RHINO Software-Defined Radio Processing Blocks

A thesis submitted to the Department of Electrical Engineering,
University of Cape Town, in fulfilment of the requirements for the degree of

Master of Science

*a*t the

University of Cape Town

by

Lekhobola Joachim Tsoeunyane

Supervised by :
Doctor Simon Winberg
and
Professor Michael Inggs

University of Cape Town

©University of Cape Town
November 30, 2015

The copyright of this thesis vests in the author. No quotation from it or information derived from it is to be published without full acknowledgement of the source. The thesis is to be used for private study or non-commercial research purposes only.

Published by the University of Cape Town (UCT) in terms of the non-exclusive license granted to UCT by the author.

University of Cape Town

Declaration

I know the meaning of plagiarism and declare that all the work in this dissertation, save for that which is properly acknowledged and referenced, is my own. It is being submitted for the degree of **Master of Science** in Electrical Engineering at the University of Cape Town. This work has not been submitted before for any other degree or examination in any other university.

Signed by candidate

Signature Removed

Signature of Author: ....
University of Cape Town

Cape Town
November 30, 2015

ABSTRACT

This MSc project focuses on the design and implementation of a library of parameterizable, modular and reusable Digital IP blocks designed around use in Software-Defined Radio (SDR) applications and compatibility with the RHINO platform. The RHINO platform has commonalities with the better known ROACH platform, but it is a significantly cut-down and lower-cost alternative which has similarities in the interfacing and FPGA/Processor interconnects of ROACH. The purpose of the library and design framework presented in this work aims to alleviate some of the commercial, high cost and static structure concerns about IP cores provided by FPGA manufactures and third-party IP vendors. It will also work around the lack of parameters and bus compatibility issues often encountered when using the freely available open resources.

The RHINO hardware platform will be used for running practical applications and testing of the blocks. The HDL library that is being constructed is targeted towards both novice and experienced low-level HDL developers who can download and use it for free, and it will provide them experience of using IP Cores that support open bus interfaces in order to exploit SoC design without commercial, parameter and bus compatibility limitations. The provided modules will be of particularly benefit to the novice developers in providing ready-made examples of processing blocks, as well as parameterization settings for the interfacing blocks and associated RF receiver side configuration settings; all together these examples will help new developers establish effective ways to build their own SDR prototypes using RHINO.

The developed library of IP cores comprises the DSP blocks and I/O interface blocks. The DSP blocks are realized with fundamental DSP algorithms which are FIR, IIR, FFT/IFFT and DDC algorithms. These DSP blocks are accompanied by a description of how they can be integrated into a common Open Standard Interconnection Bus, namely Wishbone. Furthermore, the I/O interface blocks realize the interface control logic for 1 Gigabit Ethernet and 4DSP FMC150 ADC/DAC daughter board. The 1 Gigabit Ethernet interface core uses UDP protocol to enable high speed data transfer between RHINO and external devices while FMC150 ADC/DAC provides air interface for RHINO at high sampling rates. The FM receiver is then built from the IP blocks to demonstrate the importance and reusability of the library of IP blocks in the real world context of SDR.

Testing of the IP blocks was incorporated into each step of the design process. Verification followed the Xilinx ISE tools design flow where behavioral, functional, static timing and timing

simulations were all performed. The in-circuit verification for each IP block was also performed to ensure that it actually works on spartan6 FPGA device of RHINO platform. The DSP blocks were all tested successfully in clock frequency range of 312.5 kHz to 375MHz. However, the design architecture of the DSP blocks allows them to easily adapt to clock frequencies outside this range.

Moreover, the I/O interface blocks were also tested thoroughly and successfully. The ADC and DAC were tested up to maximum sampling rates of 163.84MSPS and 61.44MSPS respectively. The 1 Gigabit Ethernet could peak the throughput rate of 98.26MSa/s when tested on a stream-based processing of RHINO platform. Lastly, the wideband FM receiver which incorporated both the Analog front-end and developed digital IP blocks was tested successfully. Testing was performed by tuning to three local FM stations and spectra for all three stations was plotted using baseband I/Q samples before FM demodulation and real-valued samples after FM demodulation. The message signals recovered through FM demodulation consisted of expected spectral components of the FM station which are mono audio, pilot tone, stereo audio and RBDS. The successfully developed library of IP blocks has proven that indeed it is useful and relevant for use in rapid prototyping of SDR applications.

ACKNOWLEDGEMENTS

I would like to gladly express my gratitude to the following people who assisted towards successful completion of this research project:

- **Dr. Simon Winberg**, my UCT supervisor, for his guidance, encouragement and providing me an excellent atmosphese for doing my research project.
- **Prof. Michael Inggs**, my UCT co-supervisor, for his advice, continuous support and immense knowledge. If it was not for a meeting we had, it have taken me years to complete.
- **Square Kilometer Array - South Africa**, for financial assistance throughout this research project
- **UCT RRSG Group Members** - I would like to thank the following colleagues in RRSG research group who were always willing to help and give suggestions:
  - Lerato Mohapi
  - Dr. Van Der Byl
  - Dr. Tong
  - Justin Coetser
  - Adrian Stevens
  - Andrew Nicol
- **My family** - my wife **'Mathato Tsoeunyane** for her unconditional love and being there for me during good and bad times. And without my lovely daughter **Puleng Tsoeunyane**, I would'nt have had courage to undertake this research project.
- **Leronti Tsoeunyane** - my late grandfather, he will forever remain my only role model. He is the reason why I have made it this far. May his soul rest in peace.
- **God The Almighty** - It is only through my strong faith in Jesus Christ my saviour, that I always felt protected and eternally blessed for having met the right people who gave their all to help me complete my research project. Glory be to God in the highest.

CONTENTS

Abstract

Acknowledgements iii

Contents iv

List of Figures x

List of Tables xiv

List of Abbreviations xvi

Nomenclature xix

1 Introduction 1

1.1 Background 1
1.2 Problem Description 3
1.3 Focus 3
1.4 Objectives 4
1.5 Methodology Overview 4
1.6 Scope and Limitations 6
1.7 Plan of Development 6

2 Literature Review 8

2.1 The Software-Defined Radio Concept 8
2.2 Reconfigurable Computing 9
2.3 IP Reuse Design 10
2.4 IP Core Libraries 12
2.5 VHDL 12
2.6 RHINO 13
2.6.1 RHINO features 13
2.6.2 RHINO Target Applications 14

2.6.3 Alternate FPGA Platforms for SDR 14
2.6.3.1 ROACH 14
2.6.3.2 USRP N200 and N210 15
2.6.3.3 BEE4 15
2.7 Digital Signal Processing Algorithms 15
2.7.1 Digital Filter 16
2.7.1.1 FIR Filter 17
2.7.1.2 IIR Filter 20
2.7.2 FFT 22
2.7.3 Digital-Down Converter 24
2.8 Gigabit Ethernet and Networking 25
2.9 Analog-to-digital and digital-to-analogue conversion card 27
2.10 ADC Noise Specifications 28
2.11 Frequency Modulation and Demodulation 29
2.12 Wishbone Bus 31
2.13 Conclusions 32

3 Methodology 35
3.1 User Requirements for IP blocks Library 35
3.1.1 Functional Requirements 35
3.1.2 Non-Functional Requirements 36
3.2 Domain Requirements 36
3.3 Design Process 37
3.4 Operational Design 38
3.4.1 DSP blocks 39
3.4.1.1 Digital Filtering 39
3.4.1.2 Fourier Transform 40
3.4.1.3 Channelization 40
3.4.2 I/O blocks 40
3.4.3 Digital Wideband FM receiver 41
3.5 Experimental Environment 41
3.5.1 Hardware 41
3.5.2 Software Tools 43
3.6 Experiments 44
3.6.1 Testing DSP cores 44
3.6.2 Testing 1Gbps Ethernet interface core 44
3.6.3 Testing ADC 44
3.6.4 Testing DAC 45
3.6.5 Testing a Streaming Core 45
3.6.6 Testing a Digital Wideband FM Receiver 46

4 Design of SDR DSP Blocks 47

4.1 FIR IP core . . . 47
4.1.1 Filter Structure . . . 48
4.1.2 Filter Coefficients Generation . . . 49
4.1.3 Parameters and Ports . . . 50
4.1.4 Timing Constraints . . . 50
4.1.5 Wishbone Interface . . . 51
4.1.6 FIR Core Test . . . 53
4.2 IIR IP Core . . . 53
4.2.1 Filter Coefficients Generation . . . 53
4.2.2 Parameters and Ports . . . 55
4.2.3 Timing Constraints . . . 56
4.2.4 Wishbone Interface . . . 56
4.2.5 IIR core Test . . . 57
4.3 FFT/IFFT IP Core . . . 57
4.3.1 Design Structure . . . 59
4.3.1.1 Butterflies . . . 60
4.3.1.2 Shift Register . . . 61
4.3.1.3 Complex Multiplier . . . 61
4.3.1.4 Twiddle Factor ROM . . . 62
4.3.1.5 Controller . . . 62
4.3.2 Parameters and Ports . . . 62
4.3.3 Core Generation Flow for Higher Length FFTs . . . 63
4.3.4 Timing Constraints . . . 63
4.3.5 Wishbone Interface . . . 65
4.3.6 FFT/IFFT core Test . . . 66
4.4 DDC IP Core . . . 66
4.4.1 DDC structure . . . 66
4.4.1.1 NCO . . . 66
4.4.1.2 Digital Mixer . . . 68
4.4.1.3 CIC Decimation filter . . . 68
4.4.1.4 Compensation Filter . . . 69
4.4.2 Parameter and Ports . . . 69
4.4.3 Timing Constraints . . . 70
4.4.4 Wishbone Interface . . . 71
4.4.5 DDC Core Test . . . 73

5 Design of SDR I/O Interface Blocks **74**
5.1 4DSP-FMC150 interface Core . . . 74
5.1.1 CDCE72010 programming settings . . . 75
5.1.1.1 PLL configuration parameters . . . 75
5.1.1.2 PLL Design . . . 76
5.1.2 ADS62P49 interface . . . 78

5.1.2.1 Sample Rate . . . 79
5.1.2.2 Bit and Word Alignment . . . 79
5.1.3 DAC3283 interface . . . 80
5.1.4 ADC and DAC Test . . . 81
5.2 UDP/IP core . . . 81
5.2.1 Overall Architecture . . . 82
5.2.1.1 Physical Layer . . . 82
5.2.1.2 Data Link Layer . . . 83
5.2.1.3 Network Layer . . . 85
5.2.1.4 Transport Layer . . . 85
5.2.2 Structure of the UDP/IP core . . . 85
5.2.3 Marvell 88E1111S/PHY initialization . . . 88
5.2.4 UDP/IP Core Interface . . . 88
5.2.5 UDP/IP Core Test . . . 89

6 Design of FM Receiver 91
6.1 Design of Digital Receiver . . . 91
6.2 Design of Analog RF Front-end . . . 95

7 Results and Discussion 97
7.1 FIR Core Test . . . 97
7.2 IIR Core Test . . . 100
7.3 FFT/IFFT Core Test . . . 101
7.3.1 Testbench . . . 102
7.3.2 Hardware Test . . . 103
7.4 DDC Core Test . . . 104
7.4.1 Noise Free System Test . . . 106
7.4.2 Adding AWGN Noise to a Modulating Signal . . . 106
7.4.3 Adding AWGN Noise to a Frequency Modulated Signal . . . 108
7.4.4 Adding 20dB AWGN Noise to a modulating signal and frequency modulated Signal . . . 108
7.5 UDP/IP Core Test . . . 115
7.5.1 ARP Test . . . 115
7.5.2 Upstream Test . . . 117
7.5.2.1 Data Transfer Test . . . 117
7.5.2.2 Transfer Speed Test . . . 117
7.5.3 Downstream Test . . . 118
7.6 Streaming Core Test . . . 122
7.6.1 Direct Streaming . . . 122
7.6.2 Stream Processing With Decimation and Filtering . . . 124
7.6.3 Testing the FFT Core inside Streaming Logic . . . 128
7.7 DAC interface core Test . . . 132

7.8 FM Receiver Test 132

8 Conclusions and Further Work 136
8.1 Conclusions 136
8.1.1 DSP IP blocks 136
8.1.2 I/O interface blocks 137
8.2 Recommendations For Further Work 139
8.2.1 Upgrade the DSP blocks 139
8.2.2 Improve the I/O interface blocks 141
8.2.3 Refine the FM receiver 142

A The Attached CD 151

B FIR IP core 153
B.1 Instantiation of the FIR core 153
B.2 Generating Testbench Data Files in Matlab 153
B.3 Plotting the results in Matlab 154

C IIR IP core 156
C.1 Instantiation of the IIR core 156
C.2 Generating Testbench Data Files in Matlab 156
C.3 Plotting the results in Matlab 158

D FFT/IFFT IP core 160
D.1 Instantiation of the FFT/IFFT core 160
D.2 Generating Testbench Data Files in Matlab 160
D.3 Plotting the results in Matlab 161
D.3.1 Decimal to 2's complement binary Conversion 162
D.4 Generating n-bit Twiddle Factors HDL ROM 162

E DDC IP core 165
E.1 Instantiation of the DDC core 165
E.2 Generating Testbench Data Files in Matlab 166
E.3 Generate Coefficients for a Compensation Filter 169
E.4 Plotting the results in Matlab 170

F UDP/IP core 172
F.1 Instantiation of the UDP/IP core 172

G ADC/DAC core 174
G.1 Instantiation of the ADC/DAC core for interfacing FMC150 174

H Digital FM Receiver 176
H.1 Top Level Design of Digital IP Blocks 176

H.2 FM demodulation function in Matlab [84] 185
H.3 Plotting the FPGA results in Matlab 185

LIST OF FIGURES

1.1 Radio transceiver architecture . . . 2
1.2 Design flow for development of IP blocks for RHINO . . . 5

2.1 Ideal Software Defined Radio Architecture [63] . . . 9
2.2 Realistic Software Defined Radio Architecture [63] . . . 9
2.3 Device technologies used for reconfigurable digital systems [66] . . . 10
2.4 Comparison of technologies used for reconfigurable digital systems [66] . . . 10
2.5 An internal structure of FPGA [9] . . . 11
2.6 Essential issues for IP reuse [30] . . . 11
2.7 RHINO-high level block diagram [87] . . . 13
2.8 Ideal linear system of direct form [11] . . . 18
2.9 Transpose form FIR filter [11] . . . 19
2.10 Optimised structures for linear-phase FIR filters ($T = z^{-1}$: Sample period delay) (i) FIR Symmetric structure when the filter order M is an odd number. (ii) FIR Symmetric structure when the filter order M is an even number. [85] . . . 19
2.11 Moving Average FIR filter [75] . . . 20
2.12 Generic structure of IIR filter [11] . . . 21
2.13 Digital biquad filters [3] . . . 22
2.14 Various architectures for pipeline FFT processor [34] . . . 23
2.15 Block diagram of a DDC [49] . . . 25
2.16 The OSI and generic Ethernet Physical Model [50] . . . 26
2.17 FMC150 block diagram [1] . . . 27
2.18 Frequency spectra of frequency-modulation waves, showing effects of varying the frequency deviation [53] . . . 31
2.19 Wishbone bus basic connection [35] . . . 32

3.1 FPGA Design Flow using Xilinx ISE [101] . . . 38
3.2 Architecture of RHINO SDR processing blocks . . . 38
3.3 IP core design process . . . 39
3.4 A flowchart showing experimental development process . . . 41
3.5 Experimental setup for the DSP cores . . . 44
3.6 Experimental setup for 1 Gigabit ethernet core . . . 45

3.7 A block diagram showing experimental setup for ADC interface core 45
3.8 A block diagram showing experimental setup for DAC interface core 45
3.9 Experimental setup for a Streaming core using ADC and 1 Gigabit Ethernet interface cores 46
3.10 Experimental setup for a digital wideband FM receiver 46

4.1 A block diagram differentiating a Core and IP Core 47
4.2 An overall architecture of a DSP IP Core 48
4.3 Architecture of FIR IP Core 48
4.4 Parallel FIR structures 49
4.5 FIR core data flow diagram 49
4.6 FIR core input/output timing waveform 51
4.7 FIR core and Wishbone slave interface 52
4.8 Architecture of IIR IP Core 53
4.9 Cascaded Direct Form I Biquad IIR filter 54
4.10 Six Cascaded second-order sections (DFI=Direct Form I) 54
4.11 IIR core input/output timing waveform 57
4.12 IIR core and Wishbone slave interface 58
4.13 The architecture of FFT IP Core 59
4.14 32-point FFT structure using Radix-2^2 Single-Path Delay Feedback algorithm . 60
4.15 The single FFT pipeline stage consisting of Butterfly Type BFI and BFII and showing how shift registers, counter, ROM and complex mulplier are connected. 61
4.16 Sign-inversion structure [81] 61
4.17 A flow diagram for generation of FFT core modules for high length FFTs . . . 64
4.18 FFT/IFFT core input/output timing waveform 64
4.19 FFT core and Wishbone slave interface 65
4.20 The architecture of DDC IP Core 67
4.21 A structure of Digital Down Converter 67
4.22 Block diagram of NCO core 67
4.23 Block diagram of a CIC core 68
4.24 DDC core input/output timing waveform 71
4.25 DDC core and Wishbone slave interface 72

5.1 CDCE72010 programming settings for FMC150 card 77
5.2 The architecture of ADS62P49 interface 79
5.3 The architecture of DAC3283 interface 81
5.4 Overall architecture of UDP/IP Stack 82
5.5 MAC core transmit operation [31] 83
5.6 MAC core receive operation [31] 84
5.7 PHY Management interface 84
5.8 Structure of UDP/IP Core based on a Gigabit Ethernet 86
5.9 ARP protocol operation data flow diagram 87

5.10 The structure of ARP packet 87
5.11 The structure of a UDP packet 88
5.12 UDP Core Write operation interface 90
5.13 UDP Core Read operation interface 90

6.1 Digital FM receiver architecture 92
6.2 Compensation Filter Response for 10-stage CIC-1 filter 94
6.3 Block diagram of a Analog RF front-end 96

7.1 Experimental environment showing Hardware and Software Tools use in this project 97
7.2 FIR core Testbench block diagram 98
7.3 The results FIR filter testbench. 99
7.4 IIR core Testbench block diagram 101
7.5 The results IIR filter testbench. 101
7.6 Testbench block diagram 102
7.7 MATLAB and FPGA results of a 1024-point FFT and IFFT core tested with rectangular pulse input waveform. 103
7.8 DDC core Testbench block diagram 105
7.9 DDC core input vector generated in MATLAB and computed by FM modulation of a 200 kHz with 94.5 MHz sampled at 122.88 MSPS. 105
7.10 A 28.38MHz carrier waveform generated in MATLAB and a local oscillator 28.38MHz signal generated by NCO core in FPGA. 106
7.11 Results of DDC Core and FM demodulator when a noise free input test signal is used. 107
7.12 FM demodulator output showing the demodulated signal with transients and after removing the transients. This applies to a test when a noise free input test signal is used. 108
7.13 Results of DDC Core and FM demodulator when 20dB AWGN noise is added to a modulating signal. 109
7.14 FM demodulator output showing the demodulated signal with transients and after removing the transients. This applies to a test where 20dB AWGN noise is added to a modulating signal. 110
7.15 Results of DDC Core and FM demodulator when 20dB AWGN noise is added to a frequency modulated signal. 111
7.16 FM demodulator output showing the demodulated signal with transients and after removing the transients. This applies to a test where 20dB AWGN noise is added to a frequency modulated input test signal. 112
7.17 Results of DDC Core and FM demodulator when 20dB AWGN noise is added to a modulating signal and frequency modulated signal. 113
7.18 FM demodulator output showing the demodulated signal with transients and after removing the transients. This applies to a test where 20dB AWGN noise is added to a modulating signal and frequency modulated input test signal. . . . 114
7.19 Wireshark Capture of FPGA broadcast ARP request 116

7.20 Trace of UDP traffic from FPGA showing the details of the UDP header 118
7.21 Trace of time taken for a single and 500 packets of UDP over 1Gbps Ethernet . 119
7.22 Measuring speed using Linux Speedometer Tool 2.8 120
7.23 Thoughput vs UDP Frame Length 120
7.24 Trace of UDP packets being transmitted to FGPA over 1Gbps Ethernet 121
7.25 Capture of received UDP data on FPGA using ChipScope Pro 121
7.26 A measured spectrum analysis for ADC input sine waveforms generated using a function generator 122
7.27 A digitized 200kHz sine wave visualized using ChipScope Pro 123
7.28 A digitized 200kHz visualized using ChipScope Pro 124
7.29 ADC digitized signals streamed via UDP 125
7.30 20MHz tone ADC ouput streamed using UDP 126
7.31 FPGA results of UDP streaming when 163.84MSPS ADC is used 127
7.32 Experimental setup for stream-based processing with CIC decimation filter and Compensation Filter 127
7.33 FPGA results of UDP streaming when a CIC and FIR filters are used to process a 200 kHz signal sampled by the ADC at 163.84 MSPS 127
7.34 Experimental setup for FFT core as tested on the FPGA 128
7.35 Results showing 512-point and 4096-point FFT of a 133kHz ADC wave using MATLAB and FFT core 129
7.36 Results showing 512-point and 4096-point FFT of a 200kHz ADC wave using MATLAB and FFT core 130
7.37 Results showing 512-point and 4096-point FFT of a 445kHz sine waveform using FFT/IFFT core 131
7.38 The spectra different sinusoids generated using NCO core and measured at the FMC150 DAC output 132
7.39 A spectrum of a baseband FM station [22] 133
7.40 The FM band signals measured before and after analogue RF front-end processing 134
7.41 The results of FM Receiver when tuning to 89MHz, 94.5MHz and 95.3MHz stations 135

8.1 Architecture of RHINO SDR processing blocks with recommended new blocks and features labelled in italic red 140

LIST OF TABLES

2.1 Computational requirement comparison [34] 24
2.2 Bessel Functions of the First Kind Rounded to Two Decimal Places [22] 30
2.3 Signal description of Wishbone bus 33

4.1 FIR core parameters 50
4.2 FIR core ports 51
4.3 Wishbone slave registers for FIR core 52
4.4 IIR core parameters 56
4.5 IIR core ports 56
4.6 Wishbone slave registers for IIR core 57
4.7 The description of formulas used for FFT architecture 59
4.8 FFT core parameters 62
4.9 FFT core pin-out 63
4.10 Wishbone slave registers for FFT/IFFT core 66
4.11 DDC core generic parameters 70
4.12 DDC core pin-out 71
4.13 Wishbone slave registers for DDC core 73

5.1 FMC150 PLL configuration parameters 75
5.2 FCM150 CDCE72010 Configuration Settings 78
5.3 Byte Enable Configurations 83
5.4 MAC core register description 85
5.5 State Machine for initialization of PHY register settings 89

6.1 Parameters of CIC-1 Filter 93
6.2 Parameters of a Compensating Filter 93
6.3 Specifications for commercial RF components 96

7.1 Bandpass filter specifications generate FIR core coefficients 98
7.2 FIR core parameter configurations 98
7.3 Bandpass filter specifications used to generate IIR core coefficients 100
7.4 IIR core parameter configurations 100

7.5 FFT/IFFT core configuration parameters as used in a testbench 102
7.6 Synthesis Report summary for FFT/IFFT core on Spartan 6 - XC6SLX150T device 104
7.7 DDC core configuration parameters as used in a testbench 104
7.8 Point-to-Point Network configurations 115
7.9 Dynamic parameters for a 49.152MSPS ADC digitizing different tones. 124
7.10 Dynamic parameters for a 163.84 MSPS ADC digitizing 200kHz tone. The ADC sample rate is decimated resulting in sample rate of 5.12 MSPS prior to UDP transmission 128
7.11 MATLAB and FPGA FFT results of ADC sines waves streamed from FPGA via UDP 128
7.12 Summary of DAC results for different tones 133
7.13 FM stations used for the FM receiver experiment 133

List of Abbreviations

- **ADC** – Analogue to Digital Converter
- **AM** – Amplitude Modulation
- **ASIC** – Application-Specific Integrated Circuit
- **BRAM** – Block Random Access Memory
- **BEE4** – Berkeley Emulation Engine 4
- **CASPER** – Collaboration for Astronomy Signal Processing and Electronics Research
- **CAT-5e** – Category 5e
- **CORDIC** – CO-ordinate Rotation DIgital Computer
- **CPLD** – Complex Programmable Logic Device
- **CPU** – Central Processing Unit
- **CRC** – Cyclic Redundancy Check
- **DAC** – Digital to Analogue Converter
- **DDC** – Digital Down Converter
- **DDR** – Double Data Rate
- **DFT** – Discrete Fourier Transform
- **DSP** – Digital Signal Processing
- **FFT** – Fast Fourier Transform
- **FIR** – Finite Impulse Response
- **FM** – Frequency Modulation
- **FMC** – FPGA Mezzanine Card
- **FPGA** – Field Programmable Gate Array

- **FSK** – Frequency-Shift Keying
- **GBE** – Gigabit Ethernet
- **GPMC** – General Purpose Memory Controller
- **GPP** – General Purpose Processor
- **HDL** – Hardware Description Language
- **IFFT** – Inverse Fast Fourier Transform
- **IIR** – Infinite Impulse Response
- **I/O** – Input/Output
- **IP** – Intellectual Property
- **IP** – Internet Protocol
- **I/Q** – In-phase and Quadrature signal components
- **ISE** – Integrated Software Environment
- **JTAG** – Joint Test Action Group
- **LGPL** – GNU Lesser General Public License
- **LPC** – Low Pin Count
- **LTI** – Linear Time-Invariant
- **LVDS** – Low Voltage Differential Signalling
- **MAC** – Media Access Control
- **NCO** – Numerically Controlled Oscillator
- **OSI** – Open Systems Interconnection
- **PC** – Personal Computer
- **PCB** – Printed Circuit Board
- **PCIe** – Peripheral Component Interconnect Express
- **PLL** – Phase Locked Loop
- **PM** – Phase Modulation
- **RBDS** – Radio Broadcast Data System
- **PWM** – Pulse Width Modulation
- **RHINO** – Reconfigurable Hardware Interface for ComputatioN and RadiO

- **RMS** – Root Mean Square
- **ROACH** – Reconfigurable Open Architecture Computing Hardware
- **RTL** – Register Transfer Logic
- **RX** – Receive
- **SDR** – Software Defined Radio
- **SKA-SA** – Square Kilimeter Array - South Africa
- **SoC** – System on Chip
- **TCP** – Transmission Control Protocol
- **TX** – Transmit
- **UDP** – User Datagram Protocol
- **USB** – Universal Serial Bus
- **USRP** – Universal Software Radio Peripheral
- **UTP** – Unshielded Twisted Pair
- **VHDL** – VHSIC Hardware Description Language
- **VHSIC** –Very High Speed Integrated Circuit
- **VNA** – Vector Network Analyzer

NOMENCLATURE

- **Analogue to digital Converter (ADC):** an electronic device that converts data from its analogue format to its digital form.
- **Digital to Analogue Converter (DAC):** an electronic device that converts data from its digital format to its analogue form.
- **Field Programmable Gate Array (FPGA):** is a set of programmable logic cells or blocks, a programmable interconnection network and a set of input and output cells around the device which can be programmed to perform a specific logic function.
- **FPGA Mezzanine Card (FMC):** an ANSI standard that defines a standard mezzanine card form factor and connector interface to an FPGA located on a carrier board.
- **Gateware:** is a digital design logic implemented on FPGA.
- **Intellectual Property (IP) core:** is a block of logic or data that is used in making a field programmable gate array (FPGA) or application-specific integrated circuit (ASIC) for a product.
- **Low Voltage Differential Signalling (LVDS):** is a standard for representing digital data using two separate voltage signals.
- **System on Chip (SoC):** is an integrated circuit (IC) that integrates all components of a computer or other electronic system into a single chip.
- **Very High Speed Integrated Circuits Hardware Description Language (VHDL):** a hardware description language used in electronic design automation to describe digital and mixed-signal systems such as FPGA.

CHAPTER 1

INTRODUCTION

The purpose of this dissertation is to present a library of IP blocks for use in Software-Defined Radio applications using RHINO board as an FPGA target platform. The blocks which are also called IP (Intellectual Property) cores will be described in VHDL and will be available under the General Public License (GPL).

This chapter outlines a brief background to the work presented in this dissertation. The problem description which is a driving force behind this work is provided along with the main focus of the dissertation. This is followed by objectives, methodology overview, scope and limitations of this work. Finally, the structure of this dissertation is briefly described.

1.1 BACKGROUND

The ever increasing introduction and evolution of wireless communication technologies and standards are changing the manner in which wireless services and applications are used [96]. The demand and usage of these services by consumers or users is growing extremely high and is constantly pushing designers beyond their limits. Wireless devices are becoming more common and users are demanding the convergence of multiple services and technologies [32] in a single wireless terminal or device. These as a result introduce potential challenges in areas of equipment design, wireless service provision, security and regulation [17].

Configurable technologies are a solution to today's increasing user needs for wireless services and applications. These types of technologies are easily upgradable, reconfigurable and can easily adapt to changes in technology standards and needs [94]. One such technology that offers all these features is a Software Defined Radio.

The advent of Software Defined Radio (SDR) has opened doors to many possibilities in the field of radio communications. Owing to its rapid growth in recent years, it has gained utmost popularity and as a result it is widely used and applied in the analysis and implementation of many Wireless Communications Systems. Traditional systems are now replaced by SDR systems because of their high configurability and increased capabilities which suit modern wireless communications technology.

SDR is a radio in which hardware components or physical layer functions of a wireless com-

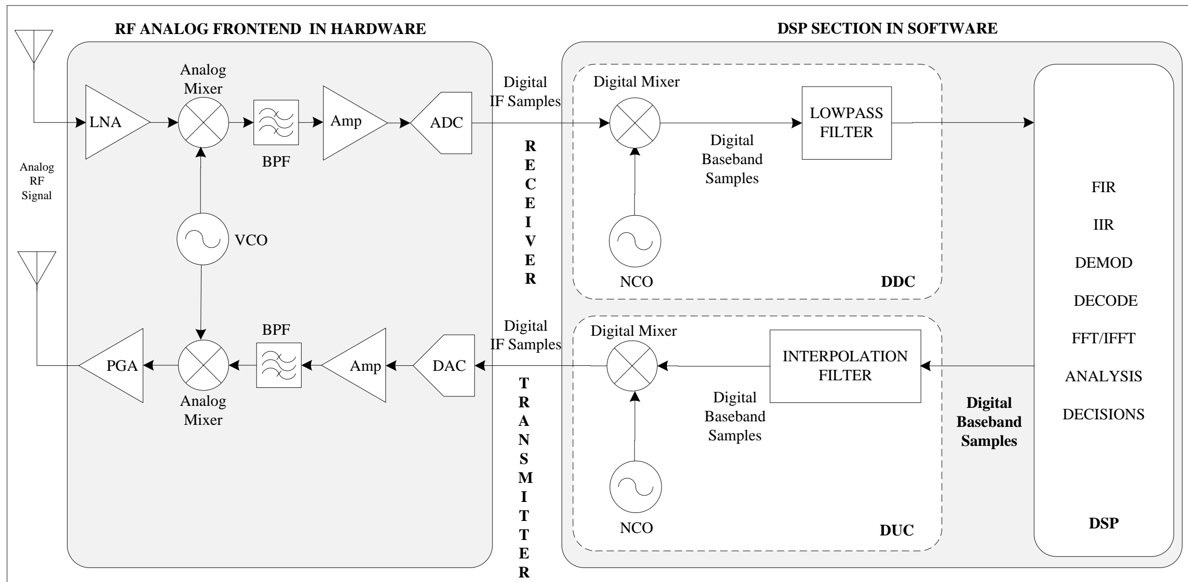

Figure 1.1: Radio transceiver architecture

munications system are all implemented in software [78]. It largely relies on a general purpose hardware that is easy to program and configure in software to enable a radio platform to adapt to multiple forms of operation such as multiband, multi-standard, multimode, multiservice and multicarrier [78, 96]. The traditional transceivers are largely based on super-heterodyne narrowband transceivers as depicted in Figure 1.1. The Software Defined Radio eliminates most of the signal pre-conditioning analog functions such as amplification and heterodyne mixing prior to analog-to-digital conversion [96, 17]. Only a wideband filter is required to reject out-of-band signals. However, high performance A/D converters are needed to achieve high sampling digitization. The A/D converters are usually costly and the trade-off between A/D converters and sampling rates remain a limitation in SDR [96].

Nevertheless, the emergence of Field Programmable Arrays (FPGAs) technology more than two decades ago has revolutionized the field of SDR. FPGAs are made of highly reconfigurable and multiple logic blocks and cells together with switch matrix to route signals between them [68]. Their flexibility and speed have made them popular and are preferred to lay a general purpose hardware platform for SDR. The reconfigurable and parallel characteristics of FPGAs enable computationally intensive and complex tasks to be processed in real-time with better performance and flexibility. These features have seen them gaining more edge over traditional general purpose processors and DSP processors [78].

Furthermore, FPGAs have led to the concept of design for reuse which is a driving factor in enhancing the productivity and improving the system-level design in SDR applications. A collection or library of parameterizable FPGA cores make design for reuse possible [100]. This library of reusable IP blocks with timing, area, power configurations is the key to SoC success as it allows mix-and-match of different IP blocks so that the SoC integrator or DSP designer can apply the tradeoffs that best suit the needs of the target application [82].

1.2 PROBLEM DESCRIPTION

The major goal of RHINO is to assist in University research groups and development teams with limited budget to rapidly prototype high performance SDR applications efficiently and at low cost [87]. For example, SDRG (Software Defined Radio Group) and RRSG (Radar Remote Sensing Group) research groups at University Of Cape Town often use RHINO in many ongoing SDR and Radar projects. SDRG goal is development and research of SDR [88] while RRSG focuses on developing advanced sensors utilizing radar technology for the user community [79]. In both groups, research is largely conducted by undergraduate and postgraduate who develop SDR and Radar systems. While RHINO is readily available for rapid prototyping of applications, students often experience challenges trying to integrate readily available third party IP blocks as well as making these compatible with RHINO. Many times this can be tedious leading to students opting for other alternative reconfigurable hardware platforms with specific technology IP libraries which are often costly.

Furthermore, the third party IP libraries are available in many forms but come at a price. The mainstream ASIC/FPGA vendors such as Xilinx and Altera provide commercial libraries of IP cores for use in wide range of SDR applications, many of which require expensive licenses to use [56]. There is a number of sources of free IP cores that are provided as open-source or ‘open-hardware’, or as other forms of open commons licensing, or released without restrictions in the public domain. Examples of these sources of free resources include the OpenCores Community, OpenSPARC T1, LEON3 Processor, GRLIB IP-Library [23], the OpenHardware.co.za Community and helpful sites such as http://www.fpga4fun.com/.

Xilinx and Altera IP Cores are costly, robust and well tested, but are only freely accessible for academic purposes [56]. These commercial IP cores are also static, making it impossible for the designer to make application-specific trade-offs [25]. Whereas OpenCores libraries are more widely accessible for free [69], but tend not to be as fully tested and parameterizable [56], particularly not for a wide range of practical SDR environments. Furthermore, the mainstream manufacturers tend to frequently use proprietary interconnection buses and use these consistently allowing blocks to be connected easily. The open libraries often have very varied interfaces making it more difficult to quickly piece together designs using these reusable components. After studying all these issues, indeed there is a need for development of reusable, portable and parameterizable IP cores designed around one open interconnection standard which will be useful for development of SDR domain specific applications.

1.3 FOCUS

This MSc project focuses on the design and implementation of a library of parameterizable and reusable Digital IP blocks with a common Open Standard Interconnection Bus, namely Wishbone [35], designed around use in SDR applications and compatibility with the RHINO platform [87]. This as a result will alleviate the commercial problems, and will work around the static structure and bus compatibility limitations of the open resources discussed in the preceding section.

RHINO hardware platform will be used in this project for running practical applications and

testing of the blocks. The HDL library that is being constructed is targeted towards both novice and experienced low level HDL developers who will use it for free, and it will give them experience of using IP Cores that support open bus interfaces in order to exploit SoC design without commercial, parameter and bus compatibility limitations. Xilinx ISE will be used to connect the library modules using low level HDL components or rather, the schematic capture tool of Xilinx ISE will be used to invoke low level HDL components through a top level design of connected blocks.

1.4 OBJECTIVES

The main goal of this project is to reduce development time and costs which are common challenges faced by students and researchers who develop SDR applications using RHINO. In order to achieve this main goal, the project needs to complete the objectives outlined below:

- Design and implement a library of modular, reusable and parameterizable IP blocks for use in SDR applications. This library of IP blocks is to be divided into two:
    1. **DSP blocks:** Developed using DSP algorithms namely FFT, IFFT, FIR, IIR and DDC.
    2. **Input/Output (I/O) interface blocks:** These are interface cores for 1 Gigabit Ethernet and ADC/DAC FMC daughter card for RHINO FPGA board.
- Perform functional verification and experimental results analysis of developed library of IP blocks.
- Build a wideband FM receiver as way to demonstrate a rapid prototyping of SDR using a developed library of blocks.
- Define Wishbone Bus slave wrapper or interface for each DSP block to allow for easy integration into SoC design.

1.5 METHODOLOGY OVERVIEW

In order to achieve the objectives outlined in the preceding section, the design methodology plays a fundamental role in the development of IP blocks for RHINO as presented in this section. The design methodology is to follow a modular approach where the individual and complex IP blocks will be composed of multiple and less complicated blocks. By learning from previously proposed design approaches [82, 19], the general design flow for development of the library of IP blocks for RHINO platform is illustrated in Figure 1.2. Each step in the entire design flow is described as follows:

- Design starts with the specification and documentation of the reusable IP core. This further describes a detailed behavior of IP core and all the parameters associated with it. The DSP algorithms used are clearly defined along with how they are implemented on the FPGA using appropriate hardware realizable structures.

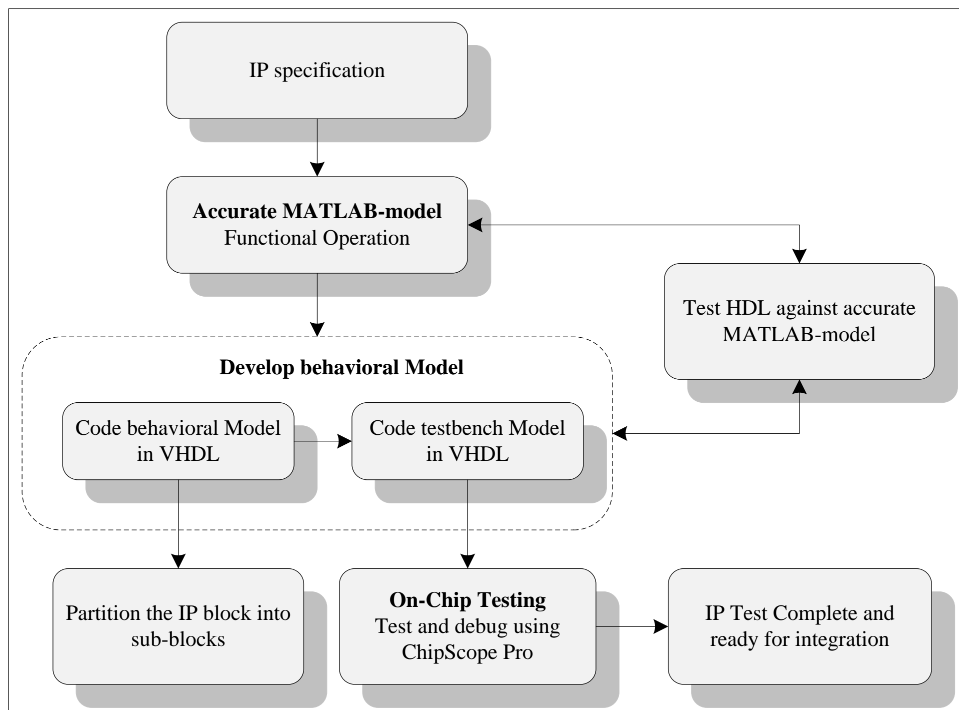

Figure 1.2: Design flow for development of IP blocks for RHINO

- Functional model of the IP core is created using accurate floating point MATLAB in order to fully understand and analyze the algorithms used before actual HDL development. In addition, the same input data to the model is used later for the HDL test-bench input.

- Behavioral model of the IP core is then developed using generic, structural and technology independent fixed-point arithmetic VHDL. Each complex IP core is broken from the top-level view or design into multiple simplified sub-blocks. In this step of the design process, timing, area and power issues are largely considered.

- Behavioral model is verified and debugged using the test-bench coded in VHDL and this is simulated to view data contained in the signals. The verification includes code coverage and behavioral (or functional) coverage. Equivalent MATLAB model results are compared with the HDL test-bench results in-order to achieve satisfactorily accurate results. However, the results obtained from the test-bench are not expected to produce 100% match with the results of the MATLAB model. The reason for this is that VHDL uses less accurate fixed-point arithmetic and MATLAB uses a more accurate floating-point arithmetic.

- In addition to HDL simulation performed in the previous step, further debugging and verification is carried out using a ChipScope Pro [20]. In this way, the physical I/O signals or ports of the FPGA-based system are monitored and analyzed on a host computer. The ChipScope Pro accomplishes this task by using its collection of IP cores that connect directly to the FPGA system being tested [20]. The IP cores namely Integrated Controller(ICON) and one or more Integrated Logic Analyzers(ILAs) are instantiated into a design [20], these allow any signal in the design to be sampled, and data to be captured

and sent to a host computer via a JTAG interface for analysis [107].

The methodology overviewed in this section is expanded further in Chapter 3 where the requirements analysis, design process, operational design, tools and experiments are discussed.

1.6 Scope and Limitations

The aim of this Msc thesis is to design and implement a library of low-level IP blocks or cores using VHDL. The IP blocks are divided into DSP blocks and I/O interface blocks as described in section 1.4. Although these blocks are expected to be tested and be fully functional on RHINO FPGA platform, they can still be used in other FPGA platforms through minor modifications in the original HDL code.

The Wishbone bus [35] interface to each DSP IP block needs to described but neither the design of a complete Wishbone Interconnection Bus architecture nor the performance analysis of implemented DSP IP blocks in the Wishbone bus is covered in this work. This implies that only the interface of how the blocks are integrated into an existing Wishbone Bus is described.

The FM Receiver is to be designed as a typical SDR prototype using the developed library of IP blocks. However, the library is also expected to be used in rapid prototyping of other SDR applications.

1.7 Plan of Development

This dissertation consists of eight chapters. **Chapter 1** outlines the background of SDR field, a need for FPGAs in reconfigurable computing and how this has led to design reuse concept commonly applied in development of library of IP cores. The chapter then goes on to provide the problem statement and objectives of this project. It then presents the methodology overview, scope and limitations. Lastly it outlines the structure of this dissertation in this section. The rest of chapters are as follows:

Chapter 2 discusses a Literature Review of the underlying theory that is necessary to formulate an approach for implementing a library of IP blocks. It starts off by reviewing the SDR technology and reconfigurable computing. It then investigates into modern IP libraries and challenges faced by designers using third party IP libraries. A brief introduction to VHDL is provided and RHINO platform is introduced along with its features that will be crucial in this project. Furthermore, common DSP algorithms, ADC, DAC and 1 Gigabit Ethernet are discussed. The Chapter concludes with the description of the Wishbone bus.

Chapter 3 outlines the requirements analysis necessary to identify specific feature expectations as demanded by the users. It then goes on to describe the hardware and software tools necessary to pave the way for a good experimental environment where the IP blocks will be tested. Then the design of the library of IP blocks is overviewed and finally the chapter shows how testing of the blocks will be carried out.

Chapter 4 discusses design and development of DSP blocks which comprise the FIR, IIR, FFT, IFFT, and DDC blocks. The wishbone interface for these blocks is also described.

Chapter 5 details the design and development of fully functional I/O interface blocks for 1 Gigabit Ethernet and FMC150 ADC/DAC card.

Chapter 6 outlines design of a digital wideband FM receiver to showcase rapid application development of SDR using the developed library of IP blocks.

Chapter 7 presents testing of the blocks which was carried out to perform functional verification and experimental results analysis developed for individual IP blocks. The tests culminate to a major test of a digital FM receiver which is built from the IP blocks developed.

Chapter 8 presents the conclusions of the results obtained in Chapters 7 and also discusses the extent to which objectives are satisfied. It then wraps up by outlining the future work which will be the refinement of the work already started in this dissertation.

CHAPTER 2

LITERATURE REVIEW

This chapter presents a review of existing literature that was performed in order to support the study undertaken in this dissertation. First a brief description of SDR field is given followed by details of reconfigurable computing. The IP reuse design concept is then discussed along with IP core libraries. Thereafter a brief introduction to VHDL and its history is provided. RHINO platform is then described and how it fits into this work. Then an introduction to DSP algorithms and I/O interface blocks commonly used in SDR applications is provided. Finally, the chapter concludes with a brief description of the Wishbone bus standard.

2.1 THE SOFTWARE-DEFINED RADIO CONCEPT

The SDR Forum, working in collaboration with Institute of Electrical and Electronic Engineers (IEEE) P1900.1 group define SDR as a "*radio in which some or all of the physical layer functions are software defined.*" [78]. SDR is realized through a reconfigurable radio platform composed of hardware and software components; however, most processing is performed in software. Since SDR relies mainly on software to compute radio processing tasks, it therefore provides profound flexibility and upgradability of radio systems. It can easily adapt to a number of operational forms such as multiband, multi-standard, multimode and multiservice [78, 65].

The ideal SDR block diagram is shown in Figure 2.1. It is composed of a transceiver and digital processing block. The goal is to bring the ADC and DAC closest to the Antenna to speed up computations [63]. The ADC converts received analogue signals from analogue domain to digital domain while the DAC converts digital signals to analogue signals. Furthermore, the filter and amplifiers condition the received RF signal before digital signal processing is performed and they also shape the digitally modulated signal before wireless transmission [92].

The more realistic architecture is illustrated in Figure 2.2. In addition to ADC, DAC, amplifiers and filters as illustrated in Figure 2.1, frequency translation from RF to baseband and vice-versa is performed in analogue mode. This happens between the antenna and ADC or DAC conversion. Control of the RF transceiver is performed via digital interface by DSP. Usually this requires the dynamic configuration of the transceiver settings and mainly depends on the requirements such as signal noise, linearity, gain and power level.

A general purpose processing element is required to perform digital operations, analysis and

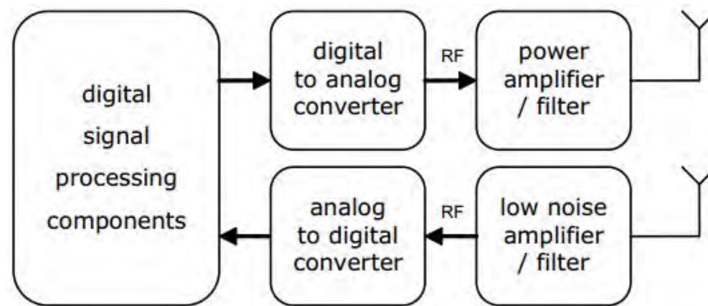

Figure 2.1: Ideal Software Defined Radio Architecture [63]

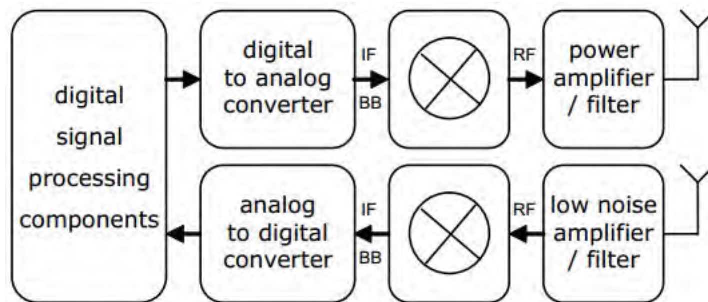

Figure 2.2: Realistic Software Defined Radio Architecture [63]

decision making [78, 37]. The processing elements such as GPP, FPGA and ASICs can be used to deliver functionality of SDR [51]. Many communication systems use general purpose processor (GPP) but this is gradually changing as designers now prefer FPGAs for computationally intensive systems. FPGAs are made of reconfigurable logic block and cells together with switch matrix to route signals between them. They also perform multiple DSP operations and support dynamic reconfiguration where the system swaps elements without any reprogramming [67].

2.2 Reconfigurable Computing

Reconfiguration is defined as the process of changing the structure of a reconfigurable device at device start-up and run-time [9]. When the reconfigurable devices such as GPPs, CPLDs, FPGAs and ASICs are used for computing as shown in Figure 2.3, the process is referred to as reconfigurable computing. Before the widespread use of FPGAs, designers preferred ASICs over GPPs when the system computational requirements were beyond that of GPP or the system had critically high production volumes [51]. ASICs offer high performance capabilities but at very high cost. They occupy less silicon area and are less power consuming. However, their drawback is that they are inflexible and expensive [9]. On the other hand, the GPPs are very flexible but at the cost of much delay due to a processor fetching instructions from memory, decoding them and writing the results back to the memory.

Different device technologies each with set a of design trade-offs [66] are shown in Figure 2.4. The FPGAs combine the merits of both ASICs and GPPs without their respective limitations. They provide the high performance of ASICs and offer architectural flexibility and low development costs like GPPs [51]. FPGAs are similar to CPLDs but are internally more complex

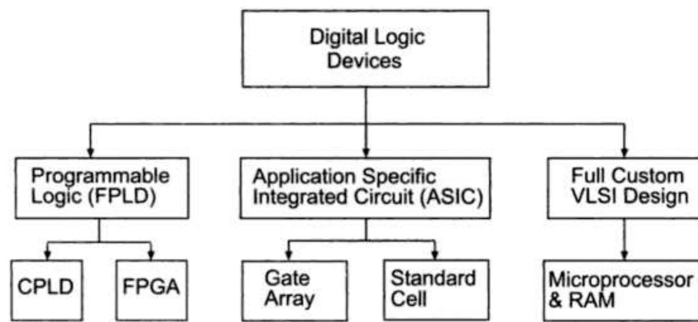

Figure 2.3: Device technologies used for reconfigurable digital systems [66]

and bigger than the CPLDs. The structure of an FPGA comprises three main parts. It has a set of programmable logic cells or blocks, a programmable interconnection network interface and a set of input and output cells around the device [9, 11]. The user application is written on one or more logic blocks. Programming of these can occur once or multiple times. The interconnection network connects the logic blocks while the I/O cells enable the FPGA device to connect with external devices. A typical internal structure of an FPGA is illustrated in Figure 2.5

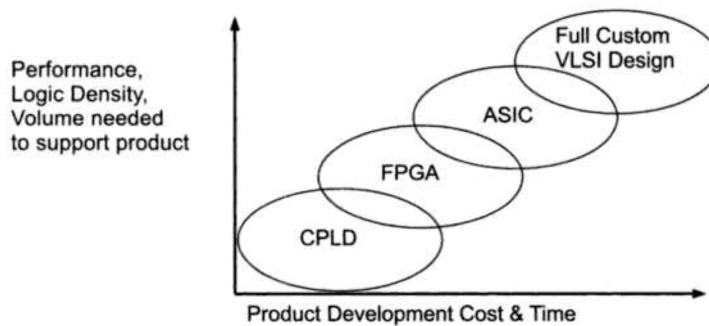

Figure 2.4: Comparison of technologies used for reconfigurable digital systems [66]

2.3 IP REUSE DESIGN

In the previous section, we have learned that FPGAs permit extremely complex functions with flexibility, at low power, reduced power and more reliability. Consequently increasing pressure on designers to meet ever-tightening time-to-market deadlines now measured in months rather than years [100]. Working more at system level, designers are heavily involved with integrating the components without close study of innermost design functionality as their aim is to speed up productivity or prototyping process.

As a result, there is a great need to develop design and verification methodologies that will speed up the design and development process. Design for reuse therefore becomes a driving factor in enhancing the productivity and improving the system-level design [100, 83]. A collection or library of parameterizable IP makes design for reuse possible. This increases flexibility to design as parameters controlling these features would be configured into code during synthesis and as a results describing hardware of the desired application [100, 83].

In IC technology, design of intellectual property is commonly discussed along with design for

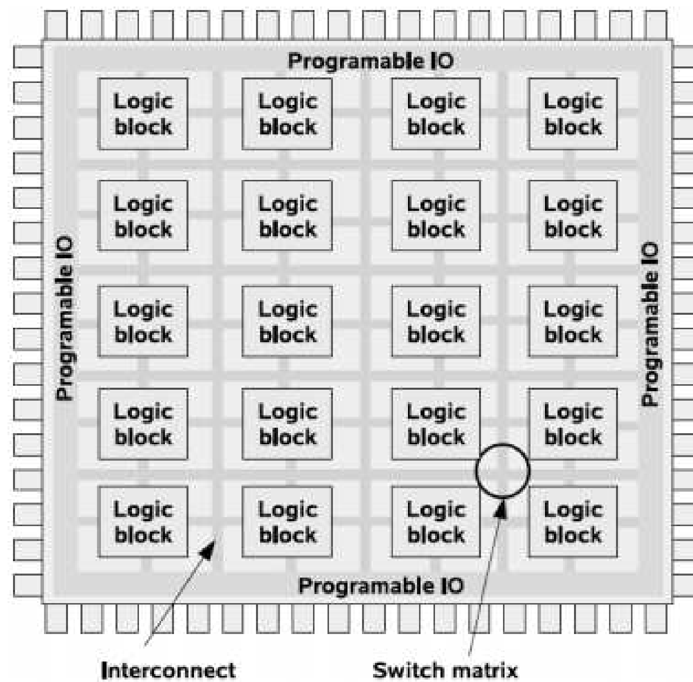

Figure 2.5: An internal structure of FPGA [9]

reuse. But what makes up the IP? In IC design world, it is referred to as RTL description of the design and it is made complete by including the documentation of the workings, functionality and tests which are as important as the design itself [100, 30]. Regardless of limited support from the semiconductor industry, there are IP reuse issues [30] that need to be considered by IP businesses and these are summarized in Figure 2.6.

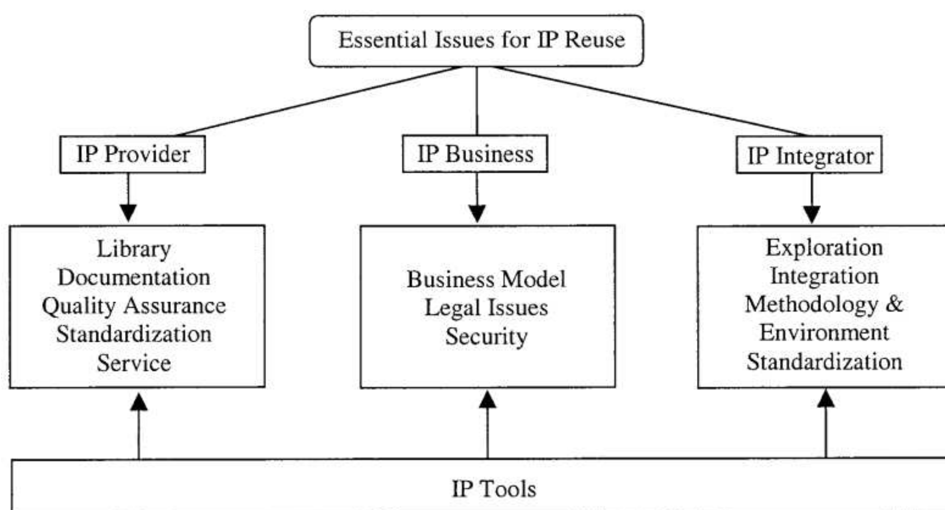

Figure 2.6: Essential issues for IP reuse [30]

2.4 IP CORE LIBRARIES

The continuous design and implementation of a library of blocks, called IP (Intellectual Property) cores is increasingly driven by the desire to meet shortest possible time-to-market. This has led to greater demands of minimal development and debugging time [71, 100].

Furthermore, hardware designers are mainly relying on pre-designed IP cores from these IP libraries to increase productivity and reduce design time. However, many of the ASIC/FPGA vendors and third-party IP libraries are static [25]. A static IP does not allow high performance to be achieved even when hardware resources or power budget is available nor achieve better performance to save both size and power consumption [25]. Integrating the third-party IP can also be a huge challenge. Very often, it is a time-consuming and error-prone task [29]. Lastly, the IP libraries developed by private vendors are extremely expensive [56].

All the above shortcomings of private vendor IP libraries have led to new open source hardware development models where reusable IP are developed and made available to the public. Two examples of communities supporting open IP cores are OpenCores and GRLIB. OpenCores has a considerable number of IP as well as Wishbone bus and are all accessible for free. However, OpenCores IP are not paramaterizable [56]. Likewise, GRLIB has a remarkable number of IP cores and are interconnected by AMBA-2.0 AHB/APB bus on a SoC design. But one drawback of using GRLIB IP cores is that not all IP cores are free [29]. Many of the open IP libraries have common characteristics which are listed below [10][25][29][71][100]:

- Modularity
- Parameterizability
- Portability
- Reusability
- Upgradability
- Specific Technology Independency
- Ability to consume less FPGA resources

2.5 VHDL

VHDL is an abbreviation for VHSIC Hardware Description Language and VHSIC stands for Very High Speed Integrated Circuits. VHDL is defined as a hardware description language for controlling the behaviour of electronic circuits [8]. It can be used for simulation, modeling, testing, design and documentation of hardware projects.

VHDL was developed by United States Department of Defense (DoD) [8] and was later adopted by the IEEE as IEEE standard IEEE1164 and IEEE1076. The first two standards were set in 1987 and 1993. Later improvements were made in 2000, 2002 and 2009.

VHDL and Verilog are popular Hardware Description Languages used to specify logic for CPLDs and FPGAs. VHDL is largely used in this work; however, some libraries coded in Verilog have been borrowed from other sources. This is not a problem as Verilog modules can be instantiated inside VHDL and both can co-exist in one design project.

2.6 RHINO

RHINO (**R**econfigurable **H**ardware **I**nterface for ComputatioN and Radi**O**) is a standalone FPGA processing board with the same computer architecture as ROACH (**R**econfigurable **O**pen **A**rchitecture **C**omputing **H**ardware). RHINO was designed at the University Of Cape Town and is largely aimed around a lower cost, totally open source FPGA board which provides a good platform for development of Software-defined Radio applications [87]. Its high level architecture is illustrated in Figure 2.7.

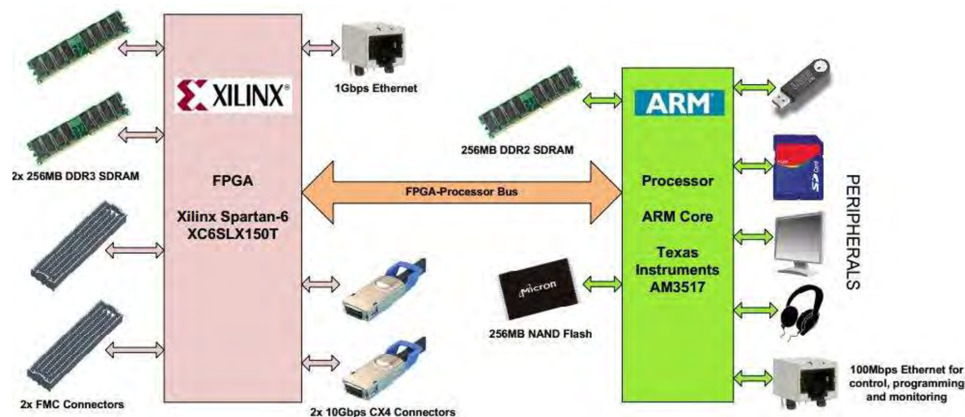

Figure 2.7: RHINO-high level block diagram [87]

2.6.1 RHINO features

Below is an outline of some key design features of RHINO, mainly which will provide a test environment for the designed Library Of SDR blocks:

1. **Xilinx XC6SLX150T FPGA:** This is a reconfigurable device which performs DSP operations hosted by the board. It supports a wide range of peripherals that enable communication by transferring data in and out of the FPGA. The FPGA is connected to ARM processor via FPGA-Processor bus which is also referred to as GPMC bus.
2. **AM3517 ARM Processor:** It is manufactured by Texas Instruments and supports Linux. It is running BORPH operating system which is a Linux variant with FPGA support.
3. **BORPH:** This stands for Berkeley Operating system for Re-Programmable Hardware. It is an extended Linux kernel that allows control of FPGA resources as if they were native computational resources [15]. This as a result allows users to program the FPGA with a given design or configuration and run it as software process within Linux.
4. **100Mbps Ethernet:** It connects directly to a processor to enable remote control and monitoring of the board as well a programming the FPGA.

5. **1Gbps Ethernet:** This interfaces with FPGA to provide high-speed network connection with remote device using standard TCP or UDP transport layer protocols to convey packets of data.

6. **FMC connectors:** FMC stands for FPGA Mezzanine Card. This enables interface with ADC, DAC and mixed signal daughter cards, supporting sample rates over 1GS/s [87].

7. **System Clock:** The FPGA board provides a global 100MHz clock that is used to drive the FPGA fabric.

2.6.2 RHINO Target Applications

The RHINO platform was designed to be a combination of an education and training platform for learning about reconfigurable computing, and as a research and prototyping platform for studies related to SDR for the application domains of Radar, Telecommunications and Radio Astronomy [39]. The design has attempted to incorporate a combination of some design features found in radio astronomy backend processing platforms (in particularly the ROACH) and features common to SDR prototyping platforms (e.g. the USRP).

The RHINO platform itself is designed around providing a comparatively low cost FPGA-based reconfigurable computing platform suited for a variety of SDR backend processing applications. RHINO is planned to provide a level of compatibility with the more powerful ROACH platform, and is intended to accommodate a trajectory for novice developers, who want to delve more deeply into RA processing, to transition to ROACH and other high-end platforms.

2.6.3 Alternate FPGA Platforms for SDR

Before RHINO was designed, other FPGA-based hardware platforms which target similar SDR applications were considered and investigated. The investigation helped to identify the strengths and weaknesses of existing hardware, and build on these previous designs when developing RHINO [87]. The three FPGA boards namely ROACH, USRP N200 and BEE4 are briefly described below.

The review of the three boards showed that the ROACH and BEE are very expensive for smaller research and development teams whereas USRP provides with low performance and insufficient resources. These reasons result in all three boards not meeting requirements for low-cost platform with high performance to be useful in SDR applications. RHINO therefore seeks to meet all requirements not met by the three FPGA platforms [87]. All the hardware features were chosen in consideration of effect RHINO would have on these SDR applications. In order to determine the hardware and software requirements for RHINO, the processing requirements for each of these applications were used [87].

*2.6.3.1 **ROACH***

ROACH is a Virtex-5 based platform, designed by SKA-SA primarily for radio astronomy applications. It forms part of the collection of FPGA boards for signal processing by the CASPER radio astronomy community.

RHINO has adopted some of the positive ROACH features such a separate on-board processor running BORPH, this provides a user with a simple interface to monitor and control the hardware design running on the FPGA. There is no need to use special JTAG programmers.

2.6.3.2 ***USRP N200 and N210***

These are FPGA boards designed by Ettus Research, specifically for SDR applications. The SDR supported applications include broadcast TV, mobile telephone network base-stations and satellite navigation, in both academic and industrial sectors.

2.6.3.3 ***BEE4***

BEE4 was first developed as a processor emulation to speed up the development of new processor architectures. It was developed by University of California, Berkeley, but the latest iterations (BEE3 and BEE4) have been developed by BEEcube. It is described as a platform where researchers can rapidly prototype a variety of architectures in a relatively short amount of time by using a repository of low-level component designs [87].

2.7 DIGITAL SIGNAL PROCESSING ALGORITHMS

As discussed in earlier sections of this chapter, it is very clear that the SDR applications strive to perform all signal processing tasks in digital domain. In the SDR field, DSP is briefly defined as continuous mathematical operations attempted in real-time. These often occur quickly and repetitively on a set of data [51]. Some common DSP algorithms include:

- Digital Filtering, e.g. Finite Impulse Response (FIR), Infinite Impulse Response (IIR), Vertibi Decoder
- Convolution
- Correlation
- Fast Fourier Transforms
- Channelization

Many algorithms were previously built using programmable digital processors. Over a decade ago, FPGAs started to replace traditional digital processors to perform DSP functions due to their high speed and flexible logic. Additionally, a DSP can be mapped directly to resources available in FPGA [52]. Despite the fast growing popularity of FPGAs, programmable processors will still be used to perform DSP functions which are not suited to FPGA such as floating computation and matrix inversion etc [80]. In some applications, they are used together to share work load whereas in others, a general-purpose DSP processor is used for system control and data movement functions while the FPGA handles peak processing functions [52].

There are numerous ways of implementing DSP algorithms on the FPGA. Careful choice of implementation and development tools can save a designer a lot of time and hard work. In

addition to that, carefully selected DSP algorithms can increase FPGA efficiency in terms of area and speed [47]. The DSP algorithms implemented in this project are reviewed below:

2.7.1 Digital Filter

Digital filter is commonly used in LTI systems to alter the attributes of a signal in time or frequency. In general terms, it passes a set of desired frequency components from a mixture of desired and undesired components [11, 59]. Design of frequency-selective discrete-time filters for practical signal processing applications often involves, in general, the following five stages [61, 59]:

1. **Specification:** Define the desired frequency response function characteristics to meet the needs of a specific application. The characteristics include filter order, passband and stopband frequencies, transition band and attenuation. This step also decides the type of filter to be designed which can be low-pass, highpass, bandpass and stopband filter.
2. **Approximation:** Approximate the desired frequency response function by the frequency response of a filter with a polynomial or a rational system function. The goal is to meet the specifications with minimum complexity, that is, by using the filter with the lowest number of coefficients.
3. **Quantization:** Quantize the filter coefficients at the required fixed-point arithmetic representation.
4. **Verification:** Check whether the filter satisfies the performance requirements by simulation or testing with real data. If the filter does not satisfy the requirements, return to Stage 2, or reduce the performance requirements and repeat stage 4.
5. **Implementation:** Implement the system obtained in hardware, in this project the FPGA is used.

Practical digital filters are implemented with fixed point arithmetic. Consequently, both the filter coefficients and input and output signals are in discrete form. These leads to four types of fixed point arithmetic effects [57]:

- **Coefficient quantization error:** This effect is visible when the actual filter response differs slightly from the ideal response. The cause of this is discretization (quantization) of the filter coefficients which has the effect of perturbing the location of the filter poles and zeroes.
- **Roundoff noise:** This is the error in the filter output that results from rounding or truncating calculations within the filter in fixed point implementations. As the name implies, this error looks like low-level noise at the filter output.
- **Limit cycles:** These are spurious oscillations found in recursive filters which occur as a result of non-linearity where the filter input is a zero or constant.

- **Overflow oscillation:** This refers to a high-level oscillation that can exist in an otherwise stable filter due to the nonlinearity associated with the overflow of internal filter calculations.

There are two commonly used digital filter and are outlined below:

2.7.1.1 ***FIR Filter***

FIR (Finite Impulse Response) is a filter with a finite duration impulse response. Many digital filters are implemented using FIR and are widely supported in terms of tools, software and IP cores [27]. Some characteristics of FIR filters are listed below [61, 83, 70, 11]:

- They have exactly linear phase.
- They are always stable.
- They are easy to implement because they lack feedback.
- They support both low and very high sample rates.
- They typically have low coefficient and arithmetic roundoff error budgets, and well-defined quantization noise.
- Any arbitrary magnitude response can be tackled using FIR sequence.

Expressed in z-domain, the transfer function $H[z]$ of FIR filter is determined by

$$H[z] = \sum_{k=0}^{N-1} h[k]z^{-k}, \tag{2.1}$$

and the Nth order FIR output $y[n]$ is given by a convolution sum namely:

$$y[n] = x[n] * h[n] = \sum_{k=0}^{N-1} h[k]x[n-k], \tag{2.2}$$

where $x[n]$ is the input sequence, z is complex variable, $h[k], k = 0, 1, ..., N-1$, are the impulse response coefficients and N is the filter length.

The design of the FIR filter involves finding the coefficients of a polynomial frequency response function that best approximates the design specifications [59]. The common methods used to determine the coefficients are:

- Windowing method

- Iterative method

The easiest method is Windowing method. If the ideal filter frequency response is $H_d(e^{jw})$ and its corresponding infinite-duration impulse response sequence is $h_d(n)$. Then the finite-duration causal impulse response corresponding to the filter coefficients is determined by multiplying $h_d(n)$ with a window function $w(n)$ [70]:

$$h_{coeff} = h_d(n) * w(n) \tag{2.3}$$

Commonly used Windowing functions are Hamming, Blackman, Rectangular, Triangular, Bartlett-Hanning, Hann and Bohman.

The iterative method designs optimal FIR filters. This means a filter has constant equiripple in the stopband and passband. The most commonly used algorithm for iterative method is Remez exchange Algorithm.

Structures for the realization of FIR filter are described below:

1. **Direct FIR Filter**
   The direct filter is graphically shown in Figure 2.8. It consists of "tapped delay lines", adders and multipliers to perform FIR function. The FIR coefficients are presented to the operand of the multipliers and one other operand is the input or delayed input samples [11].

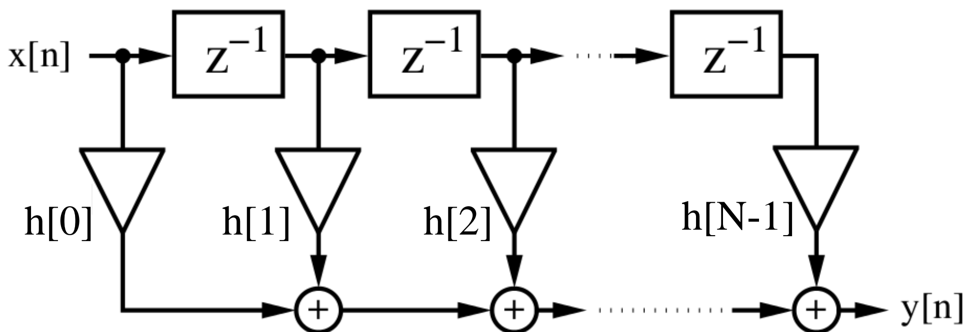

Figure 2.8: Ideal linear system of direct form [11]

2. **Transposed FIR filter**
   This filter structure supports N filter coefficients and it is a modified structure of a direct FIR implementation. Figure 2.9 shows FIR filter with a transposed structure which is a generally preferred architecture on the FPGA hardware. This is because the extra shift register is not needed for x[n] and calculating the output y[n] needs only one multiplication and one addition, hence speed is highly increased [11, 83].

3. **Even and Odd symmetric Coefficients FIR Filter**
   This FIR Filter form implements an optimized realization that exploits the symmetry

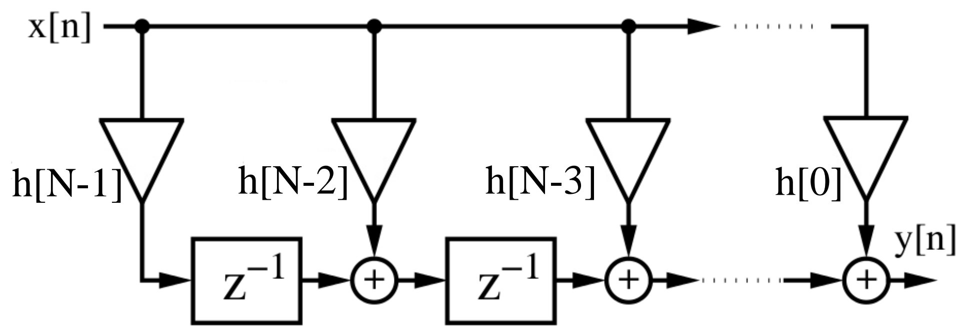

Figure 2.9: Transpose form FIR filter [11]

of frequency response coefficients. It reduces the number of multipliers to N/2 while the number of adders remains unchanged. Consequently the filter with decreased area footprint on the FPGA implementation is achieved [11, 59, 83]. Figure 2.10 shows the parallel architectures of the symmetric coefficient FIR filters.

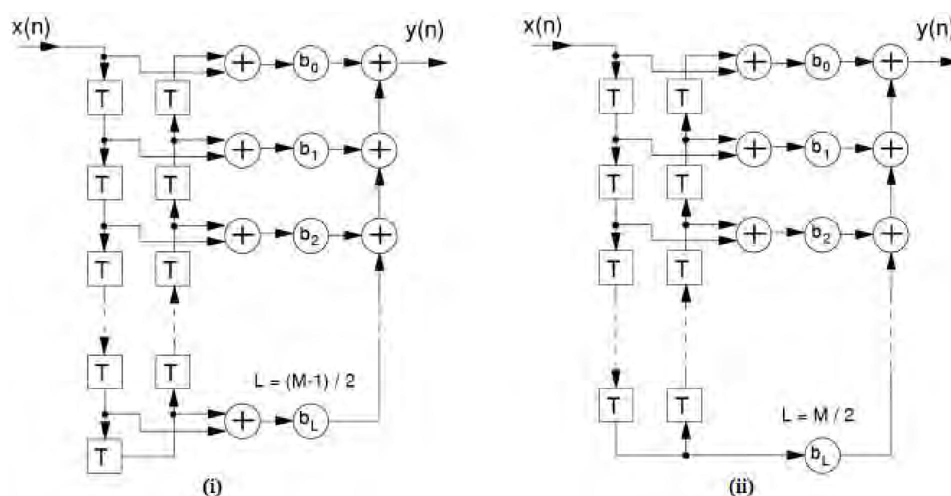

Figure 2.10: Optimised structures for linear-phase FIR filters ($T = z^{-1}$: Sample period delay) (i) FIR Symmetric structure when the filter order M is an odd number. (ii) FIR Symmetric structure when the filter order M is an even number. [85]

4. **Moving Average Filter**
   This FIR filter is illustrated in Figure 2.11 because of its wide usage in many communication systems[75]. Its output $y[n]$ is defined by:

$$y[n] = \frac{1}{N} \sum_{k=0}^{N-1} x[n-k], \tag{2.4}$$

where $x[n]$ is the input data, $k = 0, 1, ..., N-1$, and N is the filter length.

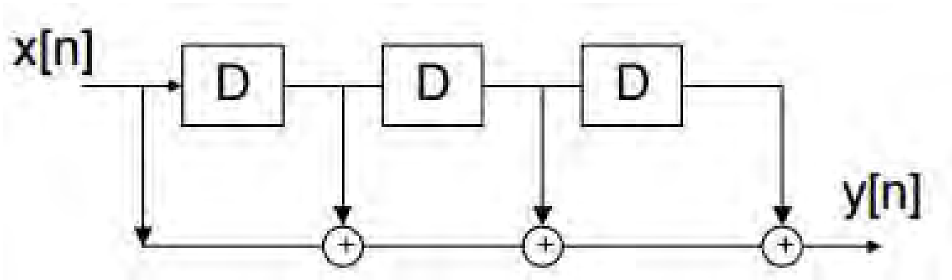

Figure 2.11: Moving Average FIR filter [75]

2.7.1.2 ***IIR Filter***

IIR filter is a filter with infinite duration impulse response. Its practical implementation can be unstable due to a recursive nature or feedback. Given the same filter order, it can be more efficient than the FIR filter because it attains both the zeros and poles while the FIR has only the zeros [11]. The IIR filter is not as widely supported as the FIR and is generally used in lower rate applications [27]. The transfer function $H[z]$ of IIR filter is given by:

$$H[z] = \frac{\sum_{k=0}^{N-1} b_k z^{-k}}{1 + \sum_{k=1}^{N-1} a_k z^{-k}} \tag{2.5}$$

and the difference equation $y[n]$ of a system performing IIR filtering is written as:

$$y[n] = \sum_{k=0}^{N-1} b_k x[n-k] - \sum_{k=1}^{N-1} a_k y[n-k], \tag{2.6}$$

where $x[n]$ is input data, z is complex variable, b_k stands for non-recursive coefficients, a_k represents recursive coefficients, and $k = 0, 1, ..., N-1$. The structure of the IIR is generally shown in Figure 2.12. Figure 2.12(a) shows separate recursive and non-recursive IIR parts and Figure 2.12(b) shows both parts merged together.

The coefficients of the IIR can be generated using different classical IIR filter types summarized below [11, 27]:

- **Elliptic filter:** It is equiripple in both the passband and stopband and has a narrow transition band.
- **Butterworth:** This type of IIR filter has maximally flat passband, flat stopband, wide transition band.
- **Chebyshev Type I:** It has equiripple passband, flat stopband, moderate transition band.

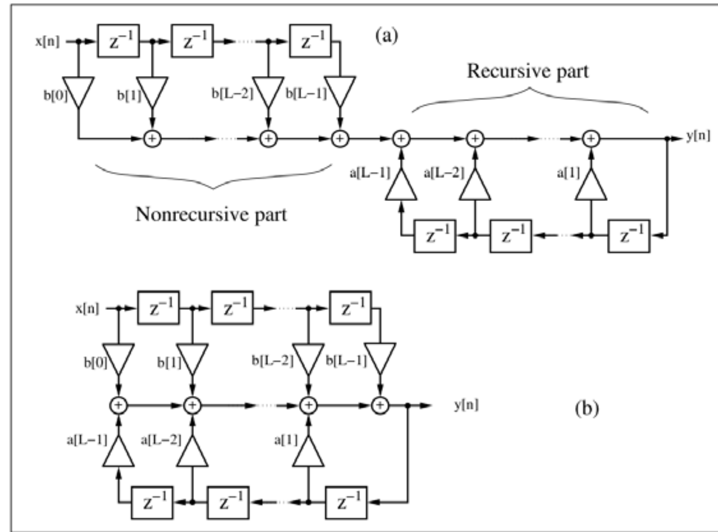

Figure 2.12: Generic structure of IIR filter [11]

- **Chebyshev Type II:** It has a flat passband, equiripple stopband, moderate transition band.
- **Bessel:** It is characterized by its fairly flat passband gain and slow initial rate of attenuation. Bessel filters generally require higher filter order than other filters for satisfactory stopband attenuation.

In fixed point arithmetic IIR realizations coefficients $(a_0...a_{N-1}, b_0...b_{N-1})$ are quantized, the resulting errors can significantly alter the desired filter characteristics. Breaking up the IIR transfer function into lower-order sections and connecting this in cascade or parallel can greatly decrease the sensitivity to quantization errors [2].

One of the mostly used lower order IIR filters is a biquad. A biquad is a second order IIR filter with two poles and two zeros [74]. The biquad can be used in a cascade to build higher order or complex filters called second order sections (SOS). It is very useful for fixed point implementations as the effects of quantization and numerical stability are negligible [64]. The biquads have two different forms namely Direct Form I and Direct Form II as shown in Figure 2.13. The biquad IIR filter transfer function $H[z]$ is defined by equation below:

$$H[z] = \frac{b_0 + b_1 z^{-1} + b_2 z^{-2}}{1 + a_1 z^{-1} + a_2 z^{-2}} \tag{2.7}$$

where z is a complex variable, a_k and b_k are both filter coefficients. The difference equation $y[n]$ of a biquad is written as:

$$y[n] = b_0 x[n] + b_1 x[n-1] + b_2 x[n-2] - a_1 y[n-1] - a_2 y[n-2], \tag{2.8}$$

where $x[n]$ is input data.

Direct form I is the most preferred for fixed point arithmetic implementation because it has a single summation point. Direct form II is suitable for floating point because it saves memory and

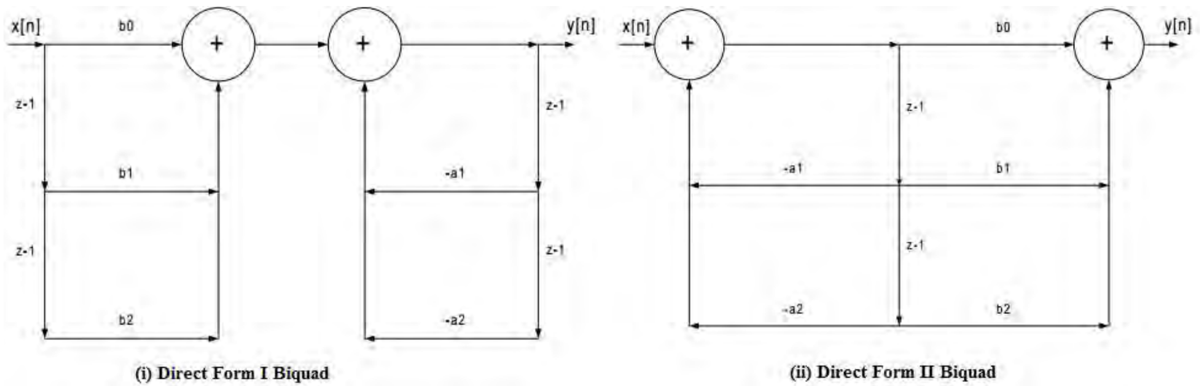

Figure 2.13: Digital biquad filters [3]

it's not sensitive to overflows in fixed point implementations. Direct form II can be enhanced further with a transposed form which has better floating point accuracy [74].

2.7.2 FFT

Fast Fourier Transform (FFT) is an efficient implementation of Discrete Fourier Transform (DFT). The function of a DFT is to map time domain data sequence into frequency domain data sequence [73]. FFT is widely used and applies in many areas such as digital communication systems, radar systems, multimedia systems etc. [73, 34, 81]. FFT output $X[k]$ is defined by the following equation:

$$X[k] = \sum_{k=0}^{N-1} x[n] W_N^{nk} \tag{2.9}$$

where $k = 0, 1, ..., N-1$ and $W_N = e^{-j\frac{2\pi}{N}}$, the root-of-unity, is also known as the *twiddle factor*.

FFTs can be realized in several architectures using various FFT algorithms. Factors such as execution speed, hardware complexity, area occupation, flexibility and precision are considered during FFT hardware implementation. Implementing parallel FFT architectures is very costly although it leads to very high performance FFT. On the other hand serial implementations are very slow which may not be ideal option for very high-speed real time systems. Pipelined architectures have emerged as a better option as they present a trade-off between pure parallel and pure serial implementations of FFT [73, 34, 81].

Radix-2, Radix-4, Radix-2^2 are amongst the commonly used FFT algorithms. These algorithms are mapped into various forms of length-N FFT architectures which can be classified into Single-path Delay Feedback (SDF), Single-path Delay Commutator (SDC), Multi-path Delay Feedback (MDF) and Multi-path Delay Commutator (MDC). Some examples of architecture types are Radix-2 Multi-path Delay Commutator (R2MDC), Radix-2 Single-path Delay Feedback (R2SDF), Radix-4 Single-path Delay Feedback (R4SDF), Radix-4 Multi-path Delay Commutator (R4MDC), Radix-4 Single-path Delay Commutator (R4SDC) and Radix-2^2

Single-path Delay Feedback (R2^{2}SDF) are all illustrated in Figure 2.14 [34, 56].

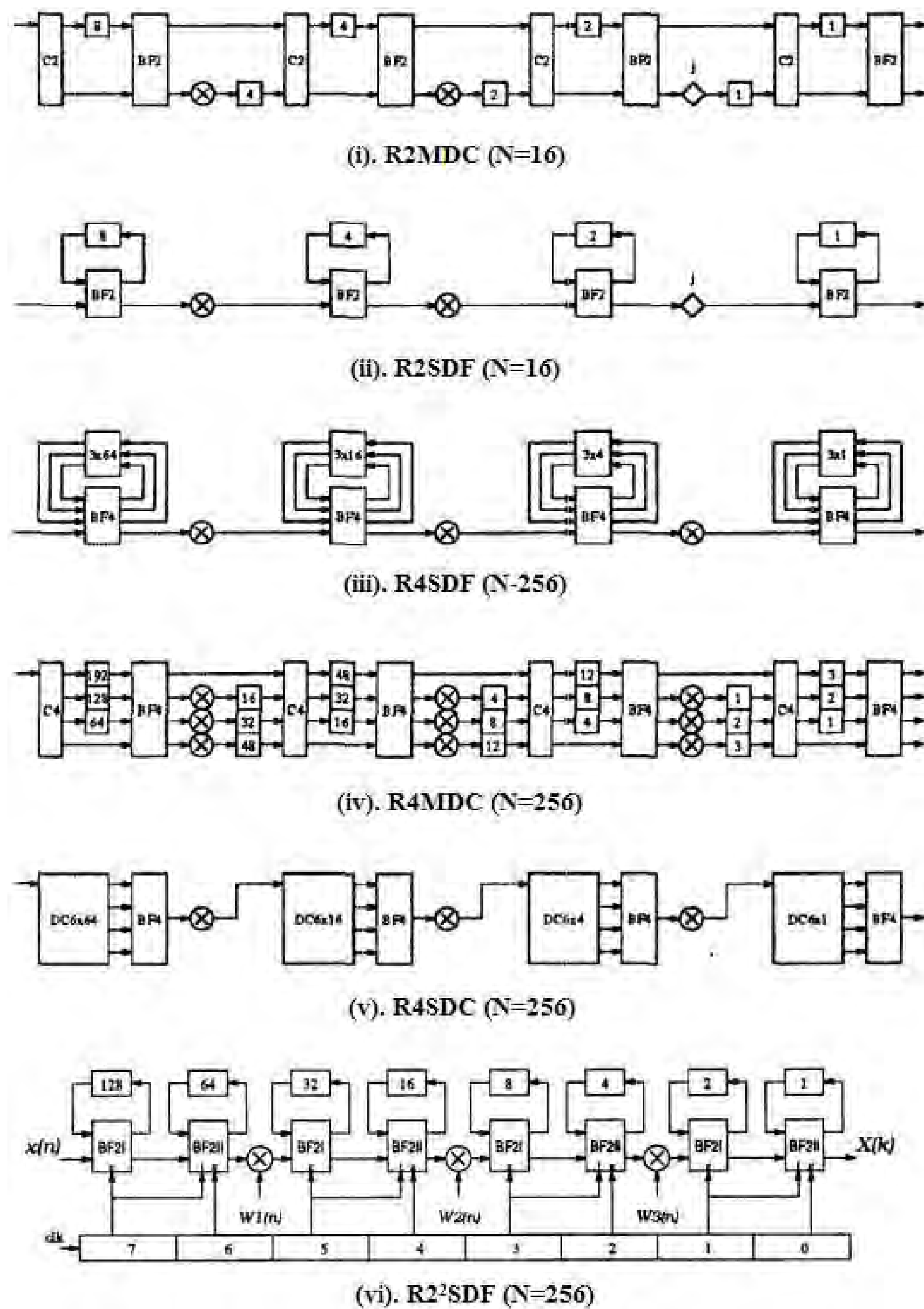

Figure 2.14: Various architectures for pipeline FFT processor [34]

These architectures are briefly explained below:

- **R2MDC:** This realizes the simplest pipeline architecture of radix-2 algorithm [34]. It has two parallel input data streams flowing forward with correct distance between data elements entering the butterfly scheduled by proper delays [34].

- **R2SDF:** It has a single data stream which passes through a multiplier at each stage and it uses registers efficiently by storing butterfly output in the feedback shift registers [34].

- **R4SDF:** This uses a CO-ordinate Rotation DIgital Computer (CORDIC) circuit, instead of a multiplier for twiddle factors to implement a pipeline FFT architecture [4].

- **R4MDC:** The R4MDC architecture is a simple way of implementing Radix-4 FFT algorithm but it has a major drawback of low utilization of computational elements [48].

- **R4SDC:** It is the most popular pipeline FFT architecture with efficient use of butterfly units and multipliers [72].

- **R2^{2}SDF:** This architecture exploits the merits of Radix-2 and Radix-4 algorithms. Its multiplicative complexity is of radix-4 algorithm and it retains the butterfly structure of radix-2 algorithm [34]. As a result, it possess spatial regularity, simple control, pipelined operation and low computational resources [56].

Furthermore the computational resources of the previously discussed FFT architectures are compared in Table 2.1. In this project, R2^{2}SDF FFT architecture will be used to implement FFT/IFFT core. It is chosen because it uses less multipliers and data memory which happen to be the dominant computational elements of the FFT architecture.

Table 2.1: Computational requirement comparison [34]

	multiplier #	**adder #**	**memory size**	**control**
R2MDC	$2(log_4N-1)$	$4log_4N$	$3N/2-2$	simple
R2SDF	$2(log_4N-1)$	$4log_4N$	$N-1$	simple
R4SDF	log_4N-1	$8log_4N$	$N-1$	medium
R4MDC	$3(log_4N-1)$	$8log_4N$	$5N/2-4$	simple
R4SDC	log_4N-1	$3log_4N$	$2N-2$	complex
R2^{2}SDF	log_4N-1	$4log_4N$	$N-1$	simple

2.7.3 Digital-Down Converter

A digital-down converter (DDC) allows the frequency band of interest to be moved down the spectrum to baseband signal near 0Hz such that further processing of signals becomes easier [70]. A DDC is sometimes referred to as channelizer. The general structure of DDC is depicted in Figure 2.15. It consists of NCO (Numerically Controlled Oscillator) with tuning capability, dual mixer and matched digital filters. The DDC takes in a band limited high sampling rate ADC signal, shifts the band of interest to DC by multiplying ADC signals with NCO sine and cosine signals using a dual digital mixer. The decimation filter reduces the high sampling rate while retaining all information. The filter is require to eliminate signals that are not with the band of interest [49]. The final output of the DDC is in complex I/Q format and it is in a good condition to be processed further using DSP functions.

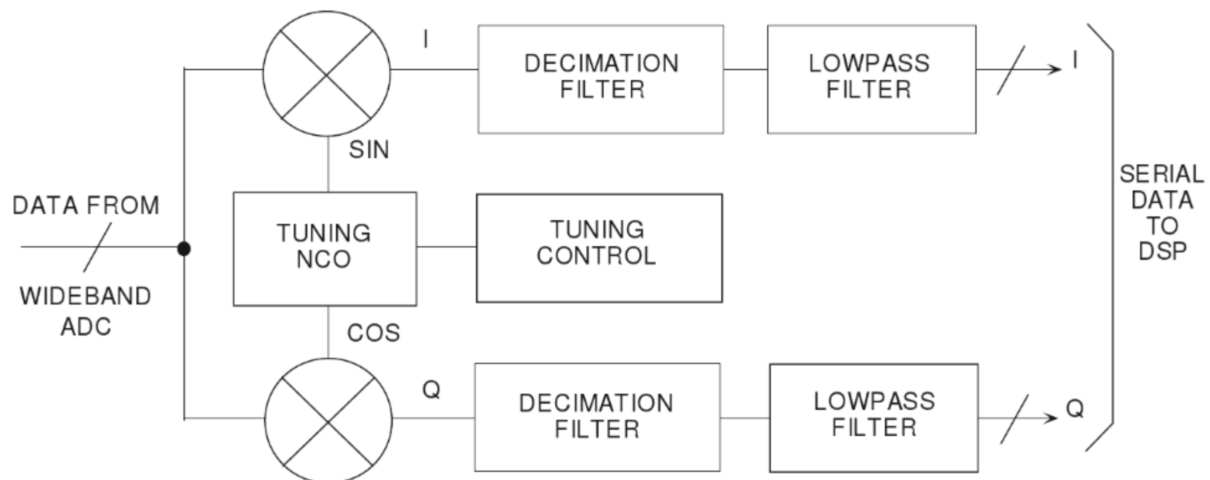

Figure 2.15: Block diagram of a DDC [49]

2.8 GIGABIT ETHERNET AND NETWORKING

When implementing I/O communication interfaces to external devices in FPGA, speed, technology and protocol top the list in the design considerations [58]. The availability of FPGAs with thousands of logic gates has made it possible to interface multiple peripheral device using standard I/O communication protocols [28]. For the most part, I/O speeds can impose a bottleneck to the system overall performance if speed, technology and protocol are not selected carefully [5]. In applications where an FPGA is required to communicate with a PC, PCI Express (PCIe) is currently the fastest solution but at the higher cost. However, there are less costly solutions which still provide sufficiently high speed connection for many applications. On such solution is Gigabit Ethernet.

Gigabit Ethernet technology is an extension of the 10/100-Mbps Ethernet standard. It provides a raw data bandwidth of 1000 Mbps while maintaining full compatibility with the installed base of over 70 million Ethernet nodes [28]. Gigabit Ethernet can operate in both operating modes namely half-duplex and full-duplex. In comparison with PCIe, it provides backward compatibility by supporting existing Ethernet systems, network operating systems and network management. Furthermore, the NIC (Network Interface Card) of the PC support Gigabit Ethernet. Not only a PC can connect to the FPGA, other embedded system devices can also connect to the FPGA via Gigabit Ethernet [28].

The OSI model shown in Figure 2.16 shows some specifics where Gigabit Ethernet implementation is largely applied. TCP or UDP can both be used as transport layer protocols to implement Gigabit Ethernet communication. TCP is a connection-oriented protocol, which means connection is maintained until application programs at both ends have finished communication. This makes it a reliable transport protocol as it ensures that all transmitted packets are received by the receiver. If the receiver detects errors in the transmitted packet or the packet gets lost, the transmitter resends the packet. TCP is therefore suited for applications that require high reliability, and transmission time is relatively less critical [26]. On the other hand, UDP is a connectionless protocol which sends totally independent frames to a receiver without ensuring

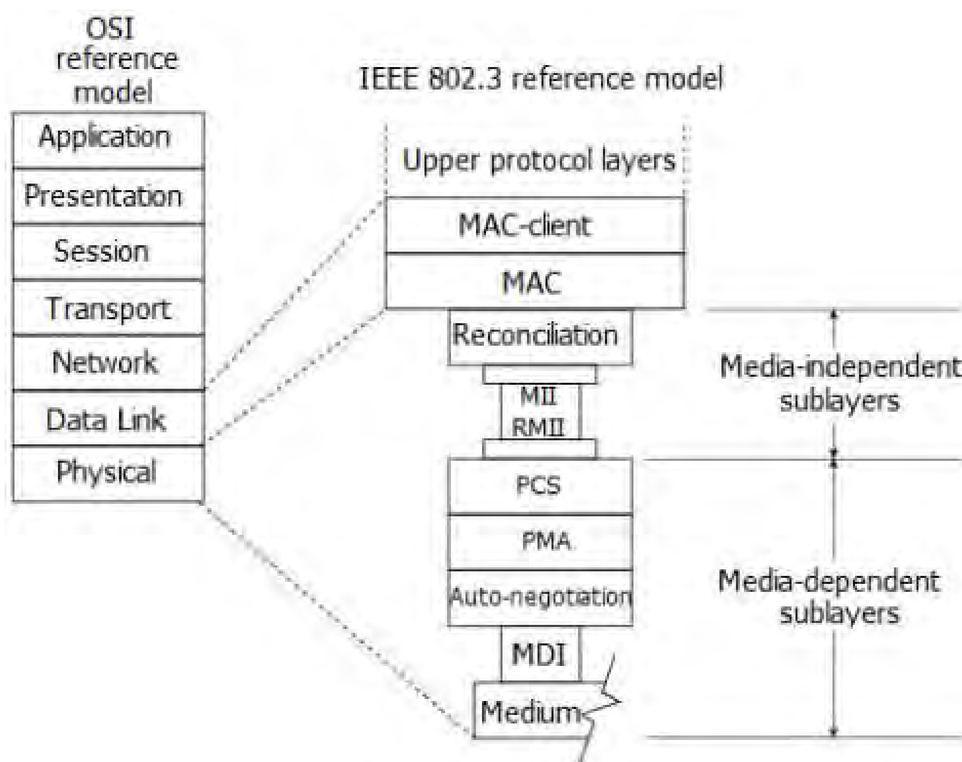

Figure 2.16: The OSI and generic Ethernet Physical Model [50]

their arrival at the destination. As a result it is unreliable transport protocol as lost packets are never retransmitted by a sender. Since UDP sends packets without error and flow control, overhead and latency are low. It is therefore suitable for applications that need fast and efficient transmission such as real-time applications [26].

Typically, IPv4 is used as network layer along with one of the transport layer protocols. Since many streaming applications involving FPGA and PC do not require retransmission of packets in the communication, UDP is preferred [58, 6] to TCP for the following reasons:

- It uses a simpler protocol mechanism without special handshaking between sender and receiver.
- It is suitable for streaming applications because of its minimal delay in transmission of packets.
- It uses less resources on FPGA and it is simple to implement

Although the UDP is a preferred transport protocol in many FPGA streaming applications, the user needs to ensure that the sender does not overwhelm the receiver with frames as this is likely to result in dropped frames [26] at receiver end. The corrupted frames will fail CRC at the receiver and will also be discarded.

Moreover, a physical layer device (PHY) is required for FPGA to connect with external devices. This is located on the board between the FPGA and the interface to external devices. Nowadays

an EMAC (Ethernet Media Access Controller) is commonly used to connect directly to a PHY device on the board. Typically one of MII, GMII, SGMII are buses are used for communication between FPGA and PHY [5].The EMAC simplifies implementation as the user only has to write wrapper files. This extra logic is necessary to define packets that comply with network and transport layer protocols that will be accepted by Operating System Kernels at the PC end.

Many EMAC IP cores are implemented and supplied by big VLSI companies. For Xilinx FPGA devices, there are two commercially available IP cores namely Xilinx Tri-Mode Ethernet MAC [102] and AXI Ethernet Lite MAC [104]. Both require very expensive licenses for designers to use. However, OpenCores provides 10/100/1000-Mbps tri-mode Ethernet MAC with enough documentation and the code accessible for free under LGPL licence, hence its open source [31]. Another open source MAC IP core is found in USRP2 software as demonstrated here [99], but it lacks sufficient documentation. OpenCores tri-mode Ethernet MAC will be used in this project for its open accessibility to public and documentation that is enough to get started.

2.9 ANALOG-TO-DIGITAL AND DIGITAL-TO-ANALOGUE CONVERSION CARD

The FMC daughter card of choice in this work is a commercial board manufactured by 4DSP namely FMC150 [1]. Its internal architecture is shown in Figure 2.17. The FMC150 provides TI's ADS62P49 dual channel 14-bit 250MSPS ADC and a TI's DAC3283 dual channel 16-bit 800MSPS DAC which can be driven by internal or external reference clock. The ADS62P49 has analogue bandwidth of 700MHz [42]. The clock management and distribution are performed by TI's CDCE72010 PLL chip [41] while the power supply and temperature monitoring are performed using TI's AMC7823 [40].

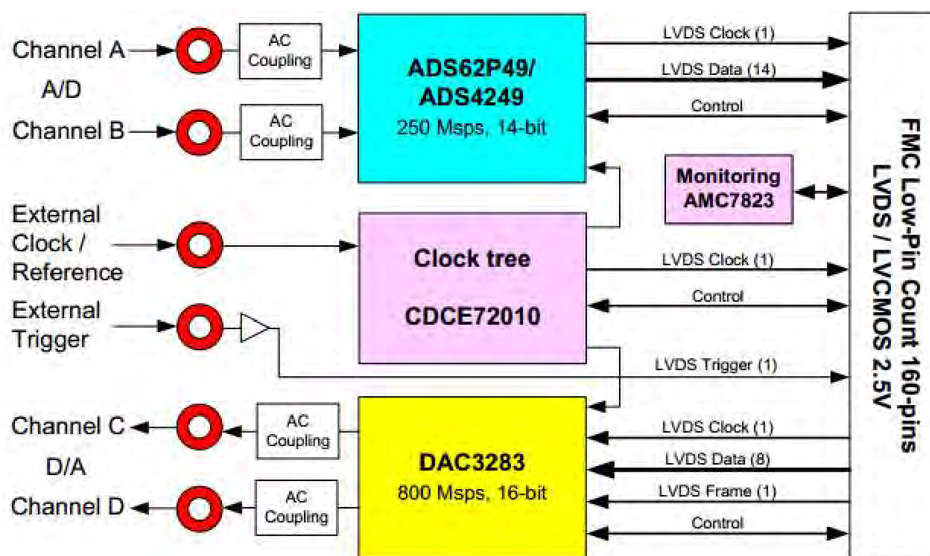

Figure 2.17: FMC150 block diagram [1]

The FMC150 card is compliant to FMC standard (ANSI/VITA 57.1). Its low-pin count (LPC) connector enables high speed interface using LVDS (Low Voltage Differential Signaling) Standard bus [1]. LVDS is a popular differential data transmission standard with a two-wire, low-swing differential signaling [45]. The major benefits include the following:

- Posibbility of low supply voltage operation
- High speed data transfer
- Good common noise rejection
- Less noise generation

2.10 ADC NOISE SPECIFICATIONS

The ADC introduces noise and distortion that degrades the quality of a sampled analogue signal. The ADC parameters provide designers a fairly accurate correlation of the performance expectations of a particular ADC [36]. These parameters are classified into two namely static parameters and dynamic parameters. The common static parameters include offset error, gain error, differential nonlinearity (DNL) and integral nonlinearity. Dynamic parameters include signal to noise ratio (SNR), signal to noise and distortion ratio (SINAD), effective number of bits (ENOB), total harmonic distortion (THD) and spurious-free dynamic range (SFDR) [13].

The static parameters are of most significance in extremely low frequency signals compared to sampling frequency. Static parameter effects are less important in high frequency applications, for this reason the dynamic parameters apply. SDR applications typically operate at very high frequencies therefore only dynamic parameters are detailed in this literature. Both the theoretical and mathematical descriptions of dynamic parameters are presented as follows [36]:

- **Signal-to-Noise Ratio (SNR):** This characterizes the ratio of the fundamental signal to the noise spectrum. It is the sum of all spectral components except DC, fundamental and the first six harmonics relative to full-scale power (dBFS) or signal power (dBc). It is defined by equation 2.10.

$$\text{SNR} = 6.02 \cdot N + 1.763 \text{ (dB)} \tag{2.10}$$

  where N is the ADC resolution.

- **Signal-to-Noise And Distortion (SINAD):** It is the combination of SNR and THD, that is, the sum of all spectral components except DC and fundamental relative to the signal power measure in dBc. It is defined by equation 2.11.

$$\text{SINAD} = 20 \cdot log_{10} \left(\frac{A_{\text{signal}}[rms]}{A_{\text{noise}}[rms]} \right) \text{ (dB)} \tag{2.11}$$

  where A_{signal} is the RMS value of the signal input to ADC and A_{noise} is the RMS value of the noise including the harmonic content.

- **Effective Number of Bits (ENOB):** This is a figure of merit which tells how close the ADC is near to the theoretical mathematical model. It calculated from SINAD using equation 2.12.

$$\text{ENOB} = \frac{\text{SINAD} - 1.763}{6.02} \text{ (bits)} \tag{2.12}$$

where all values are given in dB, and SINAD is the signal-to-noise and distortion ratio, 6.02 is to convert decibels (log_{10}) to bits (log_2), and 1.763 is the quantization error in an ideal ADC.

- **Total Harmonic Distortion (THD):** This characterizes the ratio of the sum of power of the first six harmonics to the fundamental signal power. It is measured in (dBc) and defined by equation 2.13.

$$\text{THD} = 20 \cdot log_{10} \left(\frac{\sqrt{V_2^2 + V_3^2 + \cdots + V_X^2}}{V_1} \right) \text{ (dBc)} \tag{2.13}$$

where V_2 to V_X are harmonics to the fundamental V_1.

- **Spurious Free Dynamic Range (SFDR):** This is the ratio of the level of the input signal to the level of the largest distortion components in the FFT spectrum. It is measured in dBc and is defined by equation 2.14.

$$\text{SFDR} = 20 \cdot log_{10} \left(\frac{V_{\text{f}}}{V_{\text{s}}} \right) \text{ (dBc)} \tag{2.14}$$

where V_{f} is a fundamental signal and V_{s} is highest spurious signal.

2.11 FREQUENCY MODULATION AND DEMODULATION

Frequency modulation is a type of angle modulation where frequency of the carrier is varied according to the amplitude of the information (message) signal [12]. The instantaneous frequency f_i of carrier is varied linearly with the message $m(t)$

$$f_i = \frac{1}{2\pi} \frac{d\theta_i(t)}{dt} = \frac{1}{2\pi} \theta_i(t) = f_c + k_{vco} \cdot m(t) \tag{2.15}$$

where amplitude and phase of carrier are constant. k_{vco} is the voltage-to-frequency gain of the VCO (Voltage Controlled Oscillator) expressed in units of Hz/V, and the quantity, $k_{vco} \times m(t)$, is the instantaneous frequency deviation. The frequency-modulated waveform is expressed as shown below

$$x_{FM} = A_c cos \left[2\pi f_c t + 2\pi k_{vco} \int_0^t m(\tau) d\tau \right] \tag{2.16}$$

where

- x_{FM} is FM output signal.
- f_c is the carrier frequency (i.e. frequency of unmodulated signal).
- A_c is carrier signal amplitude.

- It is assumed that the angle of unmodulated carrier is zero for simplicity $t = 0$.

The frequency deviation and modulation index are defined as follows. First let $m(t) = A_m cos(2\pi f_m t)$ denote the single-tone message (modulating) signal. Then the instantaneous frequency of FM signal becomes

$$f_i = f_c + k_f A_m cos(2\pi f_m t) = f_c + \Delta f cos(2\pi f_m t) \quad (2.17)$$

where $\Delta f = k_f A_m$ [Hz] is the **frequency deviation** [53], representing the maximum departure of instantaneous frequency of FM signal from the carrier frequency f_c. The angle of FM signal is defined by

$$\theta_i(t) = 2\pi \int_0^t f_i(\tau) d\tau = 2\pi f_c t + \frac{\Delta f}{f_m} sin(2\pi f_m t) = 2\pi f_c t + \beta sin(2\pi f_m t) \quad (2.18)$$

where $\beta = \Delta f / f_m$ [rad] is the **modulation index**, representing the maximum departure of angle of FM signal from angle $2\pi f_c t$ of unmodulated carrier. Furthermore, for a single tone message signal, the number of significant sidebands in output spectrum is the function of modulation index. This can be mathematically analyzed using n^{th} Bessel functions

$$x_{FM}[n] = \frac{A_c}{2} \sum_{k=-\infty}^{\infty} J_k(\beta) cos(\omega_c n + \omega_m k) n \quad (2.19)$$

The trigonometric function terms reduce to trigonometric functions of the sum and difference frequencies. Taking a Fourier transform results in a frequencies with the form $\omega_c \pm k\omega_m$ where k is any integer and the strength of the frequency component depends on $J_k(\beta)$.

$$\varphi_{FM}[f] = \frac{A_c}{2} \sum_{k=-\infty}^{\infty} J_k(\beta) [\delta(f - f_c - kf_m) + \delta(f + f_c + kf_m)] \quad (2.20)$$

The number of sidebands of the FM modulated signal and its associated magnitude coefficient can be found with help of Bessel function tables as shown in Table 2.2. An example of some wideband FM signals using different modulation indices is shown Figure 2.18.

Table 2.2: Bessel Functions of the First Kind Rounded to Two Decimal Places [22]

β	**J0**	**J1**	**J2**	**J3**	**J4**	**J5**	**J6**	**J7**	**J8**
0	1								
0.25	0.98	0.12							
0.5	0.94	0.24	0.03						
1.0	0.77	0.44	0.11	0.02					
2.0	0.22	0.58	0.35	0.13	0.03				
3.0	-0.26	0.34	0.49	0.31	0.13	0.04	0.01		
4.0	-0.40	-0.07	0.36	0.43	0.28	0.13	0.05	0.02	
5.0	-0.18	-0.33	0.05	0.36	0.39	0.26	0.13	0.05	0.02

Bandwidth of FM message can be estimated using Carson's rule:

$$BW_{FM} \approx 2(\beta + 1) f_m \quad (2.21)$$

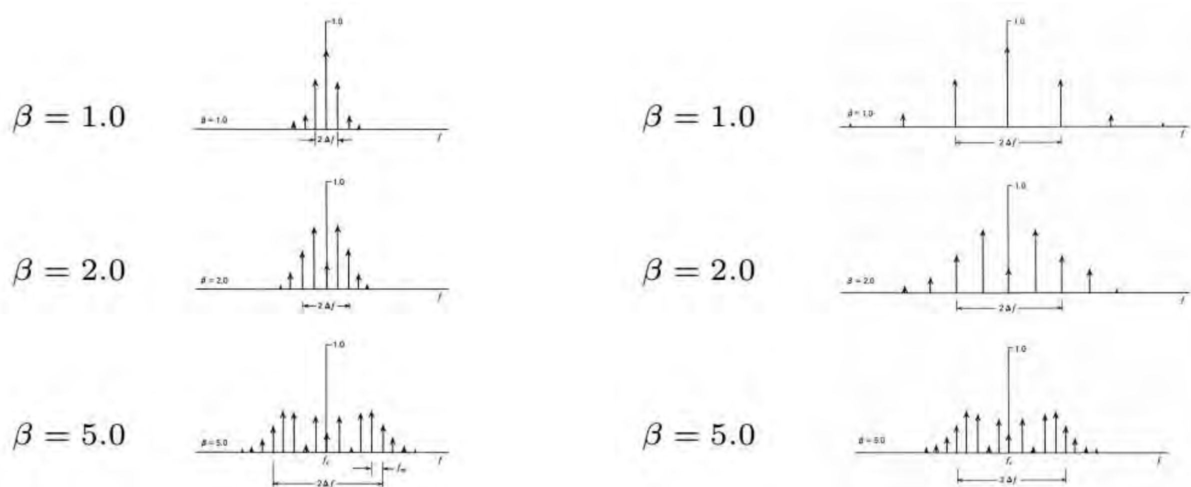

Figure 2.18: Frequency spectra of frequency-modulation waves, showing effects of varying the frequency deviation [53]

where β is modulation index.

In order to recover the message signal from the FM signal, frequency demodulation needs to be performed. The basic demodulator converts the FM signal to AM signal as below [22]

$$\Delta\theta_{demom}(t) = \frac{dx_{FM}(t)}{dt} = -A_c(2\pi f_c + 2\pi k_{vco}m(t))sin(2\pi f_c + 2\pi k_{vco}\int_0^t m(t)dt) \quad (2.22)$$

and finally the envelope detector can be used to recover $m(t)$.

2.12 WISHBONE BUS

According to WISHBONE specification [35], Wishbone is a System-on-Chip (SoC) Interconnection Architecture which defines a portable interface for use with Semiconductor IP Cores. It is designed around design reuse concept thus alleviating SoC integration problems arising in designing of internal bus for SoC applications. In comparison to other interconnection bus standards such as Advanced Microcontroller Bus Architecture (AMBA) by ARM, CoreConnect by IBM and Avalon by Altera, Wishbone is found to have an upper edge over them [90]. It has the use of flexible arbitration scheme and additional data transfer cycle (Read-Modify-Write cycle). Furthermore, its as completely open standard and there are freely available IP cores supporting Wishbone on OpenCores Community [69].

The Wishbone imposes no limitations on the creativity of the designer. It is simple to design and supports popular interconnection structures [24] such as point-to-point, data flow, shared bus and crossbar switch. Shown in Figure 2.19 is a basic Wishbone interconnection between a master and a slave and the relevant ports are described in Table 2.3. The master can be a processor or bus controller and a slave is an IP core which accelerates functions.

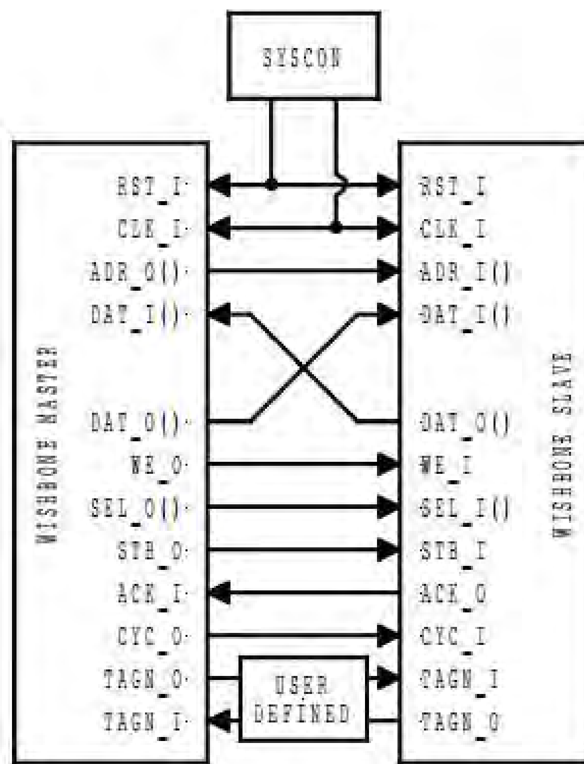

Figure 2.19: Wishbone bus basic connection [35]

2.13 CONCLUSIONS

This chapter reviewed SDR to provide a theoretical understanding needed before developing applications using RHINO platform. The reconfigurable computing was then highlighted in the context of SDR to show how it can be applied to achieve high performance computing capabilities. Thereafter, different reconfigurable computing devices such as GPP, ASIC and FPGA were studied and analysed in terms providing better performance when used in SDR applications. GPP is still popular because of its low cost, high flexibility and simplicity but at the cost of low performance. ASICs have very high performance capabilities but are very expensive. FPGA is therefore a reconfigurable device of choice in SDR because it is less costly and offers advanced computing capabilities with flexibility.

Due to increasing popularity of FPGAs, IP designers increasingly demand ready-made library of IP cores to integrate in SDR applications. Consequently, a concept of IP Reuse becomes very important and this was discussed in this chapter along with the latest trend of IP libraries. When investigating these IP libraries, it has been discovered that many of the robust and reliable IP cores are sold by commercial IP companies at high costs. There are also freely available IP cores offered by open-source communities, but these IP libraries lack support and documentation making it hard to use. The library of IP cores to be developed in this project will therefore build on strengths and weaknesses found in existing libraries studied in this chapter. The IP cores will be highly reusable, well documented, and completely free and will be available under open-source license.

Table 2.3: Signal description of Wishbone bus

Signal	Name	Description
RST_I	reset input	Global active high reset signal.
CLK_I	clock input	Global clock signal.
ADR_O/I	address output/input array	The address bus from master to slave.
DAT_I/O	Data input/output array	Data bus from slave to master.
DAT_O/I	Data output/input array	Data bus from master to slave.
WE_O/I	Write enable output/input	The write enable signal from master to slave. It is asserted by master during write operation and negated during read operation.
STB_O/I	strobe output/input	Indicates a valid data transfer cycle and it is asserted by the master.
ACK_I/O	acknowledge input/output	Indicates a normal termination of a bus cycle when set by a slave.
CYC_O/I	cycle output/input	Indicates a valid bus cycle is in progress when set by a master.

Furthermore, VHDL was introduced in this chapter because it is a hardware description language of choice that will be used to develop FPGA-synthesizable cores in this project. It is also a conventional language used in previous projects developed for RHINO. RHINO platform targets SDR domain applications namely Radio Astronomy, Radar and Telecommunications. These were briefly reviewed in this chapter to help identify IP cores for this project that will meet target application requirements.

As specified in Chapter 1, the IP cores in this project will be classified into DSP cores and I/O interface cores. The DSP cores will be based on DSP algorithms namely IIR, FIR, FFT/IFFT and DDC. The review of these algorithms was covered in this chapter and different techniques to implement them efficiently on the FPGA were covered. As a result, the proposed IP core library will use the same development techniques to achieve efficiency, high performance and reusability of the IP cores. Furthermore, a Wishbone bus was also discussed because it will be used as standard a interconnection bus for the DSP cores in this project. It is chosen because it has plenty of support by the Open-Cores community and it is completely open-source.

Additionally, the high speed FMC150 ADC/DAC daughter-card was reviewed. The interface controller for this will be developed to enable RHINO to perform ADC and DAC operations. Also the introduction to ADC dynamic parameters was discussed as they will be used later in this project to evaluate the performance characteristics of the FMC150 card. In order to ship high volumes of digital data from RHINO to external devices or a PC, the 1 Gigabit Ethernet interface core will be developed. Speed, technology and protocol used when developing Ethernet interface core for FPGAs were discussed in this chapter. Although 1 Gigabit Ethernet supports three speeds 10, 100 and 1000 Mbps, in this project only 1000 Mbps will be considered when developing the Ethernet interface core. UDP was found to be a commonly used Transport layer protocol in many FPGA platforms involving Ethernet interface. We will also use UDP to develop 1 Gigabit Ethernet interface for RHINO. We choose UDP because it incurs low latency and overhead which will be ideal for high speed streaming and real-time SDR applications. It

is also simple to implement hence this will save us plenty of time. However, it has a major drawback of unreliability due to lack of data flow control, this will be avoided by carefully choosing transmission rates tolerable by the receiver. The core will be developed with the aid of Open-Cores Tri-mode MAC core which was also discussed in this chapter. This MAC core is open-source and has continuous support.

CHAPTER 3

METHODOLOGY

This chapter starts off with details of the requirements analysis for the library of SDR IP blocks. It then goes on to discuss the design process and operational design for the proposed library. Thereafter, it describes both hardware and software tools that will be used in order to pave the way for the best development and testing environment. Then the final section overviews the experimental test for each of the designed IP blocks.

3.1 USER REQUIREMENTS FOR IP BLOCKS LIBRARY

The main purpose if this section is to provide a better understanding of the user requirements regarding the proposed library of IP cores. These requirements were studied from intensive literature conducted [10][25][29][71][100], in particular the requirements which are common in SDR applications such as Telecommunications, Radar and Radio Astronomy. The user requirements are divided into functional requirements and non-functional requirements of the SDR blocks.

3.1.1 Functional Requirements

The functional requirements describe behaviour expected of IP blocks or cores to be designed and implemented. The functional requirements are outlined as follows:

- The SDR blocks will perform DSP operations common in SDR applications and provide interface to connect the FPGA to external devices through high speed I/O communication ports or adapters.
- The blocks will be capable of capturing digitized data from the ADC card and sending out the digital data using DAC card.
- The blocks will be able to operate in a streaming mode where the ADC data will be captured and be shipped off the FPGA via 1 Gigabit Ethernet using UDP at high throughput speed typically used in SDR applications.
- The cores will not depend on a specific high level CAD tool.

- Each core will provide a simple parallel interface to enable high speed interconnection with other cores.
- The blocks will possess a hardwired control for failure protection.
- Apart from 100MHz clock provided by the system, the SDR blocks will reliably operate in the clock frequency range of 312.5kHz to 375MHz.

The above functional requirements will ensure that the IP blocks are developed in accordance with the project objectives as outlined in section 1.4.

3.1.2 Non-Functional Requirements

The non-functional requirements describe the metrics and constraints to measure the success of the developed SDR blocks. These non-functional requirements are outlined as below:

- The library of IP blocks will be publicly accessible under open source license.
- The blocks will be reusable and parameterizable for integration in many SDR applications.
- The blocks will be easily upgradable, scalable and portable.
- For parallel and cascaded IP core architectures, replication of sub-blocks will be applied.
- The system clock or cycle time will be adjustable to a working environment.
- The Wishbone slave interface for each DSP core will be defined; however, no tests will be made in a real SoC design environment.

These non-functional requirements are necessary for user to evaluate the degree to which the objectives outlined in section 1.4 have been met.

3.2 Domain Requirements

In order to ensure that all the SDR blocks conform to the same standards and consistent general functionality, the domain requirements describe the rules and actions needed when developing the blocks. Domain requirements are outlined below:

- Each IP block and relating sub-blocks will be completed with a synthesizable source code in VHDL.
- The IP block will be self-contained, that is, external dependencies such as elements, design units and packages will be avoided.

- General functionality of each core will be technology independent, using VHDL code. However, the exception is in technology specific applications such as Xilinx spartan6 where adhoc HDL primitives and libraries are used for management and routing of clock and external I/O pins.
- Each core will have a testbench showing the tests passed and will be accompanied by MATLAB scripts that generate input vectors for the core in the testbench. The scripts will also create an ideal model for a core under test, therefore the ideal model results will be compared with testbench results.
- Clock and reset signal will contain no combinational logic.
- Each DSP core will have *en* and *vld* pins. The *en* port will be used to enable or disable a global system clock while *vld* port will signal the availability of valid output sample from the core.
- Bidirectional ports will not be used. Both input and output ports will be separate.

3.3 DESIGN PROCESS

The high level design process for RHINO IP blocks is detailed in section 1.5 and illustrated in Figure 1.2. In this project, the behavioral model of the blocks will be designed in Xilinx ISE and this fits in "develop behavioral model" block of the design process shown in Figure 1.2. It is therefore important to understand the ISE design flow of the IP cores in the context of development for RHINO and this is illustrated in Figure 3.1. This comprises a number of steps which are: design entry, functional verification, design synthesis, design implementation, and Xilinx device programming [101].

Design entry involves creating a new project using the ISE and adding timing constraints, pin assignments, and area constraints of the IP block being designed.

Functional verification entails verification of the design at different points of the ISE design flow. The first verification occurs before synthesis and is called behavioral simulation (also known as RTL simulation) as shown Figure 3.1. A second verification uses SIMPRIM library, it takes place after translation and it is called functional simulation (also known as gate-level simulation). The last verification is in-circuit verification which happens after device programming.

Design synthesis converts HDL design to a flat netlist which describes the connection of logic gates which make the system.

Design Implementation undergoes translate, map, place and route processes.

Timing Verification is performed by running static timing and timing simulation.

Xilinx Device Programming involves creating a bitstream file and converting it to ".bof" file executable in BORPH operating sytem (OS). The ".bof" file is run like a normal linux C application as software process in BORPH operating system.

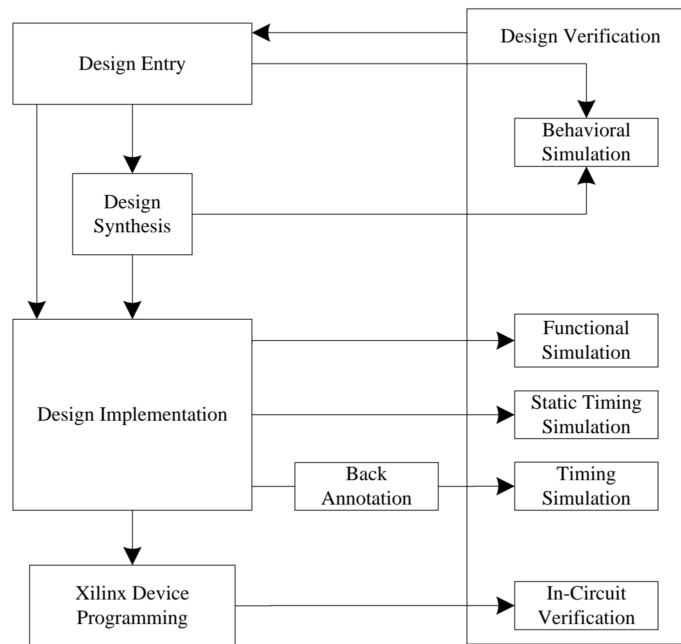

Figure 3.1: FPGA Design Flow using Xilinx ISE [101]

3.4 Operational Design

The overall system architecture of RHINO SDR processing blocks is shown in Figure 3.2. All the blocks will be designed in VHDL and run on the spartan6-XC6SLX150T FPGA device of RHINO board. The reason for using VHDL to describe the logic of SDR blocks is because it is a standard HDL language for RHINO gateware projects. Furthermore, previous FPGA projects for RHINO have been developed in VHDL.

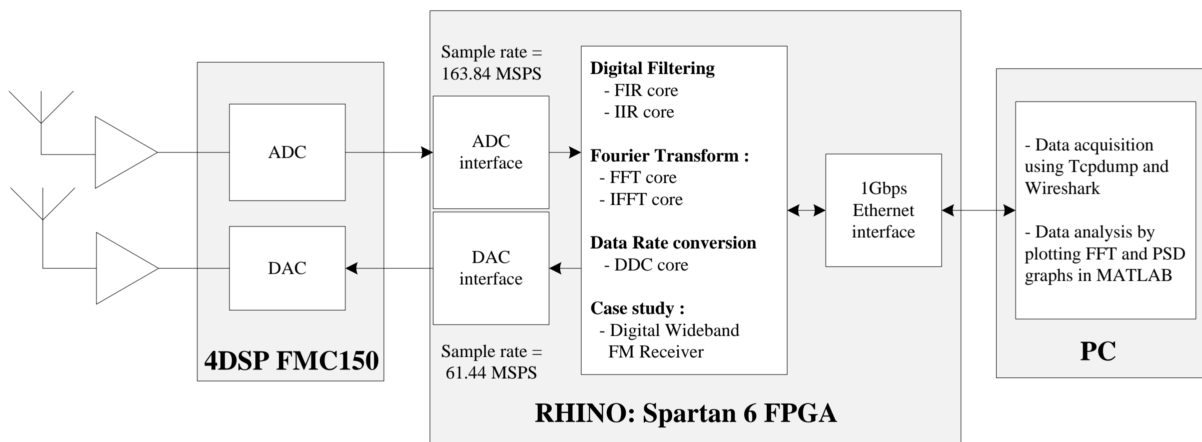

Figure 3.2: Architecture of RHINO SDR processing blocks

The design of IP cores will be categorized into two, namely DSP and I/O processing blocks or cores. The flow chart showing design process for each IP core is illustrated in Figure 3.3. The functionality and performance of the building library of SDR blocks will be exemplified

by designing a prototype of a digital wideband FM receiver which will be built from developed SDR blocks. The IP blocks are shown in Figure 3.2 and are briefly described below:

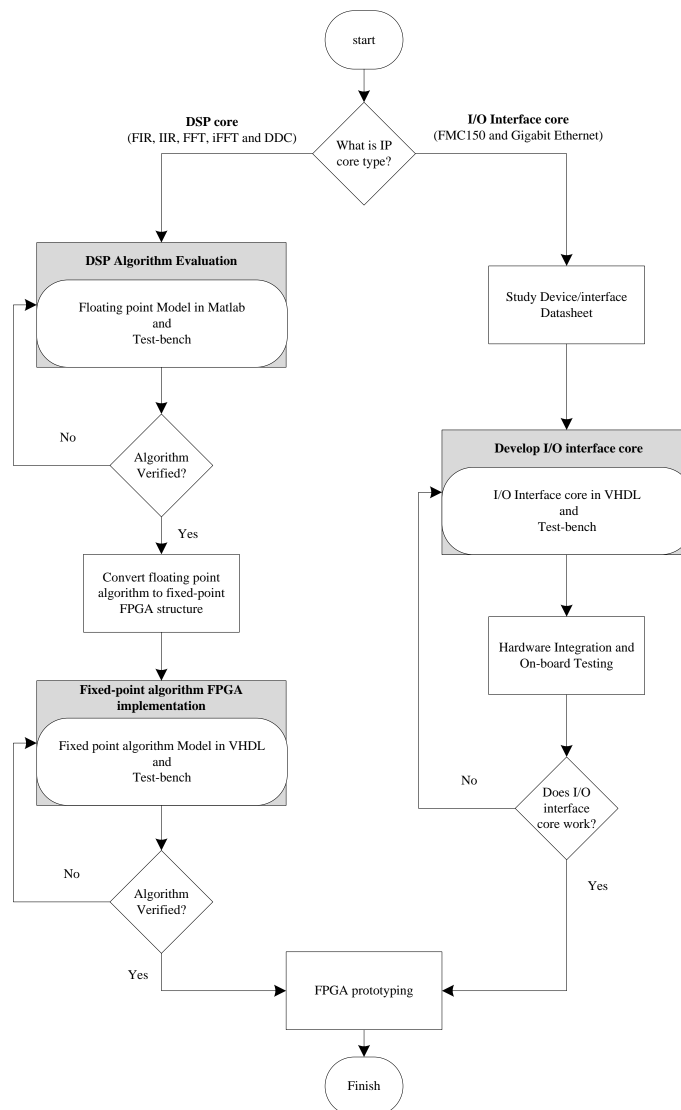

Figure 3.3: IP core design process

3.4.1 DSP blocks

By employing common DSP algorithms used in many areas of SDR, the DSP cores were chosen and classified as below:

3.4.1.1 Digital Filtering

The digital filtering cores to be developed are used in many SDR applications if not all. With support of multiple realizable structures of filters on the FPGA, the cores offer flexibility and broad choice of filter solutions for different design environments. The filter cores to be designed in this project are listed below:

- **FIR core** implements the FIR filter on the FPGA. It is chosen because it can achieve the exact linear response with unconditional stability [16], hence it is the most popular digital building block in SDR. It also forms the most computationally intensive part of the SDR namely the channelizer or IF (Intermediate Frequency) processing block.

- **IIR core** implements the IIR filter on the FPGA. It is chosen because it can achieve the same magnitude response of an FIR filter using lower order design [16]. Thus it can be the best alternative in SDR applications where resources are insufficient and fewer computations are needed.

*3.4.1.2 **Fourier Transform***

The Fast Fourier Transform is another fundamental building block of SDR-based DSP systems. Although the algorithm analysis may seem straight-forward, implementing this efficiently on the FPGA can be challenging. The architecture which comprises parallel and pipeline characteristics is realized using both Fast Fourier Transform and Inverse Fast Fourier Transform algorithms. The core is described below:

- **FFT/IFFT core** is implemented using FFT and IFFT algorithm on the FPGA. This core will be designed because it is popularly used in SDR applications such OFDM, Radar, multimedia and efficient channelizer implementations.

*3.4.1.3 **Channelization***

Channelization is made up of channellizer and it is typically the most computationally intensive [98] part of the SDR receiver as it performs IF processing at highest sampling rate. A digital down converter algorithm is often used to build a channelizer and in this project the core below will be designed.

- **DDC core** will perform data rate conversion and frequency downshifting using a digital down converter algorithm.

3.4.2 **I/O blocks**

The I/O cores are responsible for input and output data communication between the FPGA and peripheral or external devices. The I/O cores to be developed are listed below:

- 1 Gigabit Ethernet core

- ADC-DAC interface core

3.4.3 **Digital Wideband FM receiver**

The application will be designed to demonstrate that not only developed SDR blocks will be used in the FM receiver, but also in other real time SDR applications. It does so by using the developed library of blocks that include the ADC core, DDC core and 1 Gigabit Ethernet core. The I/Q FM demodulator will be implemented in Matlab on the PC and will acquire input from FM samples streamed from the FPGA via 1 Gigabit Ethernet.

3.5 EXPERIMENTAL ENVIRONMENT

The experimental development process will follow the flowchart in Figure 3.4. First the fixed point model test will be performed in Matlab as an ideal reference before performing each DSP core test. The DDC core test depends on the FIR core test. After testing all DSP cores, the process continues to 1 Gigabit Ethernet Interface core and later the FMC150 interface core. This is followed by a streaming core which depends on the results obtained from 1 Gigabit Ethernet and FMC150 interface cores. The DDC core, 1 Gigabit Ethernet and FMC150 interface cores need to be tested before performing the last cumulative experiment of the FM receiver.

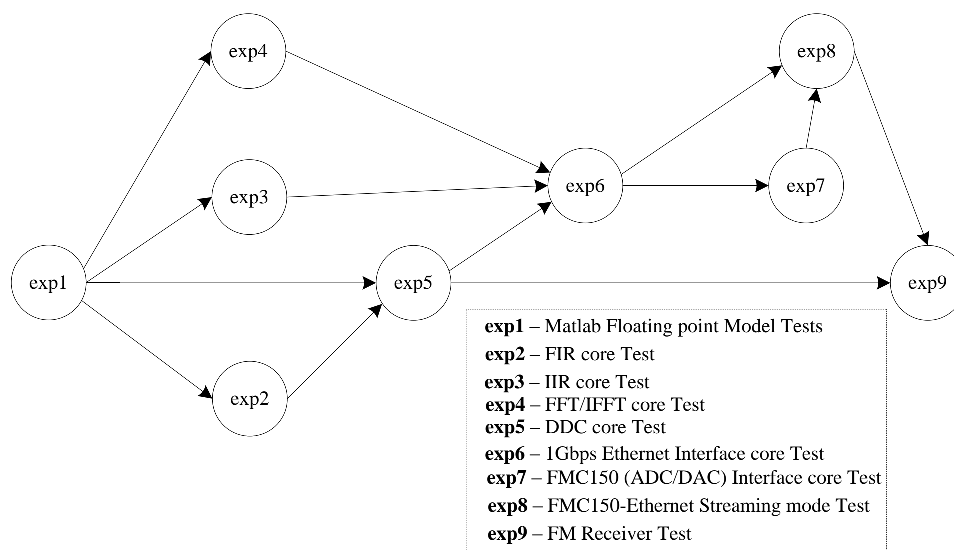

Figure 3.4: A flowchart showing experimental development process

A considerable number of hardware and software tools will be used to aid with the development and setting up of the experimental environment. The hardware tools include a Desktop PC, RHINO board, oscilloscope, function generator, spectrum analyzer and xilinx platform cable. The software tools are Xilinx ISE 14.7, ISim, ChipScope Pro, Tcmpdump, Wireshark, Matlab, ADCPro and Speedometer. All these hardware and software tools are further elaborated below.

3.5.1 **Hardware**

This section lists the hardware tools and their specifications below:

- **Desktop Computer:** A high performance machine is required for FPGA-based develop-

ment work and to run memory demanding as well as processor intensive software applications listed in section 3.5.2. The features of the PC include:

- **Operating System:** 32-bit Ubuntu 14.10
- **Memory:** 8 GiB
- **Processor:** Intel® Core™ i7-4790 CPU @ 3.60GHz $\times$ 8
- **Disk:** 976.1 GB
- **Network Adapter:** 1Gbps speed, supports 100Base-T and 1000Base-T

• **RHINO FPGA Platform:** This is an FPGA-based SDR development board that will be used to perform experimental tests and evaluate performance of SDR blocks and FM receiver prototype. Below is the list of some key features:

- **Operating System:** BORPH
- **FPGA:** Xilinx Spartan6-XC6SLX150T
- **Arm Processor:** Texas Instrument Sitara AM3517

• **Agilent DS03102A Oscilloscope:** This instrument will be used to visualize and analyze DAC output signals as well as measuring the signal amplitude versus time. The specifications are listed below:

- **Bandwidth:** 100 MHz
- **Memory Depth:** 4kpts
- **Sample Rate:** 1 Gsa/s

• **Agilent 33220A 20MHz Function/Arbitrary Waveform Generator:** It will be used to generate sine waves needed to test the ADC of the FMC150 card. Its features are listed below:

- 20 MHz Sine and Square waveforms
- Pulse, Ramp, Triangle, Noise, and DC waveforms
- 14-bit, 50 MSa/s, 64 k-point arbitrary waveforms
- AM, FM, PM, FSK, and PWM modulation types
- Linear and logarithmic sweeps and burst operation
- 10 mV_{pp} to 10 V_{pp} amplitude range

• **HP8591A Spectrum Analyzer:** This will be used to visualize and measure magnitude of signals versus frequency. The spectral analysis of DAC signals will provide more information about the characteristics of the signal. Below is the list of Spectrum analyzer specifications:

- **Frequency Range:** 9kHz - 1.8GHs (50Ω), 1MHz - 1.8GHz (70Ω)
- **Amplitude Range:** -115dBm to +30dBm (50Ω), -63dBmV to +75dBmV (70Ω)

- **RF analyzer:** will also be used for spectrum analysis and screenshot capturing of measured signals. It specifications are as follows:
  - **Frequency Range:** 5 kHz to 4/6 GHz.
  - **Directivity:** $>$ 42 dB
  - **CAT:** Distance-to-fault, return loss, cable loss
  - **VNA:** S11 mag and phase, S21 mag, time doman with gating
- **E3620A 50W Dual Output Power Supply:** will be used to provide power source for analog RF front-end. Its features are as follows:
  - **Output 1:** 0 to 25 V, 0 to 1 A
  - **Output 2:** 0 to 25 V, 0 to 1 A
  - **Power (max):** 50 W
- **Xilinx Platform Cable USB II:** The Platform Cable USB II provides integrated firmware to deliver high-performance, reliable and user-friendly configuration and programming of Xilinx FPGAs. It is used in this project for programming of Spartan6-XC6SLX150T. It works together with ChipScope Pro Analyzer to perform debugging of Spartan6-XC6SLX150T input and output signals.

3.5.2 Software Tools

In order to carry out development, simulation, experiment, testing and verification, the following software tools are installed on Linux environment except Matlab 2011.

- **Xilinx ISE 14.7:** Xilinx ISE will be used for FPGA design as it offers HDL synthesis and simulation, implementation, device fitting, and JTAG programming.
- **ISim:** This is integrated within Xilinx ISE to provide HDL simulation feature.
- **ChipScope Pro:** It is used along with Xilinx Platform Cable USB II to monitor and visualize the FPGA chip I/O signals.
- **Tcpdump:** This is a Linux command line that will be used to quickly and efficiently capture packets received by the 1Gbps Network Card.
- **Wireshark:** Wireshark will be used to visualize and analyze packets saved using Tcpdump and also monitor outgoing network traffic on 1 Gbps Network Card.
- **Netbeans 8.0.2:** This tool will be used to compile and run Java routines that will parse hexadecimal UDP frames into a vector of integer or decimal data samples sent by the FPGA.
- **Matlab 2011:** Matlab will be used for creating an ideal model for DSP cores to be designed, generate input data for DSP cores before simulation and also to graph the results obtained during experiments.

- **ADCPro:** This will be used to plot the FFT of ADC data as well as measuring dynamic parameters [44] of the ADC data. The data will be read from saved ADC data files captured using UDP stream on RHINO.
- **Speedometer:** In addition to Wireshark, this is a Linux command line tool that will be used to measure speed of incoming and outgoing traffic on 1Gbps Network Card.

3.6 Experiments

This section provides an overview of how the experiments will be performed. When testing one experiment, the results motivate that the next experiment is ready to be tested as shown in Figure 3.4. This progress establishes incremental outcomes which show progressively more insight into the robustness of operational performance of the IP blocks. In order to validate the expected correctness of the developed library of IP cores, the following experiments will be conducted.

3.6.1 Testing DSP cores

Each DSP core will be tested from input data generated from Matlab. The testbench containing a DSP core under test will then import the data where it is stored in the file. After the core has processed the data, the results will be stored in an output file as a vector of decimal samples. Matlab scripts will later be used to plot graphs and perform further signal processing of the results for analysis. The setup of the experiment to test the DSP core is shown in Figure 3.5.

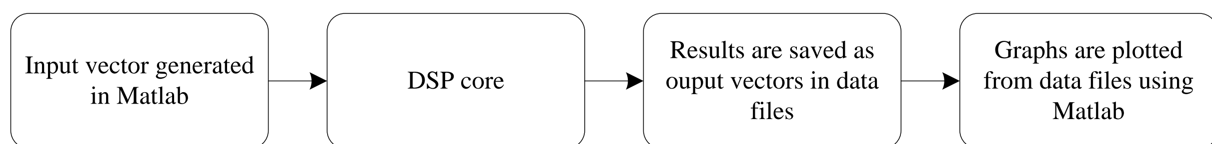

Figure 3.5: Experimental setup for the DSP cores

3.6.2 Testing 1Gbps Ethernet interface core

A 1Gbps Ethernet interface will be tested by establishing a point-to-point connection between a PC and FPGA. Both devices need to be configured with appropriate network parameters. Since the FPGA Ethernet speed is 1Gbps, it will be very important to ensure that the PC's network card also supports 1Gbps network speed. Cat5/e UTP cable will be enough to create a physical connection between PC network card and 1Gbit Ethernet interface of the FPGA. The data will then be sent from the FPGA to the PC and vice versa. The experimental setup is illustrated in Figure 3.6.

3.6.3 Testing ADC

The ADC of the FMC150 card is to be tested as shown in Figure 3.7. The test pattern generator of the ADC could be used to test the functionality of the ADC; however, this is not enough to verify that the ADC samples properly and that timing requirements are correctly met. The

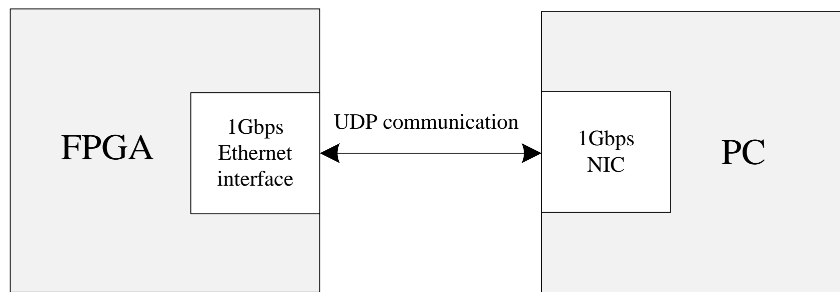

Figure 3.6: Experimental setup for 1 Gigabit ethernet core

function waveform generator is therefore used to feed sine wave of different frequencies into the analog input of the ADC. The digitized data by the ADC is captured inside FPGA and visualized using ChipScope Pro. ChipScope Pro plots amplitude versus time of the ADC data; this does not provide all the information needed to ensure full functionality when noise characteristics are considered. For this reason, data will be captured on the PC using UDP and sophisticated plots will be made as it will be demonstrated in later sections.

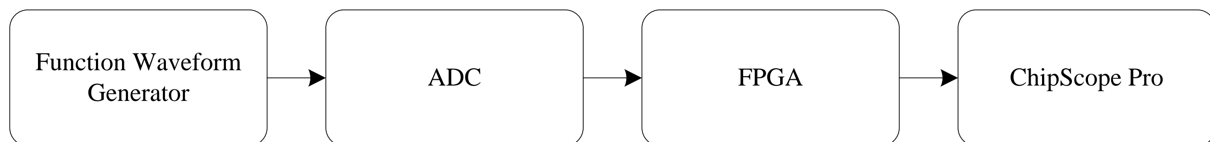

Figure 3.7: A block diagram showing experimental setup for ADC interface core

3.6.4 Testing DAC

The experimental setup for DAC is illustrated in Figure 3.8. The DAC will be tested by generating sine waves of different frequencies using NCO core inside the fpga. The FPGA will send digital samples generated by the NCO to a DAC, then the oscilloscope and spectrum analyzer will be used to visualize signal in time and frequency domain respectively.

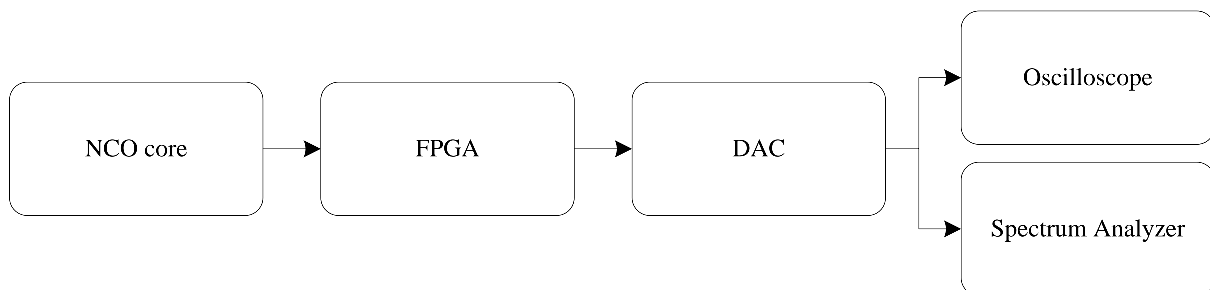

Figure 3.8: A block diagram showing experimental setup for DAC interface core

3.6.5 Testing a Streaming Core

The streaming core comprises both the ADC and Gigabit Ethernet cores. Data source is a function waveform generator which connects to analog input of the ADC. Inside the FPGA,

the digitized waveform from the ADC is relayed directly to a 1 Gigabit Ethernet core which sends ADC data to a PC in a form of UDP packets. The setup of the experiment is depicted in Figure 3.9.

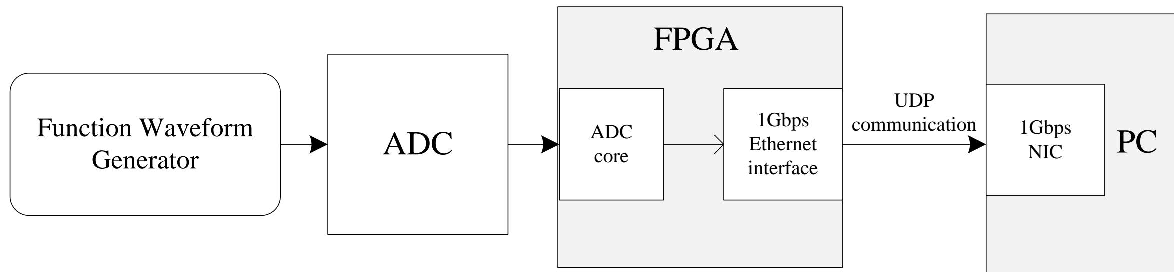

Figure 3.9: Experimental setup for a Streaming core using ADC and 1 Gigabit Ethernet interface cores

3.6.6 Testing a Digital Wideband FM Receiver

The digital FM receiver will be built and tested in VHDL simulation. Another comprehensive test will be performed on the actual hardware using the experimental setup illustrated in Figure 3.10. The aim of this experiment is to demonstrate that the developed library of SDR blocks can function according to defined specifications not only in this application, but also in other SDR domain specific applications. The FM receiver will incorporate the ADC core, DDC core, and 1 Gigabit interface core all in FPGA and arctan/differentiator FM demodulator in MATLAB running on a PC.

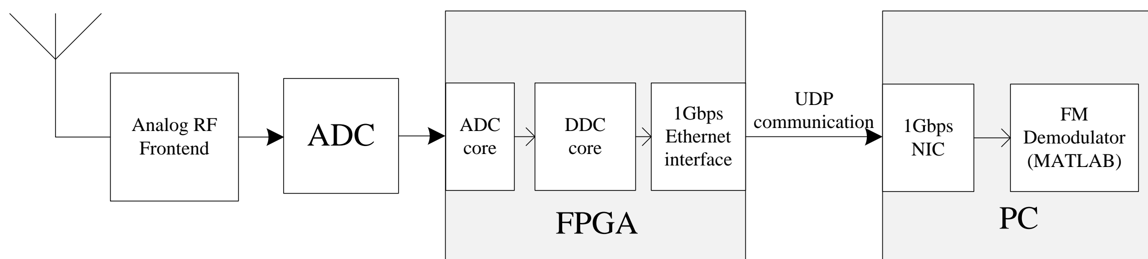

Figure 3.10: Experimental setup for a digital wideband FM receiver

CHAPTER 4

DESIGN OF SDR DSP BLOCKS

In this chapter the library of FPGA-based DSP blocks is designed. The blocks can also be referred to as the cores. Where the core or block is a standalone FPGA entity with inputs and outputs. It is synchronized and controlled by a clock and reset respectively. In order to connect a core to a standard communication bus, a bus interface functionality is required [18]. The combination of a core and the bus interface added to it is IP core as illustrated in Figure 4.1.

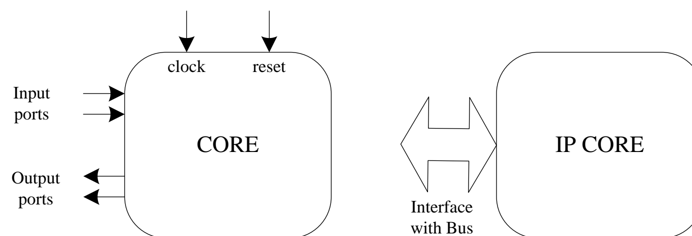

Figure 4.1: A block diagram differentiating a Core and IP Core

The designed library of DSP IP cores encompasses the FIR IP core, IIR IP core, FFT/IFFT IP core and DDC IP core. Each core has a description of a Wishbone interface to show how it can be attached to Wishbone bus in a SoC design. The goals of implementing these IP cores are to reduce complexity, increase design reuse, simplify effort of integration and ensure accurate communication and timing needs.

Figure 4.2 illustrates a general high level architecture of each IP core. It consists of a wishbone connection and a high-speed I/O connection. The wishbone control logic manages read-write operations of the slave registers while the FIFO memory stores incoming input data and outgoing processed data.

The FIR IP core will be designed first, then an IIR IP Core, followed by FFT/IFFT IP Core and lastly DDC IP Core.

4.1 FIR IP CORE

This section presents the design of FIR IP core. The FIR IP core is the FPGA implementation of FIR filter described in section 2.7.1.1. The design of the filter enables modularity and scalability

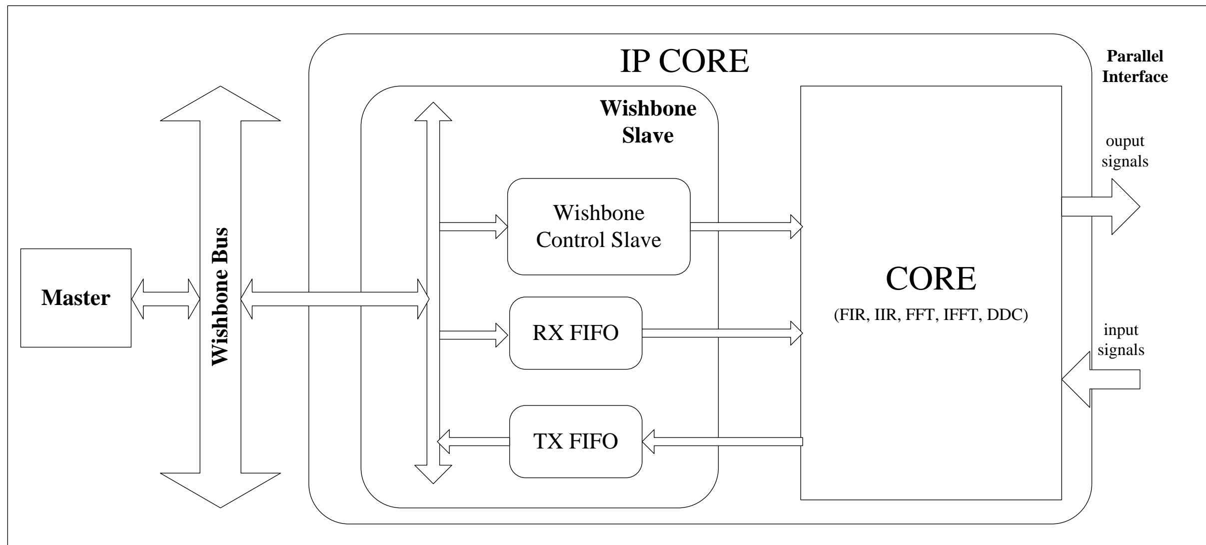

Figure 4.2: An overall architecture of a DSP IP Core

of SDR applications with assurance of maximum attainable clock speed. With support of five different FIR structures, the user has wide range of choice to synthesize efficient FIR filter that meets the design on hand. The top level block diagram of the FIR IP core is depicted in Figure 4.3.

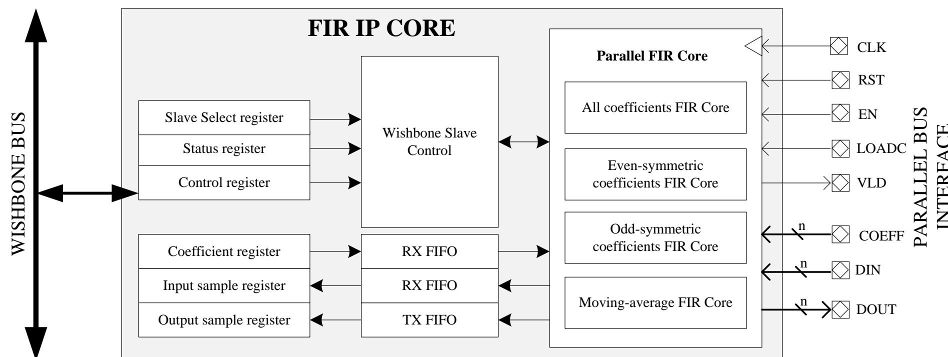

Figure 4.3: Architecture of FIR IP Core

4.1.1 **Filter Structure**

The proposed FIR core realizes a number of structures as shown in Figure 4.4. These structures include transposed parallel FIR structure, averaging FIR filter and two optimized realizations namely even and odd symmetric parallel FIR filters [11][61]. Parallel FIR architectures are designed around low-order, high performance applications while optimized architectures are to be used in high-order, applications and where resources are limited.

The FIR core operation depends mainly on the structure chosen by the designer and the diagram that summarizes the operational flow based on the selected FIR structure is shown in Figure 4.5.

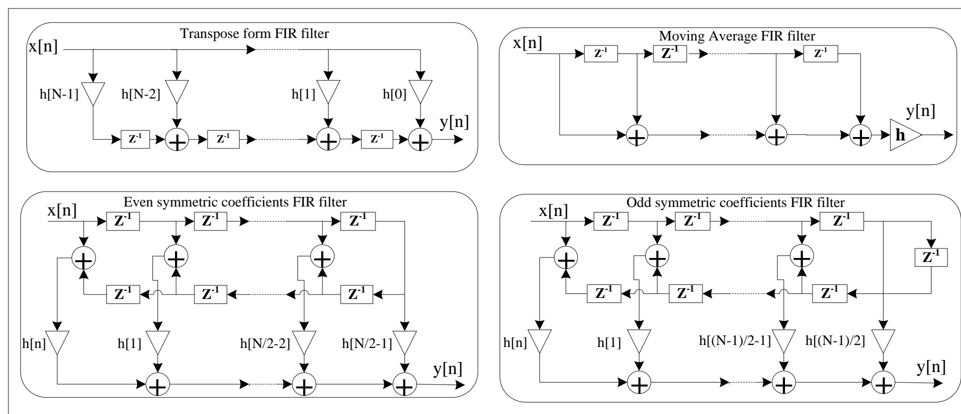

Figure 4.4: Parallel FIR structures

Except for a moving FIR filter, the other filter structures use coefficients stored in the ROM or rather load coefficients from external source. It is the user choice to decide whether to use ROM coefficients or the externally load them. The FIR core does not begin filtering process until the coefficients loading is finished. If internal coefficients are used, filtering occurs immediately without waiting for loading to happen.

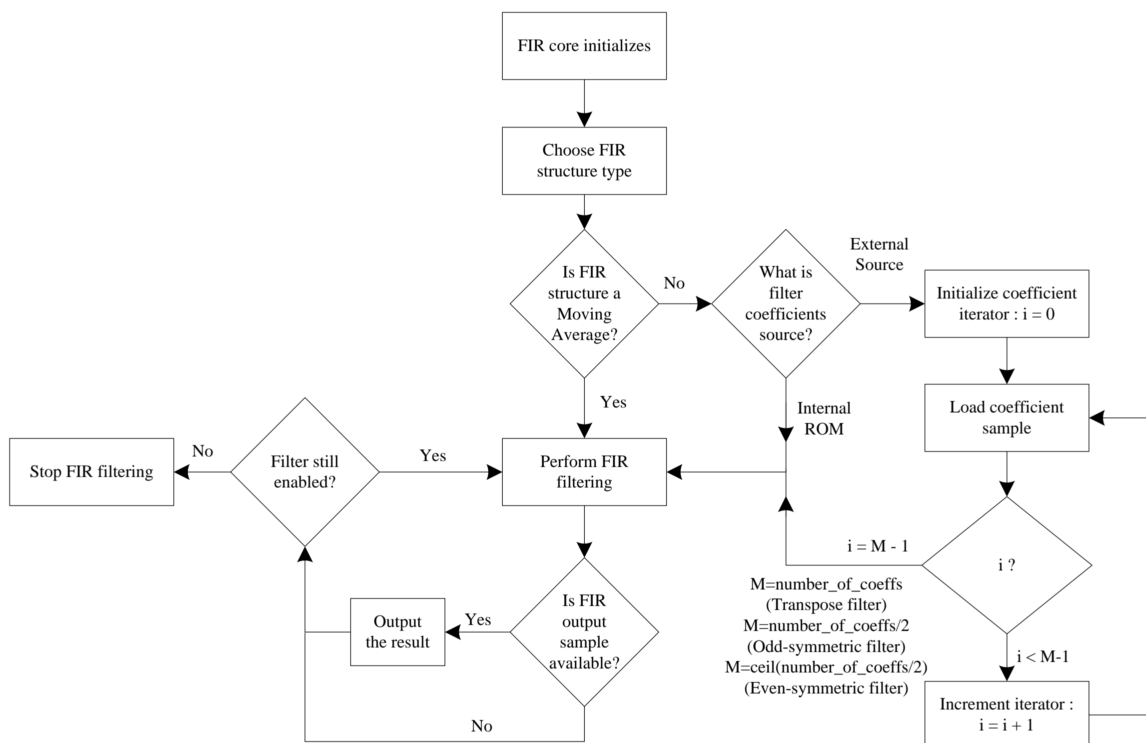

Figure 4.5: FIR core data flow diagram

4.1.2 **Filter Coefficients Generation**

The FIR core uses fixed point arithmetic to represent data. Using the windowing and iterative methods discussed in section 2.7.1.1, the coefficients of FIR core are created. However, the

resulting coefficients are fractional and some values are negative in nature. To represent these values in a format that will be used in FPGA, quantization or scaling of coefficients to n-bits by two's complement factor is applied. For example, 0.125 multiplied by 10 gives 1.25. The calculation in fixed point notation using 8 bits precision is performed by first converting 0.125 to binary 0.001. Then 0.001 in binary is shifted 7 bits to the left resulting in 10000 binary hence preserving the 8th bit to represent sign in two's complement binary. The value 10000 in binary is multiplied by 10 and gives 10100000 in binary. The product 10100000 is in turn shifted 7 bit positions to the right yielding 1.0100000 in binary which corresponds to 1.25 in decimal format.

Furthermore, the FIR core allows the coefficients to be stored initially as fixed values in a ROM or can be loaded dynamically before the FIR core is started. The word length of the coefficients can be configured by the user depending on the requirements of the application. Alternatively, default 16-bit wide coefficients can be used.

4.1.3 Parameters and Ports

The designed FIR core is equipped with generic parameters described in Table 4.1. These parameters are configured by the user for the core to meet application specific needs. These include word length of input data, output data and filter coefficient. The size of filter coefficients is also specified by the user. Other parameters are the structure of FIR implementation and the filter coefficients whose source is defined by the user. That is, whether they are stored in internal ROM or be loaded externally. Furthermore, the FIR core also provides high speed parallel interface with ports described in Table 4.2.

Table 4.1: FIR core parameters

Generic name	Description	Type	Valid range
DIN_WIDTH	Width of data input	Unsigned integer	$\geqslant 8$
DOUT_WIDTH	Width of data output	Unsigned integer	$\geqslant 8$
COEFF_WIDTH	Width of coefficients	Unsigned integer	$\geqslant 8$
NUMBER_OF_TAPS	Number filter taps	Unsigned integer	$\geqslant 2$
LATENCY	FIR latency or structure	Unsigned integer	0=transpose 1=Odd symmetric 2=Even symmetric 3=Moving Average
COEFFS	Filter coefficients	array of integers	Array size = taps size

4.1.4 Timing Constraints

Figure 4.6 provides a timing waveform of the FIR core and shows how it connects to other using high speed parallel interface. The *en* drives the core when it is set high. *Loadc* enables loading of FIR coefficients which are input into a core using *coeff[COEFF_WIDTH-1:0]* bus. Alternatively, the FIR coefficients can be stored in a ROM as constants and these are initialized when the FIR core starts. When *loadc* goes low, the input samples are fed into core using *din[DIN_WIDTH-1:0]* bus. The valid filter output samples are read on *dout[DOUT_WIDTH-1:0]* bus when *valid* signal is asserted.

Table 4.2: FIR core ports

Pin name	I/O	Description	Active state
clk	in	System Clock	Rising edge
rst	in	System reset	high
en	in	Clock enable	high
loadc	in	Load coefficient enable	high
coeff[COEFF_WIDTH-1:0]	in	coefficient input sample	data
vld	out	Valid output data available	high
din[DIN_WIDTH-1:0]	in	Filter input sample	data
dout[DOUT_WIDTH-1:0]	out	Filter output sample	data

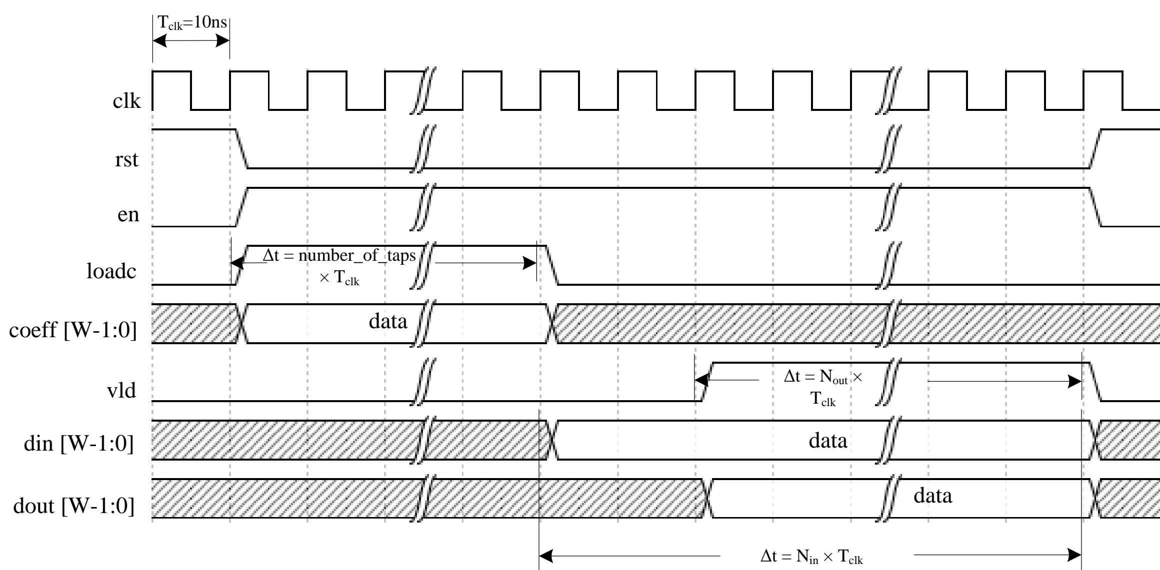

Figure 4.6: FIR core input/output timing waveform

4.1.5 Wishbone Interface

Figure 4.7 shows the FIR core connected to a Wishbone slave to enable SoC integration. The Wishbone interface is composed of high speed parallel ports and wishbone ports. Wishbone ports are described in section 2.12 and the *clk*, *rst* and *en* ports work the same way as described in Table 4.2. The ouput ports of the FIR slave provide the FIR core with the input data so that the FIR core can perform FIR filtering. These include slave *dout[15:0]* port which sends FIR input data to a *din[15:0]* port of the FIR core. Coefficient sample is sent to the FIR core input using the signal connecting *coeff[15:0]* ports on both the FIR slave and FIR core. This only takes place when the FIR core is configured to use external coefficients. Setting slave *start*/*en* signal initiates FIR core filtering process.

The structure in Figure 4.7 also consists of feedback signals from the FIR core to the FIR slave interface core. Using *dout[31:0]* port which connects to *din[31:0]* port of a slave, the FIR core sends filtered data to slave interface. This happens each time when the *vld*/*en* signal is asserted.

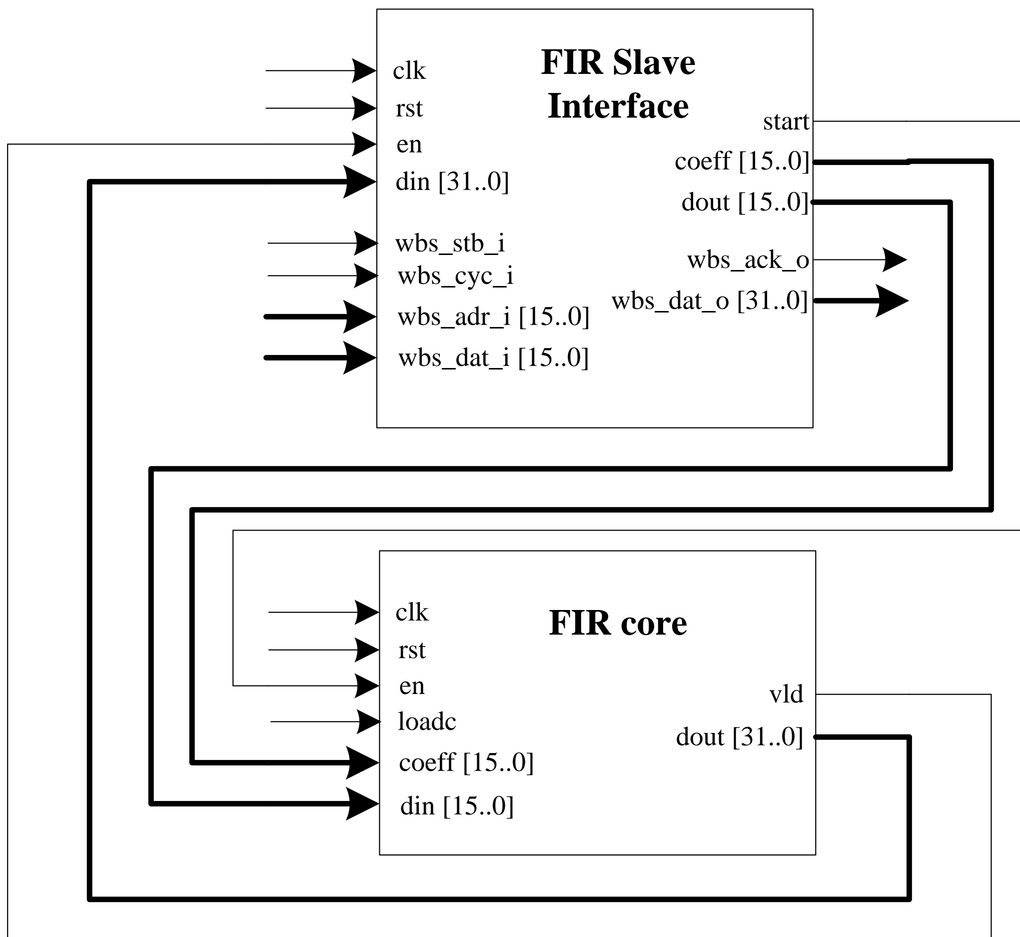

Figure 4.7: FIR core and Wishbone slave interface

Furthermore, the register description of Wishbone interface is shown in Table 4.3. The FIR IP core in the SoC design is uniquely identified by read-only *slave_select* register. To start the filtering processing, the write-only *control* register is set. A *status* register is read-only register which set high to signal the end of filtering process and a *coefficient* register is a write-only register which stores a 16-bit coefficient sample to be loaded into FIR core prior to filtering process. Lastly, the *input_sample* is a write-only 16-bit register that holds the next data sample to be filtered while *output_sample* is a read-only register that holds a filtered 32-bit data sample.

Table 4.3: Wishbone slave registers for FIR core

Register	Address	Register Value Bits
slave_select	0x0000	16
status	0x0001	1
control	0x0002	1
coefficient	0x0003	16
input_sample	0x0004	16
output_sample	0x0005	32

4.1.6 **FIR Core Test**

The FIR core test only involves high speed parallel interface in section 7.1. Although it has been briefly described how the core can use Wishbone bus interface to connect to SoC bus, it is not tested in this work.

4.2 IIR IP CORE

This section outlines the design of IIR IP core that implements IIR filter on the FPGA and details on how the IIR filter works are discussed in section 2.7.1.2. The core is built from a basic structure of a 2nd order IIR filter also known as biquad of Direct Form I [11] as illustrated in Figure 4.9. IIR core allows cascading of the biquads to build higher order IIR filters without experiencing coefficient-sensitivity problems. This IIR structure with a cascade of biquads is called second-order sections and its transfer function $H(z)$ is defined by equation 4.1. The block diagram of IIR core designed in this dissertation is shown in Figure 4.8.

$$H(z) = \prod_{i=1}^{N} H_i(z) = \prod_{i=1}^{N} \frac{b_{i0} + b_{i1}z^{-1} + b_{i2}z^{-2}}{1 + a_{i1}z^{-1} + a_{i2}z^{-2}} \tag{4.1}$$

where $i = 1, ..., N$, N is the number of second-order sections and a_i, b_i are filter coefficients.

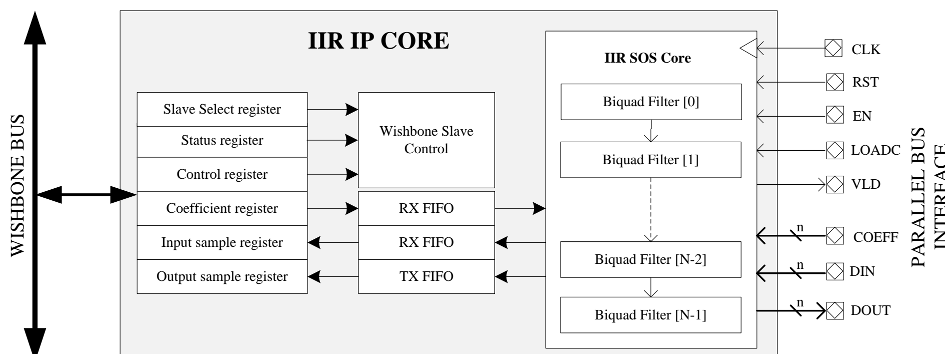

Figure 4.8: Architecture of IIR IP Core

4.2.1 **Filter Coefficients Generation**

Filter coefficients are defined as signed fixed point two's compliment arithmetic. The coefficients are generated using classic IIR filters as described in section 2.7.1.2. The generated coefficients are typically fractional and negative therefore they are quantized to n-bit precision suitable for implementation on the FPGA. However, due to recursive nature of IIR, implementation of IIR core on the FPGA is highly prone to overflows [2]. This condition is not ideal as it results in misinformation of IIR filtered data. Different techniques [2] can be used to scale the coefficients and thereafter the quantization can be applied before FPGA implementation as demonstrated in section 4.1.2. In this work, we only use one technique namely Chebychev Norm. This will ensure the IIR core never experiences the overflow by constraining the result at each node of the second-order sections structure to be less than 1.

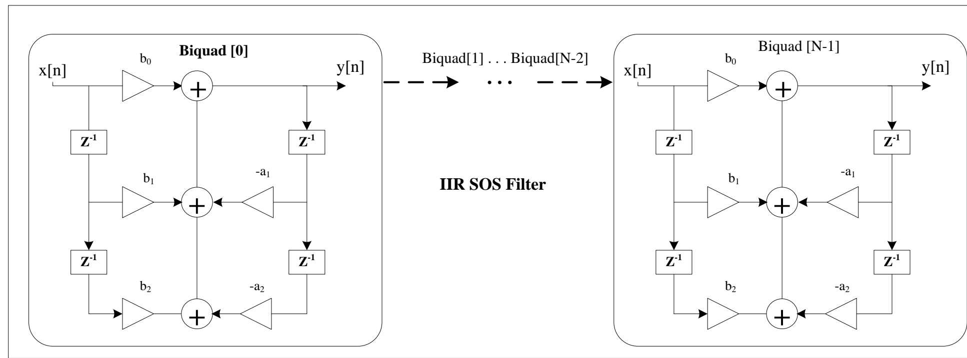

Figure 4.9: Cascaded Direct Form I Biquad IIR filter

Furthermore, a Matlab script that can be used to quickly and easily scale the IIR filter coefficients is found in Appendix C.2. It uses Chebychev Norm (Infinity-Norm) $l_\infty = \max_{\omega} |G(\omega)|$, where $G(w)$ is unscaled filter frequency response. The scaling procedure used in this design is described in [2, 86]. This is based on estimation of scaling factors $s_i = 1/l_{i\infty}$ which provide maximum amplitudes in biquad stages y_i but prevent the output adders from overflow at i^{th} stage of second-order sections structure. The cascaded frequency reponses $G_{0i}(z)$ have to be

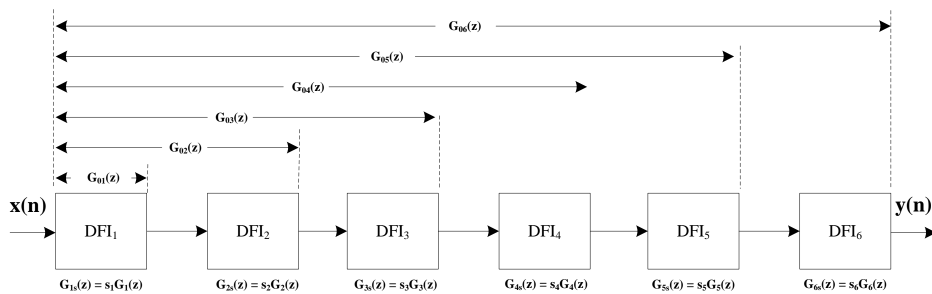

Figure 4.10: Six Cascaded second-order sections (DFI=Direct Form I)

regarded because separate scaling of $G_i(z)$ will cause decreasing magnitudes from one second-order section stage to the next [86]. The example below shows how scaling is performed for six cascaded second-order sections of direct form I illustrated in Figure 4.10.

- The scaled frequency response at i^{th} stage is
  $G_{is}(z) = s_i G_i(z)$

- Scale factor s_i ensures that the overall gain of the filter from input $x[n]$ to output y_i is unity to avoid overflow.

- Notation: to find infinity-norm for some transfer function $G(z)$, we use
  l-norm of $G_i(z) = \max_{\omega} |G(\omega)| = l_\infty(G_i(z)) = l_{G_i}$

- Calculate the Chebychev Norm of cascaded frequency response:

$$
\begin{aligned}
l_{G_{01}} &= l_\infty(G_{01}(z)) = l_\infty(G_1) \\
l_{G_{02}} &= l_\infty(G_{02}(z)) = l_\infty(s_1 G_1(z) G_2(z)) = s_1 l_\infty(G_1 G_2(z)) \\
l_{G_{03}} &= l_\infty(G_{03}(z)) = l_\infty(s_1 s_2 G_1(z) G_2(z) G_3(z)) = s_1 s_2 l_\infty(G_1(z) G_2(z) G_3(z)) \\
l_{G_{04}} &= l_\infty(G_{04}(z)) = l_\infty(s_1 s_2 s_3 G_1(z) G_2(z) G_3(z) G_4(z)) \\
&= s_1 s_2 s_3 l_\infty(G_1(z) G_2(z) G_3(z) G_4(z)) \\
l_{G_{05}} &= l_\infty(G_{05}(z)) = l_\infty(s_1 s_2 s_3 s_4 G_1(z) G_2(z) G_3(z) G_4(z) G_5(z)) \\
&= s_1 s_2 s_3 s_4 l_\infty(G_1(z) G_2(z) G_3(z) G_4(z) G_5(z)) \\
l_{G_{06}} &= l_\infty(G_{06}(z)) = l_\infty(s_1 s_2 s_3 s_4 s_5 G_1(z) G_2(z) G_3(z) G_4(z) G_5(z) G_6(z)) \\
&= s_1 s_2 s_3 s_4 s_5 l_\infty(G_1(z) G_2(z) G_3(z) G_4(z) G_5(z) G_6(z))
\end{aligned}
$$

- Using $s_i = 1/l_{i\infty}$ and the previous equations for Chebychev Norm at each stage, we obtain the scaling factors as below:

$$
\begin{aligned}
s_1 &= 1/l_{G_{01}} \\
&= 1/l_\infty(G_1(z)) \\
s_2 &= 1/l_{G_{02}} \\
&= 1/(s_1 l_\infty(G_1 G_2(z))) \\
s_3 &= 1/l_{G_{03}} \\
&= 1/(s_1 s_2 l_\infty(G_1(z) G_2(z) G_3(z))) \\
s_4 &= 1/l_{G_{04}} \\
&= 1/(s_1 s_2 s_3 l_\infty(G_1(z) G_2(z) G_3(z) G_4(z))) \\
s_5 &= 1/l_{G_{05}} \\
&= 1/(s_1 s_2 s_3 s_4 l_\infty(G_1(z) G_2(z) G_3(z) G_4(z) G_5(z))) \\
s_6 &= 1/l_{G_{06}} \\
&= 1/(s_1 s_2 s_3 s_4 s_5 l_\infty(G_1(z) G_2(z) G_3(z) G_4(z) G_5(z) G_6(z)))
\end{aligned}
$$

- $s_1 s_2 s_3 s_4 s_5 s_6 = 1$, because of the original gain of the full order $l_\infty(G(\omega)) = l_\infty(G_1 G_2 G_3 G_4 G_5 G_6) = 1$ description.

- Finally, scaling coefficients is performed:
  $\mathbf{s_1}: b_{01s} = s_1 \times b_{01}, b_{11s} = s_1 \times b_{11}, b_{21s} = s_1 \times b_{21}$
  $\mathbf{s_2}: b_{02s} = s_2 \times b_{02}, b_{12s} = s_1 \times b_{12}, b_{22s} = s_1 \times b_{22}$
  $\mathbf{s_3}: b_{03s} = s_3 \times b_{03}, b_{13s} = s_3 \times b_{13}, b_{23s} = s_3 \times b_{23}$
  $\mathbf{s_4}: b_{04s} = s_4 \times b_{04}, b_{14s} = s_4 \times b_{14}, b_{24s} = s_4 \times b_{24}$
  $\mathbf{s_5}: b_{05s} = s_5 \times b_{05}, b_{15s} = s_5 \times b_{15}, b_{25s} = s_5 \times b_{25}$
  $\mathbf{s_6}: b_{06s} = s_6 \times b_{06}, b_{16s} = s_6 \times b_{16}, b_{26s} = s_6 \times b_{26}$

4.2.2 Parameters and Ports

The IIR core is composed of generic parameters which are configurable by user. These are described in Table 4.4. The parameters include the word length of input data, output data and

coefficient. The number of biquad stages is also configured by the user. Both the recursive and non-recursive coefficients of each biquad stage are specified by the user in a form of matrix. Furthermore, the ports of the IIR core which enable high speed parallel interface are described in Table 4.5.

Table 4.4: IIR core parameters

Generic name	**Description**	**Type**	**Valid range**
DIN_WIDTH	Width of data input	Unsigned integer	$\geqslant 8$
DOUT_WIDTH	Width of data output	Unsigned integer	$\geqslant 8$
COEFF_WIDTH	Width of coefficients	Unsigned integer	$\geqslant 8$
STAGES	Number of Biquad stages	Unsigned integer	> 0
b,a	Filter coefficients	Integer Matrix	Matrix size > 1

Table 4.5: IIR core ports

Pin name	**I/O**	**Description**	**Active state**
clk	in	System Clock	Rising edge
rst	in	System reset	high
en	in	Clock enable	high
vld	out	Valid output data available	high
din[DIN_WIDTH-1:0]	in	Filter input sample	data
dout[DOUT_WIDTH-1:0]	out	Filter output sample	data

4.2.3 **Timing Constraints**

Figure 4.11 shows a timing waveform diagram of IIR core. The *en* signal activates the filtering process by core. Input to the core is presented on *din[W-1:0]* bus. The *vld* signal indicates the valid output data available on *dout[W-1:0]*.

4.2.4 **Wishbone Interface**

Figure 4.12 shows the IIR core along with a Wishbone slave connection to enable SoC integration. The Wishbone interface core has two interfaces made up of high speed parallel ports and wishbone ports. The *clk*, *rst* and *en* ports work the same way as described in Table 4.5 while the Wishbone slave ports are described in section 2.12.

The signals shown Figure 4.12 are classified into feedforward and feedback signals. Feedforward signals send data from the slave interface to the IIR core input. These include the *dout[15:0]* port sending IIR filter input data to *din[15:0]* port of IIR core and this only takes place when the *start/en* signal is asserted to activate the IIR core filtering process. The feedback signals are meant to send data out of the IIR core to the IIR slave core. They include *dout[15:0]* port of the IIR core which sends IIR filtered data to IIR slave via direct connection with *din[15:0]* of IIR slave core. This filtered data is valid when *vld/en* signal is set high.

Furthermore, the register description of Wishbone interface is shown in Table 4.6. The *slave_select* is as read-only register that uniquely identifies the IIR IP core in the SoC design. To start the

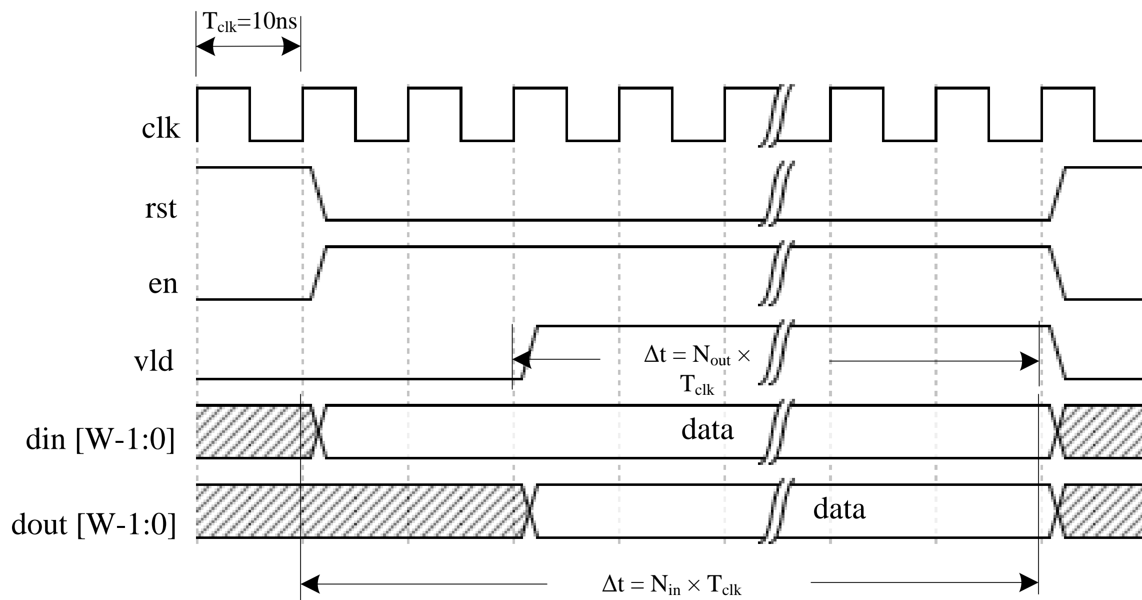

Figure 4.11: IIR core input/output timing waveform

filtering processing, the write-only *control* register is set. A status register is read-only register which set high to signal the end of filtering process, and lastly the *input_sample* is a write-only 16-bit register of to hold data the next data sample to be filtered while *output_sample* is a read-only register that keeps a filtered 32-bit data sample.

Table 4.6: Wishbone slave registers for IIR core

Register	Address	Register Value Bits
slave_select	0x0000	16
status	0x0001	1
control	0x0002	1
input_sample	0x0003	16
output_sample	0x0004	32

4.2.5 **IIR core Test**

Testing of IIR core is based on parallel interface in section 7.2 and Wishbone bus testing is not discussed.

4.3 FFT/IFFT IP CORE

This section present the design of an IP core to perform FFT computation and FFT literature is discussed in section 2.7.2. Fast Fourier Transform (FFT) is an efficient implementation of Discrete Fourier Transform (DFT). The function of a DFT is to map time domain data sequence into frequency domain data sequence [73]. FFT output $X[k]$ is defined by the equation 4.2.

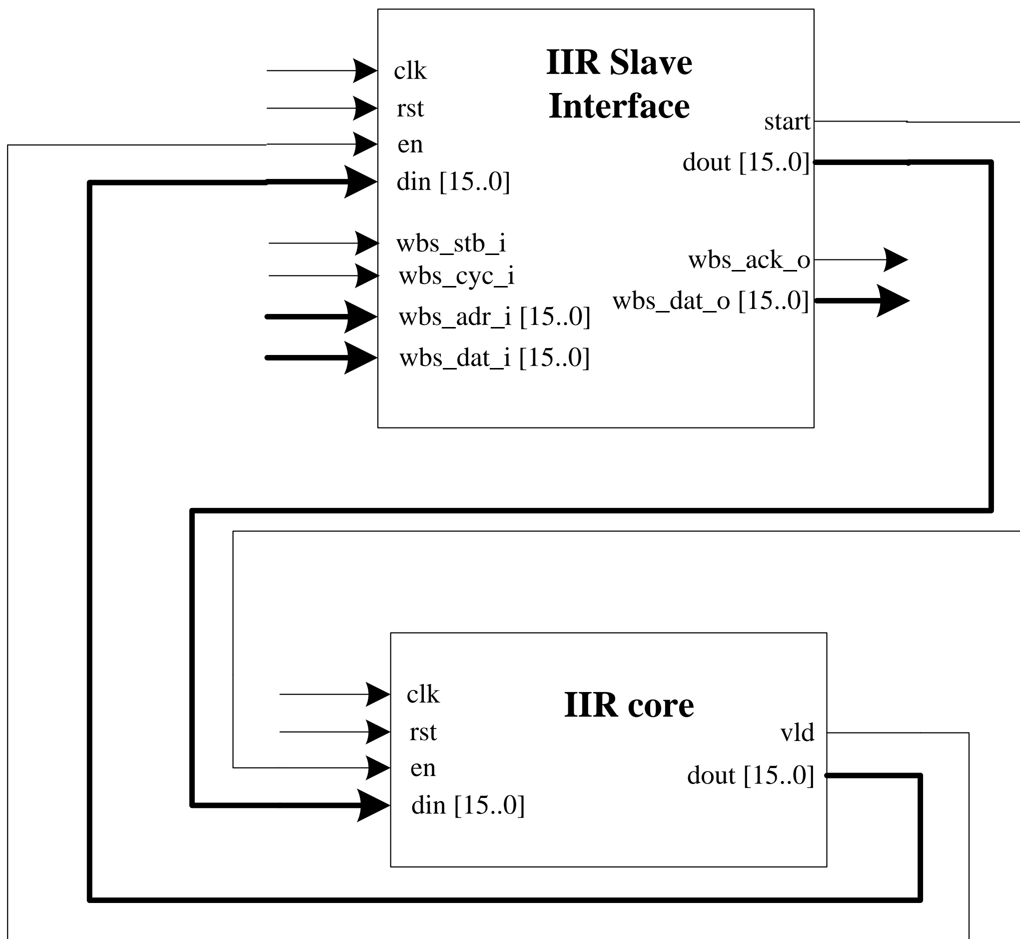

Figure 4.12: IIR core and Wishbone slave interface

$$X[k] = \sum_{k=0}^{N-1} x[n] W_N^{nk} \tag{4.2}$$

where $k = 0, 1, ..., N-1$ and N is the transform size, $W_N = e^{-j\frac{2\pi}{N}}$ is a twiddle-factor and $j = \sqrt{-1}$.

In this project, Radix-2^2 SDF algorithm [34] is exploited to implement a complex pipelined Radix-2^2 Single Path Delay Feedback Architecture of FFT. The high level block diagram of the designed FFT IP core is shown in Figure 4.13. Some benefits of using Radix-2^2 to design the FFT core is that its FFT architecture has simple pipeline control and reduced multipliers by a factor of (N-1)/2 compared to Radix-2 and Radix-4 available in Xilinx IP Cores Library [105].

Details of Radix-2^2 SDF algorithm are all covered in [34, 81]. This section only covers how the algorithm is used to design VHDL blocks that implement an FFT core. The implemented FFT core is further used to implement an IFFT core. The procedure is straightforward as the IFFT is computed by conjugating the twiddle factors of the corresponding forward FFT output [81].

The FFT Core length is configured to be 4, 816, 32, 64, 128, 256, 512, 1024, 2048 and 4096. However, larger size FFTs can be also be achieved by following guidelines outlined in section 4.3.3. The designed core is meant to be used and applied in fields where SDR is prevalent such as digital communication systems, radar systems and multimedia systems.

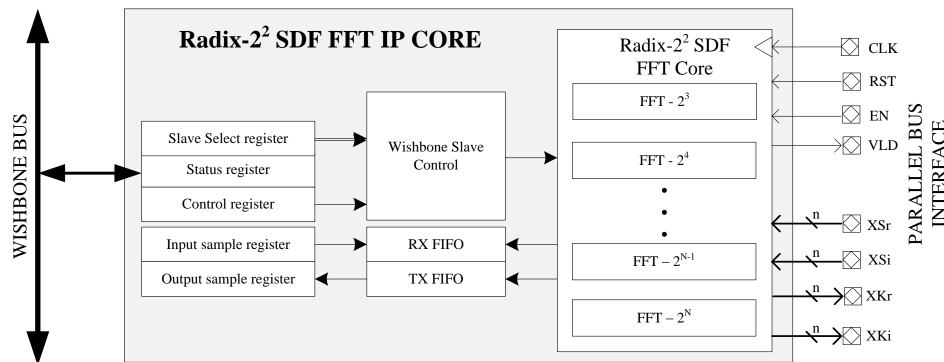

Figure 4.13: The architecture of FFT IP Core

4.3.1 Design Structure

A typical Radix-2^2 SDF FFT is illustrated in Figure 4.14. In this particular design data arrives at the input in a natural order and outputs results in a bit-reversed sequence. For an FFT with *N* points, a complete stage consists of two butterflies namely BFI and BFII, delay feedback shift register and a twiddle factor complex multiplier. On the other hand, half a stage only has a single butterfly which is BFI whereas the important formulas used to determine specific number of building blocks in the FFT architecture are clearly described in Table 4.7. The building blocks of the architecture are described below.

Table 4.7: The description of formulas used for FFT architecture

Formula	**Description**
N	Number of FFT points
$N-1$	Number of registers found in feedback registers
$log_4(N)$	Number of stages
$log_2(N)$	Number of butterflies and shift registers
$2log_2(N)$	Number of adders
$\frac{log_2(N)-1}{2}$	Number of complex multipliers

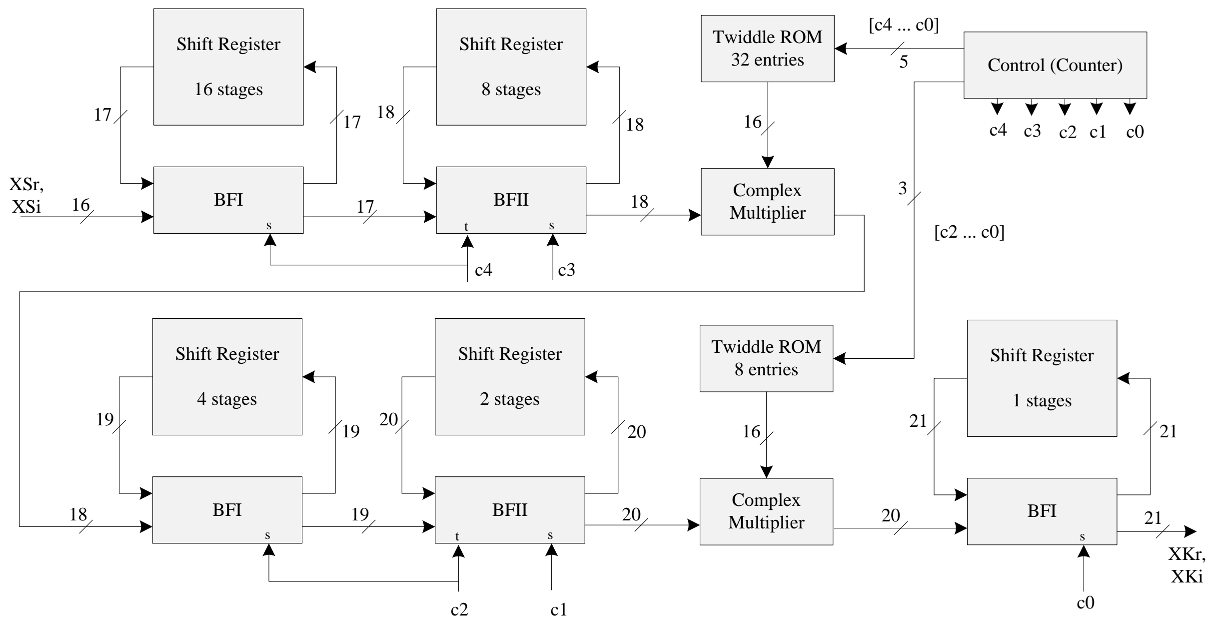

Figure 4.14: 32-point FFT structure using Radix-2^2 Single-Path Delay Feedback algorithm

4.3.1.1 **Butterflies**

A typical FFT architecture i^{th} stage is made up of one or two butterflies. The two butterflies are known as BFI and BFII and are illustrated in Figure 4.15. Both the inputs (*XSi[15:0],XSr[15:0]*) and outputs (*XKi[20:0],XKr[20:0]*) are complex valued digital samples. The four multiplexers are controlled by s control bit which is provided by a counter. When s is '0', the first butterfly remains in the idle state for $N/2 * i$ cycles. During this time, the incoming data is directed into the shift registers until they are filled. On the next $N/2$ cycles when s is set to '1', the butterfly computes a 2-point DFT using incoming data and results are stored in the shift registers.

Butterfly outputs are determined by equation 4.3. $Z(n)$ is sent out to be multiplied with twiddle factors and $Z(n + N/2)$ is stored back in the shift register. BFII performs 2-point DFT computation in a similar manner as BFI. The only exception is that BFII has extra logic to perform multiplication by $-j$ which involves real-imaginary swapping and sign inversion. Real-imaginary swapping is computed by MuXim block in Figure 4.15, and the sign inversion by MUXsg shown in Figure 4.16.

$$\begin{aligned} Z(n) &= x(n) + x(n + \frac{N}{2}) \\ Z(n + \frac{N}{2}) &= x(n) - x(n + \frac{N}{2}) \end{aligned} \tag{4.3}$$

where $0 \leqslant n < \frac{N}{2}$.

The data output bus width of each BFI is calculated as *input width + 1* and that of BFII is *input width + 2* where *input width* refers to width of data input in each stage of the FFT pipeline architecture.

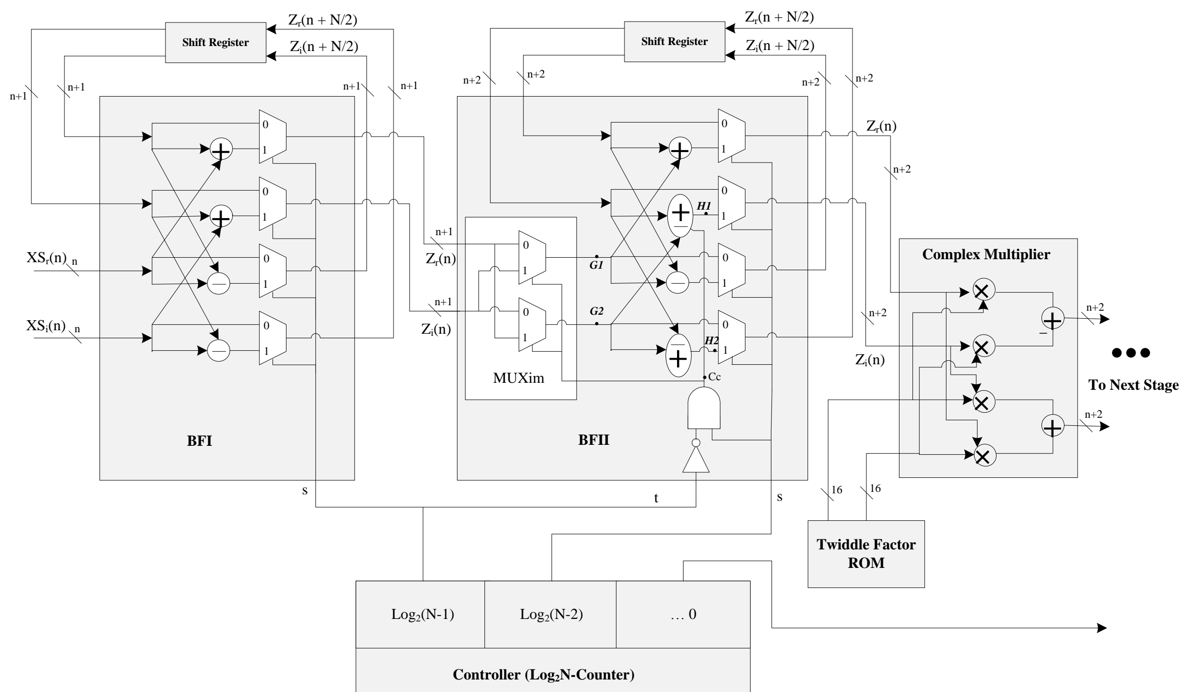

Figure 4.15: The single FFT pipeline stage consisting of Butterfly Type BFI and BFII and showing how shift registers, counter, ROM and complex mulplier are connected.

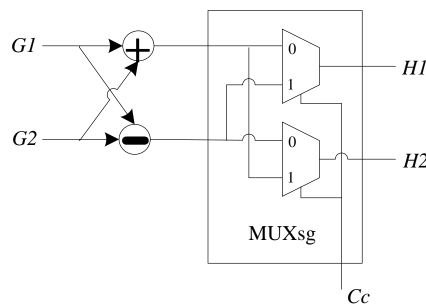

Figure 4.16: Sign-inversion structure [81]

4.3.1.2 Shift Register

The shift registers help to store data temporarily in pipeline FFT architecture. The depth of each shift register at i^{th} stage is determined by $N/(2*i)$. For each shift register, the bus width is equivalent to its corresponding butterfly output width.

4.3.1.3 Complex Multiplier

The multiplier computes the product of twiddle factor stored in ROM by BFII output. The structure of a complex multiplier is shown in Figure 4.15. The multipliers are only used in stages where exactly two butterflies apply except for the last stage.

4.3.1.4 ***Twiddle Factor ROM***

Every complete stage of Radix-2^2 FFT architecture requires that a twiddle factor be multiplied with BFII output. The twiddle factors are constant complex values stored in 16-bit ROM with depth of $N/2^{2i}$ at each ith stage. These twiddle factors are generated according to equation 4.4 and then stored in ROM. Using MATLAB script provided in Appendix D.4, the ROM HDL files containing twiddle factors can be generated easily. The appropriate twiddle factor is selected by control logic in the pipeline structure. Each ROM is addressed by a sliced vector of bits from control logic as shown in Figure 4.14. The vector slice is in a form of $log_2\left(\frac{N}{2^{2i}}\right)$. The twiddle factor at i^{th}-stage, with $i = 0, 1, ..., (log_4 N) - 2$ is given by $W_i = \{u_x\}\,; x = 0, 1, ..., \frac{N}{2^{2i}}$ with $u_x = e^{\frac{-j2\pi v}{N}}$

$$v = \begin{cases} 0, & 0 \leqslant x < a \\ 2^{2i+1} \times (x - a), & a \leqslant x < 2a \\ 2^{2i} \times (x - 2a), & 2a \leqslant x < 3a \\ 3 \times 2^{2i} \times (x - 3a), & 3a \leqslant x < 4a \end{cases} \tag{4.4}$$

where $a = \frac{N}{2^{2+2i}}$ [81] .

4.3.1.5 ***Controller***

The control logic of a Radix-2^2 FFT pipeline is implemented with a simple digital $\log_2$(N)-bit counter. The counter is used to control the butterfly multiplexers, thus enabling the butterflies to switch between operating modes described in section 4.3.1.1. Furthermore, the counter is used to address Twiddle Factor ROM which directs its output to a complex multiplier in each stage of the FFT.

4.3.2 **Parameters and Ports**

The FFT/IFFT core consists of generic parameters which make it possible for user to customize its functionality depending on the application needs. These parameters are described in Table 4.8. The parameters include the word length of the input data, output data and twiddle factor stored in ROM. The core also enables the number of FFT points to be specified by the user. Furthermore, the ports on the FFT/IFFT core enable connection to other cores using high speed parallel interface as described in Table 4.9.

Table 4.8: FFT core parameters

Generic name	**Description**	**Type**	**Valid Range**
N	Number of FFT points	unsigned integer	8, 16, 32, 64, 128, 256, 512, 1024, 2048, 4096
DIN_WIDTH	Bit width of input samples	unsigned integer	8 to 32
DOUT_WIDTH	Bit width of input samples	unsigned integer	8 to 32
TF_WIDTH	Bit width of twiddle factors	unsigned integer	$\geqslant 8$, default=16

Table 4.9: FFT core pin-out

Port name	**I/O**	**Description**	**Active State**
clk	in	System Clock	Rising Edge
rst	in	System Reset	high
en	in	Clock Enable	high
XSr[*DIN_WIDTH-1*:0]	in	Real-part input sample	data
XSi[*DIN_WIDTH-1*:0]	in	Imaginary-part input sample	data
vld	out	Valid data available	high
done	out	FFT complete	high
XKr[*DOUT_WIDTH-1*:0]	out	Real-part output sample	data
XKi[*DOUT_WIDTH-1*:0]	out	Imaginary-part output sample	data

4.3.3 Core Generation Flow for Higher Length FFTs

The designed FFT/IFFT core supports the number of FFT points specified in Table 4.8. However, a straightforward procedure can be followed to create FFT or IFFT core with more points than the maximum value of 4096. This same method can be used to generate an FFT structure of any length greater than or equal to 8 provided the FFT length is a power of two.

Figure 4.17 shows the flow of generation of HDL modules to build the top level design of the desired FFT or IFFT core by connecting butterfly stages, twiddle factor ROMs and a counter. Due to the modular structure of the designed FFT/IFFT core, its modules are reused to build custom FFT/IFFT cores.

As shown in Figure 4.17, the process starts by computing the number of stages using $log_4 N$. All the stages preceding the last stage are built using *r22sdf_stage.vhd*. In each ith stage, there is Twiddle Factor ROM whose depth is determined by $N/2^{2i}$. The ROM HDL files for FFT stages are generated using a Matlab script provided in Appendix D.4. Finally, the last stage is generated based on the FFT length used and it does not have a Twiddle Factor ROM. If the calculated number of stages is fractional, *r22sdf_odd_last_stage.vhd* file is used to build the last stage. If the computed number of the stages is a whole number, the last stage is created using *r22sdf_even_last_stage.vhd* file. The controller of the FFT is a simple $log_2(N)$-bit counter which is implemented in *counter.vhd* file. The counter has n-bit counting register that is configurable by the user.

4.3.4 Timing Constraints

A high speed parallel interface to an FFT core is illustrated in Figure 4.18. The core performs FFT function of N points as long as *en* remains high. Input digital data is represented in complex format. *XSr[DIN_WIDTH-1:0]* and *XSi[DIN_WDTH-1:0]* buses are used for input and they represent real and imaginary data respectively. *vld* goes high after *N-1* input samples to signal availability of output sample on *XKr[DIN_WIDTH-1:0]* and *XKi[DIN_WIDTH-1:0]* which are in complex values.

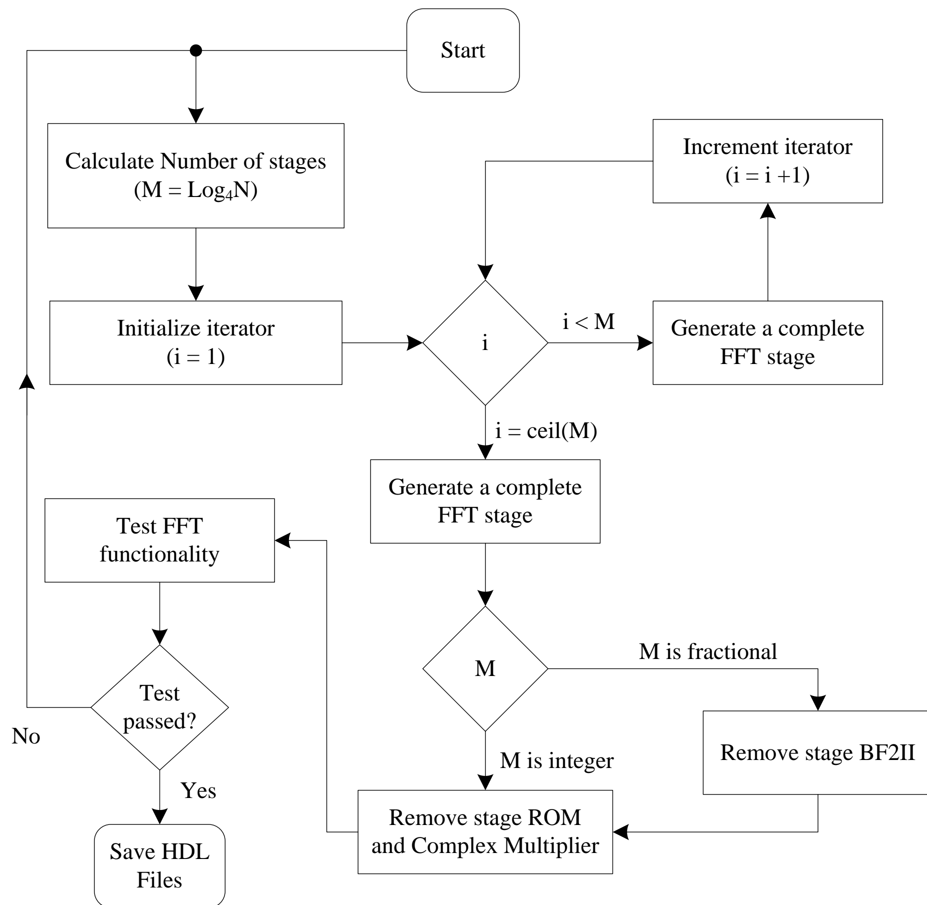

Figure 4.17: A flow diagram for generation of FFT core modules for high length FFTs

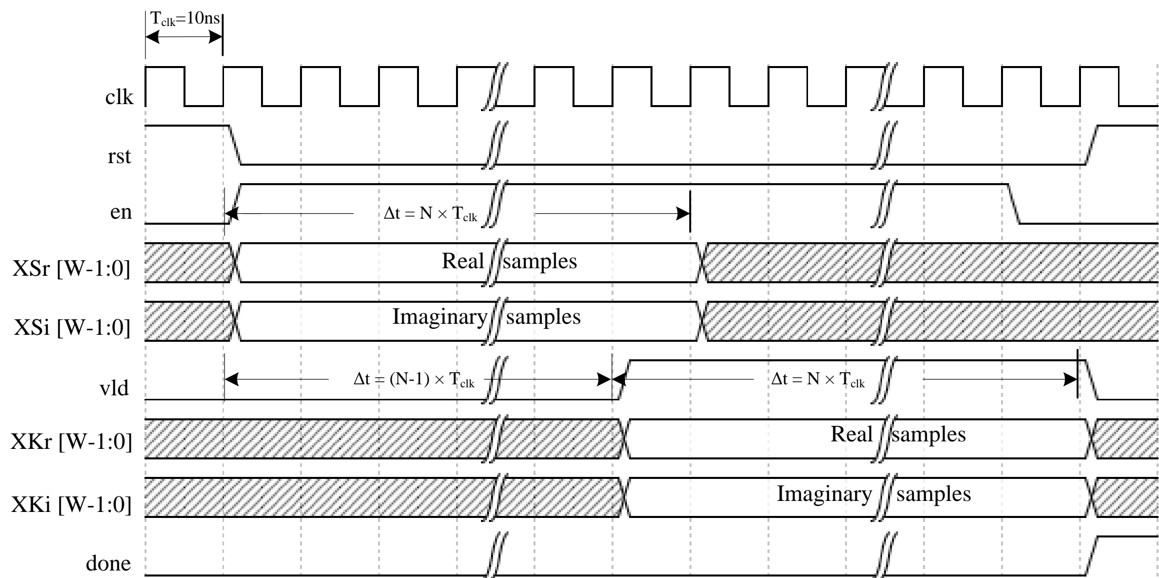

Figure 4.18: FFT/IFFT core input/output timing waveform

4.3.5 **Wishbone Interface**

In order to make an FFT/IFFT core Wishbone compatible, the Wishbone Slave Interface core is designed and connected to FFT/IFFT core as shown in Figure 4.19. The three control ports namely *clk*, *rst* and *en* operate as described in Table 4.9 and the Wishbone slave ports are described in section 2.12. The signals connecting the two blocks are divided into feedforward and feedback signals. The feedforward signals include the *start/en* signal which starts the FFT or IFFT processing on the FFT/IFFT core. Both *doutr[15:0]* and *douti[15:0]* ports are real and imaginary data ports respectively and are used to transfer input samples to corresponding *XSr[15:0]* and *XSi[15:0]* ports of the FFT/IFFT core.

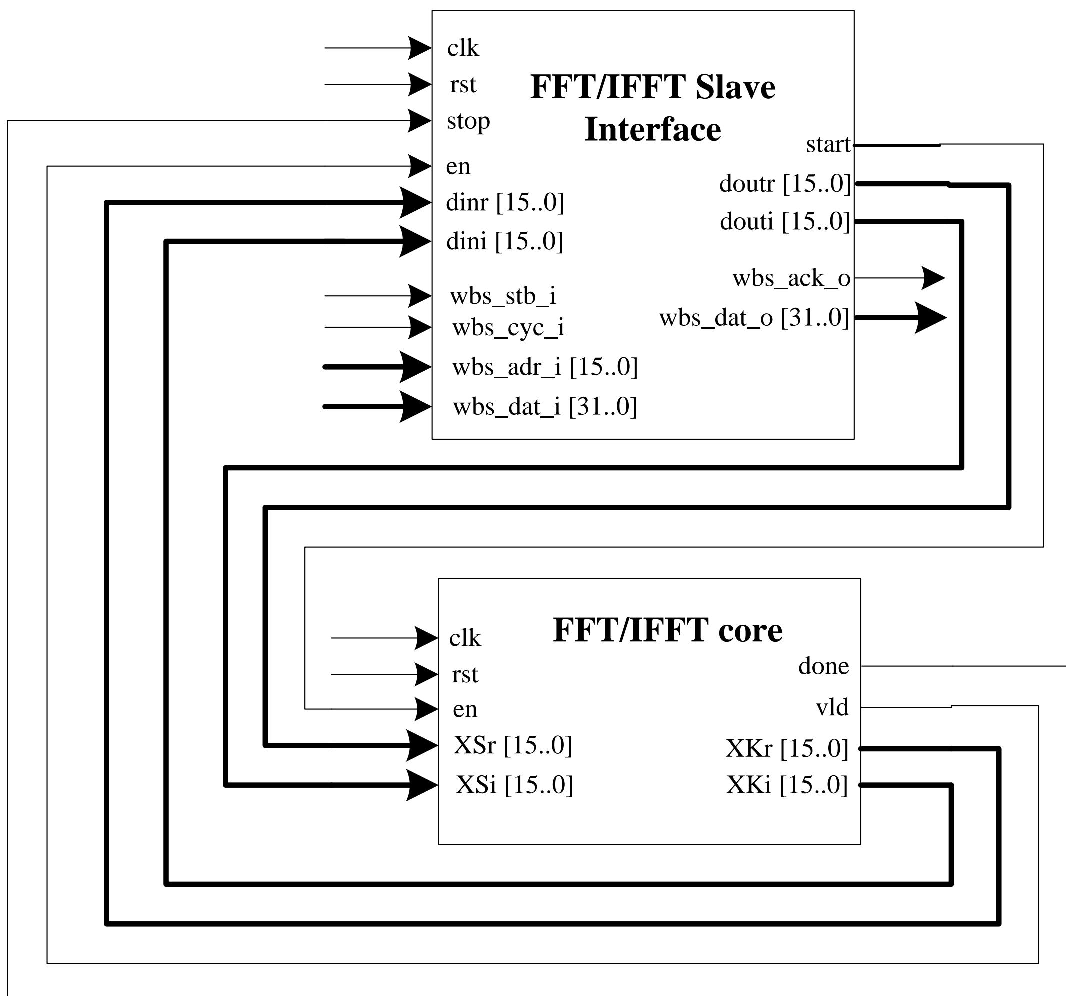

Figure 4.19: FFT core and Wishbone slave interface

Additionally, the feedback signal are used by FFT/IFFT core to send output data to slave interface core as shown in Figure 4.19. The data processed by the FFT/IFFT core is sent through imaginary and real ports namely *XKr[15:0]* and *XKi[15:0]* ports which connect directly to *dinr[15:0]* and *dini[15:0]* of the FFT/IFFT slave block. The *vld/en* signal is set high to enable output data transfer from one block to another while *done/stop* signal goes high to indicate that FFT/IFFT core has completed processing.

Furthermore, the description of FFT/IFFT Wishbone slave registers is described in Table 4.10. The *slave_select* is a read-only register used to uniquely identify the FFT/IFFT IP core. In order start the FFT/IFFT core processing, the write-only *control* register needs to be set. The end of FFT/IFFT processing is denoted by active high read-only *status* register. Lastly the write-only *input_sample* register and read-only *output_sample* register are both used for input and output data respectively. Their bit precision is 32 bits which is a concatenation of 16-bit real and imaginary input and output samples.

Table 4.10: Wishbone slave registers for FFT/IFFT core

Register	Address	Register Value Bits
slave_select	0x0000	16
status	0x0001	1
control	0x0002	1
input_sample	0x0003	32
output_sample	0x0004	32

4.3.6 **FFT/IFFT core Test**

The FFT/IFFT core test is discussed in section 7.3 using only parallel interface. Wishbone bus interface testing is not covered in this work.

4.4 DDC IP CORE

This section discusses the design of a DDC IP core. The literature for DDC algorithm is covered in section 2.7.3. The DDC performs the first processing work after ADC [95] and is used in applications where frequency down conversion, sample rate reduction and high speed filtering is required. The developed DDC core is highly configurable and can be tailored easily to meet many SDR multi-rate applications needs. Figure 4.20 illustrates the top level block diagram of the DDC IP core.

4.4.1 **DDC structure**

The DDC architecture is realized as shown in Figure 4.21. The NCO, digital mixer, CIC and FIR filter were all designed to complete the structure of the DDC as explained below.

4.4.1.1 NCO

The Numerically Controlled Oscillator (NCO) synthesizes discrete-time sine and cosine waveforms with a configurable waveform frequency as shown in Figure 4.22. The waveforms are generated from a lookup table containing a vector of sine and cosine values which are successively addressed by the phase accumulator output. The phase step of the accumulator is determined by Frequency Tuning Word (FTW) calculated using equation 4.5. n represents the width of phase in bits; f_{out} is the desired frequency of the output waveforms and f_{clk} is the frequency of the clock.

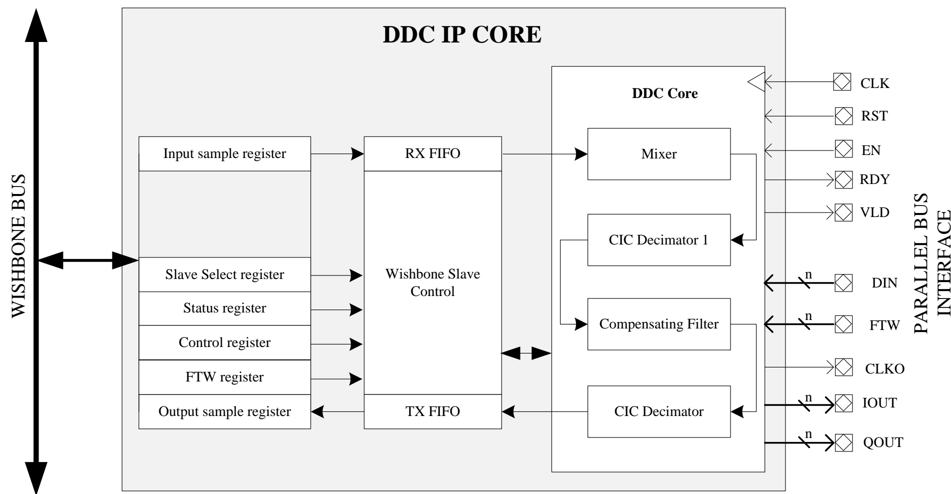

Figure 4.20: The architecture of DDC IP Core

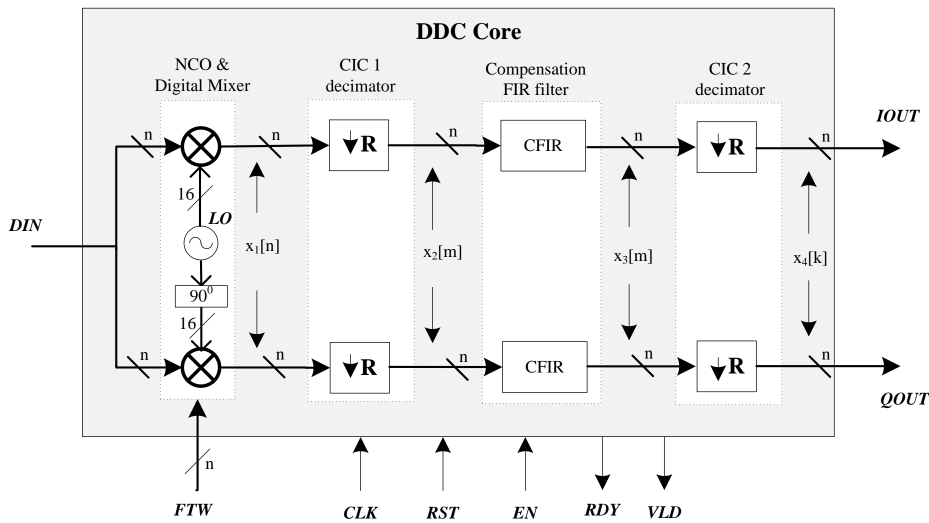

Figure 4.21: A structure of Digital Down Converter

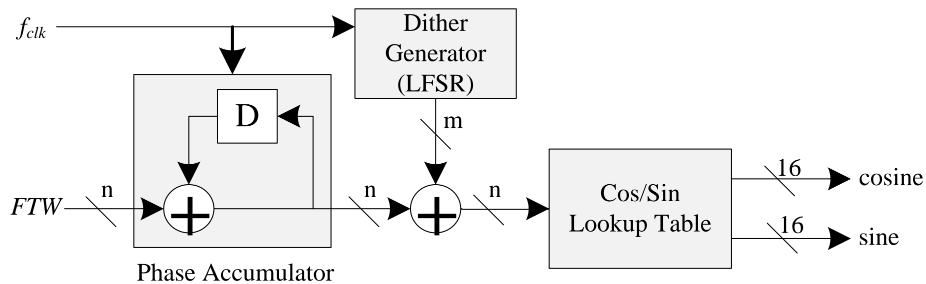

Figure 4.22: Block diagram of NCO core

$$f_{out} = \frac{FTW \times f_{clk}}{2^n} \text{ [33]} \tag{4.5}$$

Due to phase quantization, the spurious harmonics in the NCO waveform output are created. In order to equally distribute these unwanted harmonics, the random number is generated [21] using Linear Feedback Shift Register (LSFR) and added to the least significant bits of the phase accumulator. The process is referred to as phase dithering and it improves effective SFDR of the NCO-generated waveforms. The NCO of the DDC core has a configurable phase dithering in order to attain the highest possible SFDR in the output waveforms.

4.4.1.2 ***Digital Mixer***

The digital mixer is used to mix down the RF or IF signal to baseband signal for further processing. It takes in the local oscillator signal at IF frequency and multiplies it by an incoming IF signal. The product of these two signals has both the desired baseband signal and out-of-band higher order frequency components. Filtering is therefore required in order to isolate a baseband signal.

4.4.1.3 ***CIC Decimation filter***

The CIC decimation core is designed to reduce the sampling rate in the DDC. It also has a low-pass filter characteristic which is efficient and cost effective. As a result, it is used to eliminate noise emanating from a digital mixer. The simplified structure of the CIC decimation filter is illustrated in Figure 4.23.

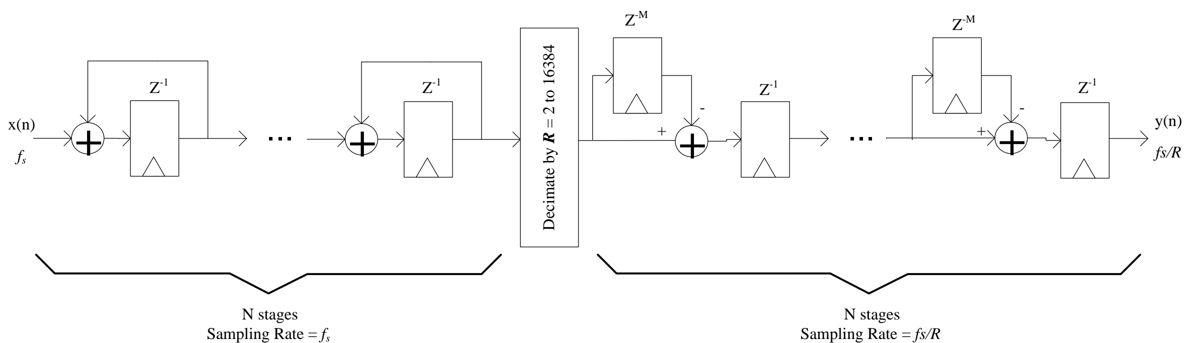

Figure 4.23: Block diagram of a CIC core

The CIC decimator is the chain of N integrator stages and N comb stages. It comprises an integrator section operating at high sampling rate f_s and comb section operating at lower rate f_s/R. These two sections are separated by a decimator which is denoted by R. The combs have a differential delay M which is used to control the filter's frequency response [91]. The system transfer function $H(z)$ and magnitude response $|H(f)|$ are defined by equation 4.6.

$$\begin{aligned} H(z) &= \frac{(1-z^{-RM})^N}{(1-z^{-1})^N} \\ &= \left[\sum_{k=0}^{RM-1} z^{-k}\right]^N \\ |H(f)| &= \left|\frac{sin(\pi M f)}{sin(\frac{\pi f}{R})}\right|^N \quad [91] \end{aligned} \tag{4.6}$$

where a complex variable $z = e^{\frac{j2\pi f}{R}}$, and f is the frequency relative to the low sampling rate f_s/R.

One drawback of using CIC to perform filtering and decimation is a non-flat response [7, 89] in the filter passband. This non-ideal behavior of the first CIC filter is corrected [7][89] by using compensation filter.

Two CIC decimators are used in this DCC core design. Most of the decimation and filtering is performed by the first filter, hence the CIC compensation is needed. The last stage CIC is optional and it used for minor filtering and sample rate reduction. Unlike the first CIC, the last CIC is not followed by a compensation filter as the CIC filter stopband attenuation is low resulting in negligible undesirable effect of the filter.

4.4.1.4 ***Compensation Filter***

The compensation filter is implemented using an FIR core designed in section 4.1. The purpose of the compensation filter is to correct the flat passband of the CIC decimation filter response. Thus the compensation filter consists of a magnitude response that is the inverse of a CIC filter response [7] as shown in equation 4.7.

$$\begin{aligned} G(f) &= \left|MR\left(\frac{sin(\frac{\pi f}{R})}{sin(\pi M f)}\right)\right|^N \\ &\approx \left|\frac{\pi M f}{sin(\pi M f)}\right|^N \\ &= |sinc^{-1}(Mf)|^N \ [7] \end{aligned} \tag{4.7}$$

The DDC core allows the user to configure parameters and coefficients of the compensation filter. The core is also accompanied by a Matlab script to design and visualize the magnitude response of both the CIC filter and a compensation FIR filter and this script is provided in Appendix E.2.

4.4.2 **Parameter and Ports**

Customizing the DDC core structure and functionality requires configuration of generic parameters described in Table 4.11. The ports of the DDC core enable it to connect to other blocks using high speed parallel interface. These ports are described in Table 4.12.

Table 4.11: DDC core generic parameters

Generic Name	Description	Type	Valid Range
DIN_WIDTH	Input data width	unsigned integer	$\geqslant 8$
DOUT_WIDTH	Output data width	unsigned integer	$\geqslant 8$
	NCO phase width	unsigned integer	$\geqslant 8$
PHASE_DITHER_WIDTH	Phase dither width	unsigned integer	$\leqslant$ phase_width
SELECT_CIC1	Use CIC1 in the DDC	bit	0 or 1
NUMBER_OF_STAGES1	Number of CIC1 stages	unsigned integer	> 0
DIFFERENTIAL_DELAY1	Differential delay of CIC1	unsigned integer	1 or 2
SAMPLE_RATE_CHANGE1	Decimation factor of CIC1	unsigned integer	> 0
SELECT_CFIR	Use compensating FIR filter of DDC	bit	0 or 1
NUMBER_OF_TAPS	Number of FIR taps/coefficients	unsigned integer	> 0
FIR_LATENCY	Choosing type of FIR structure	unsigned integer	0=Transpose, 1=Even symmetric, 2=Odd symmetric, 3=Moving average
COEFF_WIDTH	Coefficient bit width	unsigned integer	$\geqslant 8$
COEFFS	Array of quantized integer filter coefficients	array of signed integers	> 0
SELECT_CIC2	Use CIC2 in the DDC	bit	0 or 1
NUMBER_OF_STAGES2	Number of CIC2 stages	unsigned integer	> 0
DIFFERENTIAL_DELAY2	Differential delay of CIC2	unsigned integer	1 or 2
SAMPLE_RATE_CHANGE2	Decimation factor of CIC2	unsigned integer	> 0

4.4.3 Timing Constraints

The functional timing waveform diagram of the DDC core is shown in Figure 4.24. The user starts the core by asserting *en* signal. Then *rdy* goes high to signal the core is ready to receive input data on *din[DIN_WIDTH-1:0]* and start processing. In order to set the NCO to a desired frequency, *ftw[PHASE_WIDTH-1:0]* is used. This represents frequency tuning word which is set according to formula in equation 4.5. Furthermore, the baseband output samples known as *iout[DOUT_WIDTH-1:0]* and *qout[DOUT_WIDTH-1:0]* are read when *vld* is asserted.

Table 4.12: DDC core pin-out

Pin name	I/O	Description	Active State
clk	in	System Clock	Rising edge
rst	in	System Reset	high
en	in	Clock enable	high
din[DIN_WIDTH-1:0]	in	Real valued data sample	data
ftw[PHASE_WIDTH-1:0]	in	Frequency Tuning Word	data
rdy	out	DDC core ready to accept input data	high
vld	out	Valid output data available	high
clko	out	Decimated or divided clock	Rising edge
iout[DOUT_WIDTH-1:0]	out	Real output sample	data
qout[DOUT_WIDTH-1:0]	out	Imaginary output sample	data

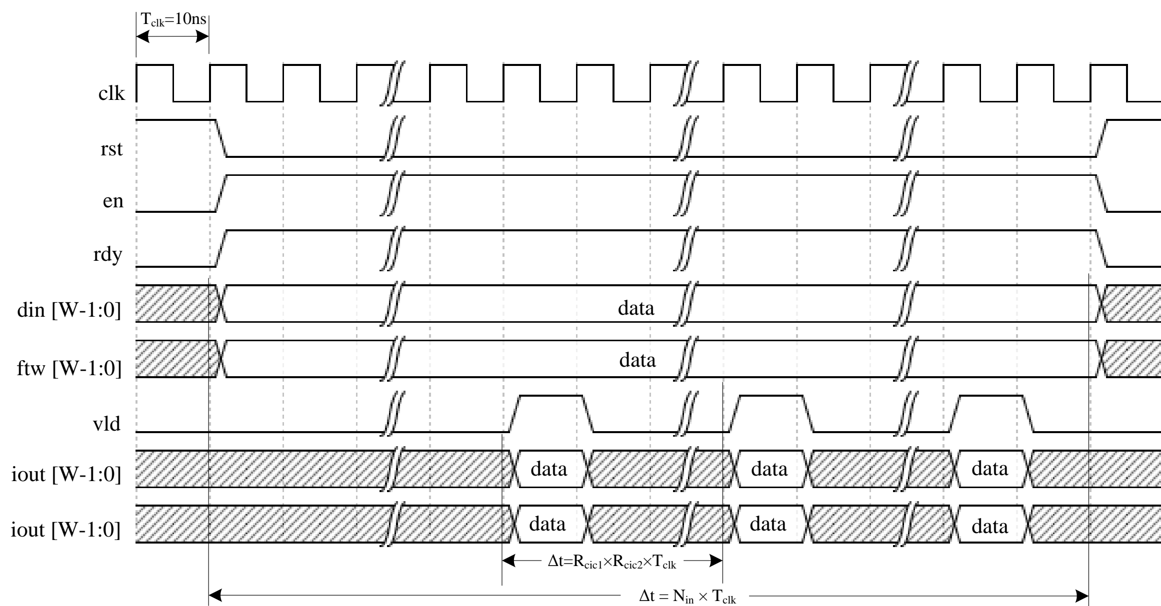

Figure 4.24: DDC core input/output timing waveform

4.4.4 Wishbone Interface

The DDC core is made to support SoC design integration by connecting to it a DDC Wishbone slave interface core as illustrated in Figure 4.25. The slave interface is composed of both wishbone ports and high speed parallel ports. The common control ports namely *clk*,*rst* and *en* are to similar ports used by DDC core as described in Table 4.11 while the Wishbone interface ports are described in section 2.12.

The signals in Figure 4.25 are classified into feedforward and feedback signals. The feedforward signals transfer data from DDC slave block to a DDC core. These include a *start/en* signal which activates DDC core processing while a signal connecting *ftw[15:0]* ports on both blocks is used to input the frequency tuning word to the DDC core. The *dout[15:0]* port presents input

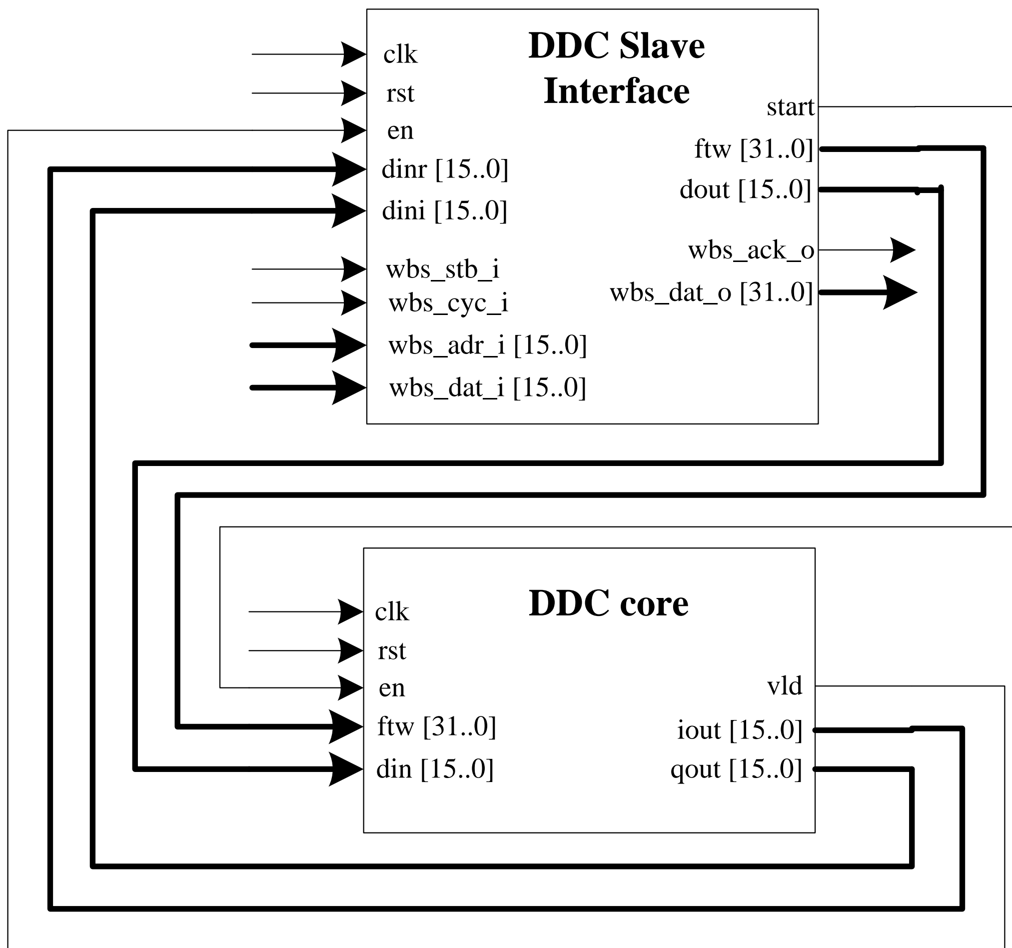

Figure 4.25: DDC core and Wishbone slave interface

samples to the DDC core via direct connection with *din[15:0]* port on the DDC core.

Additionally, the feedback signals transfer DDC core output data to the input interface of a slave block. These include the *vld/en* signal which indicates the valid data output from DDC core. The data samples processed by a DDC core are sent to a slave core via *iout[15:0]* and *qout[15:0]* I/Q ports which in turn connect to a *dinr[15:0]* and *dini[15:0]* ports of a slave interface respectively.

Furthermore, the description of DDC Wishbone slave interface registers is provided in Table 4.13. The *slave_select* is a read-only register that provides a unique identifier in the SoC design. The DDC core is activated by setting the write-only *control* register while the read-only *status* signals the end of DDC process. The frequency tuning word is held by a write-only *FTW* register. The 16-bit write-only *input_sample* register is used for input sample of the DDC core. Lastly the *ouput_sample* is a read-only output register whose bits are 32-bits which is a combination of 16-bit real output sample and 16-bit imaginary output sample.

Table 4.13: Wishbone slave registers for DDC core

Register	Address	Register Value Bits
slave_select	0x0000	16
status	0x0001	1
control	0x0002	1
FTW	0x0003	32
input_sample	0x0004	15
output_sample	0x0005	32

4.4.5 DDC Core Test

The DDC core test is presented later in section 7.4 using only parallel interface and not Wishbone bus interface.

CHAPTER 5

DESIGN OF SDR I/O INTERFACE BLOCKS

This chapter presents design and development of input/output (I/O) interface cores for RHINO. The design of ADC/DAC interface of FMC150 is discussed first and this is followed by a design of interface for 1 Gigabit Ethernet using UDP protocol to transmit and receive data packets.

5.1 4DSP-FMC150 INTERFACE CORE

FPGA devices perform all the tasks in the digital domain. As a result, they are used in high-performance and high-speed applications because digital systems exhibit close-to-ideal characteristics of signal processing. However, the external environment of FPGAs is composed of complex analog signals with the exception of other digital devices that are physically linked with the FPGA. Due to the real world that operates in an analog domain, the signal transmission and reception is performed in an analog domain using DAC and ADC daughter cards respectively.

In this project, a 4DSP-FMC150 FMC daughter card is used as a high performance ADC /DAC card to perform necessary signal conversions. The card plugs into the LPC FMC standard connector of RHINO where the FMC connector is linked to RHINO Spartan 6 FPGA via LVDS interface.

The FMC150 is designed with TIs ADS62P49/ADS4249 dual-channel 14-bit 250Msps ADC and TIs DAC3283 dual channel 16-bit 800Msps DAC. The TIs CDCE72010 PLL is the clock distribution device that provides a clock to drive the DAC and ADC. The internal clock source can optionally be locked to onboard 100 MHz or external reference clock [1].

In order to operate, control and monitor FMC150 card and make it compatible with RHINO, an FPGA- based interface should be implemented. Although the card is shipped with the reference design for several commercially available FPGA boards to allow consumers to start using it quickly, RHINO does not support the FMC150 yet.

This section presents a design of the 4DSP-FMC150 physical interface to the ADC and DAC with the aid of FMC150 control block via SPI that forms part of the 4DSP consumer reference design. The sampling rates can be changed according to user application requirements via SPI

interface, however, the example design in this section will use sample rate of 61.44 MSPS for both ADC and DAC device.

5.1.1 **CDCE72010 programming settings**

The CDCE72010 PLL provides a clock distribution system for FMC150 ADC and DAC chips. According to [41], the user may choose either the external or internal sampling clock, and one of them is synchronized with a VCXO or VCO frequency. The internal reference frequency on the FMC150 is 100 MHz which connects to a primary reference interface. The external clock is decided on by the user and it connects to a secondary reference interface. Only one reference clock can be enabled, hence they cannot function both at the same time.

The CDCE72010 consists of internal dividers, a phase frequency detector, a charge pump, an external VCXO and loop filter which all complete a PLL. Although VCXO is external to CDCE72010 chip, it is provided by FMC150 and the user can select from one of its supported frequencies which are 491.52 MHz and 737.28 MHz.

5.1.1.1 PLL configuration parameters

In order for the PLL to lock, the input frequency, dividers and VCXO needed to generate a particular set of output frequencies should all be configured properly. The product data sheet [41] provides full details of how to program the registers via SPI when modifying the parameters. Only the parameters that have been used in this design are discussed and these are summarized in Table 5.1.

Table 5.1: FMC150 PLL configuration parameters

Parameter	**Description**	**Valid Range**
M	Reference clock divider.	1 - 16384
N	VCXO/AUX/SEC divider	1 - 16384
R	Reference clock divider.	1 or 2
P	Feedback divider. P and N dividers determine the reference and feedback frequencies for the phase frequency detector. Both the reference and feedback frequencies must eventually be the same.	1 - 80
VXCO	Voltage Control Crystal Oscillator.	491.52 MHz or 737.28 MHz
K	Output Frequency divider. The output frequencies of the PLL are directly related to VCXCO input frequency.	1 - 80

5.1.1.2 PLL Design

Our design application requires three different clocks which are described as below:

1. **61.44 MHz output clock 2 (F_{out2})** - This is configured as LVPECL output and provides a sampling clock for ADC (ads62p49 chip).

2. **245.76 MHz output clock 4 (F_{out4})** - The clock is configured as LVDS and connects to the FMC connector to supply reference clock for the DAC clock and data signals inside the FPGA. *CLK_TO_FPGA_P/N* is used on the FPGA side to connect to the input clock reference.

3. **245.76 MHz output clock 7 (F_{out7})** - This is configured as LVPECL output and provides a clock for DAC (dac3283 chip).

The output frequencies are phase-locked to onboard 100 MHz input reference clock that is connected to a PRI_REF pin of cdce72010. The VCXO frequency is chosen as 491.52 MHz and this is also provided by FMC150 board. With the above parameters chosen, the goal is to now determine M, N, feedback (P), and output divider values (K). The relationship between the VCXO frequency and the input reference voltage is related by equation 5.1.

$$\begin{gathered}\frac{F_{\text{VCXO_IN}} \text{ or } F_{\text{AUX_IN}}}{\text{Frequency (PRI_REF or SEC_REF)}} = \frac{P \times M}{R \times N} \\ \text{Where :} \\ F_{\text{VCXO}} = F_{\text{out}} \times K \\ \text{Provided that :} \\ F_{\text{out}} \times K < 1500MHz\end{gathered} \tag{5.1}$$

Since the internal reference frequency is used, we choose M = 625, R = 1 and PFD = 160 kHz as recommended by the vendor [1]. At this point, the remaining unknowns are feedback dividers N and P. Choosing P = 8, the relationship in equation 5.1 is now used to determine N as shown in equation 5.2.

$$\begin{aligned}N &= \frac{F_{\text{VCXO_IN}} \times R \times M}{F_{\text{PRI_REF}} \times P} \\ &= \frac{491.52 \times 10^6 \times 1 \times 625}{100 \times 10^6 \times 8} \\ &= 384\end{aligned} \tag{5.2}$$

The output dividers are calculated as follows:

$$
\begin{aligned}
K_2 &= \frac{F_{\text{VCXO_IN}}}{F_{\text{out2}}} = \frac{491.52 \times 10^6}{61.44 \times 10^6} = 8 \\
K_4 &= \frac{F_{\text{VCXO_IN}}}{F_{\text{out4}}} = \frac{491.52 \times 10^6}{245.76 \times 10^6} = 2 \\
K_7 &= \frac{F_{\text{VCXO_IN}}}{F_{\text{out7}}} = \frac{491.52 \times 10^6}{245.76 \times 10^6} = 2
\end{aligned} \tag{5.3}
$$

Figure 5.1 shows the complete configuration made to the PLL using all the calculated parameters. The parameters are stored in ROM and are initialized at application start in order to configure FMC150 PLL registers through SPI programming. The register values are shown in Table 5.2. It is recommended that the table be studied along with register description in [41] as it provides details of the registers and default settings used for the PLL which may not have been covered in this section.

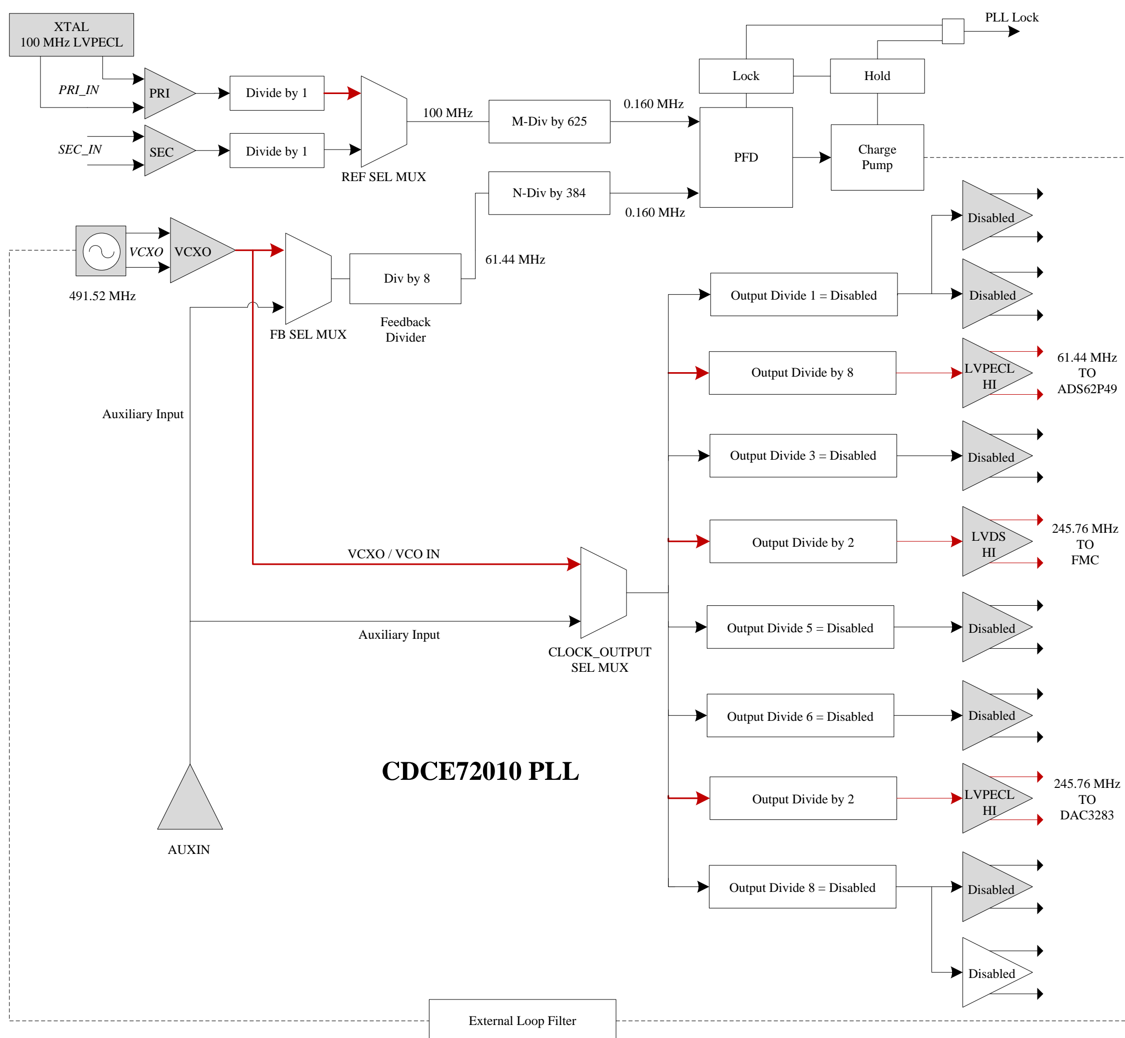

Figure 5.1: CDCE72010 programming settings for FMC150 card

Table 5.2: FCM150 CDCE72010 Configuration Settings

REGISTER	SETTING
0x00	683C0350
0x01	00000001
0x02	83080002
0x03	00000003
0x04	E9800004
0x05	00000005
0x06	00000006
0x07	83800017
0x08	00000008
0x09	00000009
0x0A	05FC270A
0x0B	0000040B
0x0C	0000180C

5.1.2 ADS62P49 interface

The DDR LVDS interface between the ADS62P49 of FMC150 and the FPGA is designed in this section where ADS62P49 is a dual channel 14-bit A/D converter with rates of up to 250 MSPS [42]. The complete LVDS receiver design shows all the necessary blocks required to capture ADC output and are all implemented on the spartan 6 FPGA as illustrated in Figure 5.2. Xilinx spartan 6 FPGA provides these I/O blocks as HDL primitives to manage differential data or clock. More details about the functionality of spartana 6 libraries can be found in [103].

The ADS62P49 uses a serialized LVDS interface in which digital data is provided to the FPGA over seven LVDS pairs per channel. This results in the designed receiver performing a deserialization of incoming signal. The main challenge is how the captured serial data is latched correctly using the bit/serial clock, and how the parallel output data is aligned correctly with the parallel clock.

As depicted in the block diagram of LVDS receiver in Figure 5.2, the received ADC differential signals are converted to single ended signals by *IBUFDS* LVDS input buffers. The signals then pass through *IODELAY2* delay block which introduces delay in each LVDS pair. This is followed by *IDDR2* which is used to transform serial data into parallel data which is eventually presented to DSP modules using two 14-bit buses.

The sampling clock is forwarded by the ADC and is obtained from the LVDS channel. This external clock is connected to the FPGA via *IBUFGDS* differential buffer. To ensure correct timing between the ADC and FPGA, auto-calibration is used to configure or change delay of *IODELAY2* block based on results of ADC pattern tests performed via *SPI control*.

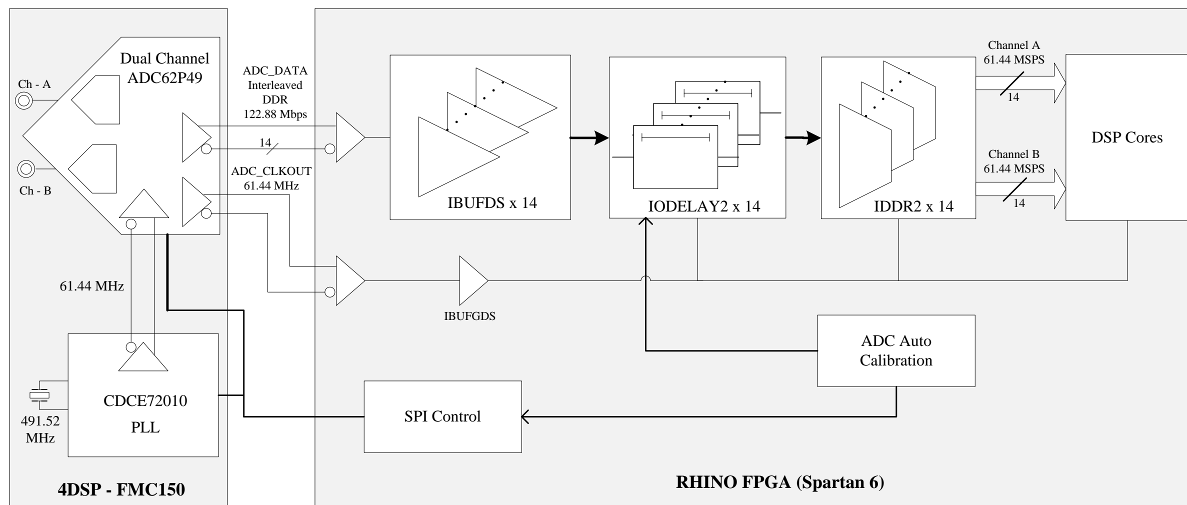

Figure 5.2: The architecture of ADS62P49 interface

5.1.2.1 Sample Rate

The ADS62P49 serial sampling frequency is 61.44Mbps. The parallel sampling clock on the FPGA is determined using the formula shown in equation Figure 5.4. The parallel clock in this design ends up being equal to the serial ADC sampling because the number of LVDS pairs used in each channel equals half of the ADC resolution. The results of using multiple LVDS pairs are increased throughput while the bit clock rate is lowered.

$$\begin{aligned} \text{Sample rate(Hz)} &= \frac{2 \times \text{lvds pairs} \times \text{bit clock(Hz)}}{\text{ADC Resolution}} \\ &= \frac{2 \times 7 \times 61.44 \times 10^6}{14} \\ &= 61.44MHz \end{aligned} \tag{5.4}$$

5.1.2.2 Bit and Word Alignment

Due to delays resulting from PCB traces and FPGA routing, meeting the timing requirements with these effects can be difficult. These effects also give rise to marginal capturing which refers to capturing of data without sufficient setup and hold times in the LVDS receiver [45]. In order to sample ADC data properly, the LVDS channels are delayed appropriately. In this design, this process is controlled by Auto-Calibration block which as illustrated in Figure 5.2. Through SPI programming, the ADC is configured for test pattern mode namely a monotonic ramp inside the FPGA. The auto-calibration operates as follows:

1. The test waits for zero-crossing and then checks if the captured *current ramp sample = previous ramp sample + 1*, if not, the delay of the *IODELAY2* is incremented until the delay of ideal sampling is found.
2. If the delay increment reaches the maximum allowed value without successful monotonic

ramp, the whole calibration is considered to have failed.

3. For successful test, an error free ramp over set maximum value of ramp must be received.

4. After successful search of an ideal delay, the delay is applied globally to two ADC channels. The pass of this test provides enough confidence in set timing requirements for interface between ADC and FPGA.

5.1.3 **DAC3283 interface**

The DAC3283 is a dual channel 16-bit 800 MSPS digital-to-analog converter with an 8-bit LVDS input data bus with on-chip termination, optional 2x and 4x interpolation filters, digital IQ compensation and internal voltage reference. It has a single 8-bit LVDS bus that accepts dual, 16-bit data input in byte-wide format [43].

This section provides a description for DAC interface design using Spartan6 FPGA. Although the DAC3283 is capable of operating at sampling rate as high as 800 MSPS, only 61.44 MSPS DAC rate is realized in this design. The same process of design can be adapted in other lower or higher sampling rate designs.

The DAC interface module takes data on the parallel side and performs 16:1 serialization over the single 8-bit LVDS bus. In a basic application with a just 1-bit LVDS bus, the resulting serial frequency would be 32 times higher than parallel frequency if DDR clock were used and data of two channels were interleaved over a single 1-bit LVDS channel. However, these figures reduce drastically as DAC3283 uses 8-bit LVDS bus to serialize and interleave dual channel 16-bit samples using a DDR sampling clock. Therefore the LVDS interface has two clock inputs, namely adcclock (serial adc data clock) and divclock(parallel side clock). The equation for calculating adcclock is shown in equation 5.5.

$$
\begin{aligned}
f_{\text{adcclock}} &= \frac{f_{\text{divclock}} \times \text{sample width} \times 2 \text{ (Dual Channel Interleaved)}}{\text{lvds pairs} \times 2 \text{ (DDR used)}} \\
&= \frac{61.44 \text{ MSPS} \times 16 \times 2}{8 \times 2} \\
&= 122.88 \text{ MSPS}
\end{aligned}
\tag{5.5}
$$

where f_{adcclock} is serial adc data clock frequency and f_{divclock} is parallel side clock frequency.

The resulting data clock sampling rate of a DAC is 122.88 MSPS when the parallel clock of 61.44 MHz is used. The calculation is shown in equation 5.5 and the schematic of DAC LVDS interface is illustrated in Figure 5.3. Serialization is done by OSERDES2 components which are available in input/out blocks library of Xilinx Spartaran6 [103]. The MMCM (Mixed Mode Clock Management) block receives a 245.76 MHz clock routed from the FMC150 to an FPGA. It generates multiple clocks derived from the input clock. The clocks are distributed to DSP cores, the OSERSES2 and a DAC.

Figure 5.3: The architecture of DAC3283 interface

5.1.4 ADC and DAC Test

The experiments for both ADC and DAC are performed in section 7.6 and 7.7 respectively. The aim is to investigate the highest possible functional ADC sampling rate on RHINO and also converting digital signals to analog at moderate DAC sampling rates using RHINO.

5.2 UDP/IP CORE

One of the high-speed I/O interfaces that a RHINO board has is the 1 Gigabit Ethernet interface. This enables the board to communicate with the external world using popular and standard Ethernet communication. Embedded Ethernet devices, personal computers and other network nodes can exploit the high computation capacity of RHINO by sending and receiving large volumes of data without limitations on high data rates.

In order to make RHINO Gigabit Ethernet interface operational, an FPGA-based Gigabit Ethernet core is needed to configure, monitor and control the Ethernet interface. This section presents a design of a UDP/IP core based on the combination of IPv4 and UDP in order to provide a high-speed and efficient solution for communication over a 1 Gigabit Ethernet. The major goal of implementing Ethernet interface on RHINO is to enable point-to-point high-speed connection to a PC so that measured signals and processed digital streams of data can be captured on the PC for analysis and storage. In addition, remote control of RHINO is also possible by sending control signals and data from a PC. Hence data transfer is supported in both directions.

FPGA devices require EMAC (Ethernet Media Access Controller) to interface with the physical layer (PHY) chip on the board [5]. RHINO uses an integrated Marvell 88E111 PHY chip. The PHY chip is needed for the FPGA to connect with external devices. The user logic can be deployed to configure [5] the EMAC physical interface in wrapper files. In our case, the wrapper files configure the Open-Cores tri-mode MAC [31] which is published under the GNU Lesser General Public License (LGPL). This is a very cost-effective and non-restrictive solution

in comparison with proprietary Media Access Controllers (MACs) such as Xilinx's Tri-Mode Ethernet Media Access Controller (TEMAC) [102] which happen to be costly. Furthermore, the Open-Cores tri-mode MAC IP core supports data rates of 10, 100 and 1000 Mb/s and is compliant with IEEE 802.3 specification [31].

Speed, technology and protocol are carefully chosen to meet high performance data transfers capabilities of Gigabit Ethernet. This is regarded as most crucial part of design when implementing all I/O interfaces as the poor selection of technologies can lead to slow data transfers which is often a bottleneck in a communication link [58, 5]. And ultimately the FPGA processing resources will not be used to their full potential.

The speed of choice is 1000 Mbps. With this speed, theoretical throughput rate slightly below 125 MB/s can be achieved and this is high enough to be used in SDR-domain applications. The technology used is Ethernet because it is low-cost, easily implementable and is commonly used in many computing devices [58]. Since the UDP/IP core will be used in real-time SDR applications where transmission speed is critical, UDP is the transport layer protocol of choice in this project because it has much lower bandwidth overhead and latency in contrast with TCP. Furthermore, given a time constraint of a project which requires project completion over a period of eighteen months, UDP will considerably save us time as it is simple to implement [54].

5.2.1 Overall Architecture

The overall architecture of UDP stack is shown in Figure 5.4. It consists of the functional sub-blocks which constitute a complete UDP/IP stack. Describing this architecture from a UDP/IP stack view-point makes it straightforward to understand design specifics with regard to technologies and protocols involved in each layer.

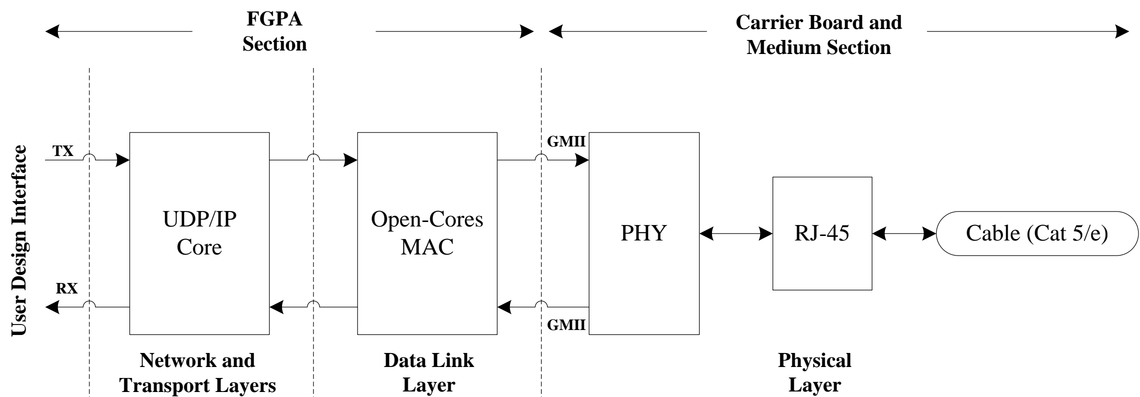

Figure 5.4: Overall architecture of UDP/IP Stack

5.2.1.1 Physical Layer

Starting with the physical layer, the protocol used here is ARP which is used to resolve both the sender and receiver MAC addresses. The 88E111 Gigabit Ethernet transceiver performs most of the physical layer operations needed and more functional details are described in [60, 87]. This PHY chip is configured for Ethernet 1000BASE-T and to operate in full-duplex. The GMII is

used as a standard data interface between a MAC and PHY chip while the MDIO bus is used to send the configuration data from the MAC to a PHY. The PHY then connects to a CAT-5/e cable through RJ-45 connector.

5.2.1.2 Data Link Layer

The data link layer comprises an Open-Cores tri-mode MAC which is responsible for delivering data over a shared physical channel. The MAC consists of three user interfaces that simplify the connection to a MAC core. The MAC is responsible for encoding and decoding user data to/from GMII and MDIO signals. One interface is used for data transmission, another one for data reception and the last one for configuration of PHY chip. All signals of the interface are clocked at the rising edge of *Clk_user*.

The transmit interface of the of the MAC is shown in Figure 5.5. This is used to send custom packets of different protocols to a destination device. In our case, UDP and ARP protocol packets are sent and will be discussed in more detail in later sections.

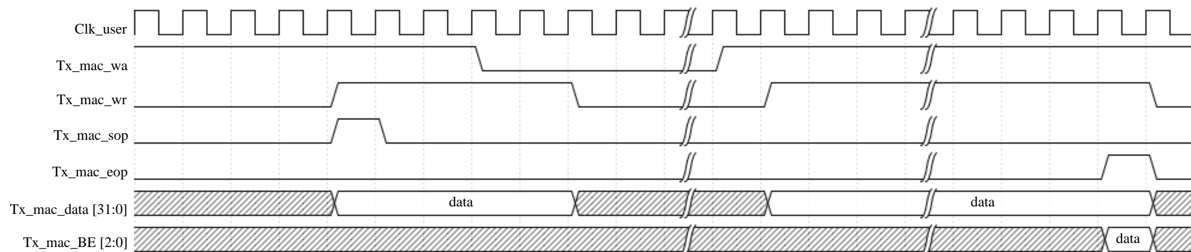

Figure 5.5: MAC core transmit operation [31]

Tx_mac_wa remains high to indicate available space in the transmit FIFO of a MAC. When *Tx_mac_wr* is high, it denotes that data write is ready and therefore *Tx_mac_sop* which signals a start of packet operation is quickly set high for one clock cycle. The packet data is then sent into MAC FIFO via 32-bit *Tx_mac_data[31:0]* bus. Data write to FIFO is paused each time *Tx_mac_wr* goes low and resumes when *Tx_mac_wr* goes high. *Tx_mac_eop* signals the end of the packet and is set high for one clock cycle. The *Tx_mac_BE[2:0]* is used for byte enable. The number of bytes and the corresponding values of *Tx_mac_BE[2:0]* are described in Table 5.3. Since our application use 32-bit bus to transmit packets, “00” is used as the value of a byte enable signal.

Table 5.3: Byte Enable Configurations

Tx_mac_BE[2:0] and Rx_mac_BE[2:0] (binary)	Number of bytes
00	4
01	1
10	2
11	3

Furthermore, the receiver interface of the MAC is illustrated in Figure 5.6. This is used to receive packets from the sender, that is, UDP and ARP packets from a remote device are received

by the user logic. *Rx_mac_ra* is a read-available signal that denotes the availability of data in the receive FIFO of the MAC. It also signals the package has been received successfully and is ready to be saved or read. *Rx_mac_rd* is asserted as long as the *Rx_mac_ra* signal is high to enable output of data received. The *Rx_mac_pa* also known as "package-available" signals the valid read data on 32-bit *Rx_mac_data[31:0]* bus. Both the *Rx_mac_sop* and *Rx_mac_eop* are used to signal start of packet and end of packet respectively. The *Rx_mac_BE[2:0]* works in the same manner as *Tx_mac_BE[2:0]* above to hold the byte enable value.

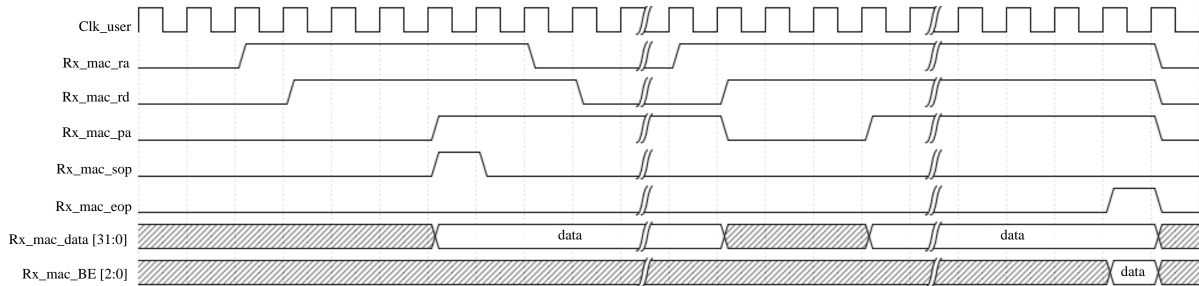

Figure 5.6: MAC core receive operation [31]

MDIO is used for configuration and status read of the PHY device. The MAC provides a simplified interface to MDIO as described in [62]. Using the FPGA user logic, the write operation is initiated by asserting *WctrlData* as shown in Figure 5.7. At this point, the PHY device address *Fiad[4:0]*, the configuration data *Ctld[15:0]*, the PHY register address *Rgad[4:0]* must hold valid values. The *Busy* signal goes high as soon as the write operation begins and it signals operation completion when it goes low.

The status read process starts by asserting *Rstat*. It also indicates that the *Fiad[4:0]* and *Rgad[4:0]* are valid. The *Busy* signal goes high to indicate that read operation is in progress. When the *Busy* signal goes low, it signals the valid status data on *Prsd[15:0]* line. Finally, the *NoPre* indicates that the preamble is sent when its set low. When it is high it means there is no preamble in the sent configuration data.

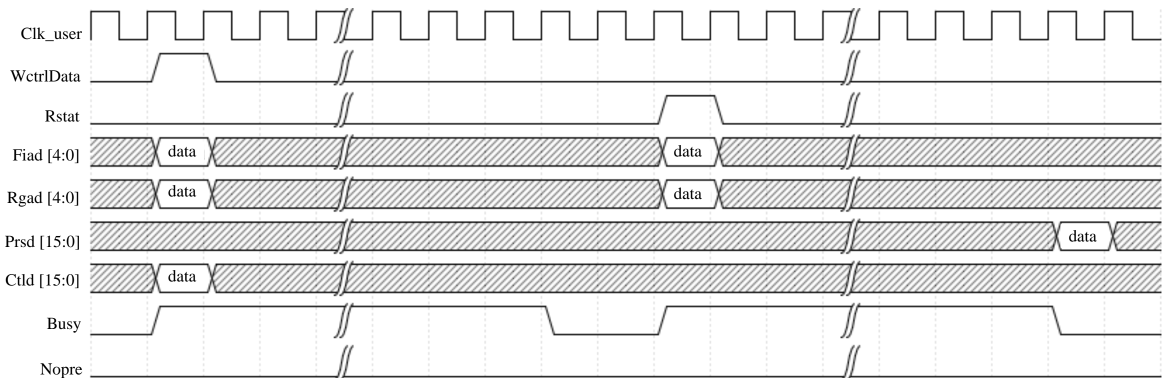

Figure 5.7: PHY Management interface

The MAC core also has specific configurations to control the core operation itself. Unlike the PHY Configuration which is done via MDIO interface, the MAC core configurations are performed by simply changing the constant register values in a configuration ROM. The registers

are fully described in [31]. Table 5.4 only shows the configurations that have been modified for RHINO UDP core while the rest remain default.

Table 5.4: MAC core register description

Register Name	Address (hex)	Value (hex)	Description
tx_pause_en	011	0001	Enables MAC to pause transmission when transmit FIFO is full.
CRC_chk_en	024	0001	Enables dropping of packets with FCS checksum error.
Speed	034	0004	Sets the Ethernet MAC core's speed level to 1000 Mbps

5.2.1.3 Network Layer

ARP is a network layer protocol used at data-link layer to map IP address to MAC address for hop-to-hop communication. Furthermore, in network layer, the internet protocol (IPv4) is used by the designed UDP core to deliver messages between the RHINO and destination device. The IP addresses are configured statically and they must be in the same subnetwork for successful communication to happen.

5.2.1.4 Transport Layer

Lastly UDP is chosen as a transport layer protocol. It is used in this design for its simplicity and the fact that it supports high speed and real-time data transfers.

5.2.2 Structure of the UDP/IP core

The architecture of the UDP core is illustrated in Figure 5.8. It consists of a UDP wrapper which simplifies usage of the core. It also has a MAC wrapper provided by open-cores which substantially reduces development time by providing functions needed to connect to PHY. The FIFOs of the MAC are driven by a system reference clock of 100 MHz. The UDP core provides GMII interface to a PHY and another interface to user design logic. On the GMII interface, the globally routed 125 MHz clock is needed to operate GMII transmit operation. While the PHY provides 125 MHz reference clock, this is not used. Rather, a 125 MHz clock is derived from the system clock using PLL primitive of spartan 6. Using ODDR2 on the spartan 6, the clock is driven and fed to the external *GIGE_GTX_CLK* output pin. If the ODDR2 is not used, the clock will never work. GMII receive operation is also driven by a 125 reference clock namely *GIGE_RX_CLK* which is generated by PHY.

The UDP wrapper core consists of sub-blocks which make it possible to send and receive ARP and UDP packets. The cores simplify the user design logic by storing static header fields of the

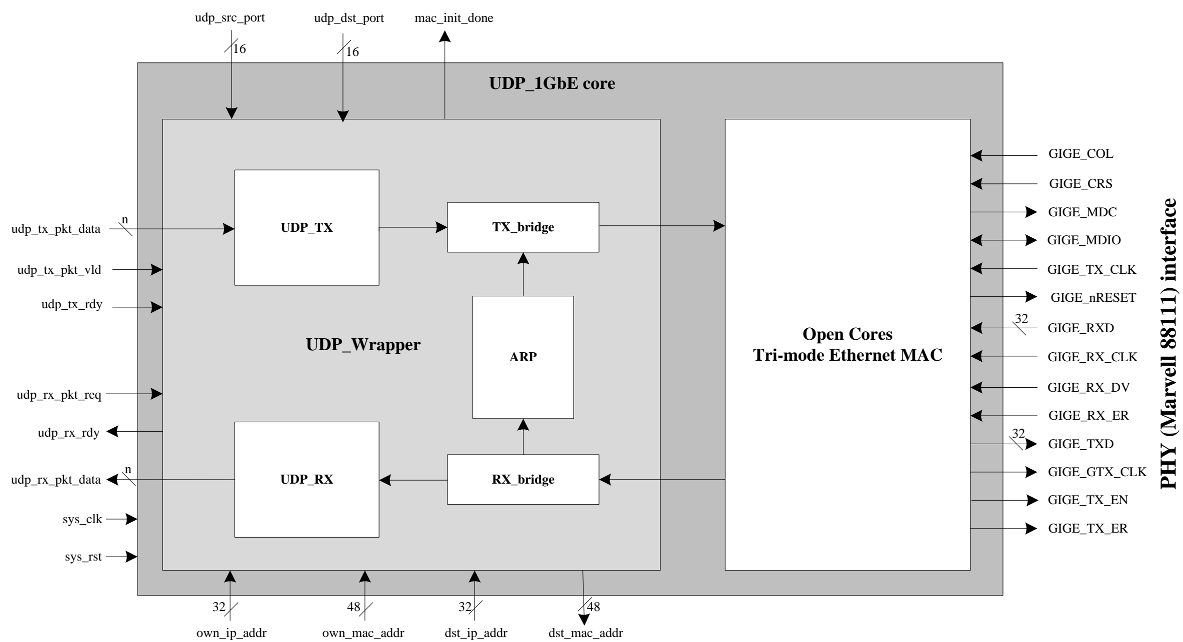

Figure 5.8: Structure of UDP/IP Core based on a Gigabit Ethernet

ARP and UDP packets in the lookup table. Only dynamic data such as the ports, ip addresses and payload are sent to the core by the user.

The *ARP* block enables the ARP process when the core initializes. This happens seamlessly and it takes place before the actual UDP packets can be sent or received. It is important that before communication the RHINO board and the remote device know each other's IP and MAC address. Initially, both devices already know each other's IP addresses as they are statically configured but they have no knowledge of the MAC addresses. This is where ARP is used to resolve the MAC addresses when the IP addresses are known by both devices.

The ARP process begins with the FPGA that sends a broadcast ARP request together with its own MAC and IP addresses and a destination IP address and polls for ARP response from a remote device. After the ARP response is received, it updates the ARP table with the received MAC address and soon after this the UDP transmission is ready to be initiated. The FPGA will also respond to ARP requests from the remote device in the midst of UDP communication.

The ARP request packet structure is shown in Figure 5.10. The operation field indicates whether the packet is a request or a response. The value of 0x01 denotes a request and 0x02 shows a response. The source and destination IP addresses are variable, the source MAC address is variable too and are all provided in user design, and the rest of the fields are static. The FPGA ARP request uses the static broadcast address "FF:FF:FF:FF:FF:FF" in the destination MAC address field of the ARP packet. For the ARP response, the destination MAC address field is filled with the known MAC address of the remote device.

Moreover, the *UDP_tx* module manages the UDP packet transmission over IP. It uses the interface shown in Figure 5.7 to send data to a destination device. The transmission requires that

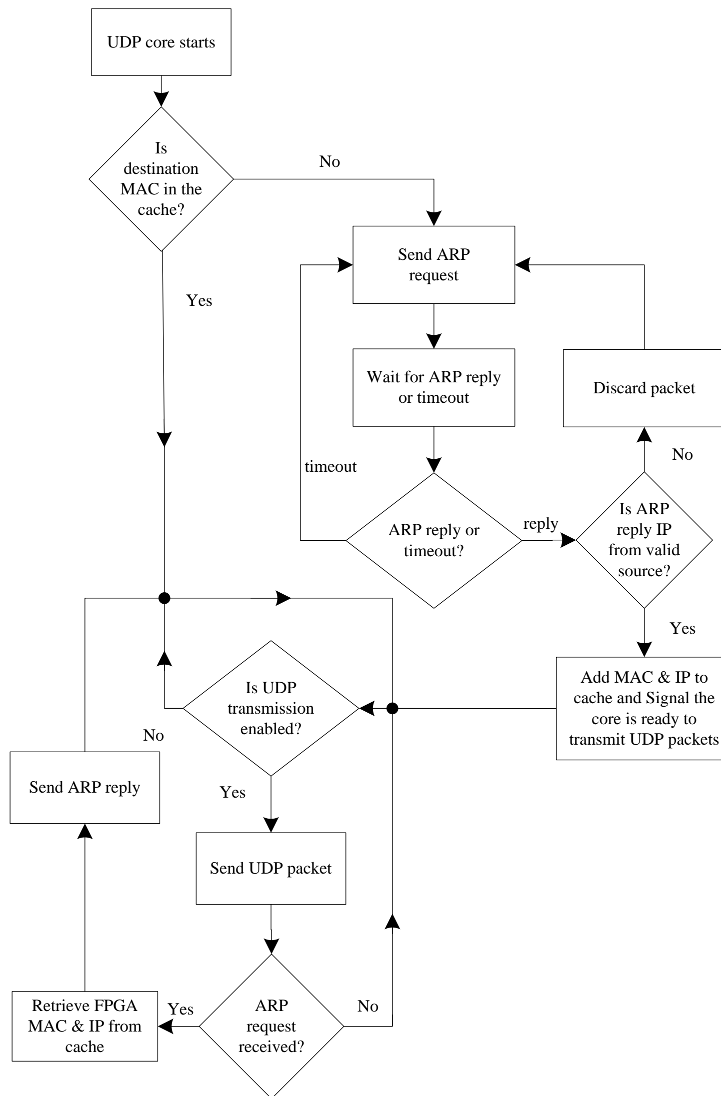

Figure 5.9: ARP protocol operation data flow diagram

0 – 7	8 – 15	16 – 23	24 – 31
Destination MAC Address [47:16]			
Destination MAC Address [15:0]		Source MAC Address [47:32]	
Source MAC Address [31:0]			
Ethernet Type (0x0806)		Hardware Type (0x0001)	
Protocol Type (0x0800)		Hardware Address Length (0x06)	Protocol Address Length (0x04)
Operation		Source MAC Address [47:32]	
Source MAC Address [31:0]			
Source IP Address [31:0]			
Destination MAC Address [47:16]			
Destination MAC Address [15:0]		Destination IP Address [31:16]	
Destination IP Address [15:0]		0x0000	

Figure 5.10: The structure of ARP packet

the user provides source and destination IP and MAC addresses along with the UDP source and destination ports. The user design also provides payload. The maximum number of bytes in the payload is 1500.

The UDP packet structure is illustrated in Figure 5.11. It comprises the MAC, UDP and IPv4 headers. The transmitter attaches four bytes of checksum to the end of each packet. This is required to check the integrity of data when it arrives at the destination. The total length field is calculated as the sum of 20 bytes of IP header, 8 bytes of UDP header and payload length. While the length field is the sum of 8 bytes of UDP header and payload length.

<table>
<tr><th>0 7</th><th>8 15</th><th>16 23</th><th>24 31</th></tr>
<tr><td colspan="4">Destination MAC Address [47:16]</td></tr>
<tr><td colspan="2">Destination MAC Address [15:0]</td><td colspan="2">Source MAC Address [47:32]</td></tr>
<tr><td colspan="4">Source MAC Address [31:0]</td></tr>
<tr><td colspan="2">Ethernet Type (0x0806)</td><td>Version Header</td><td>Different Services</td></tr>
<tr><td colspan="2">Total Length</td><td colspan="2">Identification</td></tr>
<tr><td colspan="2">Flags/Fragment offset</td><td>Time to live</td><td>Protocol</td></tr>
<tr><td colspan="2">Header Checksum</td><td colspan="2">Source IP Address [31:16]</td></tr>
<tr><td colspan="2">Source IP Address [15:0]</td><td colspan="2">Destination IP Address [31:16]</td></tr>
<tr><td colspan="2">Destination IP Address [15:0]</td><td colspan="2">Source Port</td></tr>
<tr><td colspan="2">Destination Port</td><td colspan="2">Length</td></tr>
<tr><td colspan="2">Checksum</td><td colspan="2">Data</td></tr>
<tr><td colspan="4">Data</td></tr>
</table>

Figure 5.11: The structure of a UDP packet

Lastly the *UDP_rx* block takes of received UDP packets sent by a remote device. The UDP packets are read using the receive interface shown in Figure 5.6. The destination IP and MAC addresses of UDP packets received must match with FPGA configured addresses, else the packets are dropped. The packets are also dropped if the checksum is incorrect. The maximum receiver payload still remains as 1500 bytes. The structure of the received UDP packet never changes and still looks like the one shown in Figure 5.11.

5.2.3 Marvell 88E1111S/PHY initialization

The designed UDP/IP core initialization process configures the PHY register settings accordingly before the actual UDP communication begins. MDIO is a serial communication bus that is used to transfer data between a MAC and a PHY when configuration and Status Read occurs. The PHY address used in serial communication is 0x01. Table 5.5 shows a state machine that is used to initialize the PHY. In each state, the register write occurs and it is followed by a read operation of the same register address. The write operation is considered successful when the written and read register values match. The state machine then progresses to the next state when the write is successful else initialization fails and the whole initialization process starts anew.

5.2.4 UDP/IP Core Interface

The UDP core is designed to simplify interfacing to the user top-most design entities. With all the encapsulation and decapsulation of headers in both the ARP and UDP packets taking place in the UDP core. The user only assigns communications parameters and quickly starts sending

Table 5.5: State Machine for initialization of PHY register settings

State	Action
STATE 0	Wait 5 seconds to bring PHY out of reset.
STATE 1	Set PHY to GMII Copper mode.
STATE 2	Set link speed to 1000 Mbps.
STATE 3	Set copper duplex mode to full-duplex.
STATE 4	Enable crossover.
STATE 5	Set HWCFS_MODE = GMII to Copper
STATE 6	Enable MAC pause.
STATE 7	Enable Auto-negotiation.
STATE 8	Disable 125 MHz clock output.
STATE 9	Wait 5 seconds for link to come up, if link is up within 5 seconds initialization is complete else go to STATE 0.

and receiving UDP packets to and from the remote device. The functions are performed at the rising edge of a 100 MHz system reference clock

As shown in Figure 5.12, the UDP/IP core provides an interface for sending UDP packets. The *sys_rst* keeps the core in a reset state. The UDP Core initialization commences as soon as it gets out of the system reset. At this point, the communication parameters should be valid. This includes source and destination UDP ports (*udp_src_port[15:0], udp_dst_port[15:0]*), IP addresses (*own_ip_addr[31:0], dst_ip_addr[31:0]*) and RHINO FPGA MAC address namely *own_mac_addr[47:0]*. *dst_mac_addr[47:0]* is MAC address of a remote device and it becomes valid only after initialization completes which is indicated by *mac_init_done*.

Thereafter, the UDP core raises *udp_tx_rdy* to signal that the core is ready to transmit packets. To start packet transmission, the *udp_tx_vld* is asserted by the core and this also indicates there is valid UDP packet data on *udp_tx_pkt_data[UDP_TX_DATA_BYTE_LENGTH * 8:0]* bus. The generic parameter *UDP_TX_DATA_BYTE_LENGTH* is used in the design to specify the number of bytes of the transmitted UDP frame.

There is only a slight difference between UDP Packet transmission and reception as shown in Figure 5.12 and Figure 5.13 respectively. Everything stays the same except that the *udp_rx_rdy* is set high by the UDP core to indicate that UDP packet data has been received and is ready to be read from *udp_rx_pkt_data[UDP_RX_DATA_BYTE_LENGTH * 8:0]* bus. Reading the received packets is initiated by asserting the *udp_rx_req*. The generic parameter *UDP_RX_DATA_BYTE_LENGTH* is used in the design to specify the number of bytes in the received UDP frame.

5.2.5 **UDP/IP Core Test**

In order to validate and evaluate the functionality of the implemented UDP/IP core, thorough testing of the core is performed in section 7.5. This involves investigating the throughput, speed and integrity of the transferred data.

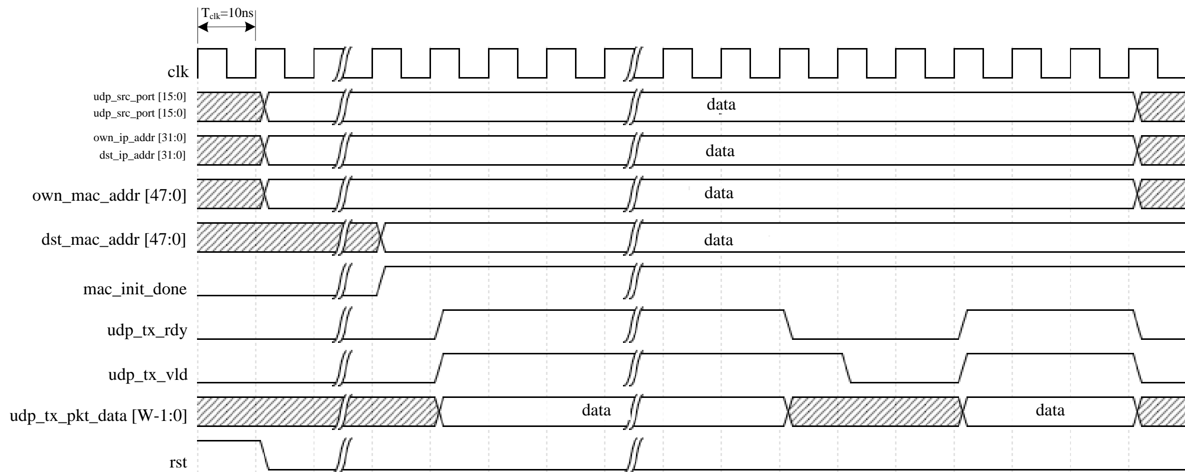

Figure 5.12: UDP Core Write operation interface

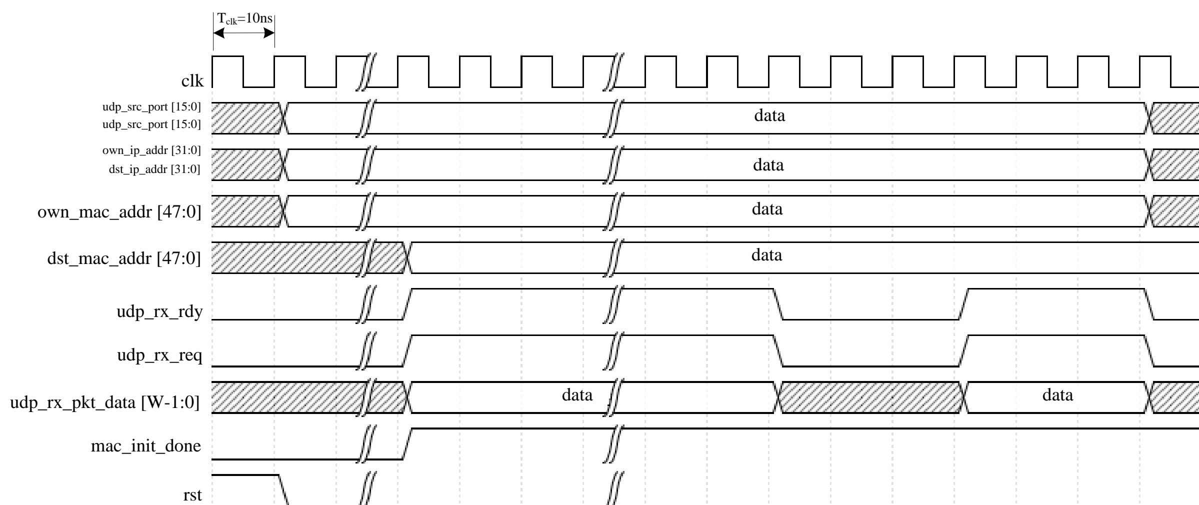

Figure 5.13: UDP Core Read operation interface

CHAPTER 6

DESIGN OF FM RECEIVER

This chapter presents the design of a wide-band digital FM receiver to show case rapid application development of SDR using a proposed library of reusable IP blocks. Using these IP blocks which incorporate DSP cores and I/O communication cores, the prototype serves as a proof of concept that the blocks can be used not only in this FM receiver design, but also in other real-time SDR applications. Choosing FM receiver is based on the fact that the receiver is more difficult than a transmitter in terms of software processing. FM is also more complex than other modulation techniques such AM and it essentially needs more processing blocks. Furthermore, the licensing issues of spectrum regulation have restrained us to use a freely available FM channels for receiving and demodulation. The fundamental concepts of frequency modulation and demodulation are described in section 2.11. The complete design of FM receiver comprises an RF analogue frontend circuitry and digital receiver which forms the largest part of the FM receiver processing.

6.1 DESIGN OF DIGITAL RECEIVER

The digital receiver processing is implemented with a DDC core and FM demodulator. The block diagram showing processing blocks is shown in Figure 6.1. Details of a DDC core operation have been described in Section 4.4 of Chapter 4.

The 20 MHz bandwidth RF signal is digitized with 14-bit precision ADC of FMC150 card. The IF signal ranges between 88 MHz and 108 MHz resulting in 20 MHz bandwidth of FM signal. The digitized FM signal is defined by equation 6.1. Typically, a very high speed ADC of at least $108MHz \times 2 = 216MHz$ is required to digitize the signal. However, this is slightly above 163.84 MHz which is the maximum ADC speed achieved on RHINO.

$$x_{FM} = A_c cos[\omega_c n + \varphi_{FM}[n]], \tag{6.1}$$

where,

where carrier phase deviation is $\varphi_{FM}[n] = k_{vco} \sum_{i=0}^{n-1} S_N[i]$, S_N is baseband signal, $k_(vco)$ is frequency sensitivity and x_{FM} is FM signal.

As an alternative to using a high speed ADC, band-pass sampling [97] is employed in this

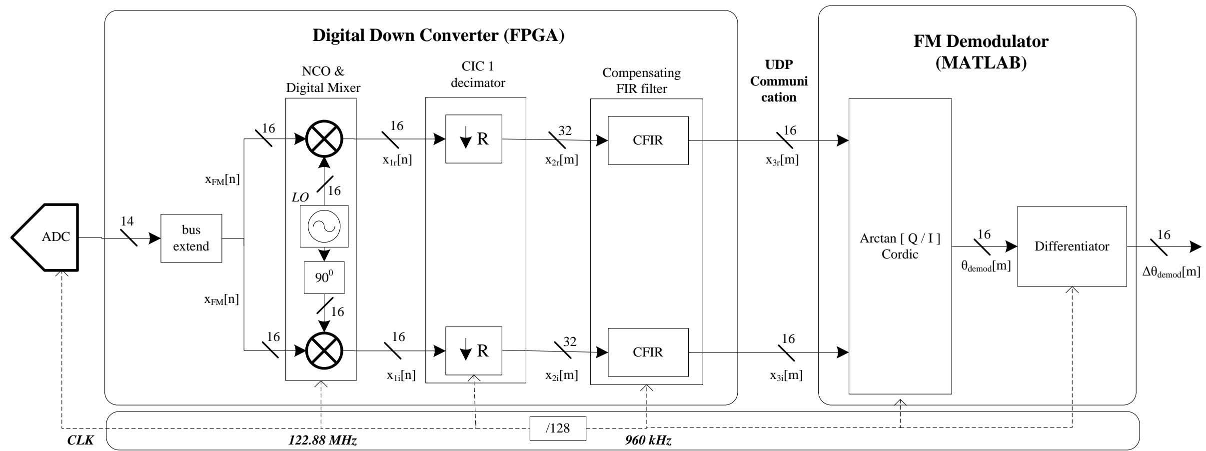

Figure 6.1: Digital FM receiver architecture

design. Bandpass sampling of FM signal enables low ADC sampling speed and frequency translation of FM channels from high centre frequency to low centre frequency. Using the bandpass criterion in equation 6.2, n falls in a range 1 to 5. We choose $n = 2$ and this results in a wide frequency range of 108MHz - 176MHz valid for ADC bandpass sampling. We choose 122.88 MSPS as the ADC bandpass sampling speed. Using this frequency, the sampled FM band signals are downshifted from 88-108MHz frequency band to 14.88-34.88MHz frequency band.

$$\frac{2f_H}{n} \leq f_s \leq \frac{2f_L}{n-1}, \tag{6.2}$$

where n is given by $1 \leq n \leq \frac{f_H}{f_H - f_L}$, f_H is high frequency and f_L is low frequency.

The 14-bit samples received from the ADC are extended to 16-bit signed words which are directed into the DDC core input. To generate a complex baseband I/Q signal, the sine and cosine waveforms are generated from the NCO core and then multiplied with the digital quadrature mixer. The frequency of the NCO output is chosen depending on the channel to be selected in the received FM band signal, that is, the output sine/cosine frequency must be equal to the frequency of band-sampled FM signal. The selected channel falls in the frequency range of 14.88 MHz and 34.88 MHz.

Although the FM channel is found in higher 88-108 MHz frequency range, the NCO frequency remains much lower than that because bandpass sampling aliases all the channels to first Nyquist Zone. Care is taken when selecting the local frequency, for instance, a 94.5 radio station would appear at 28.38 MHz after bandpass sampling. The expression for finding the frequency of a particular channel after sampling is described in equation 6.3. If the result falls above the first Nyquist when using this equation, it must be folded back into first Nyquist by subtracting the result from the ADC sampling which is 122.88 MSPS in our case.

$$f_{signal} \bmod f_{sample_rate}, \text{[14]} \tag{6.3}$$

For commercial FM broadcasting in South Africa, the maximum frequency deviation Δf is 75 kHz [46] and Carson's rule estimates the bandwidth when maximum audio message (f_m) of 15kHz is used. The bandwidth is $BW \approx 2(\beta + 1)f_m = 2(5 + 1)15kHz = 180kHz$ where β is modulation index defined by $\beta = \Delta f / f_m = 75kHz/15kHz = 5$. The commercially allocated bandwidth for each channel is 200kHz [46]. This information is therefore enough to determine the cut-off frequency. The cut-off frequency of the filter needs to be slightly above or equal to $BW/2 = 90$. This is safest point as the 180 kHz of bandwidth is normally more than enough relative to information FM broadcasters send in the allocated channel. The selectivity of the receiver is determined by the designed filter which is 80kHz at -6dB and 150kHz at -60dB. This is selective enough to isolate the selected channel from closest channels.

After mixing down the FM signal using the quadrature mixer, the image and mixer products are eliminated by the CIC filter which uses zero multipliers in its implementation. The CIC filter specification parameters are shown in Table 6.1. This CIC filter also decimates the 122.88 MSPS ADC rate to 960 kSPS by decimating ratio of 1:128. Despite its low cost, efficient and simple implementation, the CIC filter introduces undesirable droop in its filter response passband [7]. To eliminate this non-flat response in the passband of the CIC filter, the compensation FIR filter is used.

Table 6.1: Parameters of CIC-1 Filter

Parameter	**Value**
Input sample rate	122.88 MSPS
Ouput sample rate	960 kSPS
Decimation factor (R)	128
Number of CIC stages (N)	10
Differential delay (M)	1

The compensation filter specification parameters are listed in Table 6.2 while its response is shown in Figure 6.2. In this same figure, the CIC filter response is shown and the resulting total response after compensation.

Table 6.2: Parameters of a Compensating Filter

Parameter	**Value**
Input sample rate	960 kSPS
Ouput sample rate	960 kSPS
Number of coefficients	21
Cut-off frequency	90kHz
Stopband attenuation	10dB

In order to mathematically analyse the operations that the down-conversion undergoes, the equations 6.4, 6.5 and 6.6 have been provided below. They show the derivation of real and imaginary signals in the each stage of the DDC core.

$$x_1[n] = x_{FM} \cdot LO, \tag{6.4}$$

where local oscillator frequency $LO = e^{-j\omega_c \frac{n}{f_{AD}}}$ and f_{AD} is ADC sampling frequency.

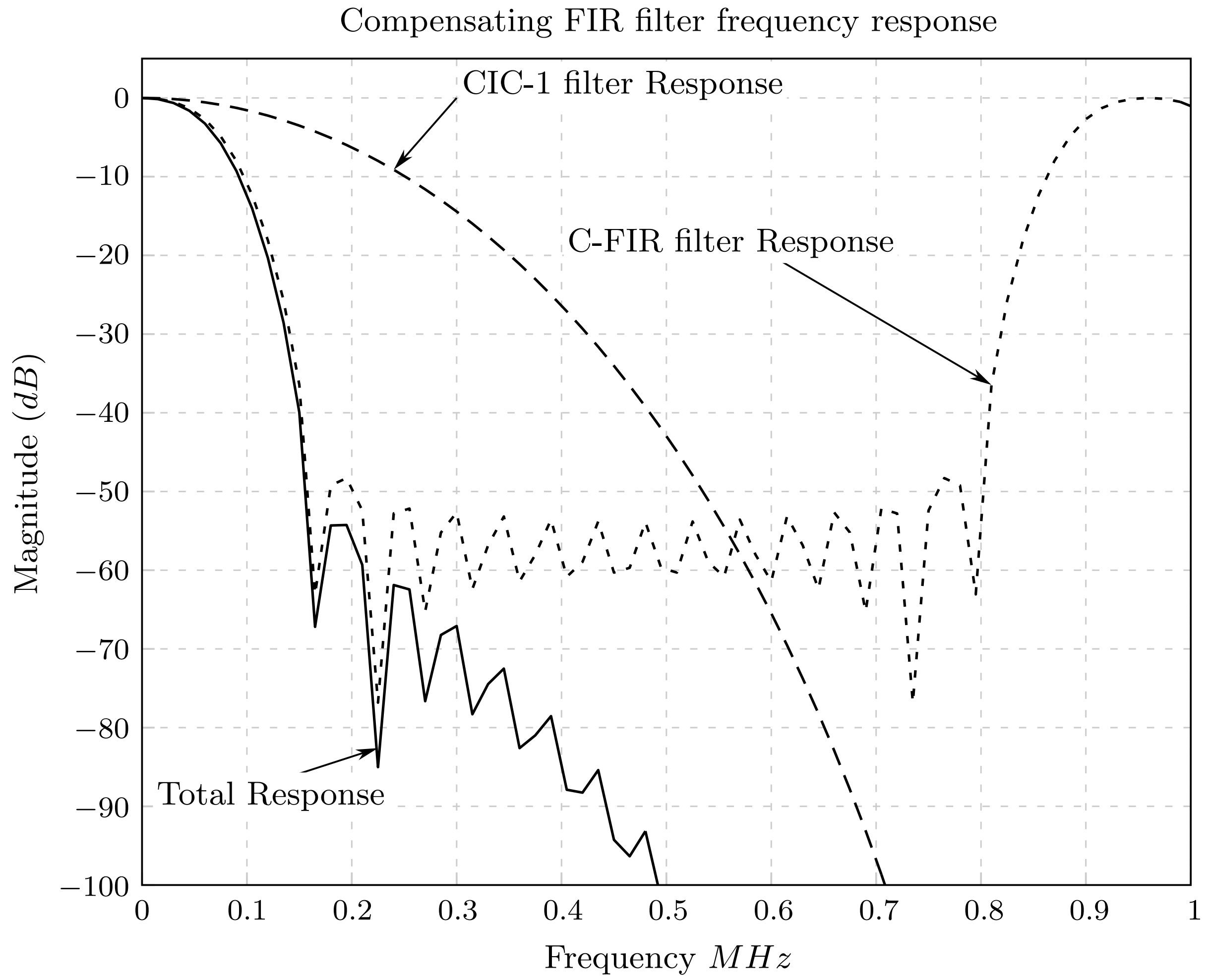

Figure 6.2: Compensation Filter Response for 10-stage CIC-1 filter

The resulting quadrature signals are expressed as below:

For Real signal :

$$\begin{aligned}
x_{1r}[n] &= x_{FM} \cdot cos[\omega_c n] \\
&= A_c \cdot cos[\omega_c n + \varphi_{FM}[n]] \cdot cos[\omega_c n] \\
&= \frac{A_c}{2}\left(cos[\omega_c n + \varphi_{FM}[n] - \omega_c n] + cos[\omega_c n + \varphi_{FM}[n] + \omega_c n]\right) \\
&= \frac{A_c}{2} cos[\varphi_{FM}[n]] + \frac{A_c}{2} cos[2\omega_c n + \varphi_{FM}[n]] \\
x_{2r}[m] &= x_{1r}[n] * h_{cic1}[n] \\
&= \frac{A_c}{2} cos[\varphi_{FM}[m]] \\
x_{3r}[m] &= x_{2r}[m] * h_{fir}[m] \\
&= \frac{A_c}{2} cos[\varphi_{FM}[m]]
\end{aligned} \tag{6.5}$$

For Imaginary signal :

$$
\begin{aligned}
x_{1i}[n] &= x_{FM} \cdot sin[\omega_c n] \\
&= A_c \cdot cos[\omega_c n + \varphi_{FM}[n]] \cdot sin[\omega_c n] \\
&= \frac{A_c}{2}\left(sin[-\omega_c n - \varphi_{FM}[n] + \omega_c n] + sin[\omega_c n + \varphi_{FM}[n] + \omega_c n]\right) \\
&= \frac{A_c}{2} sin[-\varphi_{FM}[n]] + \frac{A_c}{2} sin[2\omega_c n + \varphi_{FM}[n]] \\
x_{2i}[m] &= -1 \cdot x_{1i}[n] * h_{cic1}[n] \\
&= \frac{A_c}{2} sin[\varphi_{FM}[m]] \\
x_{3i}[m] &= x_{2i}[m] * h_{fir}[m] \\
&= \frac{A_c}{2} sin[\varphi_{FM}[m]]
\end{aligned}
\tag{6.6}
$$

where x_1 is NCO output, x_2 is CIC-1 output, x_3 is a compensation FIR filter signal, h_{cic1} is impulse response for CIC1 and h_{fir} is impulse response for a compensation FIR filter.

At this stage, the RF signal has been down-converted to complex baseband I/Q signal. The 16-bit baseband I/Q samples are concatenated and then sent to a PC as 32-bit words using UDP. At the PC end, FM demodulation is performed. The arctangent-differentiator [77] is chosen because it more efficient than its I/Q demodulator counterparts. The arctan function recovers the phase of the modulated signal followed by derivative of phase which yields the original modulating message. Equation 6.7 shows how the demodulation process is done by using the I/Q samples obtained from the last stage of the DDC core through 1 Gigabit Ethernet interface.

$$
\begin{aligned}
\theta_{dem} &= tan^{-1}\left[\frac{x_{3i}}{x_{3r}}\right] \\
&= tan^{-1}\left\{\frac{\frac{A_c}{2} sin[\varphi_{FM}[m]]}{\frac{A_c}{2} cos[\varphi_{FM}[m]]}\right\} \\
&= tan^{-1}\left\{\frac{sin[\varphi_{FM}[m]]}{cos[\varphi_{FM}[m]]}\right\} \\
&= tan^{-1}\{tan[\varphi_{FM}[m]]\} \\
&= \varphi_{FM}[m] \\
\Delta\theta_{dem}[m] &= \frac{d}{dm}\left\{k_{vco}\sum_{i=0}^{m-1} S_M[m]\right\} \\
&= k_{vco} \cdot S_M[i]
\end{aligned}
\tag{6.7}
$$

6.2 DESIGN OF ANALOG RF FRONT-END

This section presents the design of an analogue RF front-end for the wideband FM receiver. The block diagram of the frond-end design is shown in Figure 6.3. The indoor FM antenna with a variable gain of 36dB receives -65dBm FM signal in the frequency range of 88-108MHz.

The front-end also provides a bandpass filtering of FM band and a total gain of 75dB which is determined as in equation 6.8. The specifications of the components used to realize the front-end are summarized in Table 6.3.

$$\begin{aligned} \text{Total Front-End Gain (dB)} &= P_{\text{fmc150-ADC}}(dBm) + P_{\text{fm-signal}}(dBm) \\ &= 10 + 65 \\ &= 75dB \end{aligned} \tag{6.8}$$

where $P_{\text{fmc150-ADC}}$ ADC input signal power in dBm and $P_{\text{fm-signal}}$ is FM signal power in dBm.

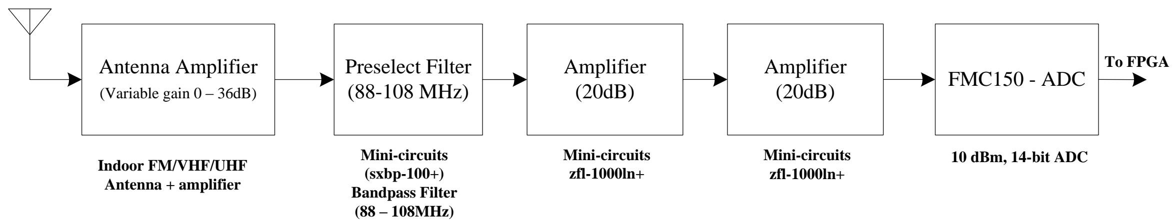

Figure 6.3: Block diagram of a Analog RF front-end

Table 6.3: Specifications for commercial RF components

Component	Manufacturer	Model Number	Specifications
Antenna	ELLIES	AAAST	**Freq range:** 88-108MHz, 175-250MHz, 470-860MHz **Gain:** 0-36dB **Noise Figure:** leq 5dB **Gain:** VHF 30dB UHF 36dB **Noise Figure:** leq 5dB
Bandpass filter	Minicircuits	sxbp-100+	**Center Freq:** 100MHz **Bandwidth:** 30MHz **Insertion Loss:** leq 3dB
RF amplifier	Minicircuits	zfl-1000ln+	**Freq Range:** 0.1 - 1000MHz **Noise Figure:** 2.9dB **Gain: Gain:** 20dB

CHAPTER 7

RESULTS AND DISCUSSION

This chapter describes the tests that were carried out in order to ensure that the IP blocks were designed and developed according to specified user requirements in section 3.1. The blocks under test were designed in Chapter 4 and 5. The wideband FM receiver which was designed in Chapter 6 using the developed IP blocks was also tested to demonstrate that developed library can be reusable and reliably functional in the SDR context. All these tests will also provide basis for conclusions and recommendations to be made in Chapter 8. The experimental setup showing hardware and software tools used is shown in Figure 7.1.

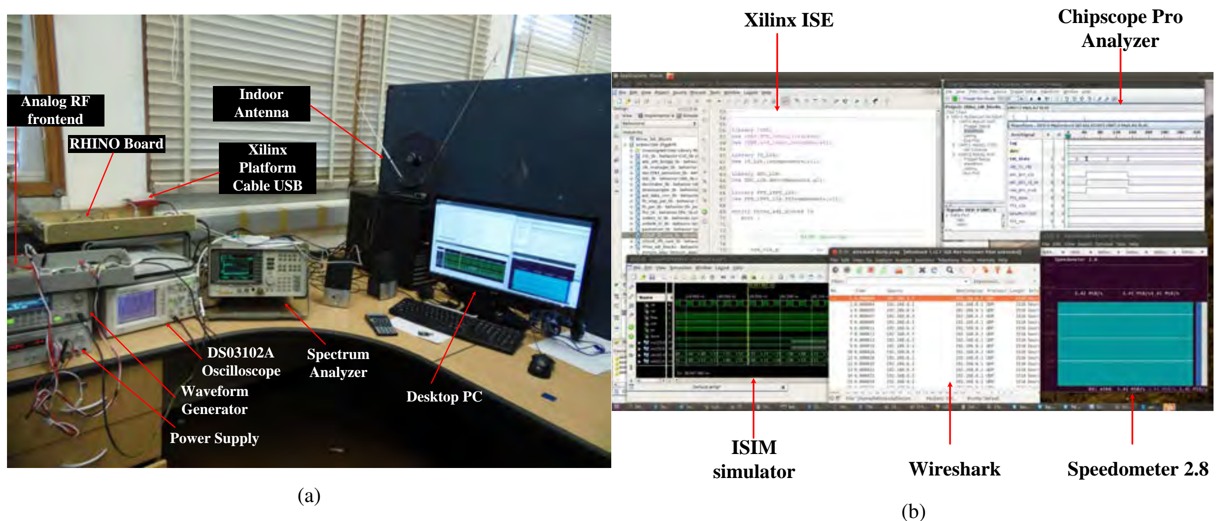

Figure 7.1: Experimental environment showing Hardware and Software Tools use in this project

7.1 FIR CORE TEST

This section describes how the FIR IP core designed in section 4.1 was verified for its validity using VHDL testbench and ISIM simulator. The results were plotted and compared to ideal Matlab filter simulation results. The VHDL component of the core is provided in Appendix B.1 while the scripts are found in Appendix B.2 and B.3.

The FIR core was verified by designing length L = 95 FIR band-pass filter to specifications

Table 7.1: Bandpass filter specifications generate FIR core coefficients

Parameter	**Value**
Sampling frequency	10 kHz
Lower cutoff frequency	2190 Hz
Higher cutoff frequency	2215 Hz
Passband ripple	3 dB
Stopband attenuation	80 dB
Number of coefficients	95

shown in Table 7.1. The resulting Parks-McClellan optimal FIR coefficients of 16-bit width are illustrated in Figure 7.3b in a form of filter frequency response. The filter was tested on an input signal consisting of a sum of sinusoids at frequencies 440, 800, 2200 and 2500 Hz as shown in Figure 7.3a. This input signal was created as vector of samples quantized to 16-bit precision using Matlab script in Appendix B.2.

Table 7.2: FIR core parameter configurations

Parameter	**Value**
DIN_WIDTH	16
DOUT_WIDTH	16
COEFF_WIDTH	16
NUMBER_OF_TAPS	95
LATENCY	0
COEFFS	A vector of filter response in Figure 7.3b

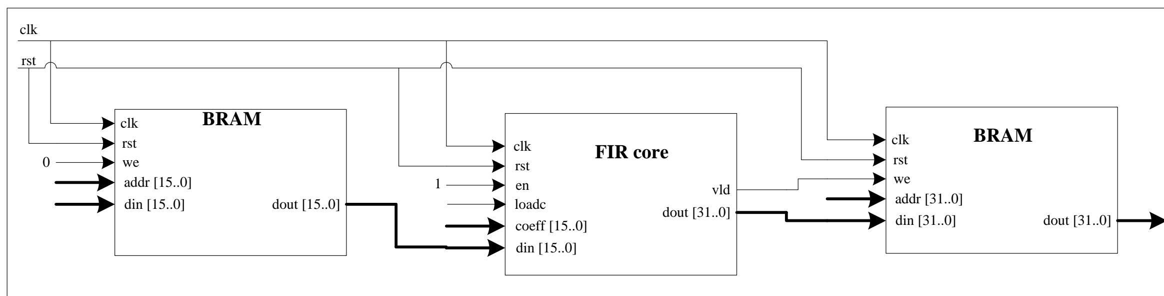

Figure 7.2: FIR core Testbench block diagram

To perform the experiment, the testbench was created as in Figure 7.2. The input signal stored in memory was processed by the FIR core to single out the 2200Hz sinusoidal component shown in Figure 7.3d. The result closely matches with the output of the ideal filter in Matlab shown in Figure 7.3c. The SNR has of the output has slightly decreased due to quantization of coefficients and results before and during core processing.

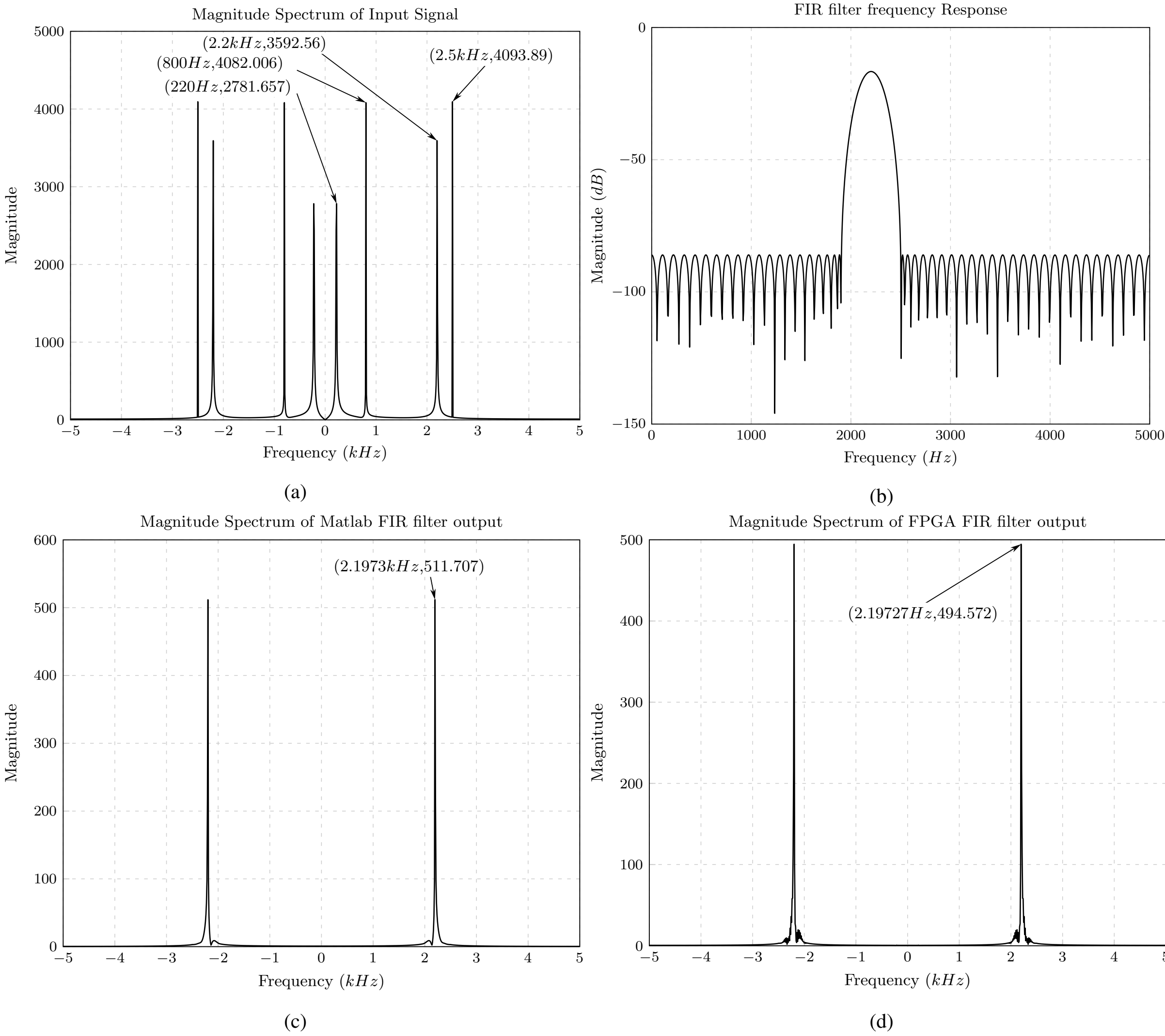

Figure 7.3: The results FIR filter testbench.

7.2 IIR CORE TEST

This section outlines testing of IIR core designed in section 4.2. The aim was to demonstrate the operation of high order IIR filter implemented with a cascade of second order sections (SOS) and using VHDL tesbench and ISIM to verify IP core functionality and validity. The coefficients were scaled as explained in section 4.2 to avoid overflow of results due to precision of an FPGA. Matlab was used to generate input vector and to compare the IP core results with ideal IIR simulation results of Matlab. All relevant Matlab scripts are provided in Appendix C.2 and C.3 whereas the VHDL component of the IIR core is provided in Appendix C.1.

Table 7.3: Bandpass filter specifications used to generate IIR core coefficients

Parameter	**Value**
Sampling frequency	10 kHz
Lower cutoff frequency	2190 Hz
Higher cutoff frequency	2210 Hz
Passband ripple	0.1 dB
Stopband attenuation	200 dB
Number of coefficients	6
Number of sections	6

This filter testing was similar to the one in section 7.1 where the sum of sine waves 220, 800, 2200, 2500 Hz shown in Figure 7.5a were used as input vector to the IIR core and 2200Hz sinusoid was isolated using a band-pass filter. The only difference is the filter specifications used to generate coefficients for both FIR and IIR cores.

Table 7.4: IIR core parameter configurations

Parameter	**Value**
DIN_WIDTH	16
DOUT_WIDTH	16
COEFF_WIDTH	16
b	A vector of filter response in Figure 7.5b
a	A vector of filter response in Figure 7.5b
STAGES	6

The IIR filter response shown in Figure 7.5b was designed with Chebyshev Type I filter to specifications shown in Table 7.3 and IIR core parameters were configured as shown in Table 7.4. The testbench of the experiment was setup as in Figure 7.4. Furthermore, the results of IIR core obtained are shown in Figure 7.5d which closely match the ideal Matlab results shown in Figure 7.5c.

Several observations were made when results obtained using FIR core in section 7.1 were compared with results of IIR core in this section. The IIR filter is highly selective and it uses fewer coefficients. This in turn led to improved results when IIR core was used.

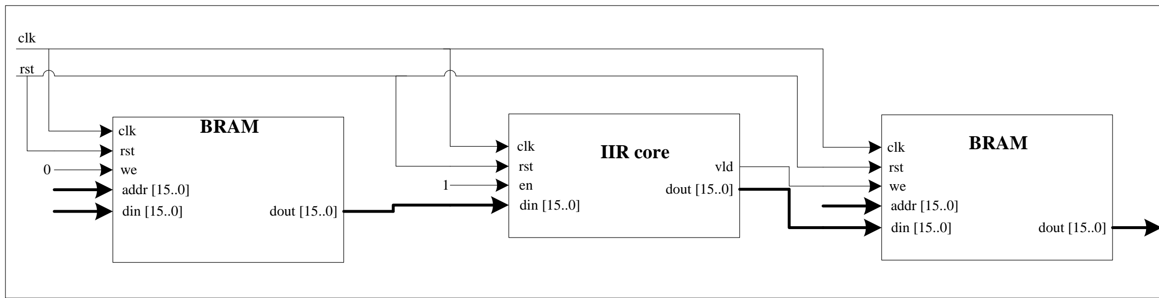

Figure 7.4: IIR core Testbench block diagram

(a)

(b)

(c)

(d)

Figure 7.5: The results IIR filter testbench.

7.3 FFT/IFFT CORE TEST

This section outlines the experiment that was performed to verify the functionality and validity of the FFT/IFFT core designed in section 4.3. The VHDL testbench and ISIM tool were used for system level verification and Matlab was used to plot the results as well as providing a floating-

point reference model for obtained results. The number of logic resources occupied by different lengths of FFT core were recorded. The Matlab scripts used are provided in Appendix D.2 and D.3 while the VHDL component of the FFT/IFFT core is provided in Appendix D.1.

For the most part, verification of the FFT/IFFT core was done using all supported N points of the core at clock speed of 100MHz, however, only a 1024-point experiment will be demonstrated in this section. Since the core operates in one of the two supported operating modes namely FFT and IFFT mode, the experiment incorporates tests for both.

7.3.1 Testbench

The block diagram of a testbench is illustrated in Figure 7.6 and the generic parameters of FFT/IFFT core were configured as in Table 7.5.

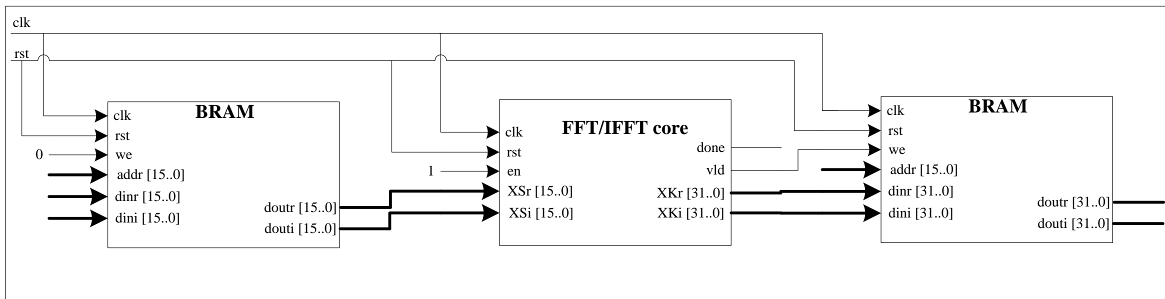

Figure 7.6: Testbench block diagram

Table 7.5: FFT/IFFT core configuration parameters as used in a testbench

Parameter	Value
N	1024
DIN_WIDTH	16
DOUT_WIDTH	22
MODE	0=FFT,1=IFFT

The testbench environment involved generating a 1024 long input vector of a rectangular pulse as shown in Figure 7.7a. This was used at the input to the core operating in FFT mode. The output of the FFT core was stored in BRAM and later used as input data to the IFFT core whose results were also kept in the final stage BRAM.

Moreover, the contents of both BRAMs were written to data files and plotted as shown in Figure 7.7. The FFT core yielded the sinc waveform in Figure 7.7c which was the expected fourier transform of a pulse waveform. This also matched with the Matlab generated FFT of the pulse wave shown in Figure 7.7b. As expected, the IFFT core produced the original rectangular pulse waveform which is illustrated in Figure 7.7d. However, the magnitude is vastly reduced due to truncation of input word length that ensured the output values were kept below the 32-bit fixed point limit when the values were growing in each pipeline stage of the FFT/IFFT core.

In order to allow the designer flexibly of choice with regard to FFT length and associated resource utilization, the synthesis report for all supported N-point FFT is provided in Table 7.6.

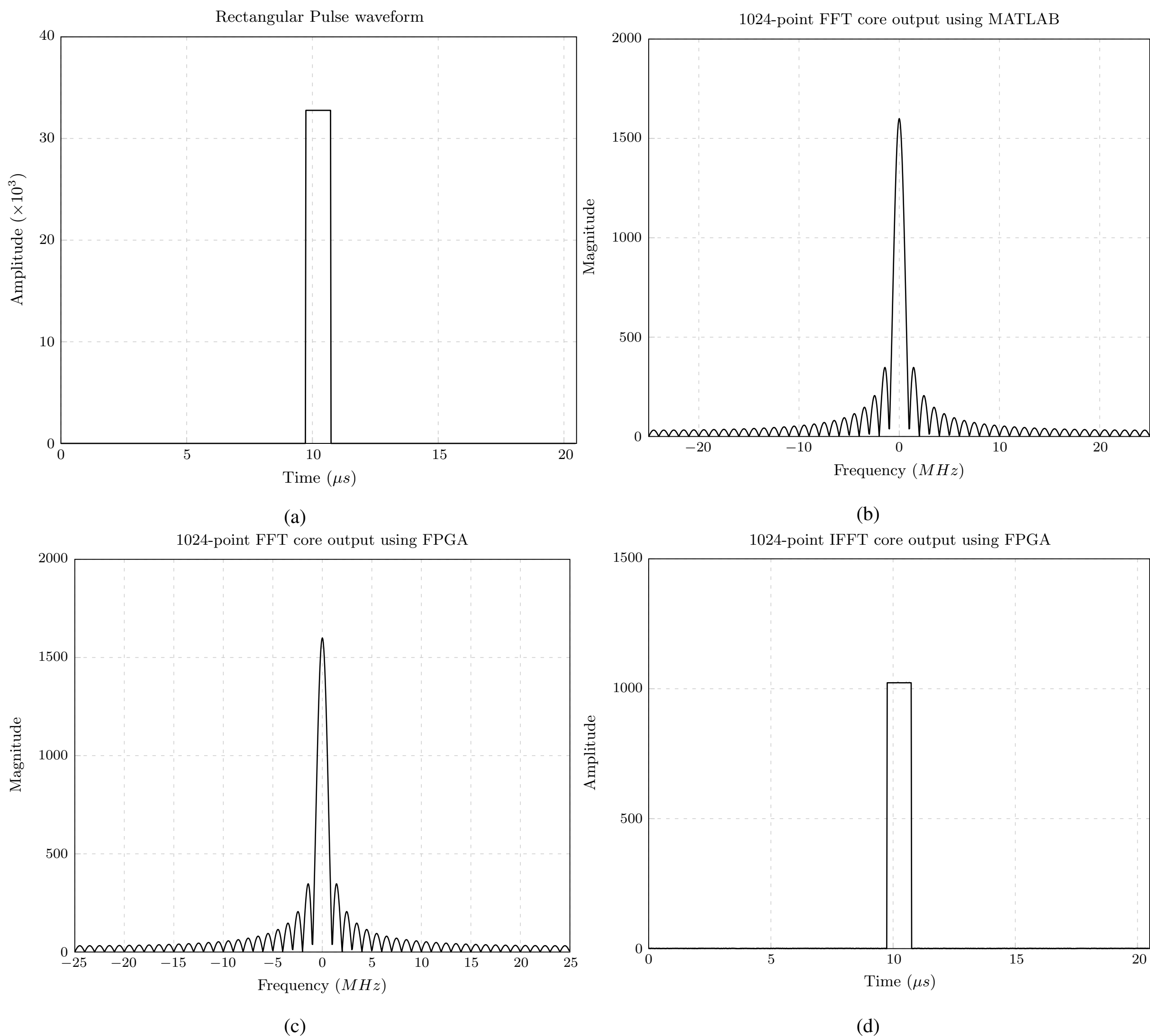

Figure 7.7: MATLAB and FPGA results of a 1024-point FFT and IFFT core tested with rectangular pulse input waveform.

These results were obtained using the same experiment setup as above but with differing lengths of FFT and input vector.

7.3.2 **Hardware Test**

A similar experiment as in the previous section was performed to test the FFT/IFFT core but this time the design needed to be fabricated on the FPGA. The input was still obtained from the BRAM containing samples of a pulse waveform. Unlike previously where results were stored in output in BRAM, the output samples were sent to a PC via Ethernet interface where results were plotted and analysed. Although this type of testing is not a realistic SDR application, the experiment was sufficient to verify the FFT/IFFT core functionality on the hardware and results obtained were no different to the ones shown in Figure 7.7. A more sophisticated typical SDR test experiment of the FFT/IFFT core is described later in section 7.6.3 of this chapter.

Table 7.6: Synthesis Report summary for FFT/IFFT core on Spartan 6 - XC6SLX150T device

FFT Length	**Logic Utilized** (92,152)	**Slice Registers** (184,304)	**Slice LUTs** (92,152)	**Block Memory** (21,680)	**DSP48A1s** (180)
N = 8	454 (1%)	260 (1%)	489 (1%)	0 (0%)	4 (2%)
N = 16	606 (1%)	383 (1%)	640 (1%)	18 (1%)	4 (2%)
N = 32	1,207 (1%)	526 (1%)	1,261 (1%)	38 (1%)	8 (4%)
N = 64	1,386 (1%)	668 (1%)	1,472 (1%)	74 (1%)	8 (4%)
N = 128	1,812 (1%)	837 (1%)	1,978 (2%)	144 (1%)	16 (8%)
N = 256	2,074 (2%)	1,045 (1%)	2,446 (2%)	288 (1%)	16 (8%)
N = 512	2,704 (2%)	1,320 (1%)	3,307 (3%)	578 (2%)	24 (13%)
N = 1024	3,105 (3%)	1,731 (1%)	4,331 (4%)	1,154 (5%)	24 (13%)
N = 2048	4,141 (4%)	2,654 (1%)	6,805 (7%)	2,304 (10%)	32 (17%)
N = 4096	5,460 (5%)	4,225 (2%)	10,551 (11%)	4,608 (21%)	32 (17%)

7.4 DDC CORE TEST

This section demonstrates how a DDC core designed in section 4.4 was tested using VHDL testbench and ISIM. The test was performed by simulating FM receiver datapath which converted FM signal from the RF to baseband signal ready to be demodulated. The specification parameters of the system are detailed in Chapter 6. Furthermore, the DDC core parameter settings are shown in Table 7.7 and the testbench is illustrated in Figure 7.8. The Matlab scripts used in this experiment are all in Appendix E.2 and E.4 while the DDC core instantiation component is provided in Appendix E.1.

Table 7.7: DDC core configuration parameters as used in a testbench

Parameter	Value
DIN_WIDTH	16
DOUT_WIDTH	32
PHASE_WIDTH	32
PHASE_DITHER_WIDTH	22
SELECT_CIC1	1
NUMBER_OF_STAGES1	10
DIFFERENTIAL_DELAY1	1
SAMPLE_RATE_CHANGE1	128
SELECT_CFIR	1
NUMBER_OF_TAPS	21
FIR_LATENCY	0
COEFF_WIDTH	16
COEFFS	Filter response in Figure 6.2
SELECT_CIC2	0
NUMBER_OF_STAGES2	0
DIFFERENTIAL_DELAY2	0
SAMPLE_RATE_CHANGE2	0

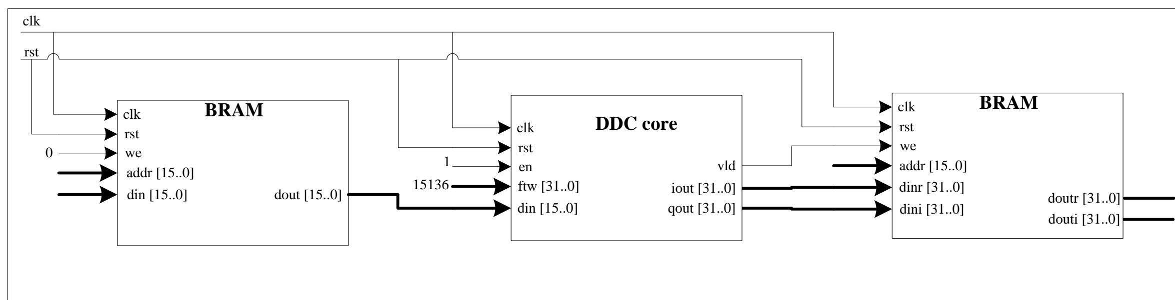

Figure 7.8: DDC core Testbench block diagram

The FM channel of interest was chosen as 94.5MHz. However, due to bandpass sampling the resulting FM signal will be centered at 28.38MHz after 122.88 MSPS sampling. Similarly, the carrier is also located at 28.38MHz as illustrated in Figure 7.10a. Using 15 kHz baseband modulating signal, four test cases were investigated. The first test investigates a system with no noise, the second one has AWGN noise added to a modulating signal, the third test only has noise introduced in FM modulated signal and the lastly the system with noisy modulating signal and modulated signal were used for a test.

Two baseband signals one without noise and the other with noise along with their spectra are shown in Figure 7.9a and Figure 7.9b respectively. The local oscillator inside the FPGA was implemented using NCO core and it generated complex sine and cosine waveforms whose magnitude spectrum is shown in Figure 7.10b. Beginning with the local oscillator (NCO) and succeeding cores in the DDC core chain, all the processes were verified in VHDL testbench and ISIM.

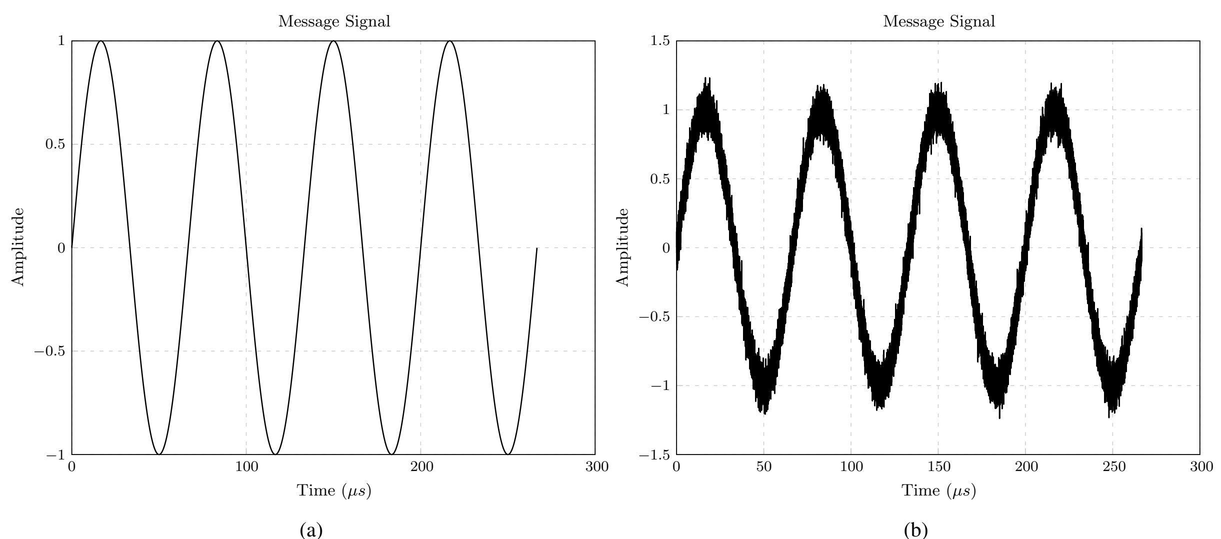

Figure 7.9: DDC core input vector generated in MATLAB and computed by FM modulation of a 200 kHz with 94.5 MHz sampled at 122.88 MSPS.

The test cases are described as follows:

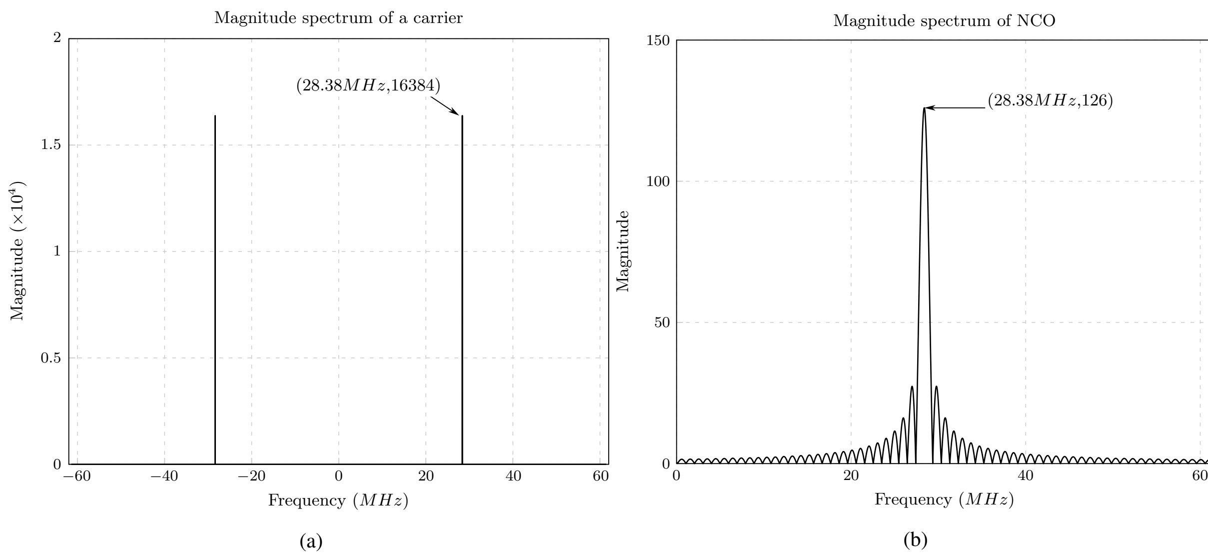

Figure 7.10: A 28.38MHz carrier waveform generated in MATLAB and a local oscillator 28.38MHz signal generated by NCO core in FPGA.

7.4.1 Noise Free System Test

This test uses a noise free FM input signal shown in Figure 7.11a. In order to convert it to baseband, NCO signals are multiplied with input FM signal using the mixer. The product of this is desired signal component centred at DC and a spurious harmonic located at 56.76MHz as shown in Figure 7.11b. This undesired signal component was removed by a CIC filter which decimated the 122.88 MSPS ADC sample rate by a factor of 1:128 resulting in 960 kSPS sample rate as shown in Figure 7.11c. The non-ideal response of the CIC filter was corrected by introducing a compensation FIR filter in the final stage of the DDC and its output is shown in Figure 7.11d.

After the digital down conversion, the FM demodulator was used to demodulate the FM signal. The magnitude spectrum and amplitude versus time graphs of the signal after demodulation are shown in Figure 7.12a and 7.12b. This output has transient response which is the effect of the FM demodulator. When the transient was removed and leaving only the steady state response, this resulted in Magnitude spectrum and time domain graphs shown in Figure 7.12c and 7.12d. The FM demodulated signal was compared to the original modulating signal shown in Figure 7.11f and the results closely match.

7.4.2 Adding AWGN Noise to a Modulating Signal

After carrying out the first experiment without noise at the system input, a second one involved adding 20dB AWGN to a 15kHz modulating signal shown in Figure 7.9b. This signal modulates a pure 28.32MHz carrier in Figure 7.10a resulting in FM signal shown in Figure 7.13a. The FM signal undergoes the same DDC core stages and finally the FM demodulator just as described in section 7.4.1. The results are shown in Figure 7.13 and Figure 7.14.

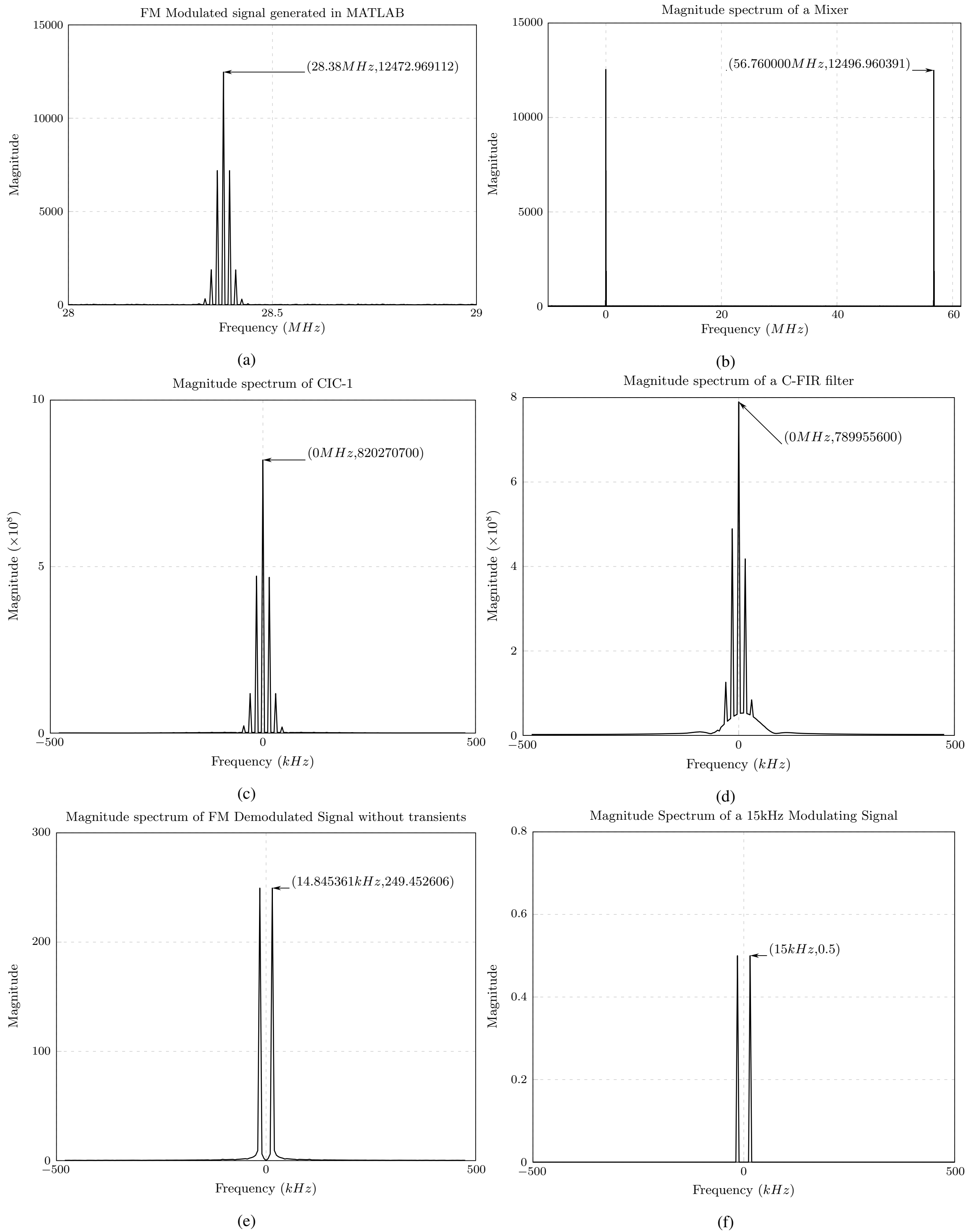

Figure 7.11: Results of DDC Core and FM demodulator when a noise free input test signal is used.

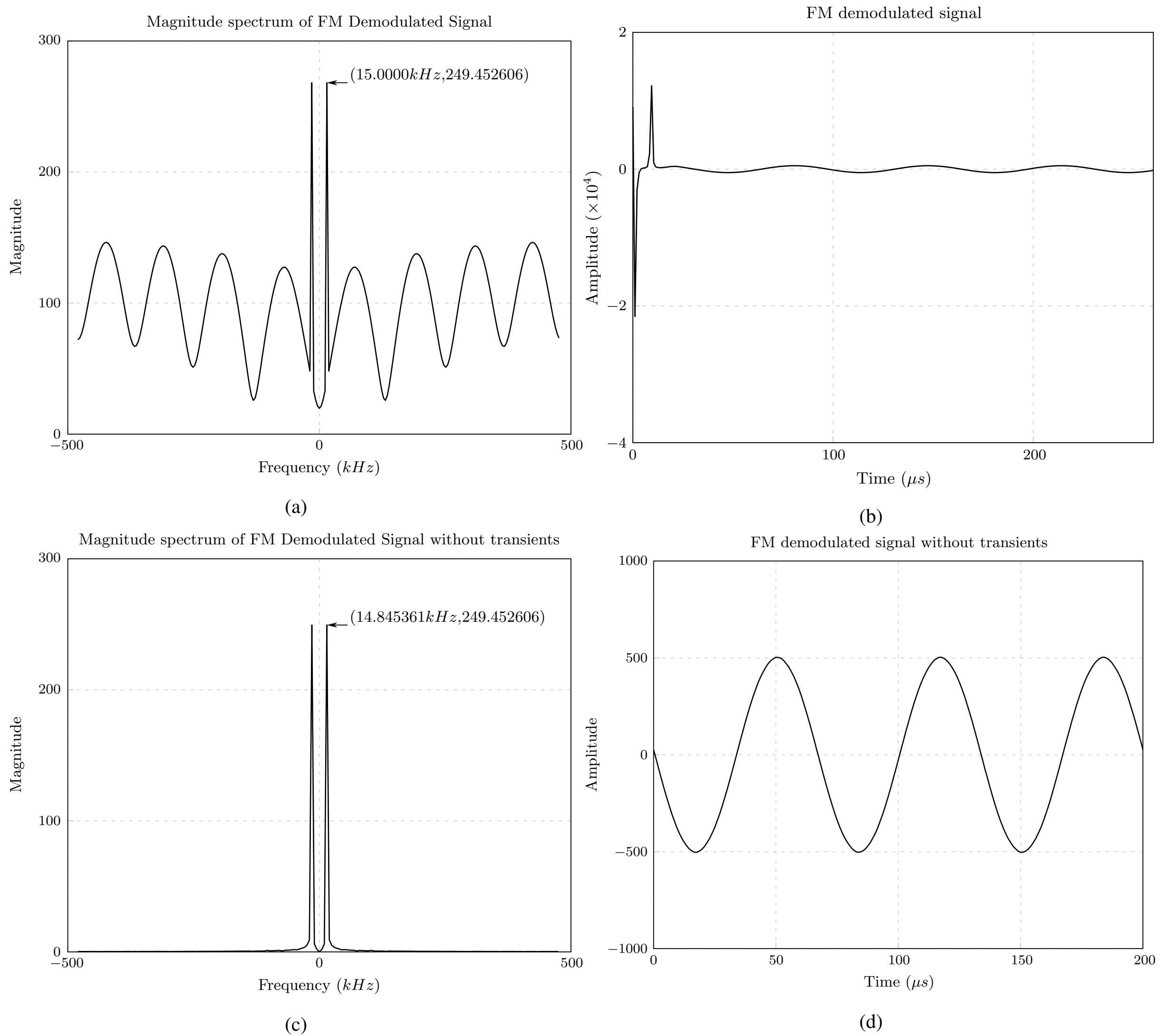

Figure 7.12: FM demodulator output showing the demodulated signal with transients and after removing the transients. This applies to a test when a noise free input test signal is used.

7.4.3 Adding AWGN Noise to a Frequency Modulated Signal

Following the second test experiment with noise added to a modulating signal before modulation, the third one was performed but this time with 20dB AGWN noise added of FM modulated signal. The modulating signal remained noise free as shown in Figure 7.9a. Consequently, the FM signal was generated to be an input test vector to a system and is shown in Figure 7.15a. The results are shown in Figure 7.15 and Figure 7.16.

7.4.4 Adding 20dB AWGN Noise to a modulating signal and frequency modulated Signal

Lastly, the test experiment with 20dB AWGN noise added to both modulating signal and frequency modulated signal was performed. The resulting FM signal which served as an input vector to a DDC core is shown in Figure 7.17a. The results are shown in Figure 7.17 and Figure 7.18.

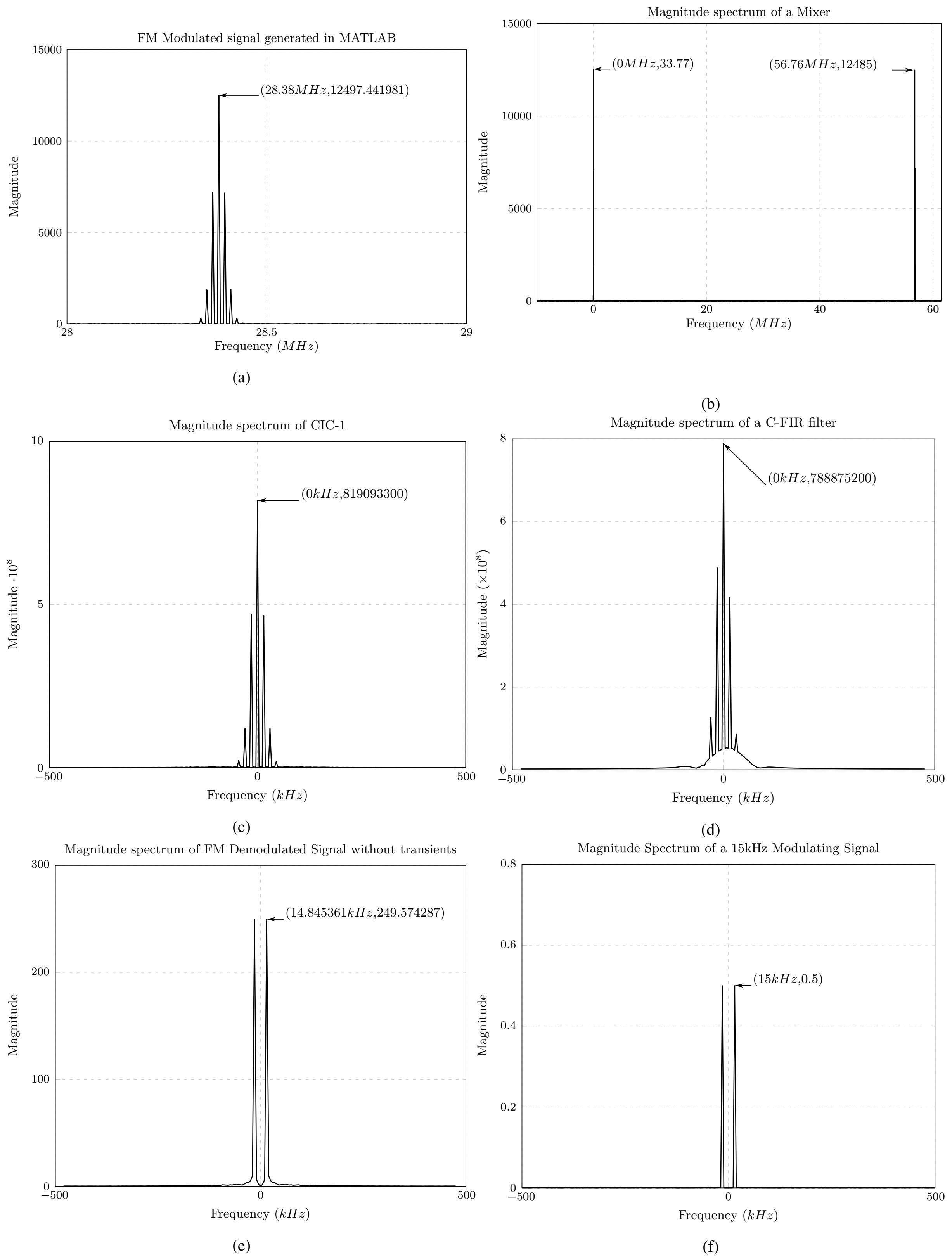

Figure 7.13: Results of DDC Core and FM demodulator when 20dB AWGN noise is added to a modulating signal.

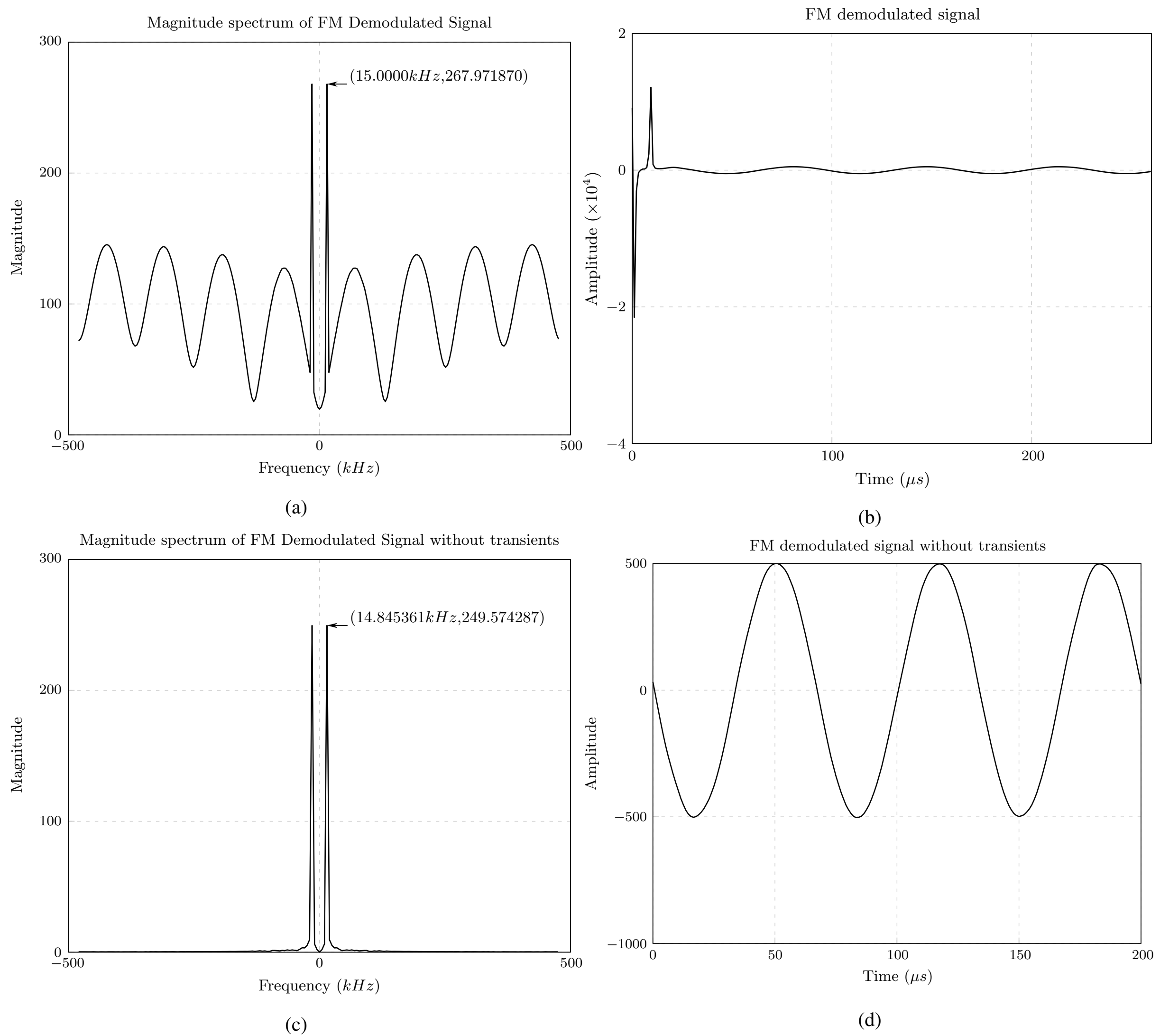

Figure 7.14: FM demodulator output showing the demodulated signal with transients and after removing the transients. This applies to a test where 20dB AWGN noise is added to a modulating signal.

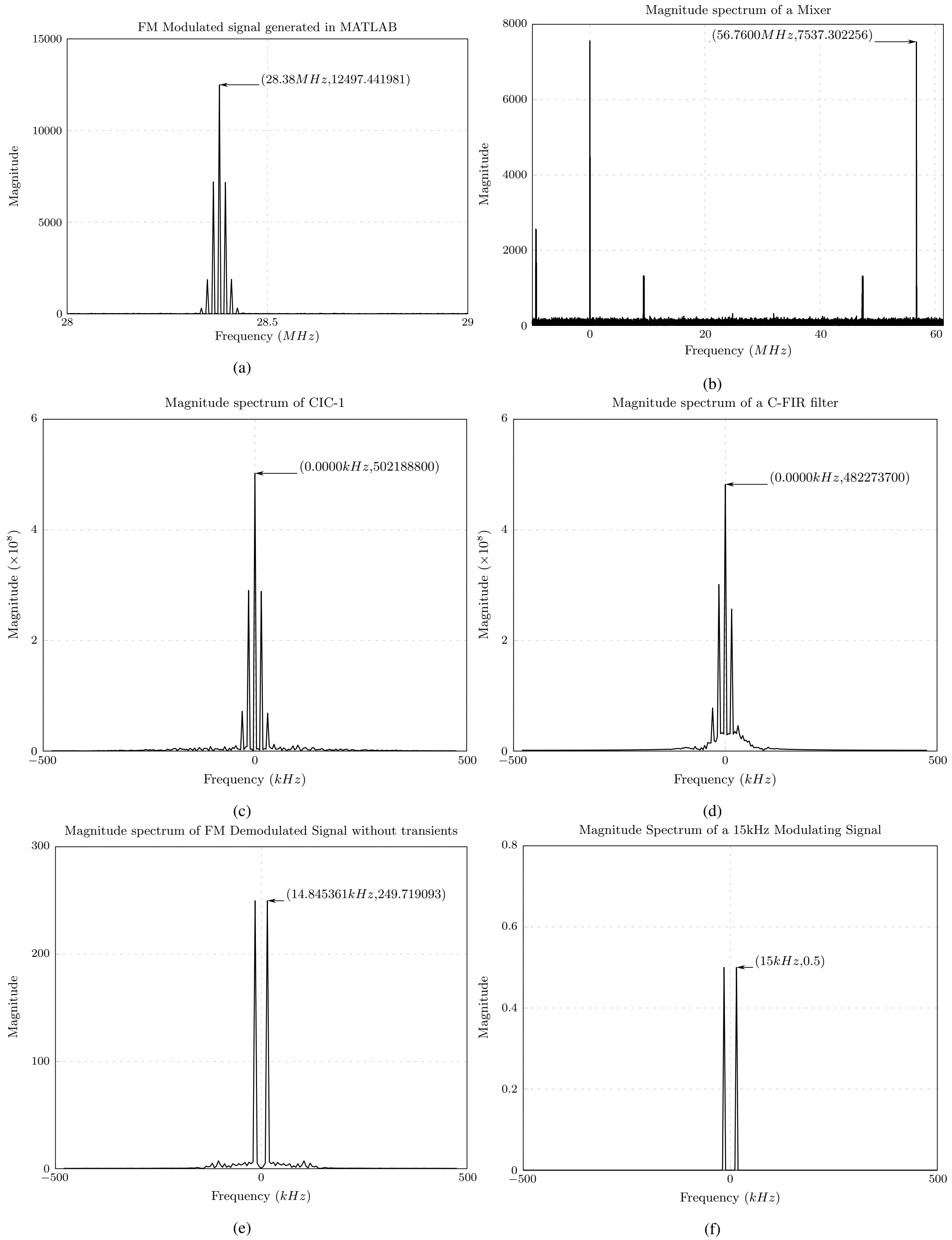

Figure 7.15: Results of DDC Core and FM demodulator when 20dB AWGN noise is added to a frequency modulated signal.

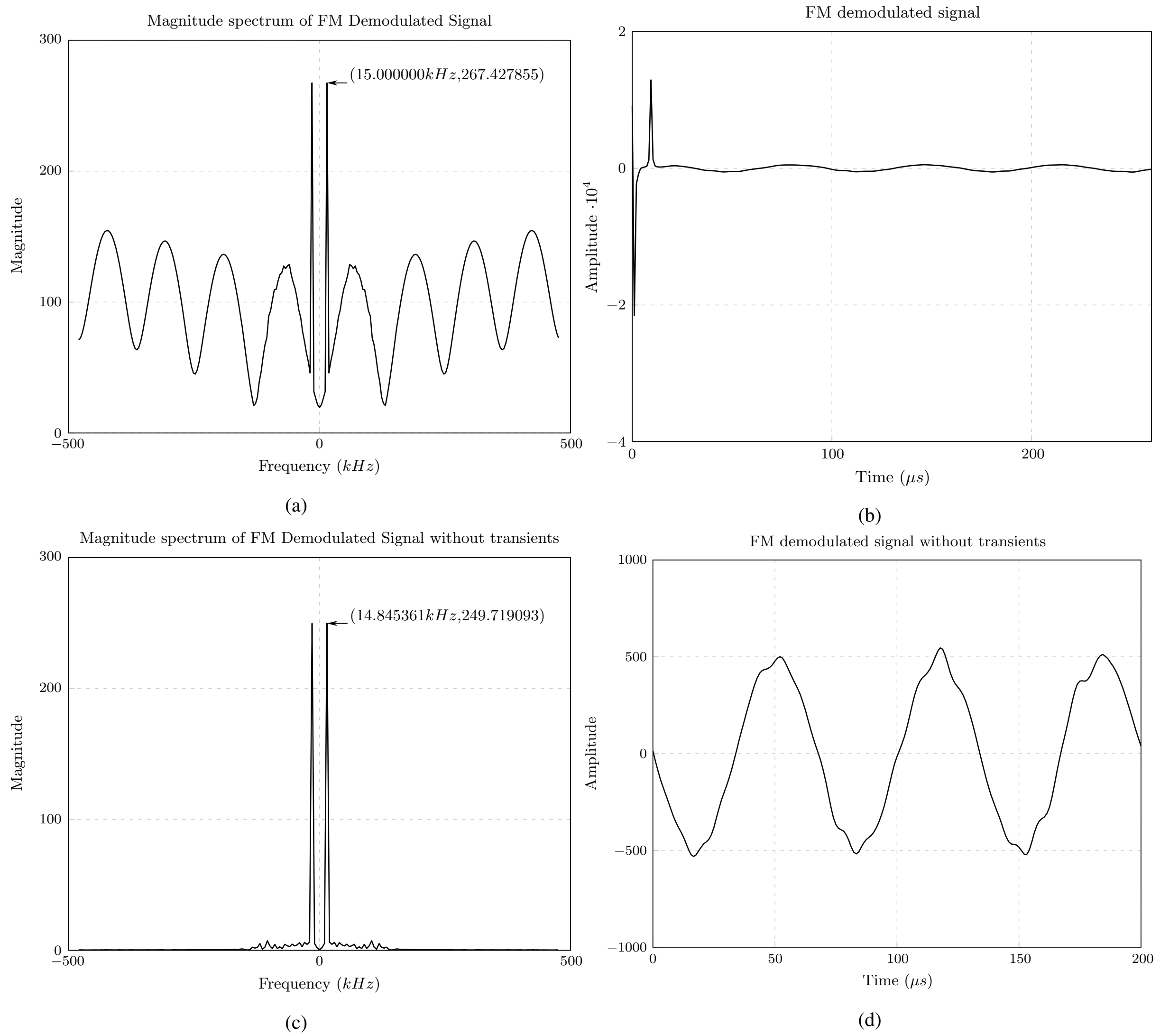

Figure 7.16: FM demodulator output showing the demodulated signal with transients and after removing the transients. This applies to a test where 20dB AWGN noise is added to a frequency modulated input test signal.

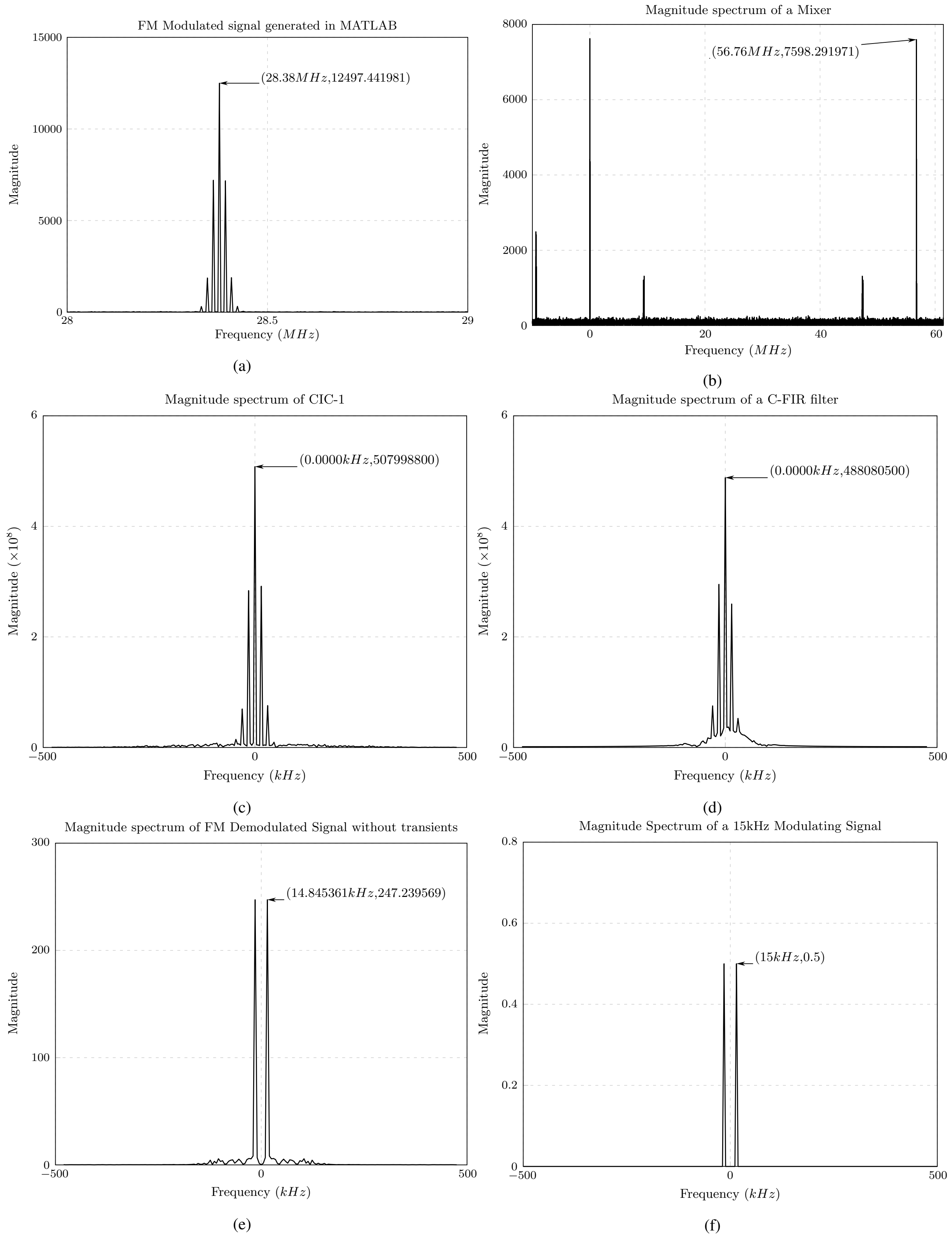

Figure 7.17: Results of DDC Core and FM demodulator when 20dB AWGN noise is added to a modulating signal and frequency modulated signal.

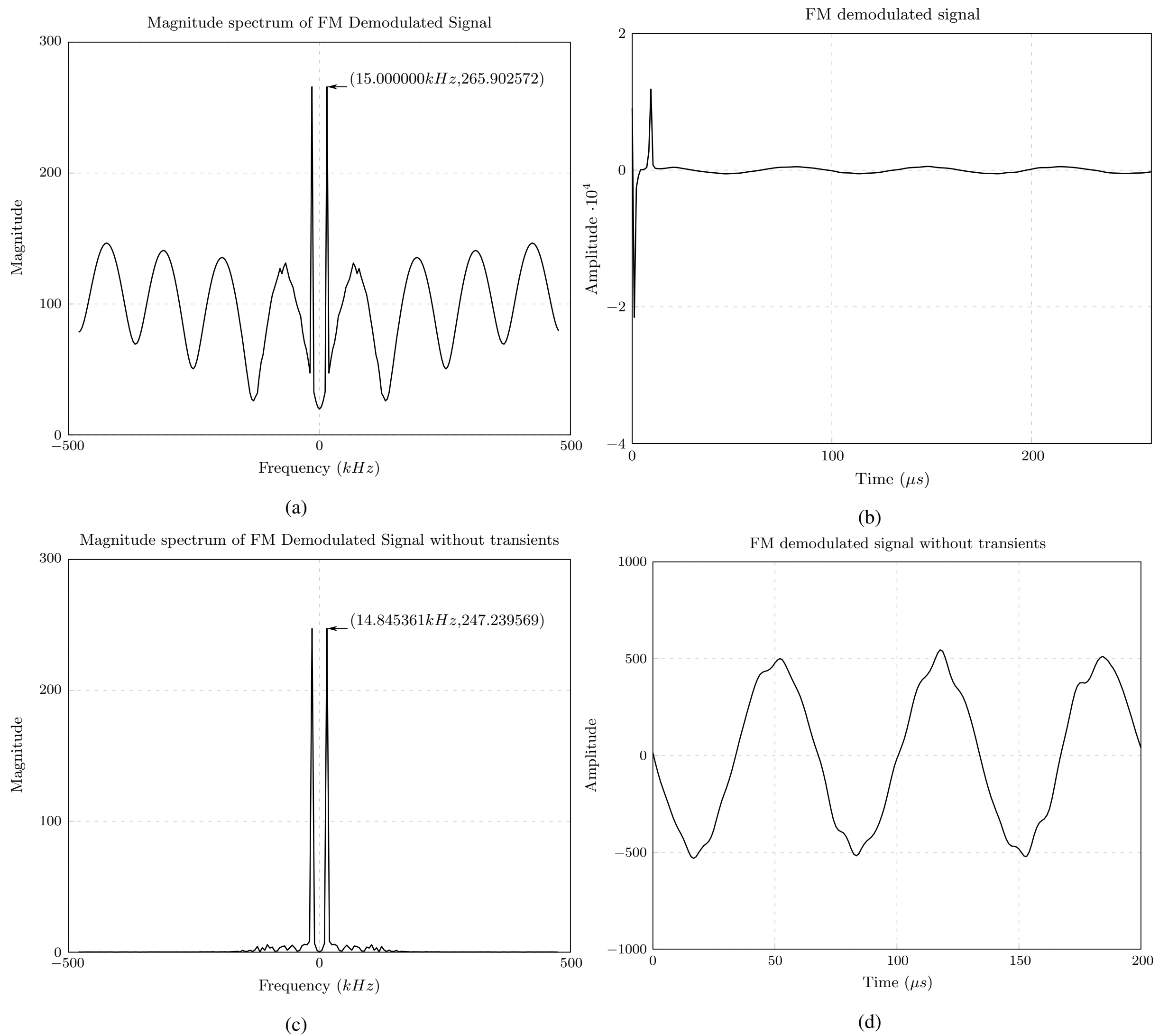

Figure 7.18: FM demodulator output showing the demodulated signal with transients and after removing the transients. This applies to a test where 20dB AWGN noise is added to a modulating signal and frequency modulated input test signal.

7.5 UDP/IP CORE TEST

This section discusses the experiment that was performed to verify and evaluate performance of a 1 Gigabit Ethernet interface using UDP/IP core designed in section 5.2. Its VHDL instantiation component is provided in Appendix F.1. The experiment mainly put emphasis on data transmission using both ARP and UDP protocols over a 1 Gigabit Ethernet. This proceeded by establishing a peer to peer connection between a PC and RHINO as shown in Figure 3.6. A physical connection was created by using a Cat5e UTP copper cable where one end connected to 1Gbps network card on the PC and another end connected to a 1Gbps adapter or interface on RHINO. The network parameters were configured as shown in Table 7.8.

Table 7.8: Point-to-Point Network configurations

Parameters	**RHINO (FPGA)**	**Host PC**
IP Address	192.168.0.3	192.168.0.1
MAC Address	00:24:ba:7d:1d:70	00:0c:29:3d:0d:2d
UDP port	9930	9930

The throughput speed was measured by sending multiple UDP packets of a fixed frame length from the FPGA to a PC. In order to ensure maximum throughput speed and minimal packet loss, each packet was sent whenever the UDP/IP core was fully ready to transmit data. A $1Hz$ sine waveform vector was used as payload in each UDP packet where the number of sine wave samples equalled the UDP frame length.

The packets received on the PC were captured with a Command Line Tcpdump Linux tool and Wireshark was used for analysis of captured packets. The outgoing packets only needed wireshark for monitoring. After data capture, the sine waveform vector in each frame was plotted to verify that it was not corrupted during transmission in the physical link. Using wireshark, the arrival times since the previous and the first packet were used to determine the amount of time taken to transmit each packet and throughput speed as shown in equation 7.1.

$$\text{Throughput Speed (MB/s)} = \frac{\text{Frame Length } (bytes) \times \text{Number of Frames}}{\text{Total Transmission Latency } (seconds)} \tag{7.1}$$

Separate tests were made based on the direction of data flow between a PC and FPGA. Thus data transfers were classified into two namely the upstream and downstream. Upstream refers to transmission of UDP data from FPGA to a PC while the downstream is transmission of UDP data from a PC to an FPGA. Before discussing test for both upstream and downstream, the ARP test was performed and is described as follows:

7.5.1 ARP Test

The ARP communication packets were recorded as shown in Figure 7.19. As marked in this figure using the first blue arrow, the FPGA sends a broadcast arp request to resolve unknown PC

MAC address. The PC caches the both FPGA ip and mac addresses and quickly replies with the MAC address as shown in first red arrow. It should be noted that the FPGA arp request precedes the UDP communication and it only happens once at start of the UDP core. The results have proved to be successful as both the request by FPGA and reply by PC were without errors.

```
No.  Time          Source          Destination     Protocol Length Info
  1 0.000000000  TexasIns_7d:1c Broadcast       ARP      60 Who has 192.168.0.1?  Tell 192.168.0.3   <- FPGA ARP requst
  2 0.000033000  AsustekC_ae:dt TexasIns_7d:1   ARP      42 192.168.0.1 is at e0:3f:49:ae:db:b2     <- PC ARP reply
 15 6.012463000  AsustekC_ae:dt TexasIns_7d:1   ARP      42 Who has 192.168.0.3?  Tell 192.168.0.1   <- PC ARP request
 16 6.012535000  TexasIns_7d:1c AsustekC_ae:d   ARP      60 192.168.0.3 is at 00:24:ba:7d:1d:70     <- FPGA ARP reply
109 51.020447000 AsustekC_ae:dt TexasIns_7d:1   ARP      42 Who has 192.168.0.3?  Tell 192.168.0.1
110 51.020515000 TexasIns_7d:1c AsustekC_ae:d   ARP      60 192.168.0.3 is at 00:24:ba:7d:1d:70
203 96.028436000 AsustekC_ae:dt TexasIns_7d:1   ARP      42 Who has 192.168.0.3?  Tell 192.168.0.1
204 96.028486000 TexasIns_7d:1c AsustekC_ae:d   ARP      60 192.168.0.3 is at 00:24:ba:7d:1d:70
▼Frame 1: 60 bytes on wire (480 bits), 60 bytes captured (480 bits) on interface 0
   Interface id: 0 (eth0)
   Encapsulation type: Ethernet (1)
   Arrival Time: Jun 20, 2015 14:50:56.489680000 SAST
   [Time shift for this packet: 0.000000000 seconds]
   Epoch Time: 1434804656.489680000 seconds
   [Time delta from previous captured frame: 0.000000000 seconds]
   [Time delta from previous displayed frame: 0.000000000 seconds]
   [Time since reference or first frame: 0.000000000 seconds]
   Frame Number: 1
   Frame Length: 60 bytes (480 bits)
   Capture Length: 60 bytes (480 bits)
   [Frame is marked: False]
   [Frame is ignored: False]
   [Protocols in frame: eth:ethertype:arp]
   [Coloring Rule Name: ARP]
   [Coloring Rule String: arp]
▼Ethernet II, Src: TexasIns_7d:1d:70 (00:24:ba:7d:1d:70), Dst: Broadcast (ff:ff:ff:ff:ff:ff)
  ▶Destination: Broadcast (ff:ff:ff:ff:ff:ff)
  ▶Source: TexasIns_7d:1d:70 (00:24:ba:7d:1d:70)
   Type: ARP (0x0806)
   Padding: 000000000000000000000000000000000000
▼Address Resolution Protocol (request)
   Hardware type: Ethernet (1)
   Protocol type: IP (0x0800)
   Hardware size: 6
   Protocol size: 4
   Opcode: request (1)
   Sender MAC address: TexasIns_7d:1d:70 (00:24:ba:7d:1d:70)
   Sender IP address: 192.168.0.3 (192.168.0.3)
   Target MAC address: 00:00:00_00:00:00 (00:00:00:00:00:00)
   Target IP address: 192.168.0.1 (192.168.0.1)
0000  ff ff ff ff ff ff 00 24  ba 7d 1d 70 08 06 00 01   .......$ .}.p...
0010  08 00 06 04 00 01 00 24  ba 7d 1d 70 c0 a8 00 03   .......$ .}.p....
0020  00 00 00 00 00 00 c0 a8  00 01 00 00 00 00 00 00   ........ ........
0030  00 00 00 00 00 00 00 00  00 00 00 00               ........ ....
Hardware type (arp.hw.type), 2 ...   Packets: 218 · Displayed: 8 (3.7%) · Dropped: 0 (0.0%)
```

Figure 7.19: Wireshark Capture of FPGA broadcast ARP request

During the course of UDP communication, the PC also sends multiple ARP requests at intervals of 60 seconds as shown if Figure 7.19 pointed by the second blue arrow. However, this time the request is unicast not broadcast and each time the FPGA replies with a valid MAC address to a PC. According to Section 2.3.2.1 of RFC1122 standard, the regular unicast arp requests occur in order to flush out-of-data cache entries. The process is also referred to as Unicast Poll while time between periodic arp requests is timeout which in this case is 60 seconds.

7.5.2 Upstream Test

This test was made by sending UDP data from an FPGA to a PC and both the data validity and transfer speed tests were carried out as below.

7.5.2.1 Data Transfer Test

In order to ensure the data integrity of sent UDP packets by the FPGA, the 1474 bytes of data were sent from the FPGA and captured on a PC using Wireshark. The captured packets are illustrated in Figure 7.20. The transmission of data was successful as the received data on a PC was also 1474 bytes long and every single character in a packet matched the one sent by the FPGA.

7.5.2.2 Transfer Speed Test

In this experiment, 500 frames were used to measure the total time it took to transmit them, hence using that to compute the throughput speed. Although different frame sizes were used to perform tests, only one test will be described to demonstrate how the throughput speed was calculated in all test cases.

Figure 7.21 demonstrates a case where 1474 bytes frame was sent from a PC to an FPGA. The size of each in each frame is highlighted in blue. It took 0.006012 seconds to transmit 500 frames as encircled in green in Figure 7.21.

Determining the transmission speed considers the 500 packets sent with frame size of 1474 bytes and all packets taking 0.006012 seconds of transmission time. The result of the computation is 122.59 MB/s as shown in equation 7.2.

$$\begin{aligned}\text{Throughput speed} &= \frac{500\text{ frames } \times 1474\text{ bytes}}{0.006012\text{ seconds}} \\ &= 122.59\text{ MB/s}\end{aligned} \tag{7.2}$$

Furthermore, the throughput speed was measured further using Linux Speedometer Tool 2.8 as shown in Figure 7.22, the result was 117 MiB/s (or 122.68 MB/s) which closely matches the result obtained using Wireshark and equation 7.2.

The theoretical limit of a Gigabit Ethernet is 125 MB/s. In the above results, 98% of theoretical figure was achieved, however, this figure will drastically change when the UDP core is used in a streaming mode. This experiment produced the best of throughput speed because data originated from the FPGA and was sent each time the UDP core was ready to transmit data. This speed is expected change whenever a data source is one of the I/O peripheral interfaces such as ADC, USB etc.

When multiple frame sizes were used to measure the speed, the results came out as depicted in Figure 7.23. The bar chart throughput increases with increase in size of a UDP frame and this was expected as defined by equation 7.2.

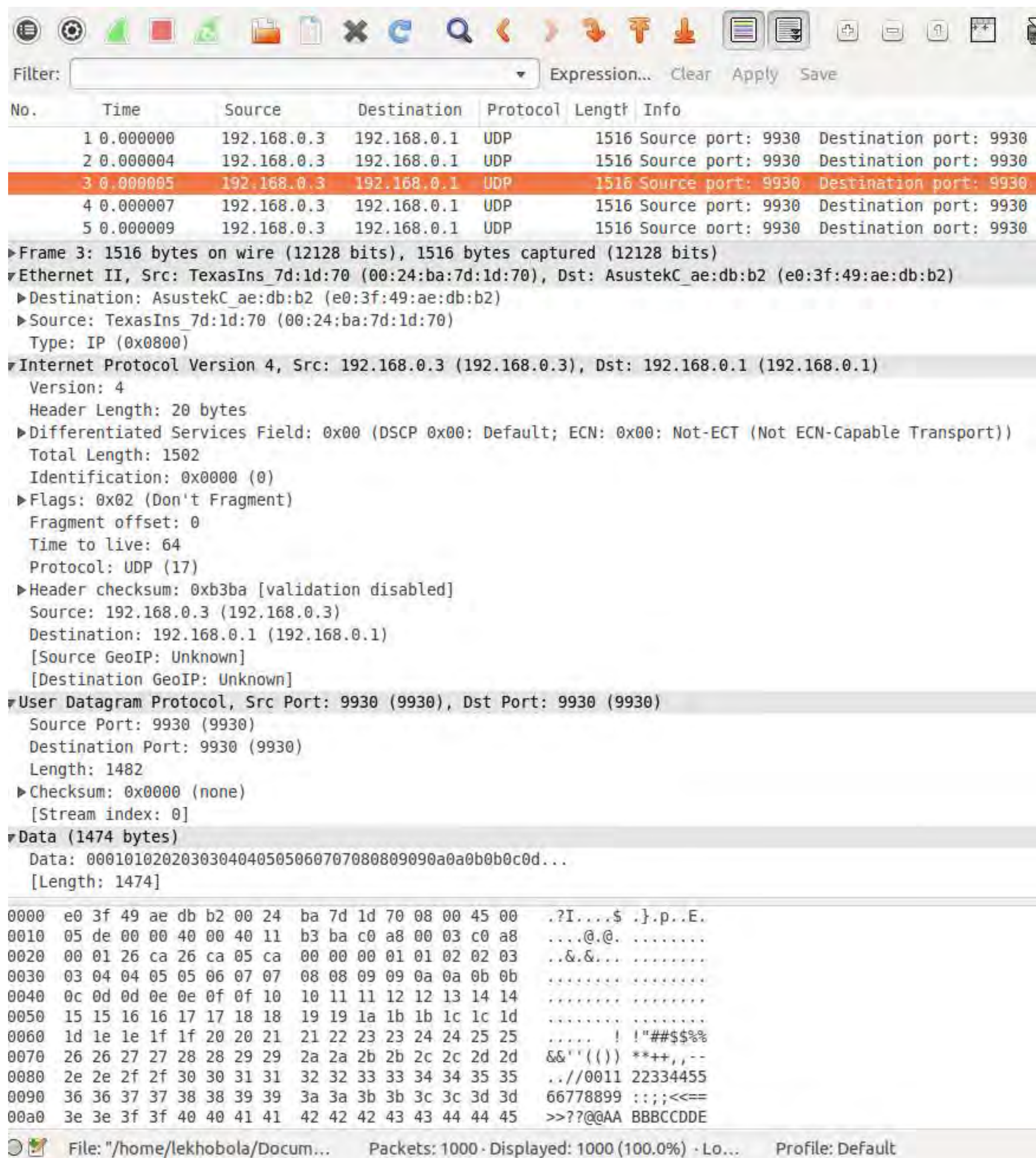

Figure 7.20: Trace of UDP traffic from FPGA showing the details of the UDP header

7.5.3 Downstream Test

Testing the downstream involved sending UDP data from the PC to an FPGA. In order to verify if the packets are indeed arriving at the FPGA, the Chipscope Pro was used. Wireshark was used to monitor the packets as they left the PC. Figure 7.24 shows as 37 bytes string encircled in red which was sent to a PC at transmission rate of 35 MB/s. The string was captured on FPGA and displayed on Chipscope Pro as illustrated in Figure 7.25.

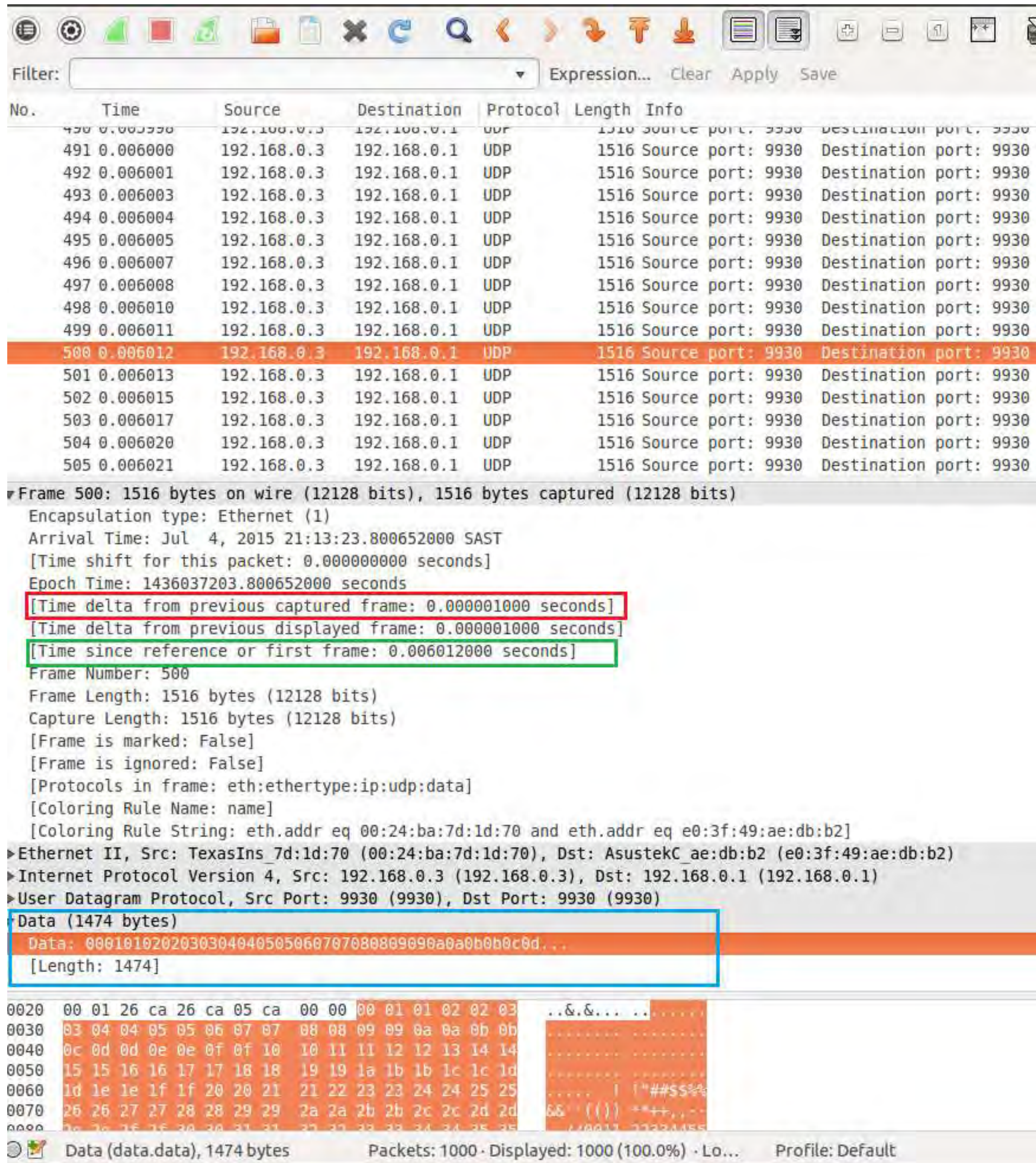

Figure 7.21: Trace of time taken for a single and 500 packets of UDP over 1Gbps Ethernet

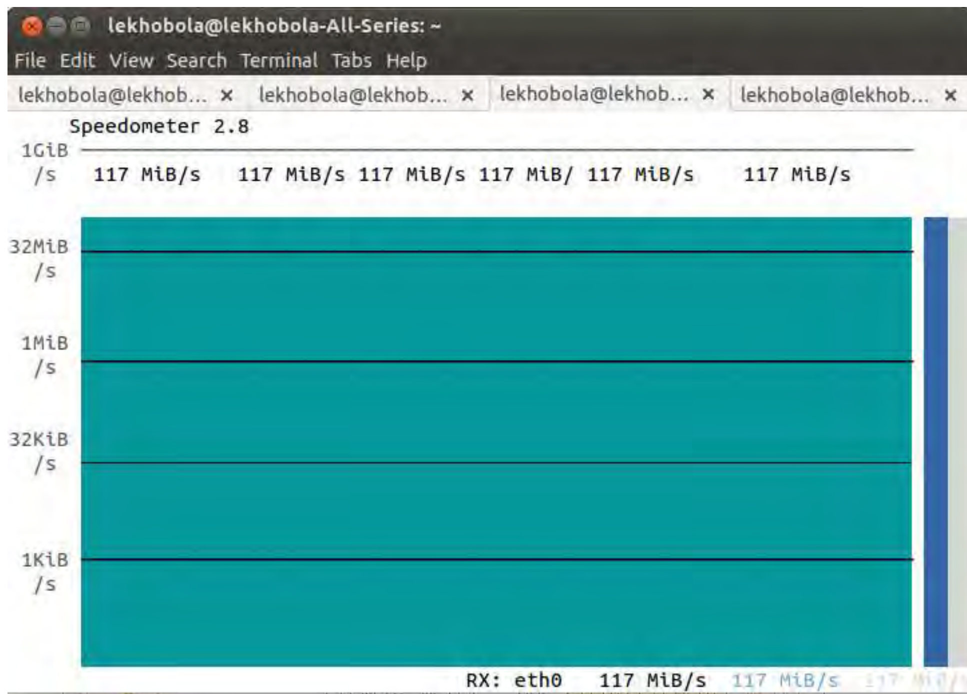

Figure 7.22: Measuring speed using Linux Speedometer Tool 2.8

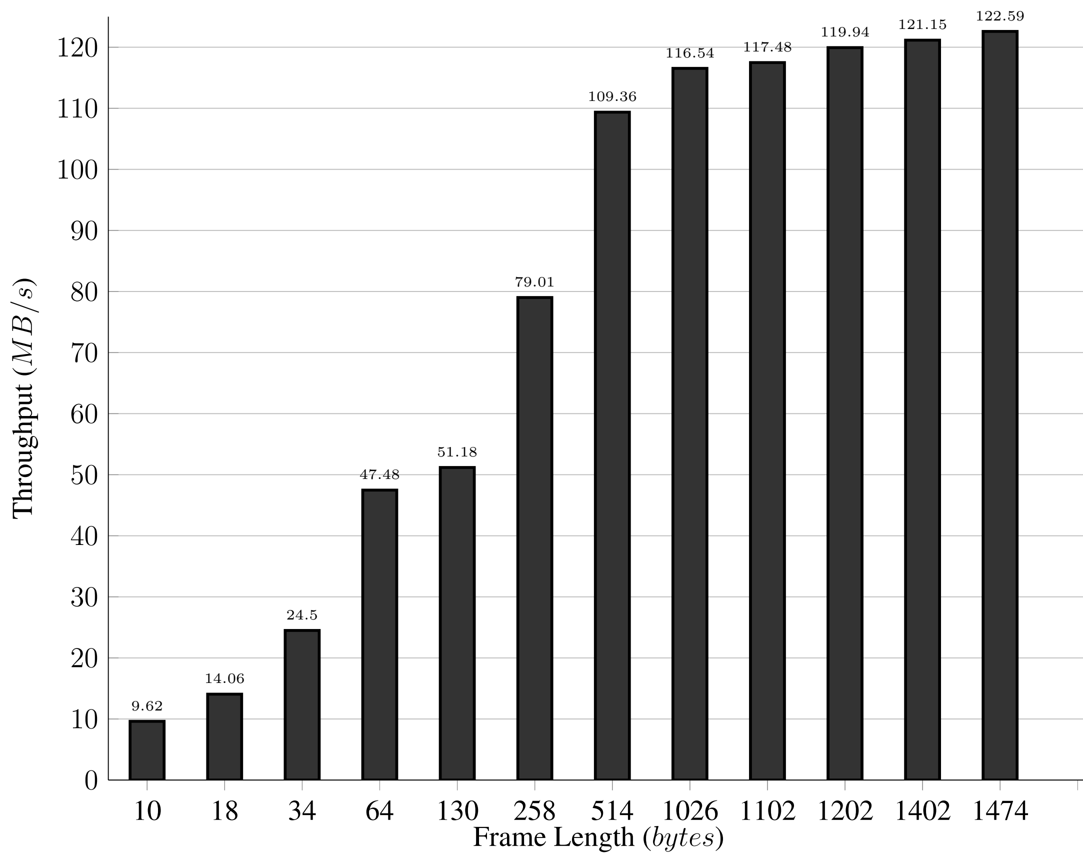

Figure 7.23: Thoughput vs UDP Frame Length

```
No.  Time        Source       Destination  Protocol  Length Info
  46 0.048629000 192.168.0.1  192.168.0.3  UDP           79 Source port: 45527  Destination port: 9930
  47 0.049705000 192.168.0.1  192.168.0.3  UDP           79 Source port: 45527  Destination port: 9930
  48 0.050778000 192.168.0.1  192.168.0.3  UDP           79 Source port: 45527  Destination port: 9930
  49 0.051850000 192.168.0.1  192.168.0.3  UDP           79 Source port: 45527  Destination port: 9930
  50 0.052931000 192.168.0.1  192.168.0.3  UDP           79 Source port: 45527  Destination port: 9930
  51 0.054003000 192.168.0.1  192.168.0.3  UDP           79 Source port: 45527  Destination port: 9930
  52 0.055068000 192.168.0.1  192.168.0.3  UDP           79 Source port: 45527  Destination port: 9930
  53 0.056180000 192.168.0.1  192.168.0.3  UDP           79 Source port: 45527  Destination port: 9930
  Interface id: 0 (eth0)
  Encapsulation type: Ethernet (1)
  Arrival Time: Jun 22, 2015 15:10:42.076144000 SAST
  [Time shift for this packet: 0.000000000 seconds]
  Epoch Time: 1434978642.076144000 seconds
  [Time delta from previous captured frame: 0.001081000 seconds]
  [Time delta from previous displayed frame: 0.001081000 seconds]
  [Time since reference or first frame: 0.052931000 seconds]
  Frame Number: 50
  Frame Length: 79 bytes (632 bits)
  Capture Length: 79 bytes (632 bits)
  [Frame is marked: False]
  [Frame is ignored: False]
  [Protocols in frame: eth:ethertype:ip:udp:data]
  [Coloring Rule Name: ___conversation_color_filter___06]
  [Coloring Rule String: (ip.addr eq 192.168.0.3 and ip.addr eq 192.168.0.1) and (udp.port eq 9930 and udp.port eq 9930)]
▶Ethernet II, Src: AsustekC_ae:db:b2 (e0:3f:49:ae:db:b2), Dst: TexasIns_7d:1d:70 (00:24:ba:7d:1d:70)
▶Internet Protocol Version 4, Src: 192.168.0.1 (192.168.0.1), Dst: 192.168.0.3 (192.168.0.3)
▼User Datagram Protocol, Src Port: 45527 (45527), Dst Port: 9930 (9930)
  Source Port: 45527 (45527)
  Destination Port: 9930 (9930)
  Length: 45
 ▶Checksum: 0x8193 [validation disabled]
  [Stream index: 0]
▼Data (37 bytes)
  Data: 4c656b686f626f6c61204a6f616368696d2054736f65756e...
  [Length: 37]

0000  00 24 ba 7d 1d 70 e0 3f  49 ae db b2 08 00 45 00   .$.}.p.? I.....E.
0010  00 41 0e 21 40 00 40 11  ab 36 c0 a8 00 01 c0 a8   .A.!@.@. .6......
0020  00 03 b1 d7 26 ca 00 2d  81 93 4c 65 6b 68 6f 62   ....&..- ..Lekhob
0030  6f 6c 61 20 4a 6f 61 63  68 69 6d 20 54 73 6f 65   ola Joac him Tsoe
0040  75 6e 79 61 6e 65 20 69  73 20 68 61 70 70 79      unyane i s happy

Data (data.data), 37 bytes     Packets: 1829 · Displayed: 1829 (100.0%) · Dropped: 0 (0.0%)
```

Figure 7.24: Trace of UDP packets being transmitted to FGPA over 1Gbps Ethernet

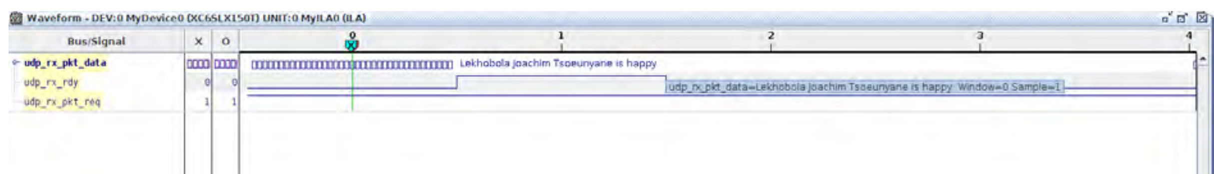

Figure 7.25: Capture of received UDP data on FPGA using ChipScope Pro

7.6 Streaming Core Test

This section discusses the streaming operation mode on RHINO. The stream-based processing incorporates ADC that digitizes analogue input and a 1 Gigabit Ethernet which uses UDP/IP core to send digital samples received directly from the ADC to a PC. The design for both ADC and UDP/IP interface cores is detailed in Chapter 5 and the VHDL instantiation components of both cores are provided in Appendix F.1 and Appendix G.1 respectively. The experimental setup was organized as illustrated in Figure 3.9.

7.6.1 Direct Streaming

The experiment of the streaming core was completed by performing a four tests using different tones 200kHz, 5MHz, 10MHz and 20MHz, all generated using a 20MHz function generator. The spectral analysis of the sine waves is shown in Figure 7.26 as measured directly from the function generator before stream-based processing by the FPGA.

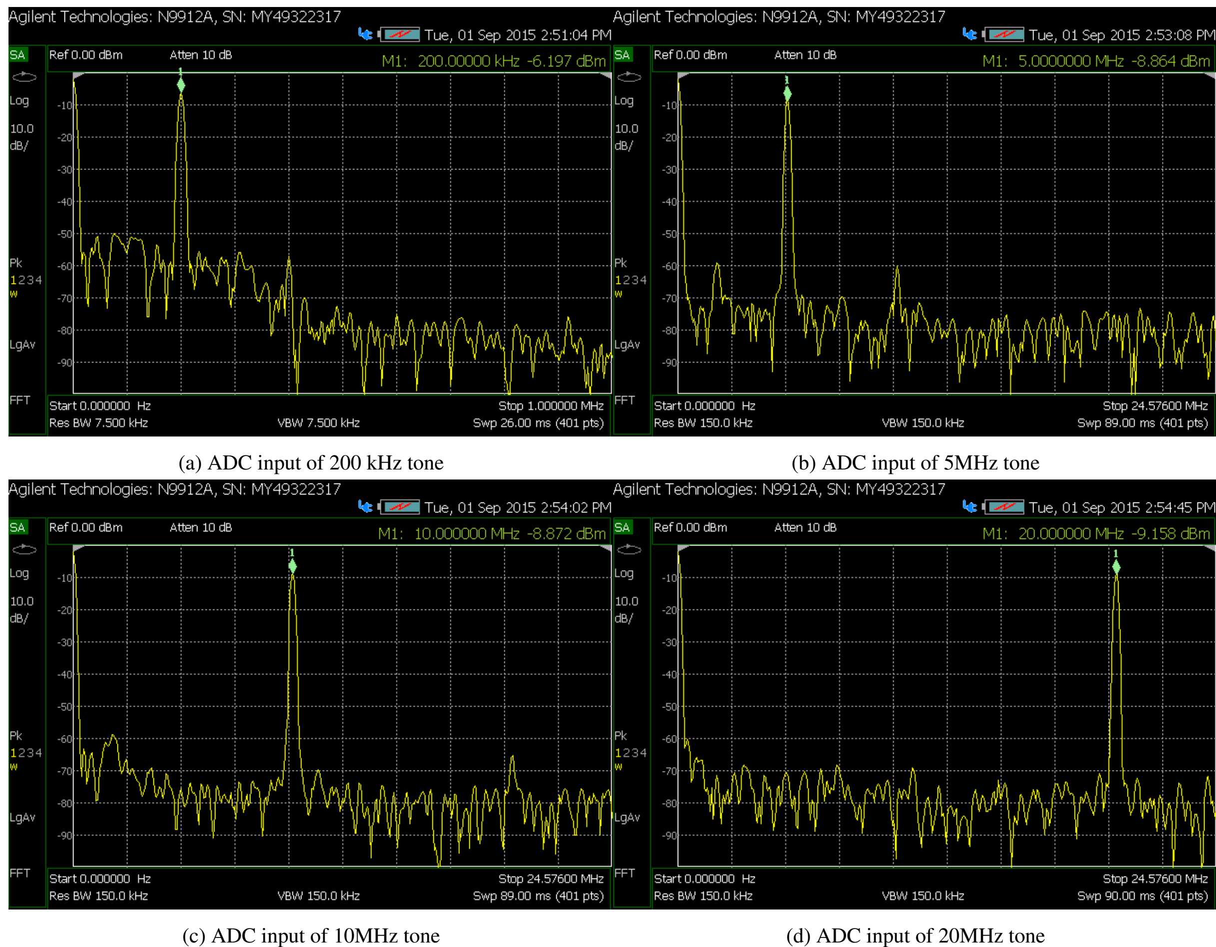

(a) ADC input of 200 kHz tone

(b) ADC input of 5MHz tone

(c) ADC input of 10MHz tone

(d) ADC input of 20MHz tone

Figure 7.26: A measured spectrum analysis for ADC input sine waveforms generated using a function generator

Each of the signals displayed in Figure 7.26 was fed into the ADC where it was converted into digital domain at ADC sampling rate of 49.152 MSPS. In order to visualize the discrete-time

domain graphs of the signals after ADC inside the FPGA, ChipScope Pro was used. One such graph showing a 200 kHz digital sine wave is illustrated in Figure 7.27.

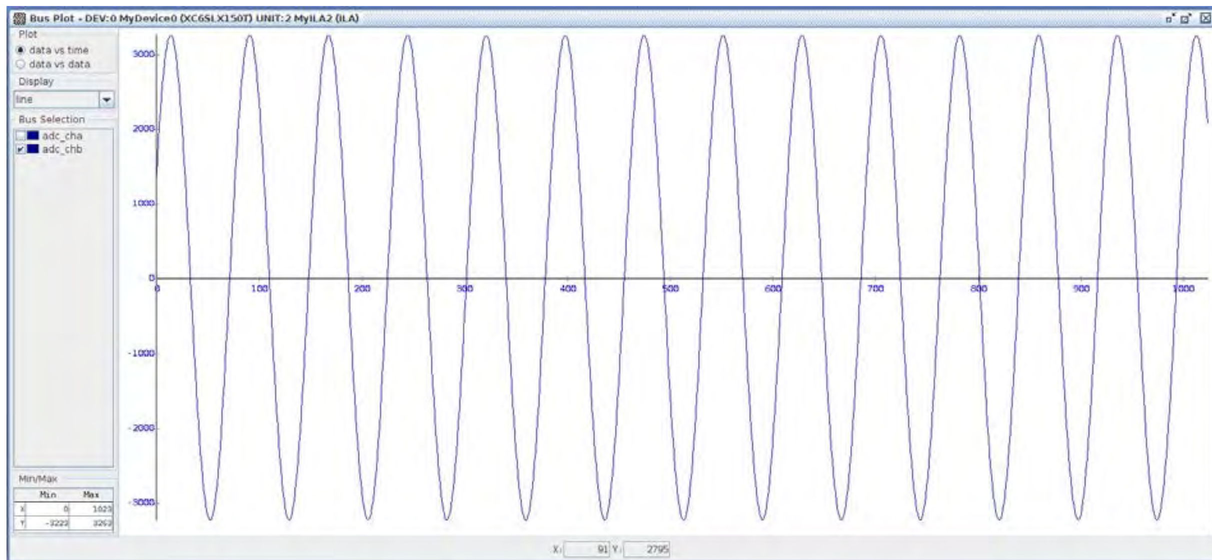

Figure 7.27: A digitized 200kHz sine wave visualized using ChipScope Pro

After acquisition of data from the ADC, the 14-bit samples were extended to 16-bit precision so that each sample was made up of two bytes. Without doing any signal processing on the signal, the 502-long double buffer was used to cache the double byte samples which were later packetized into a 502 bytes UDP frame whenever a buffer was full. The UDP packet containing ADC data was then transmitted to a PC over a 1Gbps Ethernet interface where the frames were captured and depacketized for further analysis.

At the PC end, the captured data was analysed for UDP throughput speed and dynamic parameters of the ADC. The UDP throughput speed was calculated using equation 7.1 and the result obtained was 98.62MB/s. According to B.K. Huang et al. [38], the theoretical figure of throughput in a streaming mode is 110MB/s, our results have proven that 89.65% of the ideal figure can be achieved.

In order to carry out the performance analysis of the ADC, the ADCPro software was used. ADCPro is a standalone ADC testing and performance analysis using captured ADC samples of data [44]. The most important of the dynamic parameters to be tested using ADCPro software are SNR, THD, ENOB, SFDR and SINAD. The description and formulae of these parameters is in section 2.10.

UDP data was stored on tab delimited data files where each line represented double byte or 16-bit decimal ADC sample. The files were then imported into ADCPro for analysis of signals.

Using a MultiFFT feature of the ADCPro, the 131072-point FFT was performed on 251000 samples and the key performance parameters such as SNR, THD, SINAD and SINAD were calculated. An instance of results where 200 kHz tone was analyzed as shown in Figure 7.28. This also applied to other sine waves used in the experiment.

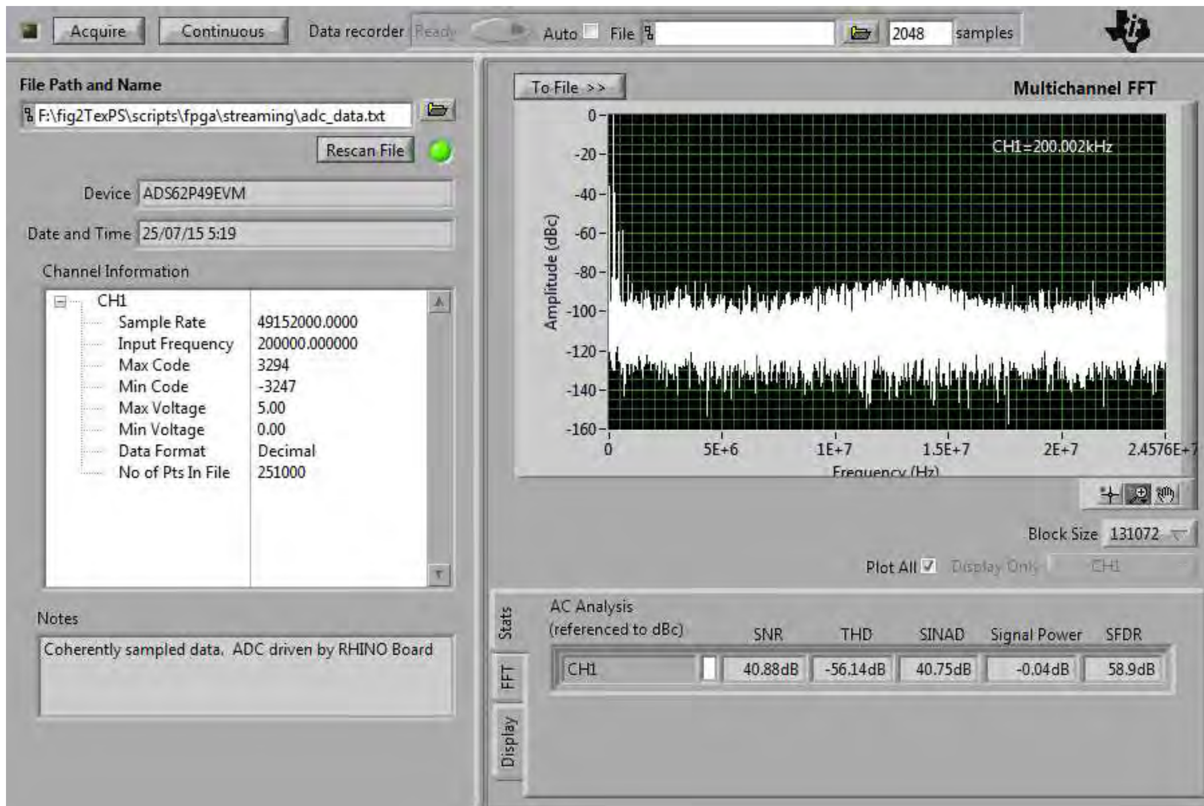

Figure 7.28: A digitized 200kHz visualized using ChipScope Pro

The FFT results of the ADCPro were exported to excel files and they were re-plotted for all the test cases as shown in Figure 7.29 and Figure 7.30 whilst the dynamic parameters are tabulated in Table 7.9.

Finally, the ENOB was determined using the equation 2.12. The results are also shown in Table 7.9.

Table 7.9: Dynamic parameters for a 49.152MSPS ADC digitizing different tones.

Measured	SNR (dBc)	THD (dBc)	SINAD(dBc)	SFDR (dBc)	ENOB (bits)
Datasheet	70	-67	69.789	80	11.3
200kHz	40.88	-56.14	40.75	58.9	6.48
5MHz	40.38	-55.85	40.26	56.0	6.39
10MHz	21.48	-51.93	21.48	52.0	3.28
20MHz	3.98	-44.25	3.98	44.3	0.363

7.6.2 Stream Processing With Decimation and Filtering

Using very high ADC sampling rates in the streaming mode results in packet loss and signal distortion. This is illustrated in Figure 7.31 where experiment setup similar to one in previous section was made, but this time using a higher ADC rate of 163.84 MSPS. The reason for this is that the increased sampling rate gave rise to ADC sample arrival rate which was higher than the UDP transmission rate. Thus leading to new samples over-writing the old data samples

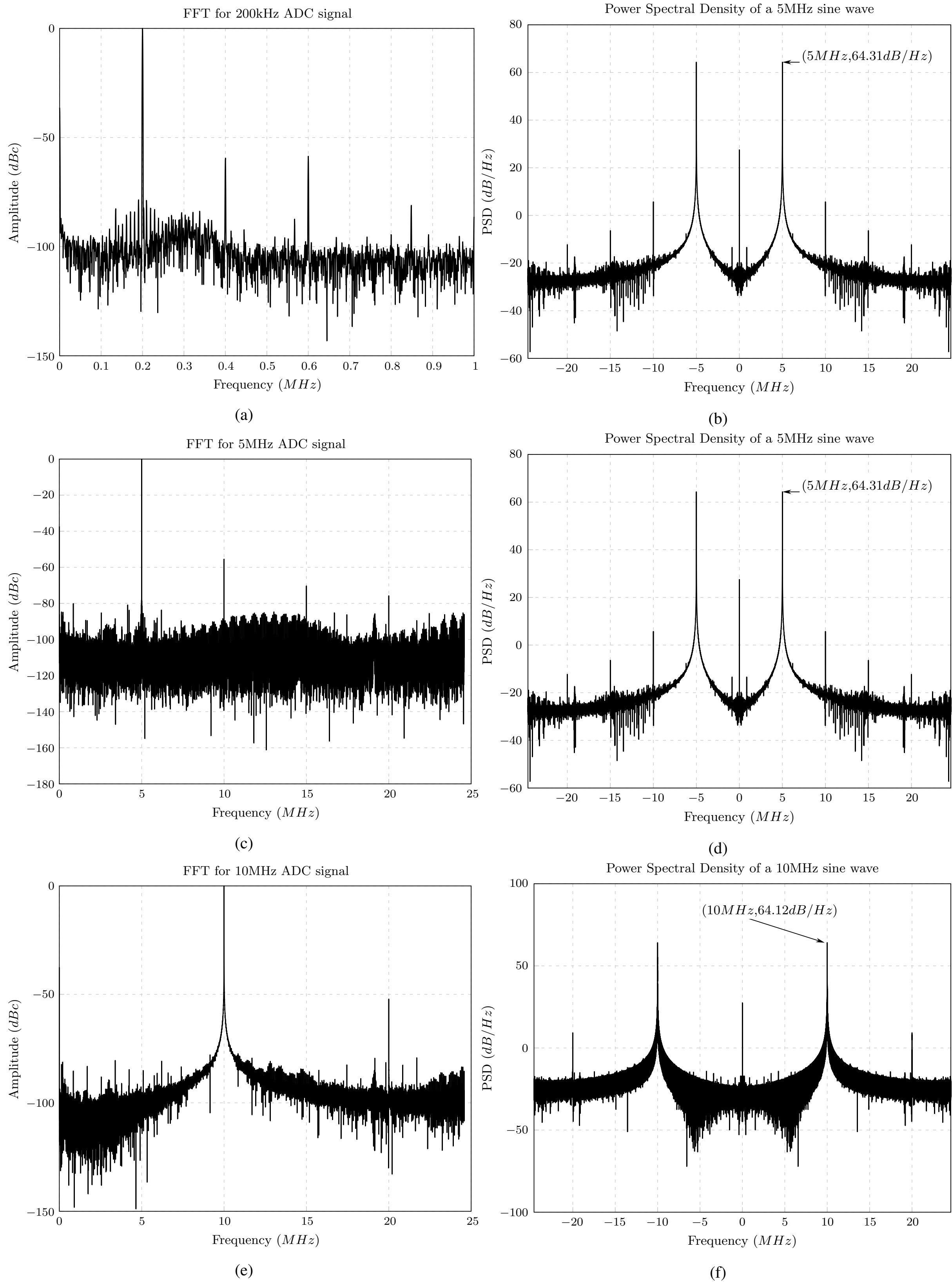

Figure 7.29: ADC digitized signals streamed via UDP

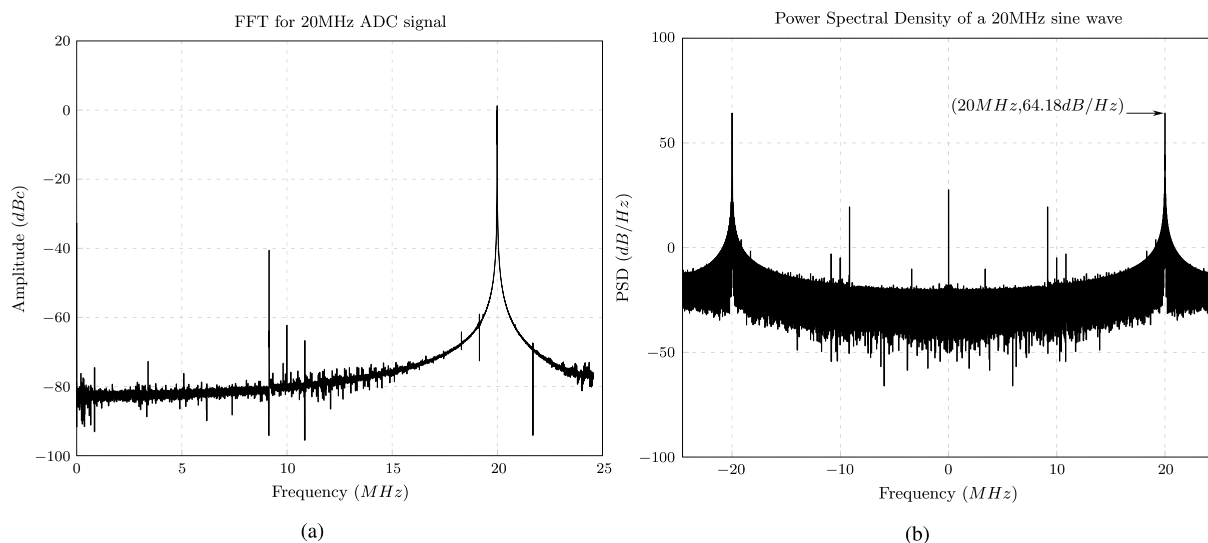

(a) (b)

Figure 7.30: 20MHz tone ADC ouput streamed using UDP

awaiting UDP transmission in a buffer. Another reason was that UDP packets were sent to UDP core faster than the Ethernet MAC could transmit the packets, hence leading to packets no being sent to a PC at all.

Although it is also possible when using UDP that packets can be dropped at the receiver, in this experiment it does not have much effect because the UDP/IP core is carefully designed not to overwhelm the receiver with packets. As long as the throughput is kept below 125MB/s the packet drops are negligible. The possibility of losing large volumes of data is when the ADC sampling rate is too high resulting in buffer overflow before the UDP/IP core transmits buffer data. This is a producer-consumer problem occurring inside the FPGA. Furthermore, the corrupted packets can fail CRC that is enabled at the receiver. This can happen in noisy environment or if a long Cat5e cable is used in a point-to-point network. However, these conditions were avoided therefore packet drops were negligible as the CRC fails occurred infrequently.

To alleviate the shortcomings of a streaming core when high ADC sampling rates were used, decimation and filtering were adopted in the design. Unlike the previous section where different signal frequencies were tested, in this experiment only a 200kHz was used. The block diagram of the setup is also illustrated in Figure 7.32. A very high 163.84 MSPS ADC sample rate was chosen and decimated by a ratio of 1:32 which resulted in a 5.12 MSPS being used for UDP transmission. A CIC decimation filter was used to perform downsampling and filtering, then followed by a Compensation FIR filter which corrected non-flat response of a CIC filter.

The results showing the FFT and PSD of the ADC signal in the presence of CIC decimator and Compensation FIR filter are depicted in Figure 7.33 and the resulting ADC dynamic parameters proving improved results are shown in Table 7.10. As observed, the decimation and filtering have a tremendous impact on the output signal. The reason being that they use relatively low data rates on the DSP side to allow for sufficient transmission rate over Ethernet.

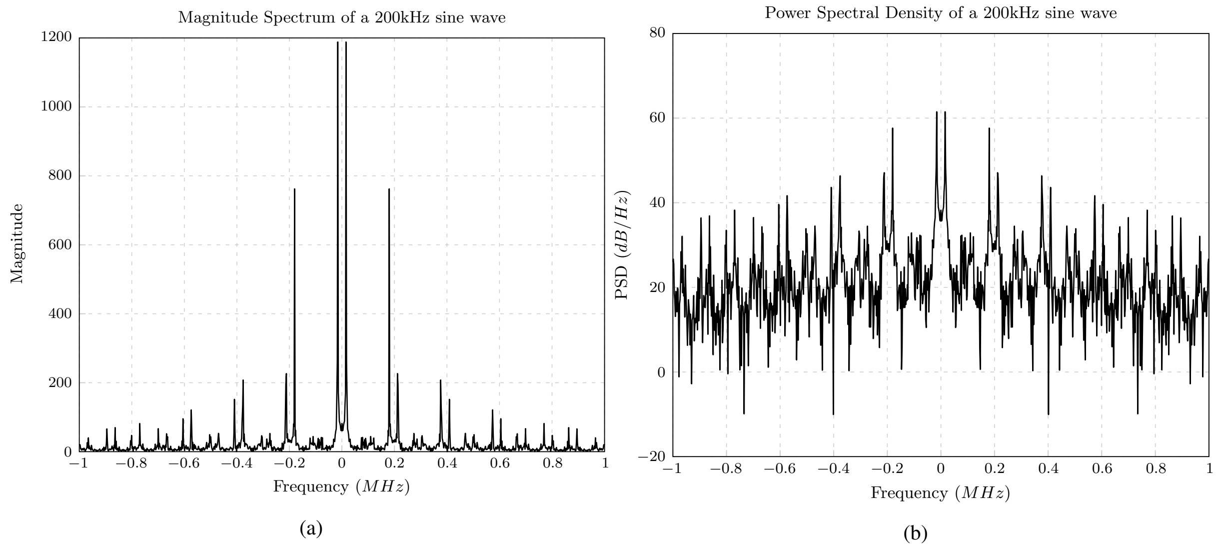

Figure 7.31: FPGA results of UDP streaming when 163.84MSPS ADC is used

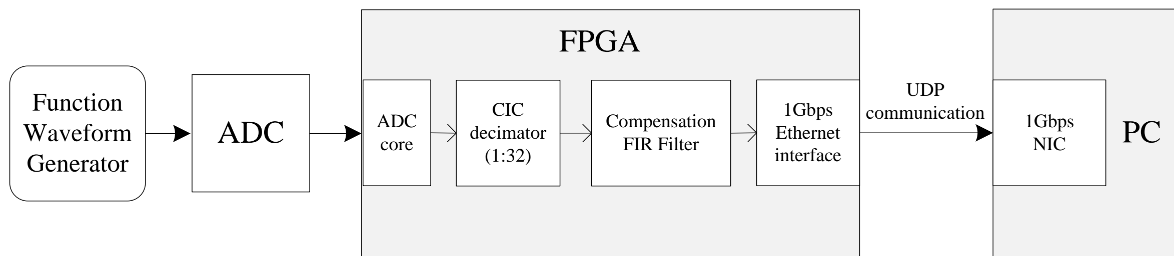

Figure 7.32: Experimental setup for stream-based processing with CIC decimation filter and Compensation Filter

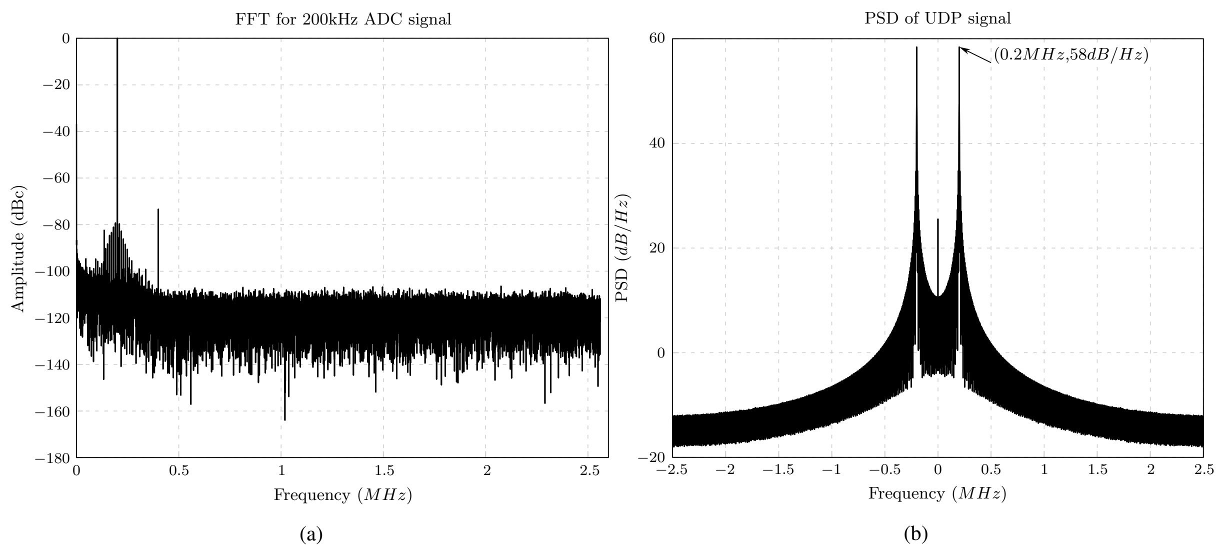

Figure 7.33: FPGA results of UDP streaming when a CIC and FIR filters are used to process a 200 kHz signal sampled by the ADC at 163.84 MSPS

Table 7.10: Dynamic parameters for a 163.84 MSPS ADC digitizing 200kHz tone. The ADC sample rate is decimated resulting in sample rate of 5.12 MSPS prior to UDP transmission

Measured	SNR (dBc)	THD (dBc)	SINAD (dBc)	SFDR (dBc)	ENOB (bits)
Datasheet	70	-67	69.789	80	11.3
200kHz	42.24	-73.35	42.24	73.4	6.72

7.6.3 Testing the FFT Core inside Streaming Logic

Having demonstrated the successful functionality of the streaming core, the FFT core was further tested by placing it between the ADC core and UDP core so that it could perform FFT of ADC digitized signals. Three tests that included 133kHz, 200kHz and 445kHz sine waveforms were used and their FFTs were performed in separate tests. In each case, the FFT lengths of 512 and 4096 were used and the lowest 6.144 MSPS sample rate for ADC was used. However, before the FFT experiment was carried out, the digital data of the three signals was captured without the FFT core. The FFT of the each three sinusoid was determined and plotted using Matlab. This served as an ideal reference model to the results processed using FFT core in FPGA. Figure 7.34 shows the setup used for the experiment.

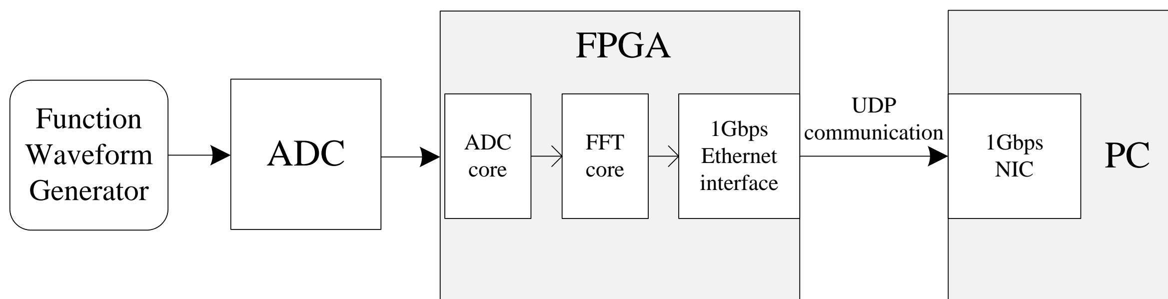

Figure 7.34: Experimental setup for FFT core as tested on the FPGA

The results of MATLAB FFT and FPGA FFT core are shown in Table 7.11 in a form of frequency and the difference between two FFT lengths. The graphs of computed FFT in MATLAB and FPGA for 133kHz, 200kHz and 445kHz ADC tones are shown in Figure 7.35, 7.36 and 7.37.

Table 7.11: MATLAB and FPGA FFT results of ADC sines waves streamed from FPGA via UDP

	MATLAB FFT frequency (kHz)			FPGA FFT Core Frequency (kHz)		
Signal	**N=512**	**N=4096**	**Difference**	**N=512**	**N=4096**	**Difference**
133kHz	132.000	133.500	1.5	132.000	133.500	1.5
200kHz	204.000	199.500	4.5	204.000	199.500	4.5
445kHz	444.000	445.500	1.5	444.000	445.500	1.5

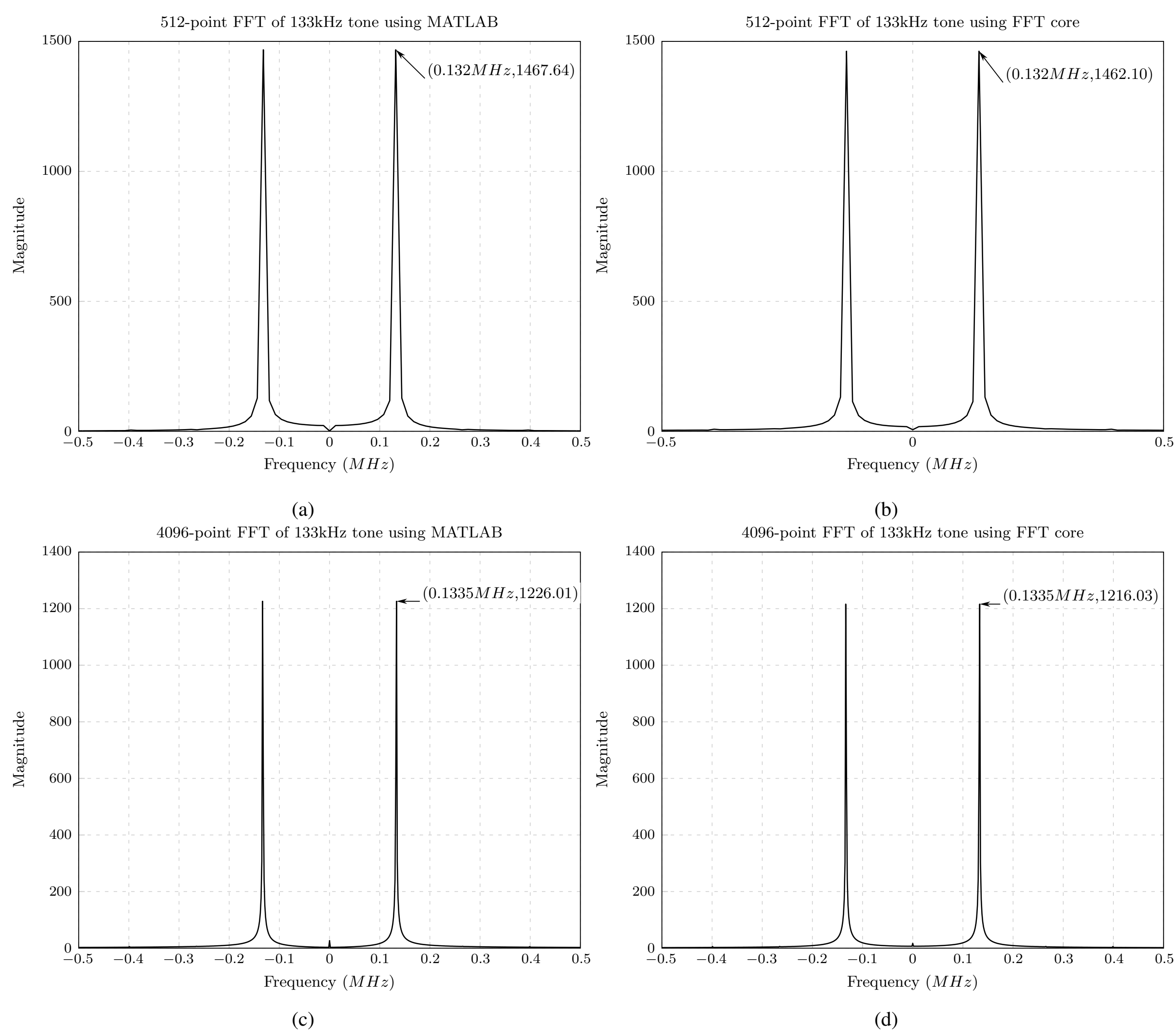

Figure 7.35: Results showing 512-point and 4096-point FFT of a 133kHz ADC wave using MATLAB and FFT core

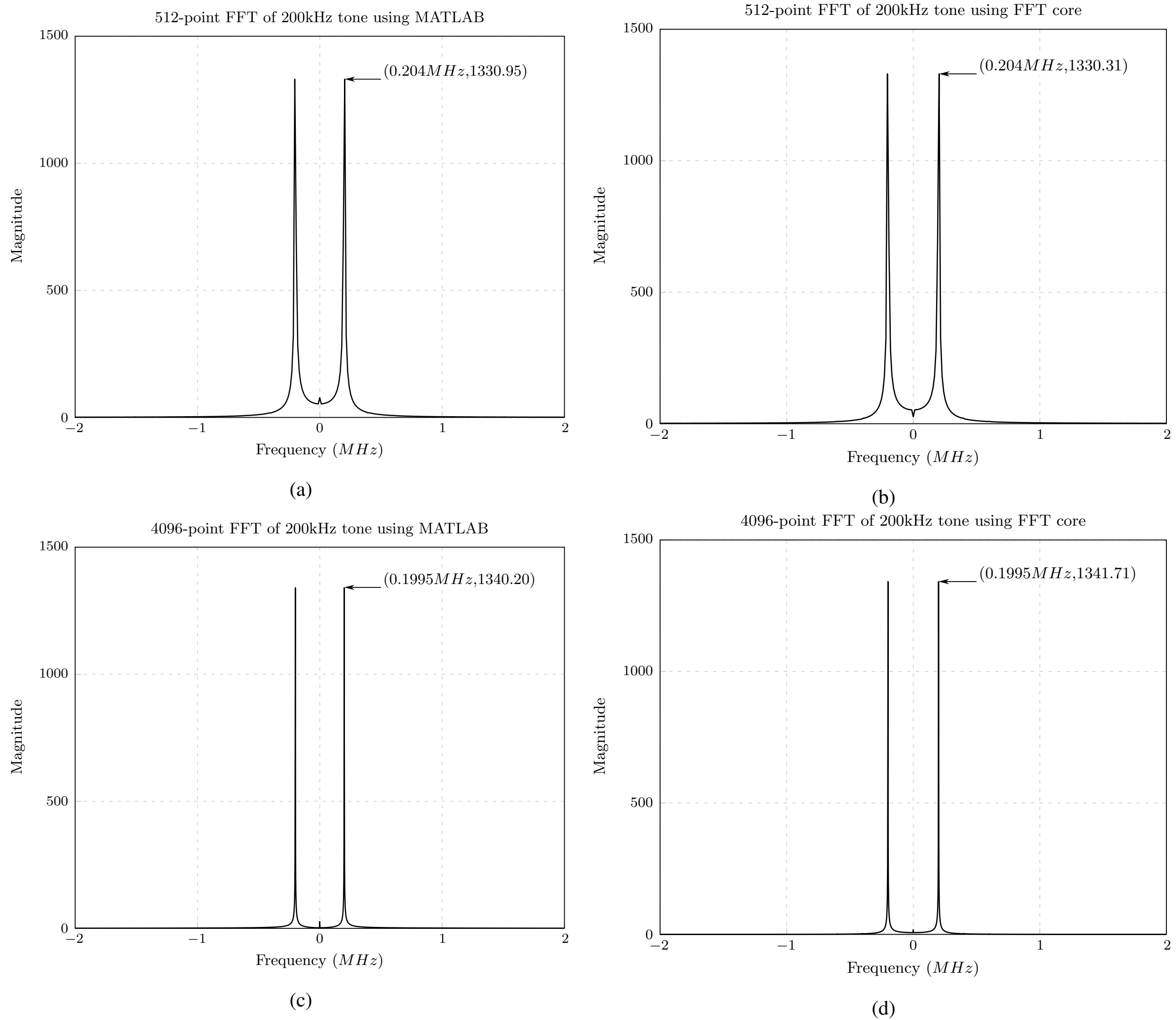

Figure 7.36: Results showing 512-point and 4096-point FFT of a 200kHz ADC wave using MATLAB and FFT core

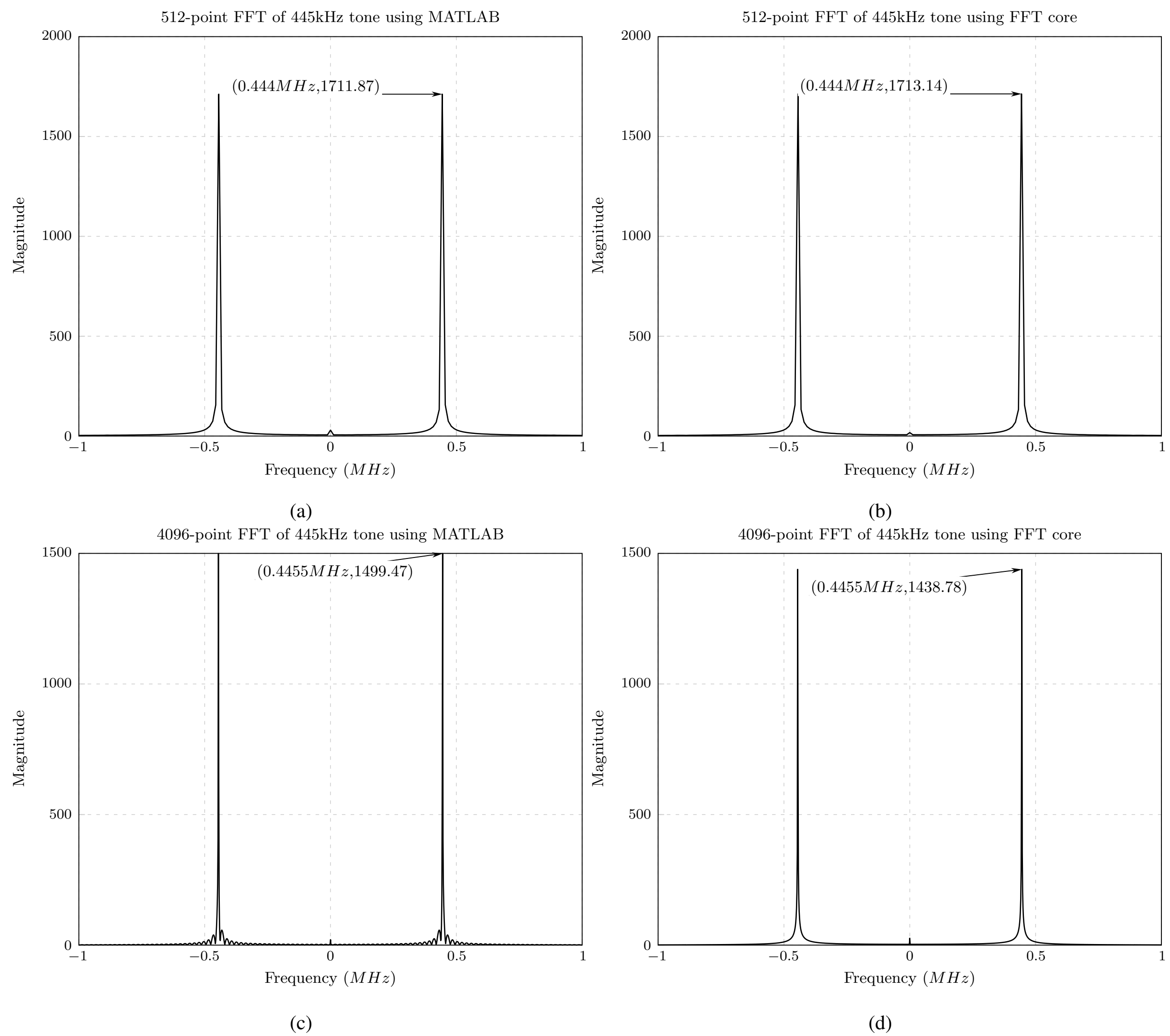

Figure 7.37: Results showing 512-point and 4096-point FFT of a 445kHz sine waveform using FFT/IFFT core

7.7 DAC interface core Test

This section presents testing of a DAC interface core for FMC150 designed in section 5.1.3. The block diagram of the experimental setup is illustrated in Figure 3.8. This experiment used a NCO core designed in section 4.4.1.1 to synthesize three different sine waveforms of frequencies 200kHz, 10MHz, 17.23MHz and 28.38MHz. The digital samples were sent to the DAC at 61.44MSPS sampling rate. The DAC in turn converted digital data into analogue signals which were measured on a spectrum analyser and the results are shown in Figure 7.38.

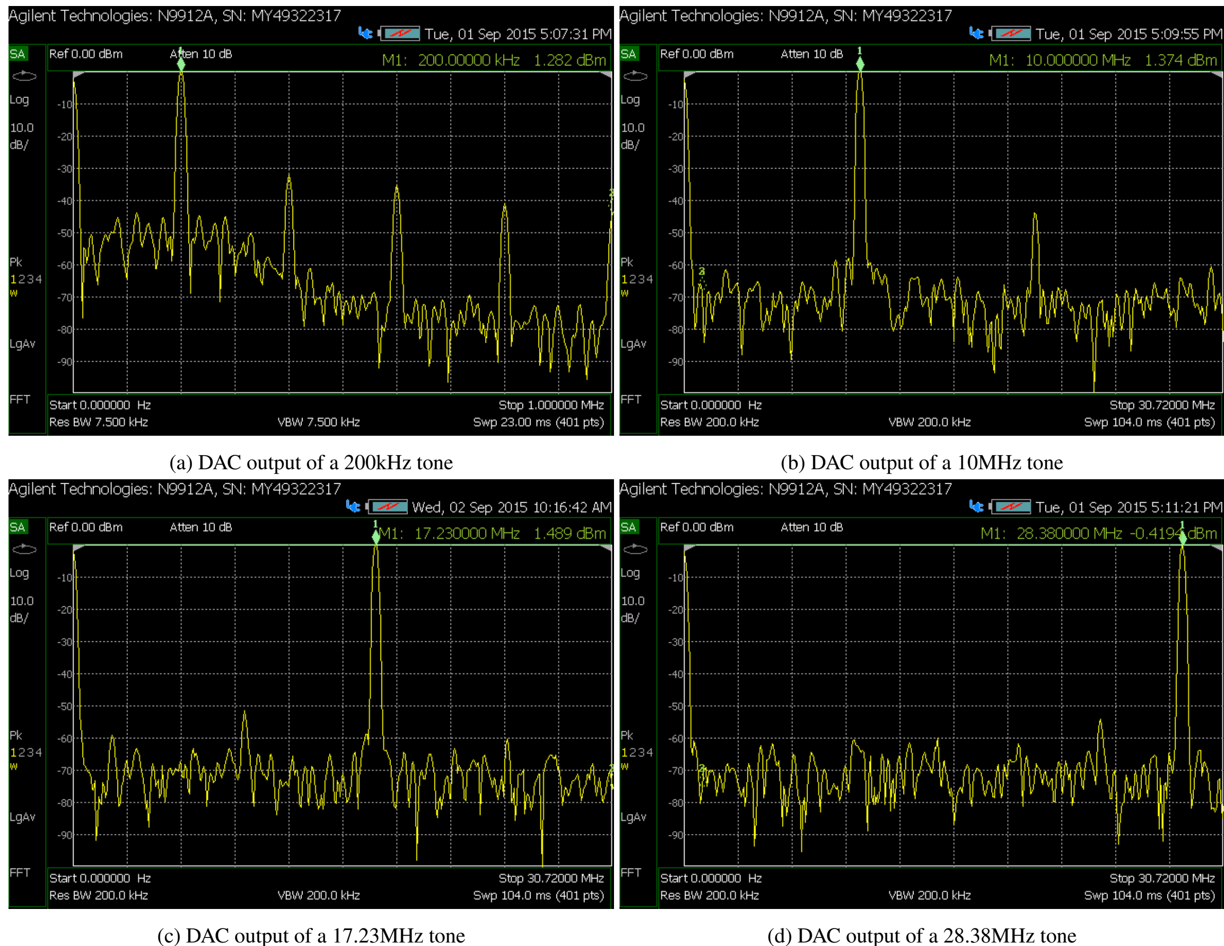

(a) DAC output of a 200kHz tone

(b) DAC output of a 10MHz tone

(c) DAC output of a 17.23MHz tone

(d) DAC output of a 28.38MHz tone

Figure 7.38: The spectra different sinusoids generated using NCO core and measured at the FMC150 DAC output

The results shown in Figure 7.38 were further summarized in Table 7.12 which shows the peak power level and SFDR of the signals measured from DAC. The power level was obtained straight from the results graph while the SFDR was calculated using equation 2.14.

7.8 FM Receiver Test

This section presents an experiment of a wideband FM receiver designed in Chapter 6 and the design is based on the FM modulation and demodulation concepts reviewed in section 2.11. The block diagram showing the experiment setup is shown in Figure 3.10. The final output of

Table 7.12: Summary of DAC results for different tones

Tone (MHz)	Fundamental Power Level (dBm)	Highest Spurious Power Level (dBm)	SFDR (dBc)
0.2	1.282	-32	33.288
10	1.374	-44	45.374
17.23	1.489	-52	53.489
28.38	-0.4194	-54	53.590

the FPGA were complex I/Q samples centered at DC. These samples were then demodulated in Matlab using arctan/differentiation FM demodulator. The output of the FM demodulator is real-valued signal. Results were then compared to an ideal FM radio baseband signal [22] depicted in Figure 7.39. The spectral content of this signal is mono audio between 0 and 15kHz, the pilot tone at 19kHz, the stereo audio between 23 and 53kHz, and RBDS at 57kHz.

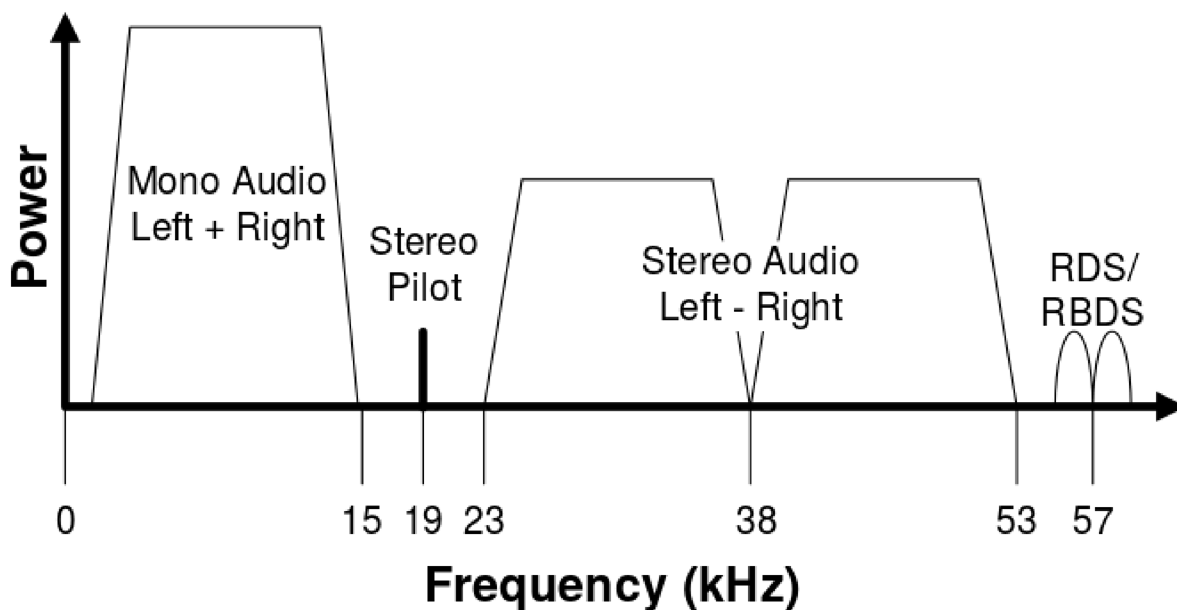

Figure 7.39: A spectrum of a baseband FM station [22]

Testing was performed by tuning to three different FM stations displayed in Table 7.13. The results showing the spectrum of the FM band measured at the antenna output and after filtering and further amplification are shown in Figure 7.40a and 7.40b respectively. These results show stations which were used for testing and are marked using respective FM station IDs.

Table 7.13: FM stations used for the FM receiver experiment

ID	FM station	Frequency
1	City Centre	89.0 MHz
2	KFM	94.5 MHz
3	Constantia Berg	95.3 MHz

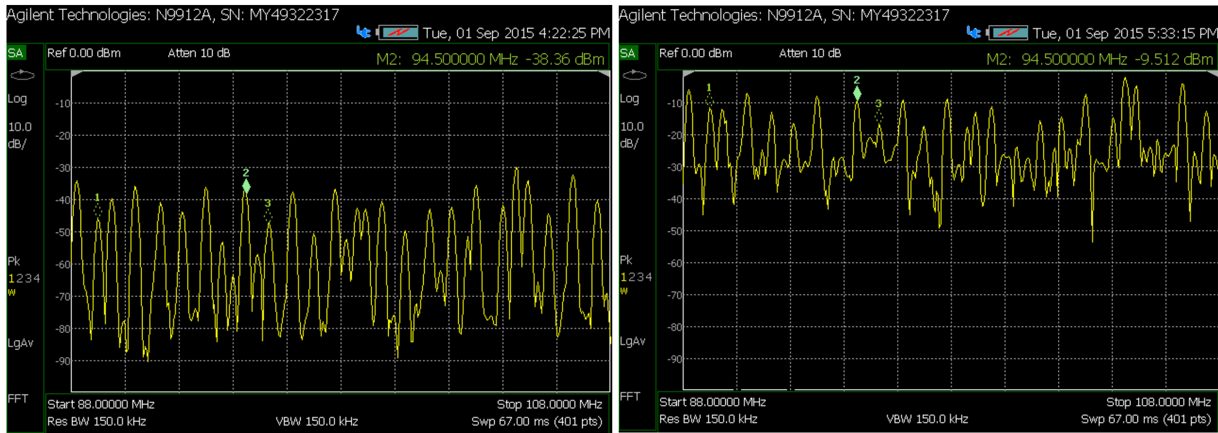

(a) The FM band signals at antenna ouput

(b) The FM band signals at front-end output

Figure 7.40: The FM band signals measured before and after analogue RF front-end processing

Furthermore, the results showing complex I/Q data before demodulation and FM demodulated signals for all FM stations are shown in Figure 7.41. The demodulated FM signal of each of the three stations was compared with ideal spectral content in Figure 7.39. The FM receiver sensitivity is -85dBm and the results clearly show the mono audio, pilot tone, stereo audio and RBDS spectral components, however; stereo audio and RBDS are not distinguished due to a weak FM signal received by the ADC. The ADC tends not to be sensitive to signals with power way below 10dBm. Increasing the analogue RF front-end gain will improve results.

Furthermore, factors which are more likely to affect the quality of the received FM signal are outlined as follows:

- The antenna gain generates profound noise as well the other amplifiers in the front-end. This noise is generated internally and it is inevitable.
- The ADC is sensitive to FM signals equal or not very far below 10dBm power level. Signals further below 10dBm are not detected by the ADC.
- The ADC also introduces noise and distortion that degrades the quality of sampled analogue FM signal as described in section 2.10.
- The man-made noise can impact the performance of the FM receiver. This generally comes from sparking equipment, and also from equipment that generates RF. This noise was highly likely as experiments were performed in RF/microwave lab where there were RF and high frequency Radar transceivers.
- The environmental factors such as weather can have tremendous impact on the integrity of the received FM signal. Lightning can cause electrical interference while heavy storm and fog can attenuate signals as they propagate through air.

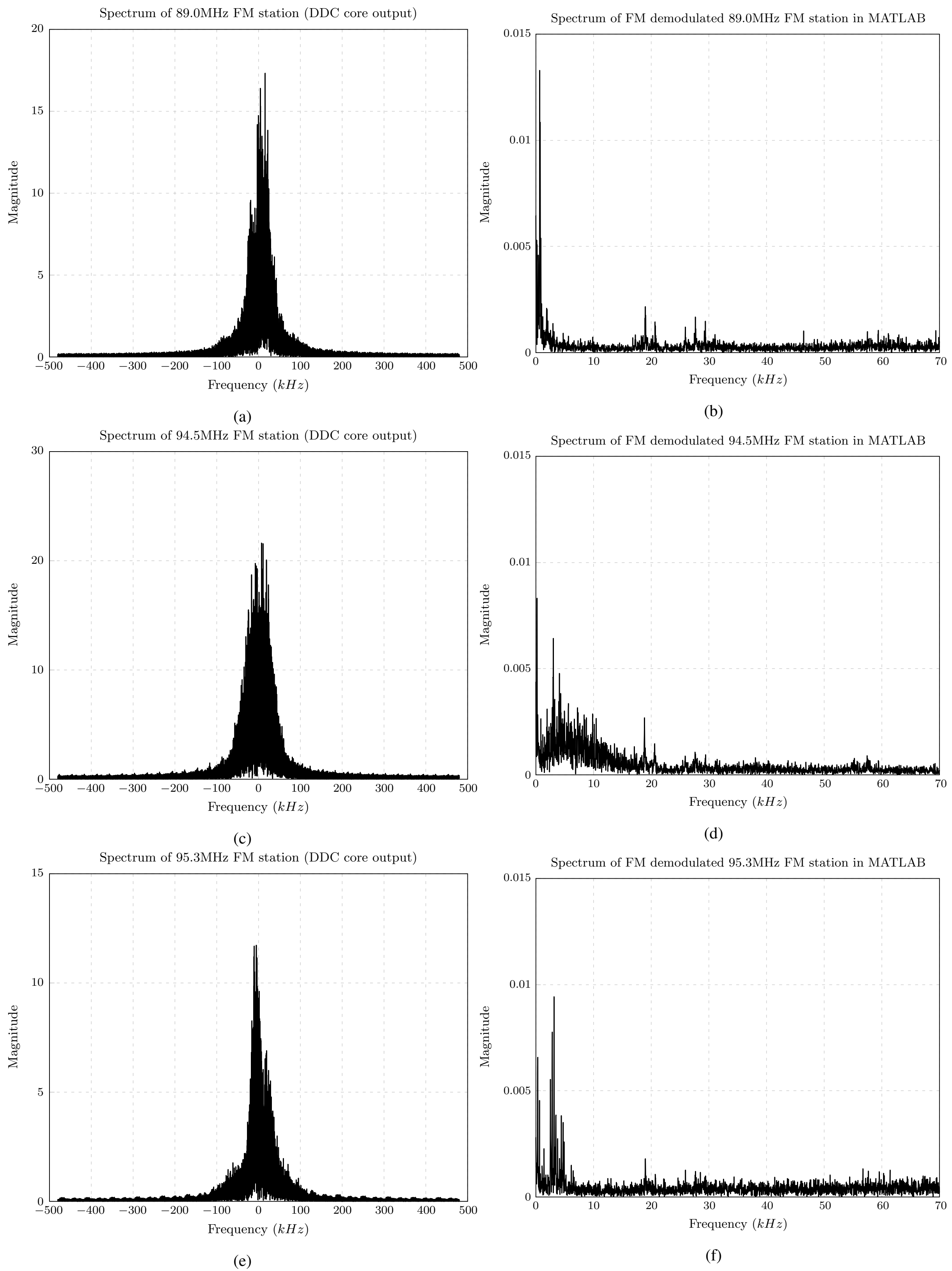

Figure 7.41: The results of FM Receiver when tuning to 89MHz, 94.5MHz and 95.3MHz stations

CHAPTER 8

CONCLUSIONS AND FURTHER WORK

This chapter presents the conclusions and future work for the SDR-based library of IP cores proposed in this dissertation.

8.1 CONCLUSIONS

The developed library of IP blocks has passed all tests discussed in Chapter 7. This section provides discussion and conclusions of the results obtained. The conclusions for the DSP IP blocks will be presented first and this will be followed by conclusions relating to the I/O interface blocks. Considerations for facilitating the reuse of these blocks by developers, in particular novice developers that have little in the way of FPGA programming experience will be highlighted.

8.1.1 DSP IP blocks

The following processing IP blocks were chosen for inclusion into the DSP IP blocks library: FIR filter, IIR filter, FFT/IFFT modules and a parameterized and highly scalable DDC block. These cores were chosen specially in consideration of common SDR processing needs and this selection was based on a thorough literature review as detailed in sections 2.3, 2.4 and 2.7. Novice developers wanting to reuse these processing cores would consequently be advised to review the theoretical operation of these blocks, possibly trying them in OCTAVE or MATLAB to gain a practical understanding of their behavior or limits, whereafter they would be familiar with the parameters concerned and be well prepared for moving to the FPGA, RHINO-based context of application of making these processing operations work in a real environment. Through the testing of these blocks done in this project, it was demonstrated in Chapter 7 that the implementation of these blocks was successful and that they could be effectively connected to other processing elements in the FPGA design to run in real time. These blocks were all designed around a common SoC interface, namely Wishbone, which was done to further improve the reusability of these blocks. In order to verify the functionality and correctness of these blocks, testing which involved behavioural and functional simulation was performed.

FIR core experimental test was performed in section 7.1 and its results were compared to high precision floating point results obtained using FIR simulation in Matlab. The comparison demonstrated that the FPGA and Matlab results are almost in the same trend; however there still

exist some deviation which is a result of quantization noise and round-off noise. Furthermore, not only was the FIR verified using behavioural and functional simulation, but the in-circuit verification was also performed in section 7.6.2 where FIR core was used as the compensation filter after decimation of high ADC sampling rate. This further justifies the extent of success to which the FIR core was designed and tested.

The IIR core was tested in section 7.2 the same way as the FIR core but with different filter design response. The results of the IIR core were similar to IIR simulation results in Matlab and there was little deviation as seen when testing FIR core. The results of IIR core are more improved because of high attenuation in the IIR filter stopband which is obtained with a smaller number of coefficients in comparison to the FIR filter.

Testing of the FFT/IFFT core was also successful and was performed in section 7.3. The results of the core operating as FFT and IFFT were compared with floating point FFT and IFFT functions in Matlab and the results obtained were similar. Furthermore, the in-circuit verification of the FFT/IFFT core was performed in a stream-based processing of ADC data as described in section 7.6.3. The results obtained were compared with Matlab calculated FFT of ADC data and were very similar to one another.

The DDC core was tested successfully using the FM signal which was created by modulating 94.5MHz carrier signal with 15kHz baseband signal as demonstrated in section 7.4. The FM signal was processed by the DDC core and Digital FM demodulator. The final output was the FM demodulated signal that had transients at the beginning but quickly faded away before the system enters into a steady state. The steady state of FM demodulated signal was identical to the original baseband 15kHz signal. The only small difference found was in the signal frequencies which were calculated as 15kHz (original modulating signal) - 14.845361kHz (FM demodulated signal) = 0.1546kHz. Furthermore, noise was added to the modulating signal and to FM signal before DDC core processing and FM demodulation. The results obtained showed that adding AWGN to modulating signal before modulation has no noticeable effect on the signal produced after FM demodulation. On the hand, adding AWGN noise to the FM signal before DDC core processing and FM demodulation results in reduced SNR of the output signal and the AWGN noise is noticeable in the output signal.

8.1.2 **I/O interface blocks**

Testing of the I/O interface blocks involved in-circuit verification of UDP Ethernet IP core and the FMC150 ADC/DAC sampling card interface core. Both of these interface blocks produced satisfactory results when tested on the RHINO board. In terms of novice engineers using the capture card, there are preparatory and time-planning considerations for this: The 4DSP FMC150 is a highly specialized card and has many configuration settings that need to be properly configured in order to make it operate in the way needed; while it is a powerful product it is, from my experience, advisable for novice users to start with ready-made configuration settings and one of the suggested RF bands in the tutorial before spending possibly days getting the settings and the structure of the RF front-end circuitry properly aligned to the application needs.

The UDP/IP core which created a reliable interface for 1 Gigabit Ethernet on RHINO was

tested first as discussed in section 7.5. The 1 Gigabit Ethernet testing was successful as UDP data could be transferred in both directions and received on both the PC and FPGA without errors. For novice developers wanting to experiment with prototyping their own SDR systems, it would likely be easier, and likely work out quicker in the long run, were they to start with, after initial OCTAVE/MATLAB experiments, to have a direct sampling core to Ethernet core connection and work on maximizing the sample throughput of this arrangement, while doing sanity checks on the RHINO's output (to check for any breaks in data acquisition) and to test algorithms on real data, before moving the processing operations (such as digital tuning and FM demodulation) onto the FPGA using the pre-built DSP blocks.

The throughput speed of the 1 Gigabit Ethernet was tested with data generated within the FPGA and the speed obtained was 122.59 MB/s which is 98% of theoretical 125 MB/s. However, when 1 Gigabit Ethernet was tested in a stream-based processing, the results dropped to 98.62 MB/s. This is still a very good result as it is only 89.65% of the streaming mode theoretical figure of 110 MB/s. The range of UDP payload supported by the designed core ranges from 1 to 1474 bytes.

The results have demonstrated that very long packets of UDP data can be transferred between the FPGA and the PC. Additionally, the practical throughput speed measured is very close to the theoretical figure and this is a good sign that the designed UDP/IP core is performing as expected. Some observations were made which will be important to take into consideration when using the UDP/IP core. They are as follows:

- Very long UDP packets get corrupted or lost when sent to a PC at high transmission speed using the 1 Gigabit Ethernet interface inside the FPGA. The reason for this is that packets are dropped by PC network card due to high traffic bursts. This issue can be resolved by increasing the receive buffer size in Linux Kernel. Another alternative is to reduce frame size or the transmission speed.
- For stream-based processing using ADC and 1 Gigabit Ethernet, high ADC sampling rates beyond 49.152MSPS lead to data loss between ADC interface core and UDP/IP. An example showing results of this problem is illustrated in Figure 7.31. The reason for this is that the arrival rate of ADC samples in the intermediary buffer is higher than the transmission rate of UDP/IP core. The buffer fills up faster than the UDP/IP core gets ready to transmit all values in the buffer and when it does, the new ADC samples will have overwritten the old ones. To work around this problem, the digital down conversion or decimation and filtering can be used as demonstrated in section 7.6.2.
- The throughput speed rises with an increase in frame size of UDP packet being transmitted. Reducing the frame size minimizes the errors in the received packet by the PC.

FMC150 ADC/DAC interface core was the second I/O interface block to be tested where ADC and DAC were tested separately. As fully described in section 7.6, ADC core was tested by supplying an ADC with sine waves of different frequency generated by a function generator. These analogue signals were converted to digital samples and then sent out to a PC as UDP packets via 1 Gigabit Ethernet. At the PC end the ADC samples were captured and the ADC

dynamic parameters were measured using ADCPro software. The results were summarized and compared to vendor-specified dynamic parameters as shown in Table 7.9. In all cases, the SNR is relatively low in comparison with the datasheet figure. The reason for this is the phase noise in the PLL generated clock that drives the ADC. SFDR, THD, SINAD and ENOB also have lower values, the reason for this is pronounced spurious harmonics due to the high level of distortion in the 10dBm input signal from a function generator. Using very low frequencies improves the results whereas increasing the function generator frequency worsens the results.

The DAC core was also tested successfully in section 7.7 where NCO core was used to supply the DAC with sine waves. The results obtained from the DAC output provided up to 53dBc of SFDR. This SFDR increases with rise in frequency of the input signal to the DAC. Furthermore, lower frequency signals have a number of spurious harmonics but they decrease when frequency increases. This effect is due to phase quantization of the NCO core.

The last experiment performed was the FM receiver as described in section 7.8. The results obtained were baseband I/Q data of received FM station and the FM demodulated signal of the tuned FM station. The testing was performed using three FM stations and results were successful. The spectra of the baseband I/Q signals represent typical FM modulated signals while FM demodulated signals have the expected spectral components that include mono audio, pilot tone, stereo audio and RBDS. The FM receiver sensitivity is -85dBm and the following section 8.2, advises on ways to improve this due to limitations of the testing equipment used.

8.2 Recommendations For Further Work

This section presents some future refinements to the developed library of IP blocks for use in SDR using RHINO as the development platform. Much work still remains for further improvements in order to get a full package of IP blocks needed for SDR application development. The IP blocks comprise both the DSP blocks and I/O interface blocks. The newly upgraded and recommended architecture of RHINO SDR processing blocks is shown in Figure 8.1 with new features labelled in italic red.

8.2.1 Upgrade the DSP blocks

The developed library of DSP IP cores was successful as it conforms to user requirements defined in section 3.1. This library also presents fundamental DSP blocks from which other more useful and robust DSP blocks can be built. Such blocks will also be compatible with Wishbone bus and will be designed be around the following DSP algorithms:

- **Polyphase Filterbank** is a channelizer structure that implements a resource efficient multichannel digital transmitter or receiver for a set of Frequency Division Multiplexed (FDM) channels that exist in a single sampled data stream [106]. The IP core will be realized using polyphase filterbank and it will be based on FFT IP core and FIR IP core both designed in this project.
- **Weighted Overlap Add Filter (WOLA) Filterbank** is a channelization technique optimized for uniformly spaced channels with identical filtering [93]. The WOLA IP core will be based on the FFT/IFFT IP core already designed in this dissertation.

- **Correlator** will be used to realize a multi-channel Correlator IP core on RHINO. This core will correlate an incoming data stream to a stored binary pattern called code sequence or coefficient sequence [55].

- **Spectrometer** is a widely used algorithm in radio astronomical receiver operating in a frequency domain [76]. The Spectrometer IP core will enable rapid development of very wideband spectral analysis systems. This IP core will be based on FFT IP core designed in this dissertation.

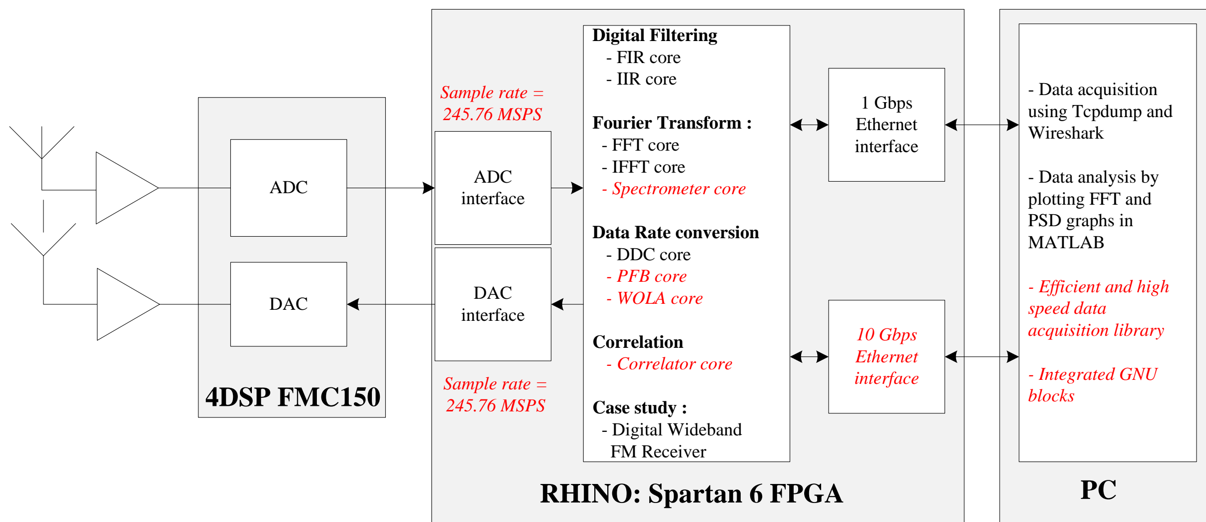

Figure 8.1: Architecture of RHINO SDR processing blocks with recommended new blocks and features labelled in italic red

Although the Wishbone interface for the developed DSP blocks has been described, implementation and thorough testing needs to be done on the practical SoC design. One example of comprehensive SoC test would be to demonstrate a SoC Design of IP blocks by integrating them into Wishbone Bus as slave soft cores and using a standalone arm processor as a master or controller. In this way, a processor would be thought of a versatile device that performs simple tasks while delegating the computationally intensive, high-speed and parallel processing tasks to the FPGA. The advantages include increased processing speed and it eases writing user applications in a more complex system. The GPMC bus connects CPU and the FPGA using GPMC controller on the CPU. The CPU views the FPGA as an external 26-bit multiplexed memory mapped device. The C Code will be developed to show how the FPGA DSP IP Cores can be called on the arm processor application while Wishbone is used in the FPGA to interconnect the IP cores and the design will be made of the following components:

- **gpmc_wb_master (master 0):** is a GPMC Wishbone master

- **wb_arbiter:** arbitrates the masters in the Wishbone bus but it may not be needed in a case where a single Master is used.

- **wb_sycon:** instantiates clocks PLLs in order to provide a Wishbone bus with clean and steady clock.

- **wb_intercon:** ties up all wishbone components that include single master and multiple slaves
- **wb_fir_ip (slave 0):** performs FIR filtering.
- **wb_fft_ip (slave 1):** performs FFT function of $N = 8, 16, ...to 4096$.
- **wb_iir_ip (slave 2):** implements IIR filter structure using second-order sections IIR filter.
- **wb_ddc_ip (slave 3):** performs Digital down converter.

8.2.2 Improve the I/O interface blocks

The developed library of I/O interface blocks for 1 Gigabit Ethernet and FMC150 daughter card worked successfully in accordance with requirements. However, some refinements are needed in order to achieve the highest possible performance as specified by relevant standards and vendors. For this reason, the following improvements are highly recommended for future work:

- Perform a comprehensive loop back test for RHINO 1 Gigabit Ethernet on a point-to-point connection with a PC. This will ensure that testing is thoroughly performed in both directions of data flow between RHINO and a PC. In the current work, comprehensive tests were performed in a flow of data from FPGA to a PC. Minor testing was performed in sending of data from PC to an FPGA.
- While throughput speed achieved on 1 Gigabit Ethernet is sufficiently high particularly for most SDR applications, this can still be improved from the current 98.62MB/s to a figure closer to 110MB/s.
- The interface core for 10 Gigabit Ethernet also needs to be designed and implemented. This will enable higher data rates not supported in 1 Gigabit Ethernet.
- Although RHINO provides interface for data communication at gigabit rates, the inefficient data acquisition at the PC end can be a massive speed bottleneck. For this reason, a development of very efficient packet sniffing application on the PC is recommended. This will capture packets at a high speed without packet loss and with no corruption of received packet data.
- The development of a packet sniffing application will be integrated in GNU blocks for real time DSP processing on the PC.
- The current maximum ADC sample rate achieved is 163.84MSPS while for DAC is 61.44MSPS. The sample rates for both ADC and DAC need to be improved to 245.76MSPS using FMC150 daughter card.

8.2.3 Refine the FM receiver

The FM receiver worked successfully according to specifications, however; there is still room for improvement to get even better results. This would be made possible by adding extra 30-35dB amplifier and using a very efficient FM only antenna in the analogue RF front-end of the FM receiver.

BIBLIOGRAPHY

[1] 4DSP. *FMC150 User Manual*. July 2013.

[2] ABOAGYE, A. K. Overflow avoidance techniques in cascaded iir filter implementations on the tms320 dsp's. *Texas Instruments* (5 1999).

[3] ABOAGYE, A. K. *Overflow Avoidance Techniques in Cascaded IIR Filter Implementations on the TMS320 DSPs*. spra509. Texas Instruments, 1999.

[4] AGHAEE, N., AND ESHGHI, M. Design of a pipelined r4sdf processor. *17th European Signal Processing Conference (EUSIPCO 2009)* (August 2009), 963–967.

[5] ALACHIOTIS, N., BERGER, S., AND STAMATAKIS, A. Efficient pc-fpga communication over gigabit ethernet. In *Computer and Information Technology (CIT), 2010 IEEE 10th International Conference on* (June 2010), pp. 1727–1734.

[6] ALACHIOTIS, N., BERGER, S., AND STAMATAKIS, A. A versatile udp/ip based pc - fpga communication platform. In *Reconfigurable Computing and FPGAs (ReConFig), 2012 International Conference on* (Dec 2012), pp. 1–6.

[7] ALTERA. *Understanding CIC Compensation Filters*. apn455. Apr. 2007.

[8] ASHENDEN, P. J., AND LEWIS, J. *The designers guide to VHDL*, 3 ed. Morgan Kaufmann, 2008.

[9] AZARIAN, A., AND AHMADI, M. Reconfigurable computing architecture survey and introduction. In *Computer Science and Information Technology, 2009. ICCSIT 2009. 2nd IEEE International Conference on* (Aug 2009), pp. 269–274.

[10] BACKER, D., CHANG, C., CHAPMAN, D., CHEN, H., DROZ, P., DE JESUS, C., MACMAHON, D., SIEMION, A., WAWRZYNEK, J., WERTHIMER, D., AND WRIGHT, M. A new approach to radio astronomy signal processing: Packet switched, fpga-based, upgradable, modular hardware and reusable, platform-independent signal processing libraries. *National Radio Science Meeting* (2006).

[11] BAESE, M. *Digital Signal Processing with Field Programmable Gate Arrays*, 3 ed. Berlin: Springer, 2007.

[12] BAKSHI, U. A., AND GODSE, A. P. *Analog Communication*, 2 ed. Technical Publications Prune, 2009.

[13] BOWLING, S. *Understanding A/D Converter Performance Specifications*. AN693. Microchip, 2000.

[14] BRANNON, B. *Basics of Designing a Digital Radio Receiver (Radio 101)*. Analog Devices.

[15] BRODERSEN, R., TKACHENKO, A., AND KWOK-HAY SO, H. A unified hardware/-software runtime environment for fpga-based reconfigurable computers using borph. In *Hardware/Software Codesign and System Synthesis, 2006. CODES+ISSS '06. Proceedings of the 4th International Conference* (Oct 2006), pp. 259–264.

[16] BURNS, P. *Software Defined Radio for 3G*. ARTECH HOUSE, 2003.

[17] CAICEDO, C. E. Software defined radio and software radio technology: Concepts and applications. `https://www.academia.edu/1319161/Software_Defined_Radio_and_Software_Radio_Technology_Concepts_and_Applications`. Accessed: 2015-03-03.

[18] CANDILORO, D. Ip-core generator for the wishbone bus. `http://www.dresd.org/files/HPPS_Candiloro_2006_ENG.pdf`, June 2006.

[19] COUSSY, P., BAGANNE, A., AND MARTIN, E. Ip cores integration in dsp system-on-chip designs. In *Signal Processing Conference, 2002 11th European* (Sept 2002), pp. 1–4.

[20] DAVIS, S. The need for thorough de-bugging capabilities in today's multi-million gate fpga designs is critical. `http://www.usbid.com/datasheets/usbid/2000/2000-q2/xl36_19.pdf`. Accessed: 2015-03-04.

[21] DE A. MELO1, C. A. R., AND DE SOUZA2, R. E. Design and implementation of a wishbonecompatible low-noise arbitrary waveform generator with dac compensation.

[22] DER, L. Frequency modulation (fm) tutorial. `http://www.silabs.com/Marcom%20Documents/Resources/FMTutorial.pdf`. Accessed: 2015-08-02.

[23] DESIGN, AND REUSE. Free ip cores projects. `http://www.design-reuse.com/download/sip/`. Accessed: 2015-03-03.

[24] DONGYE, C. Design of the on-chip bus based on wishbone. In *Electronics, Communications and Control (ICECC), 2011 International Conference on* (Sept 2011), pp. 3653–3656.

[25] FANG, F., HOE, J. C., PÜSCHEL, M., AND MISRA, S. Generation of custom DSP transform IP cores: Case study Walsh-Hadamard transform. In *High Performance Embedded Computing (HPEC)* (2002).

[26] FOROUZAN, B. A., AND CHUNG, S. *Data Communications and Networking 4th Edition*, 4th ed. McGraw-Hill Higher Education, 2007.

[27] FRANCIS, M. *Infinite Impulse Response Filter Structures in Xilinx FPGAs*. WP330 (v1.2). Xilinx, Aug. 2009.

[28] GAD, V., GAD, R. S., AND NAIK, G. Implementation of gigabit ethernet standard using fpga. *International Journal of Mobile Network Communications & Telematics - IJMNCT 2*, 4 (Aug. 2012), 31–44.

[29] GAISLER, J. *A Dual-Use Open-Source VHDL IP library*. Gaisler Research, 2004.

[30] GAJSKI, D., WU, A., CHAIYAKUL, V., MORI, S., NUKIYAMA, T., AND BRICAUD, P. Essential issues for ip reuse. In *Design Automation Conference, 2000. Proceedings of the ASP-DAC 2000. Asia and South Pacific* (June 2000), pp. 37–42.

[31] GAO, J. *10_100_1000 Mbps Tri-mode Ethernet MAC Specification*. OpenCores, Jan. 2006.

[32] GHETIE, J. Fixed wireless and cellular mobile convergence: Technologies, solutions, services. In *Telecommunications, 2007. ConTel 2007. 9th International Conference on* (June 2007), pp. 343–343.

[33] GHIWALA, G. D., THAKER, P. P., AND D.AMIN, G. Realization of fpga based numerically controlled oscillator. *IOSR Journal of VLSI and Signal Processing (IOSR-JVSP) 1*, 5 (Jan-Feb 2013), 7–11.

[34] HE, S., AND TORKELSON, M. A new approach to pipeline fft processor. In *Parallel Processing Symposium, 1996., Proceedings of IPPS '96, The 10th International* (Apr 1996), pp. 766–770.

[35] HERVEILLE, R. *Wishbone B4: WISHBONE System-on-Chip (SoC)Interconnection Architecturefor Portable IP Cores*. OpenCores, 2005.

[36] HOFNER, T. C. *Measuring and evaluating Dynamic ADC parameters*. Maxim Integrated Products, Dec. 2000.

[37] HOSKING, R. H. *Software Defined Radio Handbook*. Pentek, One Park Way, upper Saddle River, New Jersey 07458, Apr. 2012.

[38] HUANG, B. K., VANN, R. G. L., FREETHY, S., MYERS, R. M., NAYLOR, G., SHARPLES, R. M., AND SHEVCHENKO, V. F. Standardisation of fpga systems incorporating embedded linux: the mast ebw digitiser example. *Fusion engineering and design 87*, 6 (Dec. 2012), 2106–2111.

[39] INGGS, G. Putting the pieces together: The systematic development of a software defined radio toolflow for the rhino project. Master's thesis, University Of Cape Town, May 2011.

[40] INSTRUMENTS, T. *AMC7832 - Analog monitoring and control circuit*. Mar. 2005.

[41] INSTRUMENTS, T. *CDCE72010 - Ten Output High Performance Clock Synchronizer, Jitter Cleaner, and Clock Distributor*. June 2008.

[42] INSTRUMENTS, T. *ads62p48/ads62p49/ads62p28/ads62p29 : Dual Channel 14-/12-Bit, 250-/210-MSPS ADC With DDR LVDS and Parallel CMOS Outputs*. Apr. 2009.

[43] INSTRUMENTS, T. *Dual-Channel, 16-Bit, 800 MSPS, Digital-to-Analog Converter (DAC)*. Mar. 2010.

[44] INSTRUMENTS, T. *ADCPro Hardware and Software Installation Manual*. SLAU372A. Feb. 2012.

[45] INSTRUMENTS, T. *Design Consideration for Avoiding Timing Errors during High-Speed ADC, LVDS Data Interface with FPGA*. SLAA592A. June 2013.

[46] ITU. *Transmission standards for FM sound broadcasting at VHF*. Rec. ITU-R BS.450-3. 2001.

[47] JAIN, A. Verilog implementation of fpga based dsp design like fft processors. *Xilinx* (1995).

[48] JEON, D., SEOK, M., CHAKRABARTI, C., BLAAUW, D., AND SYLVESTER, D. Energy-optimized high performance fft processor. In *Acoustics, Speech and Signal Processing (ICASSP), 2011 IEEE International Conference on* (May 2011), pp. 1701–1704.

[49] KESTER, W. *The data conversion handbook*. Analog Devices, 2005.

[50] KHALILZAD, N., YEKEH, F., ASPLUND, L., AND PORDEL, M. Fpga implementation of real-time ethernet communication using rmii interface. In *Communication Software and Networks (ICCSN), 2011 IEEE 3rd International Conference on* (May 2011), pp. 35–39.

[51] KNAPP, S. *Using Programmable Logic to Accelerate DSP Functions*. Xilinx, Oct. 1995.

[52] KNAPP, S. K. Using programmable logic to accelerate dsp functions. *Xilinx* (1995).

[53] KOLUMBAN, G. Frequency modulation: Summary and repetition of the most important facts, Mar 2015.

[54] KOZIEROK, C. *The TCP/IP Guide: A Comprehensive, Illustrated Internet Protocols Reference*. No Starch Press, San Francisco, CA, USA, 2005.

[55] LATTICE. *Correlator IP core*. Lattice Semiconductor Corporation, Apr. 2005.

[56] LOPEZ-PARRADO, A., AND VALDERRAMA-CUERVO, J.-C. Openrisc-based system-on-chip for digital signal processing. In *Image, Signal Processing and Artificial Vision (STSIVA), 2014 XIX Symposium on* (Sept 2014), pp. 1–5.

[57] MADISETTI, V. K., AND WILLIAMS, D. B. *Digital Signal Processing Handbook*. CRC Press, LLC, 1999.

[58] MAHMOODI, M., SAYEDI, S., AND MAHMOODI, B. Reconfigurable hardware implementation of gigabit udp/ip stack based on spartan-6 fpga. In *Information Technology and Electrical Engineering (ICITEE), 2014 6th International Conference on* (Oct 2014), pp. 1–6.

[59] MANOLAKIS, D., AND INGLE, V. *Applied Digital Signal Processing*. Cambridge University Press, 2011.

[60] MARVELL. *88E1111 Datasheet - Intergrated 10/100/1000 Ultra Ethernet Transceiver*. Dec. 2004.

[61] MIKROELECTRONIKA. Chapter 2: Fir filters - digital filter design. `http://www.mikroe.com/chapters/view/72/chapter-2-fir-filters/`.

[62] MOHOR, I. *Ethernet IP Core Specification*. OpenCores, Nov. 2002.

[63] MOY, C., AND RAULET, M. High-level design methodology for ultra-fast software defined radio prototyping on heterogeneous platforms. *ADVANCES IN ELECTRONICS AND TELECOMMUNICATIONS* (Apr. 2010), 67–85.

[64] NEDERLAND, A. S. Designing fixed point direct form ii (biquad) iir filters with the asn filter designer. Tech. rep., Advanced Solutions Nederland, Jan. 2012.

[65] OKADA, K., AND KOUSAI, S. *Digitally-Assisted Analog and RF CMOS Circuit Design for Software-Defined Radio*. Springer Science+Business Media, 2011.

[66] OKLOBDZIJA, V. G. *Computer Engineering HandBook*. CRC Press LLC, 2002.

[67] OLIVIERI, S., AARESTAD, J., POLLARD, L., WYGLINSKI, A., KIEF, C., AND ERWIN, R. Modular fpga-based software defined radio for cubesats. In *Communications (ICC), 2012 IEEE International Conference on* (June 2012), pp. 3229–3233.

[68] OLIVIERI, S. J., JIMAARESTAD, HOWARDPOLLARD, L., WYGLINSKI, A. M., CRAIGKIEF, AND ERWIN, R. S. Modular fpga-based software defined radio for cubesats. *IEEE International Conference on Communications - Selected Areas in Communications Symposium* (June 2012), 3229–3233.

[69] OPENCORES. Opencores projects. `http://www.opencores.org/projects/`. Accessed: 2015-03-03.

[70] PANDA, A., BAGHMAR, S. K., AND AGRAWAL, S. K. Fir filter implementation on a fpga allowing signed and fraction coefficients with coefficients obtained using remez exchange algorithm. *International Journal of Advancements in Technology 1* (2010), 203–210.

[71] PIMENTEL, J., AND LE-HUY, H. A vhdl library of ip cores for power drive and motion control applications. In *Electrical and Computer Engineering, 2000 Canadian Conference on* (2000), vol. 1, pp. 184–188 vol.1.

[72] R, A., GANDHI, K., AND LAD, V. Low power r4sdc pipelined fft processor architecture. *IOSR Journal of VLSI and Signal Processing (IOSR-JVSP) 1*, 6 (Mar-Apr 2013), 68–75.

[73] RAOL, K., KIML, D., AND HWANG, J. *Fast Fourier Transform: Algorithms and Applications*. Springer Dordrecht Heidelberg London New York, 2010.

[74] REDMON, N. Biquads. http://www.earlevel.com, Apr. 2003.

[75] REYES, P., REVIRIEGO, P., RUANO, O., AND MAESTRO, J. Efficient structures for the implementation of moving average filters in the presence of seus using system knowledge. *the 2006 Radiation Effects on Components and Systems Workshop* (Sept 2006).

[76] RF-ENGINES. *RF Engines 1GHz Spectrometer Core drives unprecedented performance enhancements in radio astronomy*. RF Engines Ltd, Apr. 2005.

[77] RICE, M., PADILLA, M., AND NELSON, B. On fm demodulators in software defined radios using fpgas. In *Military Communications Conference, 2009. MILCOM 2009. IEEE* (Oct 2009), pp. 1–7.

[78] ROUPHAEL, T. J. *RF and Digital Signal Processing for Software-Defined Radio, A Multi-Standard Multi-Mode Approach*. Elsevier, 2009.

[79] RRSG. U.c.t remote radar sensign group - introducation. http://www.rrsg.uct.ac.za/intro/intro.html. Accessed: 2015-08-20.

[80] RUDRA, A. Fpga-based applications for software radio. http://www.rfdesign.com, Apr. 2004.

[81] SAEED, A., ELBABLY, M., ABDELFADEEL, G., AND ELADAWY, M. I. Efficient fpga implementation of fft/ifft processor. *International Journal of Circuits, Systems and Signal Processing 3* (2009).

[82] SALEH, R., WILTON, S., MIRABBASI, S., LEMIEUX, G., GRECU, C., IVANOV, A., HU, A., GREENSTREET, M., AND PANDE, P. P. System-on-chip: Reuse and integration. *Natural Sciences and Engineering Research Council of Canada* (2010).

[83] SAVELA, V., JARVINEN, P., NUMMELA, A., KESKINEN, J., AND NURMI, J. Utilization of a vhdl-based asic-realizable digital filter architecture library in dsp system design. *VIUF Proceedings* (1994).

[84] SCHER, A. How to capture raw iq data from a rtl-sdr dongle and fm demodulate with matlab. http://www.aaronscher.com/wireless_com_SDR/RTL_SDR_AM_spectrum_demod.html, May 2015. Accessed: 2015-08-06.

[85] SCHLICHTHÄRLE, D. *Digital filters. Basics and design. 2nd ed.*, 2nd ed. ed. Berlin: Springer, 2011.

[86] SCHWARZ, P. D. B. Iir filter design and implementation. Sep 2003.

[87] SCOTT, S. Rhino: Reconfigurable hardware interface for computation and radio. Master's thesis, University Of Cape Town, Nov. 2011.

[88] SDRG. Software defined radio group - university of cape town - electrical engineering. http://www.sdrg.ee.uct.ac.za. Accessed: 2015-08-20.

[89] SENGAR, S., AND BHATTACHARYA, P. P. Performance evaluation of cascaded integrator-comb (cic) filter. vol. 2, pp. 222–228.

[90] SHARMA, M., AND KUMAR, D. Wishbone bus architecture - a survey and comparison. *CoRR abs/1205.1860* (2012).

[91] SONG, W., AND LIU, B. Design of the cic decimation filter based on sopc builder. In *Computer Science and Information Technology (ICCSIT), 2010 3rd IEEE International Conference on* (July 2010), vol. 9, pp. 602–605.

[92] SPIRIDON, S. Software defined radio transceiver frontends in the beginning of the internet era. *COCORA: The Third International Conference on Advances in Cognitive Radio* (Apr. 2013), 18–22.

[93] TIETCHE, B., ROMAIN, O., DENBY, B., AND DIEULEVEULT, F. Fpga-based simultaneous multichannel fm broadcast receiver for audio indexing applications in consumer electronics scenarios. *Consumer Electronics, IEEE Transactions on 58*, 4 (November 2012), 1153–1161.

[94] TRIBBLE, A. C. The software defined radio: Fact and fiction. *IEEE Radio and Wireless Symposium* (Jan. 2008), 5–8.

[95] TSENG, S.-M., YU, J.-C., AND LIN, Z.-H. Software digital-down-converter design and optimization for dvb-t systems. pp. 57–61.

[96] TUTTLEBE, W. H. W. Software- defined radio: Facets of a developing technology. *IEEE Personal Communications 6*, 2 (Apr. 1999), 38–44.

[97] VAUGHAN, R., SCOTT, N., AND WHITE, D. The theory of bandpass sampling. *Signal Processing, IEEE Transactions on 39*, 9 (Sept 1991), 1973–1984.

[98] VINOD, A., AND LAI, E. Low power and high-speed implementation of fir filters for software defined radio receivers. *Wireless Communications, IEEE Transactions on 5*, 7 (July 2006), 1669–1675.

[99] WILLIAMS, J. Digilent atlys resources. `https://www.joelw.id.au/FPGA/DigilentAtlysResources`. Accessed: 2015-08-02.

[100] WOODS, R., MCALLISTER, J., LIGHTBOY, G., AND YI, Y. *FPGA-based Implementation of Complex Signal Processing Systems*. John Wiley and Sons, Ltd, 2008.

[101] XILINX. Fpga design flow overview. `http://www.xilinx.com/itp/xilinx10/isehelp/ise_c_fpga_design_flow_overview.htm`. Accessed: 2015-08-24.

[102] XILINX. *LogiCORE IP Tri-Mode Ethernet MAC v4.5*. UG138. Mar. 2011.

[103] XILINX. *Spartan-6 Libraries Guide for HDL Designs*. UG615. Mar. 2011.

[104] XILINX. *LogiCORE IP AXI Ethernet Lite MAC (v1.01.b)*. DS787. July 2012.

[105] XILINX. *LogiCORE IP Fast Fourier Transform v8.0*. DS808. July 2012.

[106] XILINX. *Polyphase Filter Bank Channelizer*. XAPP1161. Mar. 2013.

[107] XILINX. *Platform Cable USB II*. DS593. Jan. 2015.

APPENDIX A

THE ATTACHED CD

The directory structure of the attached CD is described as follows:

- **datasheets/ :** This directory contains the datasheets for hardware components used in this project.
- **Java/ :** This directory contains Netbeans project with Java files to implement depacketization of received UDP frames.
- **Matlab/ :** This directory contains the data files and Matlab files to plot the results.
- **Msc_Report_TSNLEK001.pdf :** This is a Thesis report file in PDF format.
- **Pictures/ :** This is a directory for experiment pictures.
- **RHINO/ :** This a directory for Xilinx ISe project which implements the entire library of IP cores.
  - **RHINO/Rhino_Sdr_Blocks/pcores/ :** This directory consists of all IP cores implemented in VHDL using Xilinx ISE tools.
    - **DSP/ :** The directory holds the developed DSP IP cores.
      - **CIC_Lib/ :** This is a directory that has all HDL files used to implement CIC IP core. There also Matlab script files to help with testbench and simulation.
      - **DDC_Lib/ :** The directory contains HDL files used to implement a DDC IP core. It also contains Matlab script files needed for testbench and simulation.
      - **FFT_IFFT_Lib/:** This is directory with HDL files used to implement FFT/IFFT IP core. The are also Matlab script files to help with testbench and simulation.
      - **FIR_Lib/ :** This directory holds HDL files that implement FIR IP core and Matlab script files use in testbench and simulation.
      - **IIR_Lib/ :** The directory consists of HDL files to realize IIR IP core and Matlab script files for simulation and testench.

- **NCO_Lib/ :** The directory holds HDL files that implement NCO core along with Matlab script files to help with testbench and simulation.
- **PRIMITIVES_Lib/ :** This directory has HDL entities commonly used in many of the above developed cores.

* **IO/:** The directory holds the developed I/O interface cores.
  - **fmc150_if/ :** This directory contains the HDL files for interfacing 4DSP FMC150 ADC/DAC with RHINO.
  - **UDP_1GbE_if/ :** This directory has the HDL files for controlling and driving the 1 Gigabit Ethernet on RHINO.
* **SDR/ :** This directory contains the top level designs for developed DSP IP cores and I/O interface cores.

APPENDIX B

FIR IP CORE

B.1 INSTANTIATION OF THE FIR CORE

```
Library FIR_Lib;
Use FIR_Lib.fir_pkg.all;
Use FIR_Lib.fircomponents.all;

-- FIR_PAR: A parallel implementation of an FIR filter,
--          it can be configured to operate in transpose form,
--          even symmetric form, odd symmetric form and as a
--          moving average filter.

fir_par_inst : fir_par
generic map(
        DIN_WIDTH       => DIN_WIDTH,      -- input data width
        DOUT_WIDTH      => DOUT_WIDTH,     -- output data width
        COEFF_WIDTH     => COEFF_WIDTH,    -- coefficient data width
        NUMBER_OF_TAPS  => NUMBER_OF_TAPS, -- filter length
        LATENCY         => LATENCY,        -- FIR structure type [0=tranpose, 1=odd
                                           -- symmetric,2=even symmetric,3=moving average]
        COEFFS          => COEFFS          -- array of quantized coefficients - integers
)
port map (
        clk   => clk,    -- system clock input
        rst   => rst,    -- system reset input
        en    => en,     -- clock enable input
        loadc => loadc,  -- load coefficient enable input
        vld   => vld,    -- valid output result
        coeff => coeff,  -- coefficient sample input
        din   => din,    -- input data sample
        dout  => dout    -- output data sample
);
```

B.2 GENERATING TESTBENCH DATA FILES IN MATLAB

```
% ----------------------------------------------------------------------
% This generates Parks-McClellan optimal FIR coefficients in 2's
% complement and input test data for FPGA Testbench (fir_par.vhd core)
% ----------------------------------------------------------------------
%Lowpass Filter Design parameters
rp = 3;                 % passband ripple
rs = 100;               % stopband ripple
Fs = 10000;             % sampling frequency
f = [1905 2190 2215 2500];     % cutoff frequencies
a = [0 1 0];          % desired amplitudes
% compute deviations
```

```
12 dev = [10^(-rs/20) (10^(rp/20)-1)/(10^(rp/20)+1)  10^(-rs/20)];
13 [n,fo,ao,w] = remezord(f,a,dev,Fs);
14 b = remez(n,fo,ao,w);
15 N = 1023;
16 t = 0:(1/Fs):(1/Fs*N);
17
18 %Create Input Initial Signals
19 f1 = 220;
20 f2 = 800;
21 f3 = 2500;
22 f4 = 2200;
23
24 s1 = cos(2*pi*f1*t);
25 s2 = cos(2*pi*f2*t);
26 s3 = cos(2*pi*f3*t);
27 s4 = cos(2*pi*f4*t);
28 x  = s1 + s2 + s3 + s4;
29 x = x/max(abs(x));
30
31 %Perform Filtering
32 xfiltered = filter(b,1,x);
33
34 %Writing vectors to files
35
36 BW = 16; % Input Data Width
37 CW = 16; % Coefficient data Width
38
39 % Write FIR coefficients to a file
40 fid=fopen('taps.in','wt');
41 fprintf(fid,'(');
42 for i=1:length(b);
43         fprintf(fid,'%d,',round(2^(CW-1) * b(i)));
44 end
45 fprintf(fid,')');
46 fclose(fid);
47
48 % Write test data to a file
49 fid=fopen('fpga.in','wt');
50 for i=1:length(x);
51         fprintf(fid,'%d\n',round(2^(BW-1) * x(i)));
52 end
53 fclose(fid);
54
55 % Write Matlab model results to a file
56 fid=fopen('matlab.out','wt');
57 for i=1:length(x);
58         fprintf(fid,'%d\n',round(2^(CW-1) * xfiltered(i)));
59 end
60 fclose(fid);
61
62 %Plot FIlter frequency Response
63
64 [h,f] = freqz(b,1,N+1,Fs);
65
66 subplot(2,2,2);
67 plot(f,20*log10(abs(h)),'k')
68 title('FIR filter frequency Response');
69 xlabel('Frequency ($Hz$)');
70 ylabel('Magnitude ($dB$)');
71 xlim([0,5000]);
72 grid on;
```

B.3 Plotting the results in Matlab

```
1 % ---------------------------------------------------------------------
2 % This plots FPGA and MATLAB results, it can be padded to the previous
3 % script for better plot graphical disply
```

```
4  % ----------------------------------------------------------------------
5  NFFT = 1024;
6  Ts   = 1/Fs; % sampling interval
7  f    = Fs*(-NFFT/2:NFFT/2-1)/NFFT; % frequency
8
9  fid = fopen('fpga.in');
10 fpgain = textscan(fid,'%f','Delimiter','\n');
11 fclose(fid);
12
13 fid = fopen('fpga.out');
14 fpgaout = textscan(fid,'%f','Delimiter','\n');
15 fclose(fid);
16
17 fid = fopen('matlab.out');
18 matlabout = textscan(fid,'%f','Delimiter','\n');
19 fclose(fid);
20
21 % normalized FFT of signals
22 f1 = fftshift(fft(fpgain{1},NFFT));
23 F1 = abs(f1)/(N);
24 f2 = fftshift(fft(matlabout{1},NFFT));
25 F2 = abs(f2)/(N);
26 f3 = fftshift(fft(fpgaout{1},NFFT));
27 F3 = abs(f3)/(N);
28
29 % FFT for FIR Testebech input signal
30 subplot(2,2,1);
31 plot(f/1e3,F1,'k');
32 title('Magnitude Spectrum of Input Signal');
33 xlabel('Frequency ($kHz$)');
34 ylabel('Magnitude');
35 xlim([-5,5]);
36 grid on;
37
38 % FFT for MATLAB FIR output
39 subplot(2,2,3);
40 plot(f/1e3,F2,'k');
41 title('Magnitude Spectrum of Matlab FIR filter output');
42 xlabel('Frequency ($kHz$)');
43 ylabel('Magnitude');
44 xlim([-5,5]);
45 grid on;
46
47 % FFT for FPGA FIR core output
48 subplot(2,2,4);
49 plot(f/1e3,F3,'k');
50 title('Magnitude Spectrum of FPGA FIR filter output');
51 xlabel('Frequency ($kHz$)');
52 ylabel('Magnitude');
53 xlim([-5,5]);
54 grid on;
```

APPENDIX C

IIR IP CORE

C.1 INSTANTIATION OF THE IIR CORE

```
Library IIR_Lib;
Use IIR_Lib.iir_pkg.all;
Use IIR_Lib.iircomponents.all;

-- SOS_iir_inst: An implementation of Second Order Sections IIR filter.
--           The sections are made up of IIR filter of Direct form I.
--           The word lengths, coefficients and number of sections are
--           configurable.
SOS_iir_inst : SOS_iir
generic map(
        DIN_WIDTH   => DIN_WIDTH, -- input data width
        DOUT_WIDTH  => DOUT_WIDTH, -- output data width
        COEFF_WIDTH => COEFF_WIDTH, coefficient data width
        b => b, -- non-recursive coefficients
        a => a, -- recursive coefficients
        STAGES          => STAGES -- number of IIR sections
)
port map(
        clk   => clk,    -- system clock input
        rst   => rst,    -- system reset input
        en    => en,     -- clock enable input
        vld   => vld,    -- valid output result
        din   => din,    -- input data sample
        dout  => dout    -- output data sample
);
```

C.2 GENERATING TESTBENCH DATA FILES IN MATLAB

```
%-----------------------------------------------------------------------
% This applies Chebyshev I bandpass IIR filter using SOS cascade.
% Coefficients are scaled using infinity calculation of SOS transfer
% of SOS transfer function
%-----------------------------------------------------------------------
Fs=10000; % sampling frequency
% iir filter design
[b,a]  = cheby1(6,0.1,[0.438 0.442]);

% convert iir filter coefficients to SOS coefficients
[sos,g] = tf2sos(b,a,'up','inf');
b01 = sos(1,1:3);  a01 = sos(1,4:6);
b02 = sos(2,1:3);  a02 = sos(2,4:6);
b03 = sos(3,1:3);  a03 = sos(3,4:6);
b04 = sos(4,1:3);  a04 = sos(4,4:6);
```

```
16  b05 = sos(5,1:3);  a05 = sos(5,4:6);
17  b06 = sos(6,1:3);  a06 = sos(6,4:6);
18
19  % Scale the coefficients
20  [G1,f] = freqz(b01,a01,512);
21  s1     = 1/max(abs(G1));
22  [G2,f] = freqz(b02,a02,512);
23  s2     = 1/(s1*max(abs(G1).*abs(G2)));
24  [G3,f] = freqz(b03,a03,512);
25  s3     = 1/(s1*s2*max(abs(G1).*abs(G2).*abs(G3)));
26  [G4,f] = freqz(b04,a04,512);
27  s4     = 1/(s1*s2*s3*max(abs(G1).*abs(G2).*abs(G3).*abs(G4)));
28  [G5,f] = freqz(b05,a05,512);
29  s5     = 1/(s1*s2*s3*s4*max(abs(G1).*abs(G2).*abs(G3).*abs(G4).*abs(G5)));
30  [G6,f] = freqz(b06,a06,512);
31  s6     = 1/(s1*s2*s3*s4*s5*max(abs(G1).*abs(G2).*abs(G3).*abs(G4).*abs(G5).*abs(G6)));
32
33  bs1 = s1 * b01;
34  bs2 = s2 * b02;
35  bs3 = s3 * b03;
36  bs4 = s4 * b04;
37  bs5 = s5 * b05;
38  bs6 = s6 * b06;
39
40  %Create Input Signal
41  f1 = 220;
42  f2 = 800;
43  f3 = 2500;
44  f4 = 2200;
45
46  s1 = cos(2*pi*f1*t);
47  s2 = cos(2*pi*f2*t);
48  s3 = cos(2*pi*f3*t);
49  s4 = cos(2*pi*f4*t);
50  x  = s1 + s2 + s3 + s4;
51  x = x/max(abs(x));
52
53  %Perform filtering
54  xfiltered = filter(b,a,x);
55
56
57  %Write Data To Files for Testbench
58  % Bit Width
59  BW  = 16; % input data width
60  CW  = 16; % coefficient data width
61
62  % write the IIR coefficients to a file
63  fid=fopen('coeffs.in','wt');
64  fprintf(fid,'(');fprintf(fid,'%d,',round(2^(BW-1) * bs1));fprintf(fid,'),');
65  fprintf(fid,'(');fprintf(fid,'%d,',round(2^(BW-1) * bs2));fprintf(fid,'),');
66  fprintf(fid,'(');fprintf(fid,'%d,',round(2^(BW-1) * bs3));fprintf(fid,'),');
67  fprintf(fid,'(');fprintf(fid,'%d,',round(2^(BW-1) * bs4));fprintf(fid,'),');
68  fprintf(fid,'(');fprintf(fid,'%d,',round(2^(BW-1) * bs5));fprintf(fid,'),');
69  fprintf(fid,'(');fprintf(fid,'%d,',round(2^(BW-1) * bs6));fprintf(fid,'),');fprintf(fid,'\n');
70
71  fprintf(fid,'(');fprintf(fid,'%d,',round(2^(BW-1) * a01));fprintf(fid,'),');
72  fprintf(fid,'(');fprintf(fid,'%d,',round(2^(BW-1) * a02));fprintf(fid,'),');
73  fprintf(fid,'(');fprintf(fid,'%d,',round(2^(BW-1) * a03));fprintf(fid,'),');
74  fprintf(fid,'(');fprintf(fid,'%d,',round(2^(BW-1) * a04));fprintf(fid,'),');
75  fprintf(fid,'(');fprintf(fid,'%d,',round(2^(BW-1) * a05));fprintf(fid,'),');
76  fprintf(fid,'(');fprintf(fid,'%d,',round(2^(BW-1) * a06));fprintf(fid,'),');fprintf(fid,'\n');
77  fclose(fid);
78
79  % Write testbench input test data to a file
80  fid=fopen('fpga.in','wt');
81  for i=1:length(x);
82          fprintf(fid,'%d\n',round(2^(BW-1) * x(i)));
83  end
84  fclose(fid);
```

```
% Write MATLAB IIR filter model data to a file
fid=fopen('matlab.out','wt');
for i=1:length(x);
        fprintf(fid,'%d\n',round(2^(CW-1) * xfiltered(i)));
end
fclose(fid);

% Plot FIlter frequency Response
[h,f] = freqz(b,a,1024,Fs);

subplot(2,2,2);
plot(f,20*log10(abs(h)),'k')
title('IIR filter frequency Response');
xlabel('Frequency ($Hz$)');
ylabel('Magnitude ($dB$)');
xlim([0,5000]);
grid on;
```

C.3 PLOTTING THE RESULTS IN MATLAB

```
% ----------------------------------------------------------------------
% This plots FPGA and MATLAB results, it can be padded to the previous
% script for better plot graphical disply
% ----------------------------------------------------------------------
NFFT = 1024;
Ts   = 1/Fs; % sampling interval
f    = Fs*(-NFFT/2:NFFT/2-1)/NFFT; % frequency

fid = fopen('fpga.in');
fpgain = textscan(fid,'%f','Delimiter','\n');
fclose(fid);

fid = fopen('fpga.out');
fpgaout = textscan(fid,'%f','Delimiter','\n');
fclose(fid);

fid = fopen('matlab.out');
matlabout = textscan(fid,'%f','Delimiter','\n');
fclose(fid);

% normalized FFT of signals
f1 = fftshift(fft(fpgain{1},NFFT));
F1 = abs(f1)/(N);
f2 = fftshift(fft(matlabout{1},NFFT));
F2 = abs(f2)/(N);
f3 = fftshift(fft(fpgaout{1},NFFT));
F3 = abs(f3)/(N);

% FFT for IIR Testebech input signal
subplot(2,2,1);
plot(f,F1,'k');
title('Magnitude Spectrum of Input Signal');
xlabel('Frequency ($Hz$)');
ylabel('Magnitude');
xlim([-5000,5000]);
grid on;

% FFT for MATLAB FIR output
subplot(2,2,3);
plot(f/1e3,F2,'k');
title('Magnitude Spectrum of Matlab IIR filter output');
xlabel('Frequency ($kHz$)');
ylabel('Magnitude');
xlim([-5,5]);
grid on;

```

```
47 % FFT for FPGA FIR core output
48 subplot(2,2,4);
49 plot(f/1e3,F3,'k');
50 title('Magnitude Spectrum of FPGA IIR filter output');
51 xlabel('Frequency ($kHz$)');
52 ylabel('Magnitude');
53 xlim([-5,5]);
54 grid on;
```

APPENDIX D

FFT/IFFT IP CORE

D.1 INSTANTIATION OF THE FFT/IFFT CORE

```
Library FFT_IFFT_Lib;
Use FFT_IFFT_Lib.fftcomponents.all;

-- r22sdf_fft_ifft_core_inst: This module implements a complex
--                            N-point Radix 2^2 single-path delay feedback
--                            pipelined FFT or IFFT core with configurable
--                            Input bit widths where N is powers of 2.
--                            i.e. 8, 16, 32, 64, 128, 256, 512, 1024,
--                            2048, 4096. The input samples are in  natural
--                            order and ouput samples are in bit reversed order.
r22sdf_fft_ifft_core_inst : r22sdf_fft_ifft_core
generic map(
        N          => N, -- FFT Length
        DIN_WIDTH  => DIN_WIDTH, -- input data width
        DOUT_WIDTH => DOUT_WIDTH,-- output data width
        TF_W       => TF_W,      -- twiddle factor data width. default=16
        MODE       => '0'        -- core select, '0'=FFT,'1'=IFFT
)
port map(
        clk  => clk,     -- system clock input
        rst  => rst,     -- system reset input
        en   => en,      -- clock enable input
        XSr  => XSr,     -- real-part input sample
        XSi  => XSi,     -- imaginary-part input sample
        vld  => vld,     -- valid output result
        done => done,    -- fft process complete
        XKr  => XKr,     -- real-part output sample
        XKi  => XKi      -- imaginary-part output sample
);
```

D.2 GENERATING TESTBENCH DATA FILES IN MATLAB

```
% ----------------------------------------------------------------------
% This creates a rectungal pulse which is used as the input test data to
% 1024-point FFT core.
% ----------------------------------------------------------------------
bit_width = 16;         % data width
N = 1024;               % FFT length
A = 2^(bit_width - 1);  % amplitute
Fs = 50e6;              % sampling frequency in KHz
t = -Fs/2:Fs/N:Fs/2-Fs/N;

%makes the actual square pulse
```

```
12 x1T = round(A * rectpuls(t,50*(Fs/N)));
13
14 %write data input to a file in binary format
15 fid=fopen('../tb/fpga.in','wt');
16 for i=1:N;
17         fprintf(fid,"%s %s\n",conv2bin(real(x1T(i)),bit_width),conv2bin(imag(x1T(i)),bit_width));
18 end
19 fclose(fid);
20
21 %write data to a file in decimal format for later plots
22 fid=fopen('../tb/matlab.in','wt');
23 for i=1:N;
24         fprintf(fid,"%d %d\n",real(x1T(i)),imag(x1T(i)));
25 end
26 fclose(fid);
27
28 x1F = fft(x1T,N);
29
30 %write ideal FFT results using MATLAB
31 fid=fopen('../tb/matlab.out','wt');
32 for i=1:N;
33         fprintf(fid,"%d %d\n",real(x1F(i)),imag(x1F(i)));
34 end
35 fclose(fid);
```

D.3 Plotting the results in Matlab

```
1  % ---------------------------------------------------------------------
2  % This plots FPGA and MATLAB results of the FFT and IFFT core output
3  % ---------------------------------------------------------------------
4  Fs   = 50e6; % sampling frequency
5  N    = 1024; % number of samples
6  NFFT = N; % FFT length
7  Ts   = 1/Fs; % sampling interval
8  t    = [0:Ts:(N*Ts)-Ts];
9  f    = Fs*(-NFFT/2:NFFT/2-1)/NFFT; %frequency
10
11 matlabInRaw = dlmread('matlab.in',' ');
12 matlabOutRaw = dlmread('matlab.out',' ');
13 fpgaOutRaw = dlmread('fpga.out',' '); % file generate by FPGA testbench
14 ifftoutRaw = dlmread('fpga_ifft.out',' '); % file generate by FPGA testbench
15
16 matlabin = complex(matlabInRaw(:,1),matlabInRaw(:,2));
17 matlabout = complex(matlabOutRaw(:,1),matlabOutRaw(:,2));
18 fpgaout = complex(fpgaOutRaw(:,1),fpgaOutRaw(:,2));
19 ifftout = complex(ifftoutRaw(:,1),ifftoutRaw(:,2));
20
21 % normalized FFT of signal
22 f1 = fftshift(matlabout);
23 F1 = abs(f1)/(N);
24 f2 = fftshift(fpgaout);
25 F2 = abs(f2)/(N);
26
27
28 % IIR Testebech input signal
29 subplot(2,2,1);
30 plot(t/1e-6,matlabin/1e3);
31 title('Rectangular Pulse waveform');
32 xlabel('Time ($\mu s$)');
33 ylabel('Amplitude ($\times 10^3$)');
34 xlim([0,20.5]);
35 grid on;
36
37 % FFT in MATLAB
38 subplot(2,2,2);
39 plot(f/1e6,F1);
40 title('1024-point FFT core output using MATLAB');
```

```
41 xlabel('Frequency ($MHz$)');
42 ylabel('Magnitude1');
43 xlim([-25,25]);
44 grid on;
45
46 % FFT in FPGA
47 subplot(2,2,3);
48 plot(f/1e6,F2);
49 title('1024-point FFT core output using FPGA');
50 xlabel('Frequency ($MHz$)');
51 ylabel('Magnitude');
52 xlim([-25,25]);
53 grid on;
54
55 % IFFT in MATLAB
56 subplot(2,2,4);
57 plot(t/1e-6,abs(ifftout));
58 title('1024-point IFFT core output using FPGA');
59 xlabel('Time ($\mu s$)');
60 ylabel('Amplitude');
61 xlim([0,20.5]);
62 grid on;
```

D.3.1 Decimal to 2's complement binary Conversion

```
1  % -----------------------------------------------------------------------
2  % Converts decimal to 2'complement binary
3  % -----------------------------------------------------------------------
4  function bin=conv2bin(num,Nbits);
5  % num : integer value to be converted to binanary
6  % Nbits: number of the binary bits in the output string
7
8  if(Nbits <= 8)
9          bin = dec2bin(typecast(int8(num),'uint8'));
10 elseif(Nbits <= 16)
11         bin = dec2bin(typecast(int16(num),'uint16'));
12 elseif(Nbits <= 32)
13         bin = dec2bin(typecast(int32(num),'uint32'));
14 elseif(Nbits <= 64)
15         bin = dec2bin(typecast(int64(num),'uint64'));
16 end
17 if(length(bin) < Nbits)
18     zero_count = Nbits - length(bin);
19         for i = 1:zero_count
20                 bin = strcat('0',bin);
21         end
22 elseif(length(bin) > Nbits)
23         bin = substr(bin,length(bin)-Nbits + 1,Nbits);
24 end
```

D.4 GENERATING N-BIT TWIDDLE FACTORS HDL ROM

```
1  function r22sdf_twiddle_rom_gen(N,tf_bit_width);
2  % ---------------------------------------------------------------------------------------
3  % This generates DIF R2^2-SDF FFT ROM of twiddle factors in 2's complement number format
4  % ---------------------------------------------------------------------------------------
5  % [hd]           = r22sdf_twiddle_rom_gen(N,tf_bit_width)
6  % N
7  % tf_bit_width   = Bit width of twiddle factors
8  % ---------------------------------------------------------------------------------------
9  %
10 % at kth stage, k = 0,1,...ceil(log(N)/log(4))-2
11 % a[i] = e^(j*2*pi*p/N) = cos(2*pi*p/N) + jsin(2*pi*p/N)
12 % i = 0,1,2,...,(N/2^2k-1)
```

```
13  % m = N/2^(2+2k)
14  % p = 0
15  %   = 2 * 2^((2*k)+1) * (i  m) [ m  i < 2*m ]
16  %   = 2^(k*2) * (i  2*m)       [ 2*m  i < 3*m ]
17  %   = 3 * 2^(2*k) * (i  3*m)   [ 3*m  i < 4*m ]
18  %
19  % -----------------------------------------------------------------------------
20
21  % compute the number of stages
22  stages_count = ceil(log(N)/log(4))-1;
23  for k = 0:stages_count-1;
24
25  % calculate rom depth for kth stage
26  rom_depth = N/(2^(2*k));
27  % compute width of a rom height address
28  addr = log2(rom_depth);
29
30  % create vhdl file for kth fft stage
31  file_name = sprintf("data/fft%d_tf_rom_s%d.vhd",N,k);
32  fid=fopen(file_name,'wt');
33  fprintf(fid,"--****************************************************\n");
34  fprintf(fid,"--* Company:        University of Cape Town\n");
35  fprintf(fid,"--* Engineer:       Lekhobola Joachim Tsoeunyane\n");
36  fprintf(fid,"--*******************************************************\n");
37  fprintf(fid,"--* Create Date:    %s \n",datestr(now));
38  fprintf(fid,"--* Design Name:    Pipelined R2^2 DIF-SDF FFT      \n");
39  fprintf(fid,"--* Module Name:    fft%d_tf_rom_s%d.vhd\n",N,k);
40  fprintf(fid,"--* Project Name:   RHINO SDR Processing Blocks\n");
41  fprintf(fid,"--* Target Devices: Xilinx - SPARTAN-6     \n");
42  fprintf(fid,"--********************************************************\n");
43  fprintf(fid,"--* Dependencies: none
44                           \n");
45  fprintf(fid,"--*************************************************************
46  ***********\n");
47  fprintf(fid,"LIBRARY IEEE;\n");
48  fprintf(fid,"USE IEEE.STD_LOGIC_1164.ALL;\n");
49  fprintf(fid,"USE IEEE.STD_LOGIC_UNSIGNED.ALL;\n");
50  fprintf(fid,"--**************************************************************
51  ***********\n");
52  fprintf(fid,"--* This module implements the stage-%d of twiddle factor
53  ROM for a %d-point      \n",k,N);
54  fprintf(fid,"--* pipelined R2^2 DIF-SDF FFT. Each value is a complex
55   number{imaginary,complex} \n");
56  fprintf(fid,"--* ********************************************************
57  ************\n");
58  fprintf(fid,"--* params:\n");
59  fprintf(fid,"--* addr_w - rom address bit width \n");
60  fprintf(fid,"--* data_w - output data bit width \n");
61  fprintf(fid,"--* ports:\n");
62  fprintf(fid,"--* [in]  addr     - Twidde factor ROM address to read\n");
63  fprintf(fid,"--* out] doutr - Twiddle factor read from rom addr - real value\n");
64  fprintf(fid,"--* [out] douti - Twidder factor read from rom addr - imaginary value\n");
65  fprintf(fid,"--*********************************************************************\n");
66  fprintf(fid,"--* Notes: Do not modify this file as it is auto-generated using matlab
67  script    \n");
68  fprintf(fid,"--*********************************************************************\n");
69  fprintf(fid,"entity fft%d_tf_rom_s%d is\n",N,k);
70  fprintf(fid,"   generic(\n");
71  fprintf(fid,"           addr_w : natural := %d;\n",addr);
72  fprintf(fid,"           data_w : natural := %d\n",tf_bit_width);
73  fprintf(fid,"   );\n");
74  fprintf(fid,"    port (\n");
75  fprintf(fid,"        addr  : in  std_logic_vector (addr_w - 1 downto 0);\n");
76  fprintf(fid,"        doutr : out std_logic_vector (data_w - 1 downto 0);\n");
77  fprintf(fid,"        douti : out  std_logic_vector(data_w - 1 downto 0)\n");
78  fprintf(fid,"   );\n");
79  fprintf(fid,"end fft%d_tf_rom_s%d;\n\n",N,k);
80
81  fprintf(fid,"architecture Behavioral of fft%d_tf_rom_s%d is\n",N,k);
```

```
82  fprintf(fid,"   type complex is array(0 to 1) of std_logic_vector(data_w - 1 downto 0);\n");
83  fprintf(fid,"   type rom_type is array(0 to (2 ** addr_w) - 1) of complex;\n\n");
84
85  fprintf(fid,"   constant rom : rom_type := (\n");
86
87
88  % starting index for twiddle rom
89  s = rom_depth / 4;
90
91  printf("stage %d, factors = %d \n", k, rom_depth);
92  for i = 0:rom_depth-1;
93  % compute twiddle factor index
94  m = N/2^(2+(2*k));
95  if (s < m)
96          p = 0;
97  elseif(s < (2*m))
98          p = 2^(2*k+1)*(s-m);
99  elseif(s < (3*m))
100         p = 2^(2*k)*(s-(2*m));
101 elseif(s < (4*m))
102         p = (3*2^(2*k))*(s-(3*m));
103 end
104
105 s = s+1;
106 if(s == rom_depth)
107         s = 0;
108 end
109
110 % find a twiddle factor
111 tf = exp(-1j*2*pi*(p/N))
112 % real and imaginary of a twiddle factor
113 realval = real(tf);
114 imagval = imag(tf);
115 % round twiddle factor
116 rounded_real = realval*(2^(tf_bit_width-2));
117 rounded_imag = imagval*(2^(tf_bit_width-2));
118 % convert twiddle to binary
119 real_bin = conv2bin(rounded_real,tf_bit_width);
120 imag_bin = conv2bin(rounded_imag,tf_bit_width);
121 % write to file
122 if(i < rom_depth - 1)
123         fprintf(fid,"(\"%s\",\"%s\"),\n",real_bin,imag_bin);
124 else
125         fprintf(fid,"(\"%s\",\"%s\")\n",real_bin,imag_bin);
126 end
127
128 end
129 fprintf(fid,");\n");
130 fprintf(fid,"begin\n");
131 fprintf(fid,"   doutr <= std_logic_vector(rom(conv_integer(addr))(0));\n");
132 fprintf(fid,"   douti <= std_logic_vector(rom(conv_integer(addr))(1));\n");
133 fprintf(fid,"end Behavioral;\n");
134 fclose(fid);
135 end
```

APPENDIX E

DDC IP CORE

E.1 INSTANTIATION OF THE DDC CORE

```
Library FIR_Lib;
Use FIR_Lib.fir_pkg.all;

Library DDC_Lib;
Use DDC_Lib.ddccomponents.all;

-- DDC__inst: This implements a Digital Down Converter on the FPGA.
--               The cores mainly on other sub-blocks such as NCO,
--               digital mixer, CIC and compensation FIR filter.
ddc_inst : ddc
generic map(
        DIN_WIDTH               => DIN_WIDTH,    -- input data width
        DOUT_WIDTH              => DOUT_WIDTH,   -- output data width
        -- NCO Configurations
        PHASE_WIDTH             => PHASE_WIDTH, -- NCO phase width
        PHASE_DITHER_WIDTH      => PHASE_DITHER_WIDTH,  -- Phase dither width
        -- CIC 1 configurations
        SELECT_CIC1             => SELECT_CIC1, -- select CIC decimator 1
        NUMBER_OF_STAGES1       => NUMBER_OF_STAGES1,   -- number of stages
        DIFFERENTIAL_DELAY1     => DIFFERENTIAL_DELAY1, --differential Dealy
        SAMPLE_RATE_CHANGE1     => SAMPLE_RATE_CHANGE1, --decimation factor
        -- Compensation FIR configuratons
        SELECT_CFIR             =>  SELECT_CFIR,        -- use FIR filter
        NUMBER_OF_TAPS          => NUMBER_OF_TAPS,      -- number of filter coefficients
        FIR_LATENCY             => FIR_LATENCY, -- FIR filter structure type
        COEFF_WIDTH             => COEFF_WIDTH, -- coefficient data width
        COEFFS                  => COEFFS,      -- array of quantized filter coefficients
        -- CIC 2 configurations
        SELECT_CIC2             => SELECT_CIC2, -- select CIC decimator 2
        NUMBER_OF_STAGES2       => NUMBER_OF_STAGES2,   -- number of stages
        DIFFERENTIAL_DELAY2     => DIFFERENTIAL_DELAY2, -- differential delay
        SAMPLE_RATE_CHANGE2     => SAMPLE_RATE_CHANGE2  -- decimation factor
)
port map(
        clk  => clk,    -- system clock input
        rst  => rst,    -- system reset input
        en   => en,     -- clock enable input
        din  => din,    -- input data sample
        ftw  => ftw,    -- frequency tuning word
        vld  => vld,    -- valid output result
        iout => iout,   -- real-part baseband output sample
        qout => qout    -- imaginary-part baseband output sample
);
```

E.2 Generating Testbench Data Files in Matlab

```
%----------------------------------------------------------------------
% This generates an FM signal as the input test factor to the DDC core
% testbench.
%----------------------------------------------------------------------
N  = 8192*4;     % total # of samples
Fs = 122.88e6;   % perform undersampling of FM signal
Ts = 1/Fs;       % sampling interval
fc = 94.5e6;     % carrier frequency

t  = [0:Ts:(N*Ts)- Ts]; % time index for samples

% system impedance (ohms)
R = 50;

% FM modulate a test signal.
ModFreq = 15e3;              % Modulating frequency
carrier = cos(2*pi*fc*t);


msg = awgn(sin(2*pi*ModFreq*t), 20, 'measured');  % compute vector

mi = 1; % Modulation Index
fmmsg = 2^15 * cos(2*pi*fc*t + mi*msg);

% PLOTS
startplot = 1;
endplot   = 1000;

NFFT = N; % FFT length
Ts   = 1/Fs;  % sampling interval
f    = Fs*(-NFFT/2:NFFT/2-1)/NFFT; % frequency

figure(1);
subplot(2,2,1);
plot(t/1e-6, msg,'k');
title('Message Signal');
xlabel('Time ($\mu s$)');
ylabel('Amplitude');
grid on;

% FFT for a baseband signal
f1 = fftshift(fft(msg,NFFT));
F1 = abs(f1)/(N);

subplot(2,2,2);
plot(f/1e3,F1,'k');
title('Magnitude Spectrum of a Message Signal');
xlabel('Frequency ($kHz$)');
ylabel('Magnitude');
xlim([-50,50]);
grid on;

% FFT for a carrier signal
f2 = fftshift(fft(2^15*carrier,NFFT));
F2 = abs(f2)/(N);

subplot(2,2,3);
plot(f/1e6,F2/1e4,'k');
title('Magnitude spectrum of a carrier');
xlabel('Frequency ($MHz$)');
ylabel('Magnitude ($\times 10^4$)');
xlim([-62,62]);
grid on;

% FFT for FM signal
f3 = fftshift(fft(fmmsg,NFFT));
F3 = abs(f3)/(N);
```

```
68
69  subplot(2,2,4);
70  plot(f/1e6,F3,'k');
71  title('Magnitude spectrum of FM Modulated signal');
72  xlabel('Frequency ($MHz$)');
73  ylabel('Magnitude');
74  xlim([27,29]);
75  grid on;
76
77  %-------------------------------------------------------------------
78  % Digital Down Conversion (DDC) SIMULATION BEFORE IMPLEMENTATION ON FPGA
79  %-------------------------------------------------------------------
80
81  %
82  %-------------------------------------------------------------------
83  %nco = ideal_dds(Fs,17.5e6,N); % digital local oscillator
84  %fLO = 2*Fs - fc;
85  fLO = Fs - fc;
86  LO  = exp(-1*1j*2*pi*fLO*t);
87
88  % normalized FFT of signal
89  f4=(fftshift(fft(LO,N))/(N));
90
91  % power spectrum
92  F4 = 10*log10((abs(f4).^2)/R*1000);
93
94  figure(2);
95  subplot(2,2,1);
96  plot(f,F4);
97  title('spectrum of a Local Oscillator ( LO[n] )');
98  xlabel('Frequency [hertz]');
99  ylabel('Magnitude [dB]');
100 xlim([-30e6,0]);
101
102 %
103 %-------------------------------------------------------------------
104 mixer = fmmsg .* LO;                          % mix FM signal with LO
105
106 % normalized FFT of signal
107 f5=(fftshift(fft(mixer,N))/(N));
108
109 % power spectrum
110 F5 = 10*log10((abs(f5).^2)/R*1000);
111
112 subplot(2,2,2);
113 plot(f,F5);
114 title('Spectrum of a mixer signal ( b[n] )');
115 xlabel('Frequency [hertz]');
116 ylabel('Magnitude [dB]');
117 xlim([-10e6,30e6]);
118
119 %
120 %-------------------------------------------------------------------
121 Mcic = 1;    % Differential delays in the filter.
122 Ncic = 10;    % Filter sections
123 Rcic = 128; % Decimation factor
124
125 g = ones(1,Rcic*Mcic);
126 h = g;
127 for i=1:Ncic;
128         h = conv(h,g);
129 end;
130
131 cic_filtered  = conv(mixer,g);
132 cic = cic_filtered([1:Rcic:length(cic_filtered)]);
133 cic = cic(1:round(length(mixer)/Rcic));
134
135 Fs = round(Fs/Rcic);
136 Ts = 1/Fs;
```

```
137 N = round(N/Rcic);
138 t = [0:Ts:(N*Ts)- Ts];
139
140 dF = Fs/N;                          % hertz
141 f = -Fs/2:dF:Fs/2-dF;               % hertz
142
143 % normalized FFT of signal
144 f6=(fftshift(fft(cic,N))/(N));
145
146 % power spectrum
147 F6 = 10*log10((abs(f6).^2)/R*1000);
148
149 subplot(2,2,3);
150 plot(f,F6);
151 title('Spectrum of a CIC output ( c[n] )');
152 xlabel('Frequency [hertz]');
153 ylabel('Magnitude [dB]');
154 xlim([-1.5e6,1.5e6]);
155
156
157 %
158 %-----------------------------------------------------------------------
159
160 Hfir= cfir(Rcic,Mcic,Ncic,95e3,122.88e6);
161
162 % filter the mixer spurs
163 pfir = filter(Hfir,1,cic);
164
165 % normalized FFT of signal
166 f7=(fftshift(fft(pfir,N))/(N));
167
168 % power spectrum
169 F7 = 10*log10((abs(f7).^2)/R*1000);
170
171 subplot(2,2,4);
172 plot(f,F7);
173 title('Spectrum of a filter output [I[n] and Q[n]');
174 xlabel('Frequency [hertz]');
175 ylabel('Magnitude [dB]');
176 xlim([-1.5e6,1.5e6]);
177
178 % Write test data to a file
179 fid=fopen('../../tb/coeffs.in','wt');
180 fprintf(fid,"%d,",round(Hfir*2^15));
181 fclose(fid);
182
183 %
184 %-----------------------------------------------------------------------
185 Mcic = 1;    % Differential delays in the filter.
186 Ncic = 1;    % Filter sections
187 Rcic = 2;    % Decimation factor
188
189 g = ones(1,Rcic*Mcic);
190 h = g;
191 for i=1:Ncic;
192         h = conv(h,g);
193 end;
194
195 cic1 = pfir;
196 cic_filtered  = conv(cic1,g);
197 cic = cic_filtered([1:Rcic:length(cic_filtered)]);
198 cic = cic(1:round(length(cic1)/Rcic));
199
200 Fs = round(Fs/Rcic);
201 Ts = 1/Fs;
202 N = round(N/Rcic);
203 t = [0:Ts:(N*Ts)- Ts];
204
205 dF = Fs/N;                          % hertz
```

```
206 f = -Fs/2:dF:Fs/2-dF;            % hertz
207
208 %-----------------------------------------------------------------------
209 %
210 %-----------------------------------------------------------------------
211
212 % Initialize the variables.                                            %
213
214 phase = zeros(1,length(cic));
215 freq = zeros(1,length(cic)-1);
216
217 phase = atan2(imag(cic),real(cic));
218 freq = phase(1)
219 freq = diff(phase)./diff(t);
220
221 freq = -1 .* freq;
222
223 % amplify the output
224 %freq = (1/max(freq(50:length(freq)))) * freq;
225
226 %-------------------------------------------------------------------------%
227 figure(3)
228 subplot(2,2,1)
229 plot(t(1:length(t)-1),freq);
230 title('FM Demodulated Signal');
231 xlabel('Time (seconds)');
232 ylabel('Amplitude');
233 %ylim([-1,1]);
234
235 % normalized FFT of signal
236 f8=(fftshift(fft(freq,N))/(N));
237
238 % power spectrum
239 F8 = 10*log10((abs(f8).^2)/R*1000);
240
241 subplot(2,2,2)
242 plot(f,F8);
243 title('Spectrum of a Demodulated Signals');
244 xlabel('Frequency [hertz]');
245 ylabel('Magnitude [dB]');
246 xlim([-20e3,20e3]);
```

E.3 Generate Coefficients for a Compensation Filter

```
1  function [h]= cfir(R,M,N);
2  %%%%%% CIC filter parameters %%%%%%
3  %R,M,N
4  %h = filter response
5  B = 16; %% Coeffi. Bit-width
6  Fs = 122.88e6;%% (High) Sampling freq in Hz before decimation
7  Fc = 80e3; %% Pass band edge in Hz
8
9  L = 20; %% Filter order; must be even
10 Fo = R*Fc/Fs; %% Normalized Cutoff freq; 0<Fo<=0.5/M;
11
12 p = 2e3; %% Granularity
13 s = 0.25/p; %% Step size
14 fp = [0:s:Fo]; %% Pass band frequency samples
15 fs = (Fo+s):s:0.5; %% Stop band frequency samples
16 f = [fp fs]*2; %% Normalized frequency samples; 0<=f<=1
17 Mp = ones(1,length(fp)); %% Pass band response; Mp(1)=1
18 Mp(2:end) = abs( M*R*sin(pi*fp(2:end)/R)./sin(pi*M*fp(2:end))).^N;
19 Mf = [Mp zeros(1,length(fs))];
20 f(end) = 1;
21 h = fir2(L,f,Mf); %% Filter length L+1
```

E.4 PLOTTING THE RESULTS IN MATLAB

```
%-----------------------------------------------------------------------
% Plotting the results of the DDC core output
%-----------------------------------------------------------------------
N  = 8192*4;     % total # of samples
Fs = 122.88e6;  % perform undersampling of FM signal
Ts = 1/Fs;       % sampling interval
f    = Fs*(-NFFT/2:NFFT/2-1)/NFFT; % frequency

% Numerially-Controlled Oscillator
ncoOutRaw = dlmread('nco.out',' ');
ncoOut = complex(ncoOutRaw(:,1),ncoOutRaw(:,2));

% normalized FFT of signal
f4 = fftshift(fft(ncoOut,NFFT));
F4 = abs(f4)/(N);

figure(2);
subplot(2,2,1);
plot(f/1e6,F4,'k');
title('Magnitude spectrum of NCO');
xlabel('Frequency ($MHz$)');
ylabel('Magnitude');
xlim([0,61.44]);
grid on;

% Mixer Stage of DDC

mixerOutRaw = dlmread('mixer.out',' ');
mixerOut = complex(mixerOutRaw(:,1),mixerOutRaw(:,2));

% normalized FFT of signal
f5 = fftshift(fft(mixerOut,NFFT));
F5 = abs(f5)/(N);

subplot(2,2,2);
plot(f/1e6,F5,'k');
title('Magnitude spectrum of a Mixer');
xlabel('Frequency ($MHz$)');
ylabel('Magnitude');
xlim([-10,61.44]);
grid on;

%CIC Stage 1
NFFT = round(N/153);
Ts   = 1/(Fs/153);
Fs   = 1/Ts;                    % sampling interval
f    = Fs*(-NFFT/2:NFFT/2-1)/NFFT;

cic1OutRaw = dlmread('cic1.out',' ');
cic1Out = complex(cic1OutRaw(:,1),cic1OutRaw(:,2));

% normalized FFT of signal
f6 = fftshift(fft(cic1Out,NFFT));
F6 = abs(f6)/(N);

subplot(2,2,3);
plot(f/1e3,F6/1e4,'k');
title('Magnitude spectrum of CIC-1');
xlabel('Frequency ($kHz$)');
ylabel('Magnitude ($\times 10^4$)');
%xlim([-400,400]);
grid on;

%Compensation FIR Stage 1
cfirOutRaw = dlmread('cfir.out',' ');
cfirOut = complex(cfirOutRaw(:,1),cfirOutRaw(:,2));

```

```
68  % normalized FFT of signal
69  f7 = fftshift(fft(cfirOut,NFFT));
70  F7 = abs(f7)/(N);
71
72  subplot(2,2,4);
73  plot(f/1e3,F7/1e4,'k');
74  title('Magnitude spectrum of a C-FIR filter');
75  xlabel('Frequency ($kHz$)');
76  ylabel('Magnitude ($\times 10^4$)');
77  %xlim([-400,400]);
78  grid on;
79
80  % CIC Stage 2
81  NFFT = round(N/153/2);
82  Ts   = 1/(Fs/2);
83  Fs   = 1/Ts;
84  f    = Fs*(-NFFT/2:NFFT/2-1)/NFFT;
85
86  cic2OutRaw = dlmread('cic2.out',' ');
87  cic2Out = complex(cic2OutRaw(:,1),cic2OutRaw(:,2));
88
89  % normalized FFT of signal
90  f8 = fftshift(fft(cic2Out,NFFT));
91  F8 = abs(f8)/(N);
92
93  figure(3);
94  subplot(2,2,1);
95  plot(f/1e3,F8/1e4,'k');
96  title('Magnitude spectrum of CIC-2');
97  xlabel('Frequency ($kHz$)');
98  ylabel('Magnitude ($\times 10^4$)');
99  xlim([-200,200]);
100 grid on;
```

APPENDIX F

UDP/IP CORE

F.1 INSTANTIATION OF THE UDP/IP CORE

```
Library IO_Lib;
Use IO_Lib.iocomponents.all;

-- UDP_1GbE_inst: 1Gbe Ethernet interface using UDP protocol

UDP_1GbE_inst : UDP_1GbE
generic map(
                UDP_TX_DATA_BYTE_LENGTH => UDP_TX_DATA_BYTE_LENGTH, -- Number of TX packet bytes
                UDP_RX_DATA_BYTE_LENGTH => UDP_RX_DATA_BYTE_LENGTH -- Number of RX packet bytes
 )
port map(
                -- user logic interface
                own_ip_addr     => own_ip_addr, -- FPGA IP address : default=x"c0a80003"
                own_mac_addr    => own_mac_addr,-- FPGA MAC address : default=x"0024ba7d1d70"
                dst_ip_addr     => dst_ip_addr,-- Destination IP address: default=x"c0a80001"
                dst_mac_addr    => dst_mac_addr,        -- Destination MAC address

                udp_src_port    => udp_src_port,-- source UDP port : default=x"26CA"
                udp_dst_port    => udp_dst_port,-- destination UDP : default=x"26CA"

                udp_tx_pkt_data => udp_tx_pkt_data, -- udp TX packet
                udp_tx_pkt_vld  => udp_tx_pkt_vld,      -- enable data transmission
                udp_tx_rdy      => udp_tx_rdy,  -- udp core ready to transmit

                udp_rx_pkt_data => udp_rx_pkt_data, -- udp receive packet
                udp_rx_pkt_req  => udp_rx_pkt_req,      -- request to RX packet
                udp_rx_rdy      => udp_rx_rdy,  -- RX packet ready in the buffer

                mac_init_done   => mac_init_done,-- UDP initialization complete

                -- MAC interface
                GIGE_COL        => GIGE_COL,
                GIGE_CRS        => GIGE_CRS,
                GIGE_MDC        => GIGE_MDC,
                GIGE_MDIO       => GIGE_MDIO,
                GIGE_TX_CLK     => GIGE_TX_CLK,
                GIGE_nRESET     => GIGE_nRESET,
                GIGE_RXD        => GIGE_RXD,
                GIGE_RX_CLK     => GIGE_RX_CLK,
                GIGE_RX_DV      => GIGE_RX_DV,
                GIGE_RX_ER      => GIGE_RX_ER,
                GIGE_TXD        => GIGE_TXD,
                GIGE_GTX_CLK    => GIGE_GTX_CLK,
                GIGE_TX_EN      => GIGE_TX_EN,
                GIGE_TX_ER      => GIGE_TX_ER,
```

```
46
47                  -- system control
48                  clk_125mhz      => clk_125mhz,
49                  clk_100mhz      => clk_100mhz,
50                  sys_rst_i       => sys_rst_i,
51                  sysclk_locked   => sysclk_locked
52  );
```

APPENDIX G

ADC/DAC CORE

G.1 INSTANTIATION OF THE ADC/DAC CORE FOR INTERFACING FMC150

```
Library IO_Lib;
Use IO_Lib.iocomponents.all;

-- fmc150_if_inst: 1Gbe Ethernet interface using UDP protocol

fmc150_if_inst : fmc150_if
port map(

  --RHINO Resources
  sysrst           => sysrst,
  clk_100MHz       => clk_100MHz,
  mmcm_locked      => mmcm_locked,

  clk_61_44MHz     => clk_61_44MHz,
  clk_122_88MHz    => clk_122_88MHz,
  mmcm_adac_locked => mmcm_adac_locked,

  -------------- user design interface -----------------------
  -- ADC
  adc_cha_dout     => adc_cha_dout,
  adc_chb_dout     => adc_chb_dout,

  -- DAC
  dac_chc_din      => dac_chc_din,
  dac_chd_din      => dac_chd_din,

  calibration_ok   => calibration_ok,

  -------------- physical external interface -----------------

  --Clock/Data connection to ADC on FMC150 (ADS62P49)
  clk_ab_p         => clk_ab_p,
  clk_ab_n         => clk_ab_n,
  cha_p            => cha_p,
  cha_n            => cha_n,
  chb_p            => chb_p,
  chb_n            => chb_n,

  --Clock/Data connection to DAC on FMC150 (DAC3283)
  dac_dclk_p       => dac_dclk_p,
  dac_dclk_n       => dac_dclk_n,
  dac_data_p       => dac_data_p,
  dac_data_n       => dac_data_n,
  dac_frame_p      => dac_frame_p,
  dac_frame_n      => dac_frame_n,
```

```
46      txenable          => txenable,
47
48      --Clock/Trigger connection to FMC150
49      clk_to_fpga       => clk_to_fpga,
50      ext_trigger       => ext_trigger,
51
52      --Serial Peripheral Interface (SPI)
53      spi_sclk          => spi_sclk,
54      spi_sdata         => spi_sdata,
55
56      -- ADC specific signals
57      adc_n_en          => adc_n_en,
58      adc_sdo           => adc_sdo,
59      adc_reset         => adc_reset,
60
61      -- CDCE specific signals
62      cdce_n_en         => cdce_n_en,
63      cdce_sdo          => cdce_sdo,
64      cdce_n_reset      => cdce_n_reset,
65      cdce_n_pd         => cdce_n_pd,
66      ref_en            => ref_en,
67      pll_status        => pll_status,
68
69      -- DAC specific signals
70      dac_n_en          => dac_n_en,
71      dac_sdo           => dac_sdo,
72
73      -- Monitoring specific signals
74      mon_n_en          => mon_n_en,
75      mon_sdo           => mon_sdo,
76      mon_n_reset       => mon_n_reset,
77      mon_n_int         => mon_n_int,
78
79      --FMC-0 Present status
80      nfmc0_prsnt       => nfmc0_prsnt
81    );
```

APPENDIX H

DIGITAL FM RECEIVER

H.1 TOP LEVEL DESIGN OF DIGITAL IP BLOCKS

```
Library IEEE;
Use IEEE.STD_LOGIC_1164.ALL;
Use IEEE.std_logic_unsigned.all;

Library IO_Lib;
Use IO_Lib.iocomponents.all;

Library NCO_Lib;
Use NCO_Lib.ncocomponents.all;

Library DDC_Lib;
Use DDC_Lib.ddccomponents.all;

entity rhino_sdr_blocks is
        port (

                -- RHINO Resources
                sys_clk_p           : in          std_logic;
                sys_clk_n           : in          std_logic;
                sys_rst_i           : in          std_logic;

                -- Status LEDs
                fmc150_pll_ok       : out         std_logic;
                fmc150_calib_ok     : out    std_logic;
                gbe_init_ok         : out    std_logic;

                -- FMC150 interface -----------------------
                --Clock/Data connection to ADC on FMC150 (ADS62P49)
                clk_ab_p            : in     std_logic;
                clk_ab_n            : in     std_logic;
                cha_p               : in     std_logic_vector(6 downto 0);
                cha_n               : in     std_logic_vector(6 downto 0);
                chb_p               : in     std_logic_vector(6 downto 0);
                chb_n               : in     std_logic_vector(6 downto 0);

                --Clock/Data connection to DAC on FMC150 (DAC3283)
                dac_dclk_p          : out    std_logic;
                dac_dclk_n          : out    std_logic;
                dac_data_p          : out    std_logic_vector(7 downto 0);
                dac_data_n          : out    std_logic_vector(7 downto 0);
                dac_frame_p         : out    std_logic;
                dac_frame_n         : out    std_logic;
                txenable            : out    std_logic;

                --Clock/Trigger connection to FMC150
```

```
46                  clk_to_fpga         : in    std_logic;
47                  ext_trigger         : in    std_logic;
48
49                  --Serial Peripheral Interface (SPI)
50                  spi_sclk            : out   std_logic; -- Shared SPI clock line
51                  spi_sdata           : out   std_logic; -- Shared SPI sata line
52
53                  -- ADC specific signals
54                  adc_n_en            : out   std_logic; -- SPI chip select
55                  adc_sdo             : in    std_logic; -- SPI data out
56                  adc_reset           : out   std_logic; -- SPI reset
57
58                  -- CDCE specific signals
59                  cdce_n_en           : out   std_logic; -- SPI chip select
60                  cdce_sdo            : in    std_logic; -- SPI data out
61                  cdce_n_reset        : out   std_logic;
62                  cdce_n_pd           : out   std_logic;
63                  ref_en              : out   std_logic;
64                  pll_status          : in    std_logic;
65
66                  -- DAC specific signals
67                  dac_n_en            : out   std_logic; -- SPI chip select
68                  dac_sdo             : in    std_logic; -- SPI data out
69
70                  -- Monitoring specific signals
71                  mon_n_en            : out   std_logic; -- SPI chip select
72                  mon_sdo             : in    std_logic; -- SPI data out
73                  mon_n_reset         : out   std_logic;
74                  mon_n_int           : in    std_logic;
75
76                  --FMC Present status
77                  nfmc0_prsnt         : in    std_logic;
78
79                  -- 1Gbps MAC interface
80
81                  GIGE_COL                                  : in std_logic;
82                  GIGE_CRS                                  : in std_logic;
83                  GIGE_MDC                                  : out std_logic;
84                  GIGE_MDIO                   : inout std_logic;
85                  GIGE_TX_CLK                 : in std_logic;
86                  GIGE_nRESET                 : out std_logic;
87                  GIGE_RXD                                  : in std_logic_vector( 7 downto 0 );
88                  GIGE_RX_CLK                         : in std_logic;
89                  GIGE_RX_DV                          : in std_logic;
90                  GIGE_RX_ER                  : in std_logic;
91                  GIGE_TXD                                  : out std_logic_vector( 7 downto 0 );
92                  GIGE_GTX_CLK             : out std_logic;
93                  GIGE_TX_EN                          : out std_logic;
94                  GIGE_TX_ER                          : out std_logic
95          );
96  end rhino_sdr_blocks;
97
98  architecture Behavioral of rhino_sdr_blocks is
99
100         --
101         component clk_manager is
102         port(
103                 --External Control
104                 SYS_CLK_P_i   : in   std_logic;
105                 SYS_CLK_N_i   : in   std_logic;
106                 SYS_RST_i     : in   std_logic;
107
108                 clk_ab_p                  : in std_logic;
109                 clk_ab_n            : in std_logic;
110
111                 -- Clock out ports
112                 clk_125mhz     : out std_logic;
113                 clk_122_88mhz  : out std_logic;
114                 clk_100mhz     : out std_logic;
```

```
115                 clk_61_44mhz  : out std_logic;
116                 clk_25mhz     : out std_logic;
117
118                 -- Status and control signals
119                 RESET         : out std_logic;
120                 sysclk_locked : out std_logic;
121                 adcclk_locked : out std_logic
122         );
123     end component clk_manager;
124
125         component adc_eth_bridge
126          generic(
127                 MEM_DATA_BYTES : natural;
128                 MEM_DEPTH                : natural
129         );
130         port(
131                 rst              : in   std_logic;
132                 clk              : in   std_logic;
133                 en          : in   std_logic;
134                 rd_en            : in   std_logic;
135                 vld              : out  std_logic;
136                 new_pkt_rcvd : in   std_logic;
137                 din              : in   std_logic_vector(8 * MEM_DATA_BYTES - 1 downto 0);
138                 dout             : out  std_logic_vector(8 * MEM_DATA_BYTES * MEM_DEPTH - 1 downto 0);
139                 count          : out std_logic_vector(6 downto 0)
140           );
141         end component;
142
143         -- Debugging Components and Signals
144         component icon
145           PORT (
146                  CONTROL0 : INOUT STD_LOGIC_VECTOR(35 DOWNTO 0);
147                  CONTROL1 : INOUT STD_LOGIC_VECTOR(35 DOWNTO 0);
148                  CONTROL2 : INOUT STD_LOGIC_VECTOR(35 DOWNTO 0));
149
150         end component;
151
152         component ila0
153           PORT (
154                  CONTROL : INOUT STD_LOGIC_VECTOR(35 DOWNTO 0);
155                  CLK : IN STD_LOGIC;
156                  DATA : IN STD_LOGIC_VECTOR(69 DOWNTO 0);
157                  TRIG0 : IN STD_LOGIC_VECTOR(3 DOWNTO 0));
158
159         end component;
160
161         component ila1
162           PORT (
163                  CONTROL : INOUT STD_LOGIC_VECTOR(35 DOWNTO 0);
164                  CLK : IN STD_LOGIC;
165                  DATA : IN STD_LOGIC_VECTOR(47 DOWNTO 0);
166                  TRIG0 : IN STD_LOGIC_VECTOR(7 DOWNTO 0));
167
168         end component;
169
170         component vio
171           PORT (
172                  CONTROL : INOUT STD_LOGIC_VECTOR(35 DOWNTO 0);
173                  ASYNC_OUT : OUT STD_LOGIC_VECTOR(31 DOWNTO 0));
174
175         end component;
176
177
178         signal CONTROL0 : STD_LOGIC_VECTOR(35 DOWNTO 0);
179         signal CONTROL1 : STD_LOGIC_VECTOR(35 DOWNTO 0);
180         signal CONTROL2 : STD_LOGIC_VECTOR(35 DOWNTO 0);
181         signal ila_data0 :  STD_LOGIC_VECTOR(69 DOWNTO 0);
182         signal ila_data1 :  STD_LOGIC_VECTOR(47 DOWNTO 0);
183         signal trig0 : STD_LOGIC_VECTOR(3 DOWNTO 0);
```

```
184        signal trig1 : STD_LOGIC_VECTOR(7 DOWNTO 0);
185        signal vio_data :  STD_LOGIC_VECTOR(31 DOWNTO 0);
186
187        -- End
188
189
190        --
191
192        attribute S: string;
193        attribute keep : string;
194
195        -- FMC150 signals
196        attribute S of GIGE_RXD   : signal is "TRUE";
197        attribute S of GIGE_RX_DV : signal is "TRUE";
198        attribute S of GIGE_RX_ER : signal is "TRUE";
199
200        constant UDP_TX_DATA_BYTE_LENGTH : integer := 64;
201        constant UDP_RX_DATA_BYTE_LENGTH : integer := 37;
202        constant TX_DELAY                                      : integer := 10;
203
204        signal adc_cha_dout      : std_logic_vector(13 downto 0);
205        signal adc_chb_dout      : std_logic_vector(13 downto 0);
206
207    signal dac_chc_din      : std_logic_vector(15 downto 0);
208        signal dac_chd_din      : std_logic_vector(15 downto 0);
209
210        signal clk_100MHz                      : std_logic;
211        signal mmcm_locked      : std_logic;
212        signal dac_fpga_clk     : std_logic;
213
214        ------------------------- MAC signals -------------------------------------
215        signal udp_tx_pkt_data  : std_logic_vector (8 * UDP_TX_DATA_BYTE_LENGTH - 1 downto 0);
216        signal udp_tx_pkt_vld   : std_logic;
217        signal udp_tx_pkt_sent  : std_logic;
218        signal udp_tx_pkt_vld_r : std_logic;
219        signal udp_tx_rdy                 : std_logic;
220
221        signal udp_rx_pkt_data  : std_logic_vector(8 * UDP_RX_DATA_BYTE_LENGTH - 1 downto 0);
222        signal udp_rx_pkt_data_r: std_logic_vector(8 * UDP_RX_DATA_BYTE_LENGTH - 1 downto 0);
223        signal udp_rx_pkt_req   : std_logic;
224    signal udp_rx_rdy              : std_logic;
225        signal udp_rx_rdy_r     : std_logic;
226
227        signal dst_mac_addr     : std_logic_vector(47 downto 0);
228        signal tx_state                 : std_logic_vector(2 downto 0)  := "000";
229        signal rx_state                 : std_logic_vector(2 downto 0)  := "000";
230
231        signal adc_pkt_vld         : std_logic;
232        signal adc_pkt_data     : std_logic_vector (8 * UDP_TX_DATA_BYTE_LENGTH - 1 downto 0);
233        signal adc_pkt_rd_en    : std_logic;
234        signal tx_delay_cnt             : integer := 0;
235
236        signal mac_init_done    : std_logic;
237        signal calibration_ok_r : std_logic;
238        signal new_pkt_rcvd     : std_logic;
239
240        signal clk_61_44MHz     :  std_logic;
241        signal clk_122_88MHz    :  std_logic;
242        signal clk_ab_l                   : std_logic;
243
244        signal clk_368_64MHz    : std_logic;
245        signal clk_25MHz        : std_logic;
246
247        signal clk_125mhz       : std_logic;
248        signal adcclk_locked    : std_logic;
249        signal sysclk_locked    : std_logic;
250        signal sysrst                   : std_logic;
251
252        -------------- Down-sampler -----------------------------------------
```

```
253         signal ds_vld  : std_logic;
254         signal ds_dout : std_logic_vector(15 downto 0);
255
256
257         -------------- FFT Core -------------------------------------------
258         signal fft_rst  : std_logic;
259         signal fft_vld  : std_logic;
260         signal fft_done : std_logic;
261         signal XKr              : std_logic_vector(31 downto 0);
262         signal XKi      : std_logic_vector(31 downto 0);
263
264         signal XKr_r    : std_logic_vector(27 downto 0);
265         signal XKi_r     : std_logic_vector(27 downto 0);
266
267         -------------- Interconnect ------------------------------------------
268         signal bridge_rst : std_logic;
269         signal bridge_en  : std_logic;
270         signal tag                      : std_logic_vector(8 downto 0) := (others =>'0');
271         signal counter_samples : std_logic_vector( 6 downto 0);
272
273
274         -------------- Test Vector in ROM----------------------------------------
275         signal rom_addr  : std_logic_vector(5 downto 0);
276         signal rom_doutr : std_logic_vector(15 downto 0);
277         signal rom_douti : std_logic_vector(15 downto 0);
278         signal trigger   : std_logic;
279
280         ------------------------- DAC -------------------------------------
281         signal FTW : std_logic_vector(31 downto 0);
282
283         ------------------------ DDC --------------------------------------
284         signal DDC_FTW  :  std_logic_vector(31 downto 0) := (others=>'0');
285         signal IOUT      : std_logic_vector (15 downto 0);
286         signal QOUT              : std_logic_vector (15 downto 0);
287         signal ddc_vld  : std_logic;
288         type fm_type is array(0 to  8191) of std_logic_vector(15 downto 0);
289         signal fm_counter : integer range 0 to 8191 := 0;
290         signal fm_data : std_logic_vector(15 downto 0);
291         signal fm_addr : std_logic_vector(12 downto 0);
292 begin
293
294         -------------------------- Status LEDs-----------------------------
295         fmc150_pll_ok    <= pll_status;
296     fmc150_calib_ok  <= calibration_ok_r;
297         gbe_init_ok      <= mac_init_done;
298
299         --------------------------------------------------------------------
300         --
301         --------------------------------------------------------------------
302         fmc150_if_inst : fmc150_if
303         port map(
304
305           --RHINO Resources
306           sysrst        => sysrst,
307           clk_100MHz    => clk_100MHz,
308           mmcm_locked   => sysclk_locked,
309
310           clk_61_44MHz  => clk_61_44MHz,
311           clk_122_88MHz => clk_122_88MHz,
312           mmcm_adac_locked      => adcclk_locked,
313
314           dac_fpga_clk  => dac_fpga_clk,
315           -------------- user design interface ----------------------------
316           -- ADC
317           adc_cha_dout  => adc_cha_dout,
318           adc_chb_dout  => adc_chb_dout,
319
320           -- DAC
321           dac_chc_din   => dac_chc_din,
```

```
322            dac_chd_din   => dac_chd_din,
323
324            calibration_ok        => calibration_ok_r,
325
326            -------------- physical external interface -----------------------
327
328            --Clock/Data connection to ADC on FMC150 (ADS62P49)
329            clk_ab_p      => clk_ab_p,
330            clk_ab_n      => clk_ab_n,
331            cha_p => cha_p,
332            cha_n => cha_n,
333            chb_p => chb_p,
334            chb_n => chb_n,
335
336            --Clock/Data connection to DAC on FMC150 (DAC3283)
337            dac_dclk_p    => dac_dclk_p,
338            dac_dclk_n    => dac_dclk_n,
339            dac_data_p    => dac_data_p,
340            dac_data_n    => dac_data_n,
341            dac_frame_p   => dac_frame_p,
342            dac_frame_n   => dac_frame_n,
343            txenable      => txenable,
344
345            --Clock/Trigger connection to FMC150
346            clk_to_fpga   => clk_to_fpga,
347            ext_trigger   => ext_trigger,
348
349            --Serial Peripheral Interface (SPI)
350            spi_sclk      => spi_sclk,
351            spi_sdata     => spi_sdata,
352
353            -- ADC specific signals
354            adc_n_en      => adc_n_en,
355            adc_sdo       => adc_sdo,
356            adc_reset     => adc_reset,
357
358            -- CDCE specific signals
359            cdce_n_en     => cdce_n_en,
360            cdce_sdo      => cdce_sdo,
361            cdce_n_reset  => cdce_n_reset,
362            cdce_n_pd     => cdce_n_pd,
363            ref_en        => ref_en,
364            pll_status    => pll_status,
365
366            -- DAC specific signals
367            dac_n_en      => dac_n_en,
368            dac_sdo       => dac_sdo,
369
370            -- Monitoring specific signals
371            mon_n_en      => mon_n_en,
372            mon_sdo       => mon_sdo,
373            mon_n_reset   => mon_n_reset,
374            mon_n_int     => mon_n_int,
375
376            --FMC-0 Present status
377            nfmc0_prsnt   => nfmc0_prsnt
378          );
379
380
381          --1Gbe Ethernet interface
382
383          UDP_1GbE_inst : UDP_1GbE
384          generic map(
385                          UDP_TX_DATA_BYTE_LENGTH => UDP_TX_DATA_BYTE_LENGTH,
386                          UDP_RX_DATA_BYTE_LENGTH => UDP_RX_DATA_BYTE_LENGTH
387           )
388          port map(
389                          -- user logic interface
390                          own_ip_addr     => x"c0a80003",
```

```
391                     own_mac_addr    => x"0024ba7d1d70",
392                     dst_ip_addr     => x"c0a80001",
393                     dst_mac_addr     => dst_mac_addr,
394
395                     udp_src_port    => x"26CA", --9930
396                     udp_dst_port    => x"26CA",
397
398                     udp_tx_pkt_data => udp_tx_pkt_data,
399                     udp_tx_pkt_vld  => udp_tx_pkt_vld,
400                     udp_tx_rdy      => udp_tx_rdy,
401
402                     udp_rx_pkt_data => udp_rx_pkt_data,
403                     udp_rx_pkt_req  => udp_rx_pkt_req,
404                     udp_rx_rdy      => udp_rx_rdy,
405
406                     mac_init_done   => mac_init_done,
407
408                     -- MAC interface
409                     GIGE_COL        => GIGE_COL,
410                     GIGE_CRS        => GIGE_CRS,
411                     GIGE_MDC        => GIGE_MDC,
412                     GIGE_MDIO       => GIGE_MDIO,
413                     GIGE_TX_CLK     => GIGE_TX_CLK,
414                     GIGE_nRESET     => GIGE_nRESET,
415                     GIGE_RXD        => GIGE_RXD,
416                     GIGE_RX_CLK     => GIGE_RX_CLK,
417                     GIGE_RX_DV      => GIGE_RX_DV,
418                     GIGE_RX_ER      => GIGE_RX_ER,
419                     GIGE_TXD        => GIGE_TXD,
420                     GIGE_GTX_CLK    => GIGE_GTX_CLK,
421                     GIGE_TX_EN      => GIGE_TX_EN,
422                     GIGE_TX_ER      => GIGE_TX_ER,
423
424                     -- system control
425                     clk_125mhz     => clk_125mhz,
426                     clk_100mhz     => clk_100mhz,
427                     sys_rst_i      => sysrst,
428                     sysclk_locked  => sysclk_locked
429             );
430
431             clk_manager_inst : clk_manager
432             port map(
433                     --External Control
434                     SYS_CLK_P_i  => sys_clk_p,
435                     SYS_CLK_N_i  => sys_clk_n,
436                     SYS_RST_i    => SYS_RST_i,
437
438                     clk_ab_p                  => clk_ab_p,
439                     clk_ab_n          => clk_ab_n,
440
441                     -- Clock out ports
442                     clk_125mhz    => clk_125mhz,
443                     clk_122_88mhz => clk_122_88mhz,
444                     clk_100mhz    => clk_100mhz,
445                     clk_61_44mhz  => clk_61_44mhz,
446                     clk_25mhz     => clk_25mhz,
447                     -- Status and control signals
448                     RESET         => sysrst,
449                     sysclk_locked => sysclk_locked,
450                     adcclk_locked => adcclk_locked
451             );
452
453
454             --Digtal Down Converter
455
456             ddc_inst : ddc
457             generic map(
458                     DIN_WIDTH                        => 16,
459                     DOUT_WIDTH                       => 16,
```

```
460                     -- NCO Configurations
461                     PHASE_WIDTH              => 32,
462                     PHASE_DITHER_WIDTH => 22,
463                     -- CIC 1 configurations
464                     SELECT_CIC1              => '1',
465                     NUMBER_OF_STAGES1        => 10,
466                     DIFFERENTIAL_DELAY1 => 1,
467                     SAMPLE_RATE_CHANGE1 => 128,
468                     -- Compensating FIR configuratons
469                     SELECT_CFIR      => '1',
470                     NUMBER_OF_TAPS   => 21,
471                     FIR_LATENCY      => 0,
472                     COEFF_WIDTH      => 16,
473                     COEFFS   => (-78,-132,-217,-247,-57,516,1534,2880,4261,5301,5689,
474                                 5301,4261,2880,1534,516,-57,-247,-217,-132,-78),
475                     -- CIC 2 configurations
476                     SELECT_CIC2      => '0',
477                     NUMBER_OF_STAGES2       => 1,
478                     DIFFERENTIAL_DELAY2 => 1,
479                     SAMPLE_RATE_CHANGE2 => 2
480             )
481             port map(
482                     CLK   => clk_61_44mhz,
483                     RST   => sysrst,
484                     EN         => '1',
485                     DIN   => (1 downto 0 => adc_chb_dout(13)) & adc_chb_dout,
486                     FTW   => DDC_FTW,
487                     VLD   => ddc_vld,
488                     IOUT => IOUT,
489                     QOUT => QOUT
490             );
491
492             DDC_FTW <= vio_data;
493
494
495             --Interconnect Buffer for ADC and UDP/IP cores
496
497             Adc_ChB_Eth_Bridge_Inst : adc_eth_bridge
498             generic map(
499                     MEM_DATA_BYTES => 4,
500                     MEM_DEPTH               => 16
501             )
502             port map(
503                     rst                     => sysrst,
504                     clk                     => clk_61_44mhz,
505                     en                      => ddc_vld,
506                     rd_en                   => adc_pkt_rd_en,
507                     vld                     => adc_pkt_vld,
508                     new_pkt_rcvd => new_pkt_rcvd,
509                     din                     => IOUT & QOUT,
510                     dout                    => adc_pkt_data
511             );
512
513
514             --Contontrol State Machine
515
516             tx_proc : process(sysrst,clk_61_44MHz)
517             begin
518                     if(sysrst = '1') then
519                     elsif(rising_edge(clk_61_44MHz)) then
520                             --fm_addr <= fm_addr + 1;
521                             case tx_state is
522                                     when "000" =>
523                                             udp_tx_pkt_vld_r <= '0';
524                                             adc_pkt_rd_en    <= '0';
525                                             if(adc_pkt_vld = '1') then
526                                                     tx_state <= "001";
527                                             end if;
528                                     when "001" =>
```

```
529                                                 if(udp_tx_rdy = '1') then
530                                                         udp_tx_pkt_vld_r <= '1';
531                                                         adc_pkt_rd_en    <= '1';
532                                                         udp_tx_pkt_data  <= adc_pkt_data;
533                                                         tx_state         <= "010";
534                                                 end if;
535                                         when "010" =>
536                                                 udp_tx_pkt_vld_r <= '0';
537                                                 adc_pkt_rd_en    <= '1';
538                                                 if(adc_pkt_vld = '0') then
539                                                         tx_state         <= "000";
540                                                 end if;
541                                         when others =>
542                                                 null;
543                                 end case;
544                         end if;
545                 end process;
546                 udp_tx_pkt_vld <= udp_tx_pkt_vld_r;
547 
548 
549                 --DAC test using NCO
550 
551                 NCO_inst :  NCO
552                 generic map(
553                         FTW_WIDTH                => 32,
554                         PHASE_WIDTH              => 32,
555                         PHASE_DITHER_WIDTH => 22
556                 )
557                 port map(
558                         CLK   => dac_fpga_clk,
559                         RST   => sysrst,
560                         FTW   => ftw,
561                         IOUT => dac_chc_din,
562                         QOUT => dac_chd_din
563                 );
564 
565                 --FTW <= x"01DAAAAB";
566                 FTW <= vio_data;
567 
568 
569         --Debugging Section in ChipscopePro
570 
571         ila_data0(0)  <= udp_tx_rdy;
572              ila_data0(1)  <= adc_pkt_vld;
573              ila_data0(2)  <= adc_pkt_rd_en;
574              ila_data0(3)  <= new_pkt_rcvd;
575              ila_data0(4)  <= fft_done;
576              ila_data0(5)  <= fft_vld;
577              ila_data0(6)  <= fft_rst;
578              ila_data0(12 downto 7)  <= rom_addr;
579 
580              ila_data0(15 downto 13)  <= tx_state;
581 
582              ila_data0(31 downto 16)  <= fm_data;
583              ila_data0(57 downto 51)  <= counter_samples;
584              --ila_data0(66   downto 51)  <= rom_doutr;
585              ila_data0(67)  <= bridge_en;
586 
587              TRIG0(0)  <= adc_pkt_vld;
588 
589          ila_data1(13 downto 0)  <= adc_cha_dout;
590          ila_data1(27 downto 14)<= adc_chb_dout;
591 
592 
593              ------ instantiate chipscope components -------
594              icon_inst : icon
595                port map  (
596                        CONTROL0 => CONTROL0,
597                        CONTROL1 => CONTROL1,
```

```
598                         CONTROL2 => CONTROL2
599                         );
600
601                ila_data0_inst : ila0
602                port map (
603                         CONTROL => CONTROL0,
604                         CLK     => clk_100MHz,--clk_245_76MHz,
605                         DATA    => ila_data0,
606                         TRIG0   => TRIG0);
607
608                ila_data1_inst : ila1
609                  port map (
610                         CONTROL => CONTROL2,
611                         CLK => clk_61_44MHz,
612                         DATA => ila_data1,
613                         TRIG0 => TRIG1);
614
615                vio_inst : vio
616           port map (
617                 CONTROL => CONTROL1,
618                 ASYNC_OUT => vio_data);
619          --------------------------------------------------------------------
620          -- End
621          --------------------------------------------------------------------
622 end Behavioral;
```

H.2 FM demodulation function in Matlab [84]

```
1  function [y_FM_demodulated] = FM_IQ_Demod(y)
2  %This function demodualtes an FM signal. It is assumed that the FM signal
3  %is complex (e.g. an IQ signal) centered at DC and occupies less than 90%
4  %of total bandwidth.
5
6
7  %filter design!
8  b = firls(30,[0 .9],[0 1],'differentiator'); %design differentiater
9  d=y./abs(y);%normalize the amplitude (i.e. remove amplitude variations)
10 rd=real(d); %real part of normalized siganl.
11 id=imag(d); %imaginary part of normalized signal.
12 y_FM_demodulated=(rd.*conv(id,b,'same')-id.*conv(rd,b,'same'))./(rd.^2+id.^2);%demodulate!
13
14 end
```

H.3 Plotting the FPGA results in Matlab

```
1  % ----------------------------------------------------------------------
2  % This plots FPGA results using data files containing FM samples captured
3  % using UDP.
4  % ----------------------------------------------------------------------
5  Fs = 122.88e6/128;
6
7  %--------------------- 89.0MHz FM station ------------------------------
8  fpgaOutRaw = dlmread('89.0/udp_capture',' ');
9  fpgaout = complex(fpgaOutRaw(:,1),fpgaOutRaw(:,2));
10
11 N    = length(fpgaout);
12 NFFT = N;
13 f1   = fftshift(fft(fpgaout,NFFT));
14 F1    = abs(f1)/N;
15 f    = Fs*(-NFFT/2:NFFT/2-1)/NFFT;
16
17 subplot(3,2,1);
18 plot(f/1e3,F1,'k');
19 title('Spectrum of 89.0MHz FM station (DDC core output)');
```

```
20  xlabel('Frequency ($kHz$)');
21  ylabel('Magnitude'); grid on;
22  %xlim([-1e6,1e6]);
23
24  [fm_demod_signal] = FM_IQ_Demod(fpgaout);
25  f2 = fftshift(fft(fm_demod_signal,NFFT));
26  F2 = abs(f2)/N;
27
28  subplot(3,2,2);
29  plot(f/1e3,F2,'k');
30  title('Spectrum of FM demodulated 89.0MHz FM station in MATLAB');
31  xlabel('Frequency ($kHz$)');
32  ylabel('Magnitude');
33  xlim([0,70]);grid on;
34
35  %--------------------- 94.5MHz FM station -----------------------------
36  fpgaOutRaw = dlmread('94.5/udp_capture',' ');
37  fpgaout = complex(fpgaOutRaw(:,1),fpgaOutRaw(:,2));
38
39  N    = length(fpgaout);
40  NFFT = N;
41  f1   = fftshift(fft(fpgaout,NFFT));
42  F1    = abs(f1)/N;
43  f    = Fs*(-NFFT/2:NFFT/2-1)/NFFT;
44
45  subplot(3,2,3);
46  plot(f/1e3,F1,'k');
47  title('Spectrum of 94.5MHz FM station (DDC core output)');
48  xlabel('Frequency ($kHz$)');
49  ylabel('Magnitude'); grid on;
50  %xlim([-1e6,1e6]);
51
52  [fm_demod_signal] = FM_IQ_Demod(fpgaout);
53  f2 = fftshift(fft(fm_demod_signal,NFFT));
54  F2 = abs(f2)/N;
55
56  subplot(3,2,4);
57  plot(f/1e3,F2,'k');
58  title('Spectrum of FM demodulated 94.5MHz FM station in MATLAB');
59  xlabel('Frequency ($kHz$)');
60  ylabel('Magnitude');
61  xlim([0,70]);grid on;
62
63  %--------------------- 95.3MHz FM station ------------------------------
64  fpgaOutRaw = dlmread('95.3/udp_capture',' ');
65  fpgaout = complex(fpgaOutRaw(:,1),fpgaOutRaw(:,2));
66
67  N    = length(fpgaout);
68  NFFT = N;
69  f1   = fftshift(fft(fpgaout,NFFT));
70  F1    = abs(f1)/N;
71  f    = Fs*(-NFFT/2:NFFT/2-1)/NFFT;
72
73  subplot(3,2,5);
74  plot(f/1e3,F1,'k');
75  title('Spectrum of 95.3MHz FM station (DDC core output)');
76  xlabel('Frequency ($kHz$)');
77  ylabel('Magnitude'); grid on;
78
79  [fm_demod_signal] = FM_IQ_Demod(fpgaout);
80  f2 = fftshift(fft(fm_demod_signal,NFFT));
81  F2 = abs(f2)/N;
82
83  subplot(3,2,6);
84  plot(f/1e3,F2,'k');
85  title('Spectrum of FM demodulated 95.3MHz FM station in MATLAB');
86  xlabel('Frequency ($kHz$)');
87  ylabel('Magnitude');
88  xlim([0,70]);grid on;
```